TALJAARD, ROSA ELIZABETH

APPLICATION OF SEQUENTIAL INJECTION ANALYSIS AS PROCESS ANALYZERS

MSc UP 1996

Application of sequential injection analysis as process analyzers

by

Rosa Elizabeth Taljaard

Submitted in partial fulfilment of the requirements for the degree

MAGISTER SCIENTIAE

in the Faculty of Science
University of Pretoria
Pretoria
March 1996

Application of sequential injection analysis as process analyzers

by

Rosa Elizabeth Taljaard

Supervisor: Professor Jacobus F. van Staden

Department of Chemistry

University of Pretoria

Degree: Magister Scientiae

SYNOPSIS

The use of chemical analyzers in the process control strategy represents a significant shift in the thinking of many process control engineers. Increasing pressure on the chemical manufacturing industry to produce higher quality products, in an economically viable and environmentally acceptable manner, increases the requirement to maintain strict control of plant conditions throughout the production process.

The sophisticated instrumentation of laboratory facilities is unlikely to be suitable for manufacturing environments and hence dedicated systems offering long-term dependability must be developed. The simplicity of the sequential injection (SI) manifold and its low need for maintenance makes it an ideal tool in process analysis.

Having established the manifold design principles, sequential injection analysis (SIA) is evaluated as an approach to sample manipulation. Methods for use in pharmaceutical companies and hospitals (determination of calcium) and for environmental monitoring (determination of sulphate, phosphate and ammonia) are proposed. The usefulness and advantages of sequential injection analysis over conventional flow injection analysis (FIA) is demonstrated.

Die toepassing van sekwensiële-inspuitanalise as proses analiseerders

deur

Rosa Elizabeth Taljaard

Leier: Professor Jacobus F. van Staden

Departement Chemie

Universiteit van Pretoria

Graad: Magister Scientiae

SAMEVATTING

Die gebruik van chemiese analiseerders in die strategiese beplanning van prosesbeheer verteenwoordig 'n betekenisvolle wending in die denkrigting van die wetenskaplike bestuurkorps van die chemiese nywerheid en die gevolglike innovasie van navorsers in die bedryf. Verhoogde druk op die chemiese nywerheid om steeds hoër kwaliteit produkte, in 'n ekonomies lewensvatbare en omgewingsvriendelike omgewing, te lewer, verhoog terselfdertyd die vereiste om strenger kontrole gedurende die produksieproses uit te oefen.

Gesofistikeerde laboratoriumtoerusting is nie noodwendig altyd geskik om voortdurend in 'n nywerheidsomgewing te funksioneer nie. Gevolglik was dit noodsaaklik om sisteme te ondersoek en te ontwikkel wat ekonomies lewensvatbaar is en langtermyn stabiliteit en

betroubaarheid in so 'n omgewing sal lewer. Die eenvoud van die sekwensiële-inspuit (SI) analiseerder, asook die lae onderhoudskoste, leen hom uitstekend tot 'n prosesanaliseerder.

Nadat die beginsels vir die ontwerp van die sisteem vasgestel is, is sekwensiële-inspuitanalise aangewend as 'n benadering tot monster manipulasie. Metodes vir gebruik in die farmaseutiese industrie of hospitale (bepaling van kalsium) asook vir omgewings waarnemings (bepaling van sulfaat, fosfaat en ammoniak) is voorgestel. Die aanwending en voordele van hierdie tegniek bo konvensionele vloei-inspuitanalise (VIA) is aangetoon.

Acknowledgements

First, I like to thank my supervisor, Prof van Staden, for his constant enthusiasm, patience and valuable aid during my studies.

I also like to thank my parents and sisters for their encouragement and motivation. They have, often unknowingly, provide that vital support when it appears that nothing is about to work.

A number of friends have helped me in various ways, and I like to thank them all, while mentioning specifically only a few - Niel Malan for helping me from the start of this project to put up my instruments and for the number of programmes he programmed and reprogrammed to suit a specific need. Hanneli du Plessis for her valuable advise and aid in writing the thesis. Maré Linsky, Esna Britz and Neels Hattingh for their constant encouragement, tolerance, motivation and advice.

I also want to express my gratitude towards the following persons:

- Dr Deon Barnes and dr Derek Auer, from MINTEK, for their valuable advise, especially during the first part of this study.
- Triana Louw, from the Institute for Water Quality Studies, for providing most of the reference samples analyzed in this study.
- The FRD for financial support.

To Him who by means of His power working in us is able to do so much more than we can ever asks for, or even think of: to God be the glory.

Ephesians 3 : 20 - 21.

Table of Contents

CHAPTER 1

Sequential Injection - New Mechanics, Old Principles?

1.1 Introduction

Sequential injection analysis (SIA), introduced in 1990 [1,2] is a simple and convenient concept of flow analysis. Although this technique is today a mere six years old, its roots can be traced back as far as 1974 [3]. Since then the concept of flow injection analysis (FIA) grew tremendously in its application in analytical chemistry. To understand where sequential injection fits in and why Růžička referred to it as 'a new look at a familiar landscape' [3] it is best to start at the very beginning.

Flow injection belongs to a family of methods, based on sample injection into a continuously flowing unidirectional carrier stream, which carries the analyte through a chemical modulator into a detector (Fig. 1.1). This broad group of methods embraces besides flow injection (FI) or flow injection analysis (FIA) also chromatography, electrophoresis and field flow fractionation. The individual members in this family differ in one fundamental respect, *viz.*, the function of the chemical modulator, which alters the original square wave input, provided by sample injection, into a chromatogram, electropherogram, fractogram or fiagram. This is why the function of the chemical modulator, or forces within it, are associated with the names of individual techniques such as chromatography (column), electrophoresis (electric

field), field flow fractionation (external force) and flow injection (reactor) [4].

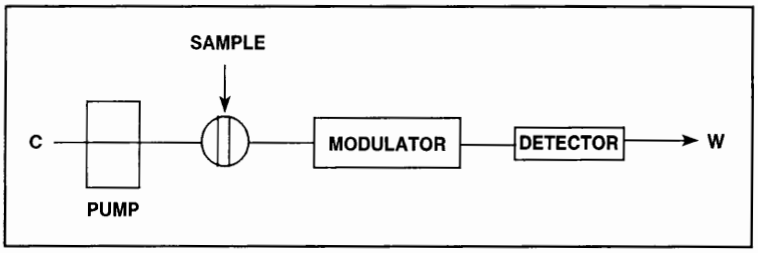

Fig. 1.1 Flow scheme of analytical techniques based on injection of an analyte into a moving carrier stream (C - carrier and W - waste).

In the beginning there was the realization that colorimeter-based serial assays could be carried out more efficiently in a flowing stream of reagent into which the sample was injected as a discrete narrow zone [5] and that FIA could be used to carry out serial assays even in a routine laboratory with modest means. All that was needed was a multichannel pump, an injection valve, a reaction coil, a flow-through detector and a recorder (Fig. 1.2). Except for the last component, which was replaced when computers invaded laboratories some ten years later, this basic flow scheme remained essentially unchanged.

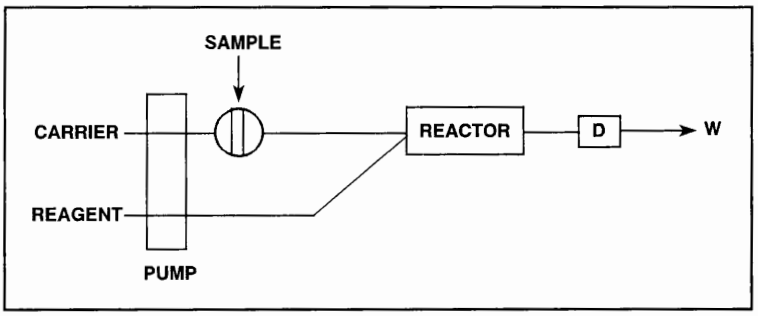

Fig. 1.2 Scheme of a flow injection system. D is the detector and W is waste.

It is well recognized that in the flow injection apparatus (Fig. 1.2) two processes take place simultaneously: physical dispersion of the sample zone within the carrier stream of reagent and a chemical reaction between the analyte molecules thus supplied. As the detector is tuned to sense species produced by this chemical derivatization, the readout has the form of a peak into which the original square wave input (as provided by injection) has been transformed.

In its simplest form the reactor is a tube that has been tightly coiled to promote radial mixing of sample and reagent. If several reagents must be added in succession, additional streams are confluenced and coils are added. Amongst the first procedures adapted to FIA were classical colorimetric methods where chart recorders were used to obtain a fiagram. Over the last 20 years the range of detectors has grown and so has the variety of reactor designs, to accommodate solvent extraction [6], gas diffusion [7], photodegradation, coulometric reagent generation and titrations [8]. In addition, miniaturized packed reactors (typically 1.5 mm i.d., 30 mm long), containing solid reagents [9], reductants [8], immobilized enzymes [10], ion exchangers [11] or silica or polymer-based C_{18} materials [12], were introduced to convert, catalyse or preconcentrate analyte molecules. Important research in the biological science is done using both flow injection cytoanalysis and flow-injection renewable surface (FI-RS) techniques [3].

When FIA research became orientated towards the exploitation of concentration gradients formed by the dispersion process [13] new techniques using stopped-flow, reversed flow, sinusoidal flow, reagent injection, sequential injection [1] and single solution calibration were developed. Of these techniques, stopped-flow injection became the cornerstone of future developments and allowed the implementation of sequential injection analysis (SIA).

1.2 Stopped flow injection

Optimization of a flow injection system is a balancing act, where dispersion of the sample zone and its mixing with a reagent must be weighed against the time required to achieve a desired chemical conversion of an analyte into a detectable species. This is so because the parabolic profile established during the injection process expands further during sample zone transport through an open-tubular channel, ultimately leading to an undesired zone broadening and consequent loss of sensitivity and sampling frequency.

In stopped flow injection, the unidirectional carrier stream moves until a suitable section of the dispersed sample zone is positioned in the observation field of the detector for stopped-flow reaction measurements. It is unfortunate that most flow-injection (FI) procedures utilize continuous flow, because such a format is not advantageous and is difficult to optimize. Indeed, by stopping the flow when the mixture of sample with the reagent reaches the flow cell, many advantages are gained [8]. First, as dispersion ceases while chemical reaction continues, the sensitivity of determination increases because the reactants and the product are no longer diluted. Second, as neither carrier nor reagent solution is pumped during the stopped-flow period, the consumption of solutions (and waste generation) is much reduced. Third, a selected section of the dispersed sample zone is trapped within the flow cell, making reaction rate measurements possible, whereby it is the slope of the reaction rate curve, as recorded during the stopped-flow interval, which allows the analyte to be quantified.

1.3 Gradient techniques

It has been well established that a dispersed sample zone, while travelling through a detector, offers an infinite number of sample/reagent ratios [8]. In its simplest form, gradient dilution has been used to accommodate highly concentrated samples within the dynamic range of a detector. This has been done by selecting a readout collected with a time delay or at a peak tail rather than simply reading peak height. In this way, dilutions up to 20 000-fold have been obtained [14] for process control applications.

Going one step further, one may select an infinite number of readouts from a single analyte zone. By viewing the dispersed zone as a matrix of concentrations versus time, into which the original square wave impulse has been transformed, the original input can be seen as digitized into a infinite number elements of fluid, each of them representing a progressively more diluted standard [8]. This concept is the basis of a single solution calibration method.

1.4 Sequential injection

The next step in the development of flow injection methodology is based on dispersion and mutual penetration of sample and reagent zones. Sequential injection (SI) [1] uses a selector (rather than injection) valve (Fig. 1.3), through which precisely measured volumes of sample solution and reagent solution are aspirated into a holding coil (HC) by means of a pump which is capable of a precise controlled stop-go-forward-reverse movement.

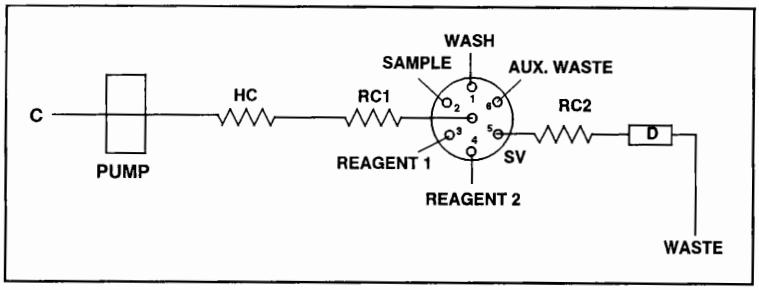

Fig. 1.3 Flow scheme of a sequential injection system. HC - holding coil, RC - reaction coil, SV - selection valve, C - carrier and D -detector.

Following the first step of zone sequencing, during which the sample and reagent zones are stacked in the holding conduit adjacent to each other (Fig. 1.4A), the valve is switched into the detector position. In the next step, the flow is reversed (Fig. 1.4B) so that the stacked zones are propelled through the valve and the reactor into the detector. As the central streamline moves at a rate that is twice the speed of the mean flow velocity, whereas the elements of fluid more adjacent to the walls move at lesser rates, the cores of the sequenced zones penetrate each other [3]. During this movement the flow reversal creates a complex region (Fig. 1.5) within which the analyte is being transformed into detectable species. The fundamental requirement for SI to succeed is to achieve maximum zone penetration through a deliberate increase in axial dispersion, obtained by means of the flow reversal and channel design [1, 16, 17]. SI is mechanically far simpler than conventional FI, as it uses only a single pump, single valve and single channel. The flow path does not have to be reconfigurated if the injection volumes, reaction times or mutual zone dispersion are to be modified, as these parameters can be altered via computer control. As additional reagents, reactors and detectors can be clustered around the selection valve (the apparent limit being only the number of available ports), multi-reagent chemistry and multi-detector assays can in principle be carried out in a single sequential injection (SI) system.

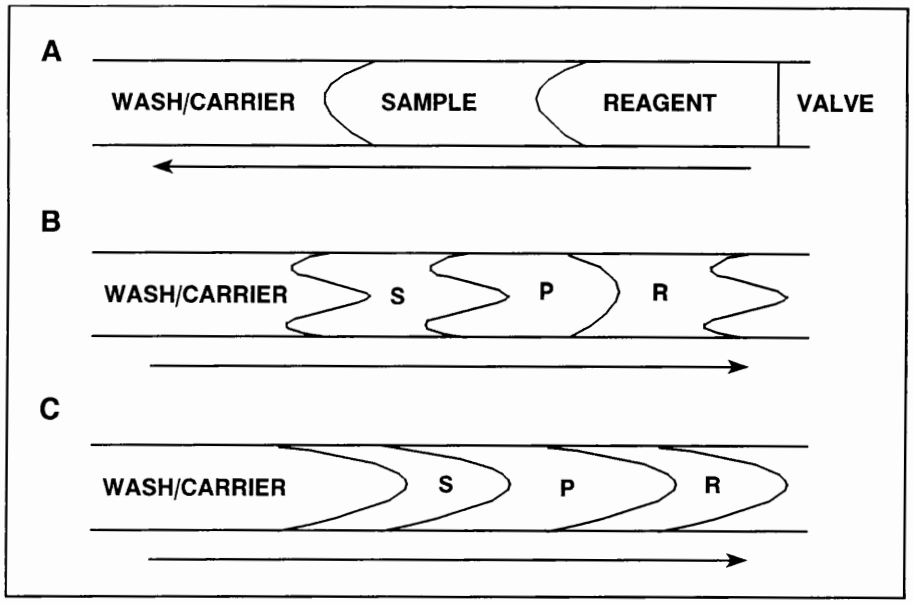

Fig. 1.4 Principle of sequential injection. Profile of zones after injection (A), immediately after flow reversal (B) and in reactor 2 (C). S - sample, R - reagent and P - formed product zones.

How does sequential injection (SI) differ from flow injection (FI) and what are the drawbacks? The answer lies in the differences in dispersion patterns as observed in FI and SI channels (Figs. 1.5 and 1.6). The characteristic feature of the FI pattern is that the injected zone flows past a confluence point where two streams merge in a synchronous fashion, so that an equal volume of reagent solution is added to each element of the passing carrier stream. The result is a concentration gradient of an analyte within the constant background of a reagent. As several confluence points can be serially placed on the main carrier line, several reagents can be serially added to the passing analyte zone, thus following the protocol of manual assays which require serial addition of several reagents. The only price paid is the multitude of manifold lines and the need of a multichannel pump. In contrast, no confluence points are used in SI, where the multiposition valve is used to sequence the zones into the holding coil. Such a valve cannot serve as a confluence point as it connects only two (and not three ports) at a time. The result is a initially sharp boundary

between adjacent zones and, therefore, only a partial overlap of analyte and reagent peaks is possible. There is also a limitation to the number of zones that can be mixed by flow reversal in a tubular reactor, three being the maximum [16]. Consequently, if several reagents need to be added serially, as it is often the case in enzymatic assays, the only alternative in SI is the use of a mixing chamber, as was used in the determination of factor XIII, which required six reagents [17]. A mixing chamber is also needed when extensive dilution of the analyte is required, typical for process control applications [18].

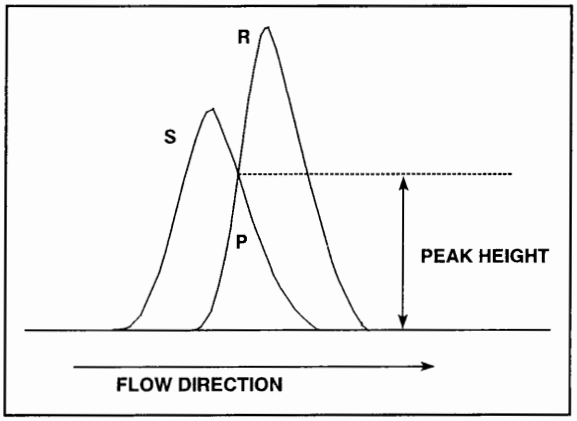

Fig. 1.5 Concentration profiles as seen by the detector in a SIA system. S - sample, R - reagent and P - formed product zones.

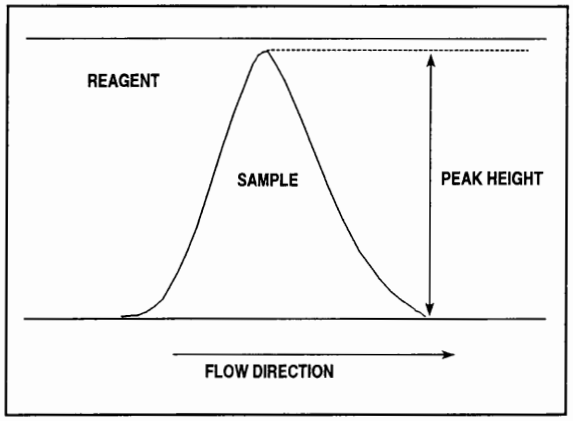

Fig. 1.6 Concentration profile as seen by the detector in a FIA system.

1.5 Advantages and disadvantages of FIA

1.5.1 Advantages

This approach to automated wet-chemical analysis did provide several excellent features that are absent in many continuous analyzers and sensors [19, 20]. Of note are the advantages in

the area of calibration, self-diagnosis and self-cleaning:

(i) Calibrants are subjected to the same treatment as the samples.

(ii) The baseline provides an immediate indication of a drifting detector or fouling of the system.

(iii) Because only a small sample bolus is injected into a continuous flowing stream the analyzer is constantly flushed with a clean solution.

(iv) The ability to make use of highly reactive, oxidizable, light-sensitive or otherwise unstable reagents which can be generated *in situ* sometimes makes this approach the only possible solution to monitor a particular process stream.

(v) There are several additional advantages such as high sampling frequency (almost twice as much samples can be analyzed with FIA than with SIA), good reproducibility and computer-compatible hardware which ensures that process analyzers are conveniently incorporated into existing or planned process control systems. Unlike SIA a FIA system does not need to be computer controlled.

1.5.2 Disadvantages

Many flow injection analyzers made their way successfully into the plant environment. Criticism, however, soon began to emerge against yet another laboratory success that was transferred to the process environment. Although many of these installations continued to perform with acceptable reliability, four main critisms were levelled against flow injection analysis [19]:

(i) The tendency of the narrow-bore tubing and fittings of the flow manifold to became blocked.

(ii) The need to develop a new manifold for each application.

(iii) The complexity of many of the manifolds.

(iv) The vulnerability of the peristaltic pump tubing, which require regular checking and replacement. It is difficult to maintain a constant flow rate for extended periods of time. Differences in temperature, solution viscosity and elasticity of pump tubing result in variations in flow rate.

Other disadvantages that act as barriers to the extensive wide scale deployment of flow injection process analyzers can be summarized as follows [20]:

(i) Most flow injection methods are suitable for the determination of single elements. Few multi-element detectors are presently used.

(ii) In spite of the fact that FIA uses pump speed typically of the order 1 $m\ell.min^{-1}$, this still translates into about 10 ℓ of reagent per stream per week. This proves to be excessive, particularly when expensive reagents are being used as carrier solution.

(iii) The chemical kinetics are concealed within the physical process of dispersion. While most chemistries are extremely rapid (kinetic studies are not practical under these conditions), kinetic differences in slower reactions can be employed to add a measure of selectivity to otherwise unspecific methods [20]. Constant flow conditions prelude this approach.

(iv) A requirement for increased reaction time implies the use of longer reaction coils. Longer reaction coils result in increased dispersion which may be undesirable.

Of course these barriers do not apply to all applications and flow injection process analyzers will continue to enjoy wide application.

1.6 Advantages and disadvantages of SIA

1.6.1 Advantages

In laboratory applications manual reconfiguration of the flow channel, high reagent consumption due to continuous flow operation, frequent servicing of peristaltic pumps and frequent recalibration of the system are acceptable. In a process environment these are prohibitive in terms of cost and manpower. Early studies in the field of SIA [1] soon showed that a single manifold was sufficient, irrespective of the chemistry to be employed. The manifold, once optimized, could be 'cast in stone'. There is apparently no limit to how many solutions (reagents, samples and standards) or devices (reactor coils, mixing chambers and detectors) can be nested around the valve. Indeed, an SI cluster may serve as a single and multichannel analyzer. Alternatively, a series of standards can be permanently nested around the valve, being ready for automated recalibration whenever needed [3].

The biggest advantage of SI compared to FI is that there is no need for physical reconfiguration of the flow path. Any changes (injected sample volume, reaction time, sample dilution and reagent : analyte ratio) are accomplished via flow programming rather than by physical reconfiguration of the flow path. Indeed, SI is fully computer compatible, as it allows all changes including system calibration, to be controlled from a computer keyboard, a feature that will allow its future optimization through the use of artificial intelligence [3]. The SI system is further robust, reliable and require a low frequency of maintenance.

1.6.2 Disadvantages

There are presently two drawbacks of SI to be mentioned. First, since aspiration of the wash solution and sequencing of the zone in the holding coil take some time (typically 30 seconds), the sampling frequency of the SI system is presently half that of a conventional FI system, where filling of the injection valve is a matter of a few seconds. Secondly, SI requires specialized software, since the sequencing, injection and data collection are entirely computer driven. This, however, is not an obstacle in using the technique [15].

1.7 From flow injection to sequential injection via the random walk model

The conceptual consequences of these technical developments, are intriguing, as the replacement of monotonous constant flow leads to reconsideration of the role of the flow transport in a flow injection system. Using the random walk model as a basis, it has been postulated that no net flow is needed for the successful operation of a flow injection system [1]. This phenomenon is described in Chapter 2.

1.8 Process analyzers

The use of chemical analyzers in the process control strategy represents a significant shift in the thinking of many process control engineers. Most of the process control systems currently used, are based on physical measurements such as flow rate, pressure, electrical resistance, etc. While this has resulted in processes which are operated under statistical control, verification of the process performance can only really be achieved by chemical analysis,

usually in a remote plant laboratory. This approach is seen as unacceptable in the design of quality management systems for the production process. In such systems, the emphasis is on quality assurance during the process rather than after-the-fact. Process analysis brings the process controller a step closer to ensuring excellent control of the plant and real time quality assurance. At this stage, lengthy development times, the cost of these analyzers and their maintenance requirements mean that only a few critical streams are monitored.

What process control engineers really want is a whole battery of chemical sensors in a fully distributed system. A high degree of redundancy (where the sensing elements are constantly being renewed and old and failing elements are decommissioned on an ongoing basis to be replaced by new sensing elements) would ensure reliability and facilities for cross validation [20].

1.9 Aim of this study

As sample injection, controlled dispersion and reproducible timing are the cornerstones of both flow injection (FI) and sequential injection (SI), much of what has been learnt from the classical flow schemes can be applied to zone sequencing. Although the mechanics of SI are much simpler than that of FI, the complexity of gradient formed by zone penetration with reversed flow still has to be unravelled. The greatest challenge is the theory of flow dynamics, which will led to optimization of flow systems based on flow stopping and reversal. Until then, the fundamentals of sequential injection will have to be explored experimentally and are summarized in empirical rules as described in Chapters two and three.

Increasing pressure on the chemical manufacturing industry to produce higher quality products, in an economically viable and environmentally acceptable manner, increases the requirement to maintain strict control of plant conditions throughout the production process. It was aimed, in this study, to develop new and adapt old methodologies to use in the plant situation. This was done because monitoring of only physical parameters, while most important, become inadequate [20].

The sophisticated instrumentation of laboratory facilities is unlikely to be suitable for manufacturing environments and hence dedicated systems offering long-term dependability must be developed. The simplicity of the SIA manifold and its low need for maintenance makes it an ideal tool as process analyzer. Methods for use in pharmaceutical companies or hospitals (determination of calcium) and for environmental monitoring (determination of sulphate, phosphate and ammonia) are proposed.

The determination of calcium is based on the fast complexation reaction between Ca^{2+} ions and cresolphthalein complexone (CPC). One of the problems experienced in this type of determination is the large background values originating from coloured free indicator species. The determination of sulphate is based on the turbidimetric determination of barium sulphate. Care must be taken in this type of procedure to stabilize the formed colloidal suspension in order to obtain reproducible results. Phosphate and ammonia are both based on slower complexation reactions. Because stopped-flow periods can easily be incorporated into SIA procedures, SIA is a very suitable technique for these determinations.

1.10 References

1. J. Růžička and G. D. Marshall, **Anal. Chim. Acta.**, **237** (1990) 329.
2. J. Růžička, G. D. Marshall and G. D. Christian, **Anal. Chem.**, **62** (1990) 1861.
3. J. Růžička, **Analyst**, **119** (1994) 1925.
4. J. Růžička, **Anal. Chim. Acta.**, **261** (1992) 3.
5. J. Růžička and E. H. Hansen, **Anal. Chim. Acta.**, **78** (1975) 145.
6. B. Karlberg and S. Thelander, **Anal. Chim. Acta.**, **98** (1978) 1.
7. H. Baadenhuijsen and H. E. H. Seuren-Jacobs, **Clin. Chem.**, **25** (1979) 443.
8. J. Růžička and E. H. Hansen, **Flow Injection Analysis**, 2nd ed.; Wiley, New York, 1988.
9. A. M. Almuaibed and A. Townshed, **Anal. Chim. Acta.**, **245** (1991) 115.
10. L. Gorton and L. Ogren, **Anal. Chim. Acta.**, **130** (1981) 45.
11. S. Olsen, L. C. R. Pessenda, J. Růžička and E. H. Hansen, **Analyst**, **108** (1983) 905.
12. J. Růžička and A. Arndahl, **Anal. Chim. Acta.**, **216** (1988) 243.
13. J. Růžička, **Anal. Chem.**, **55** (1983) 1040A.
14. M. Gisin and T. Thommen, **Anal. Chim. Acta.**, **190** (1986) 165.
15. T. Gübeli, G. D. Christian and J. Růžička, **Anal. Chem.**, **63** (1991) 2407.
16. J. Růžička and T. Gübeli, **Anal. Chem.**, **63** (1991) 1680.
17. M. Guzman, C. Pollema, J. Růžička and G. D. Christian, **Talanta**, **40** (1993) 1.
18. M. Gisin, T. Thommen and K. F. Mansfield, **Anal. Chim. Acta.**, **179** (1986) 149.
19. G. D. Marshall and J. F. van Staden, **Process Control and Quality**, **3** (1992) 251.
20. G. D. Marshall, **Sequential-injection Analysis**, PhD-Thesis, University of Pretoria, 1994.

CHAPTER 2

Theoretical Background

2.1 Introduction

A sequential injection (SI) manifold must be designed to achieve mixing between reagent and analyte such that the reagent is in sufficient excess at the maximum of the profile to ensure the greatest degree of reaction. Dilution of the formed product zone should, however, be minimized so as to avoid an unnecessary loss in sensitivity. The design of a SI manifold can be considered as the search for optimum dispersion characteristics.

Karlberg [16] has called flow injection analysis "the art of controlling sample dispersion in a narrow tube". The dispersion coefficient is governed by the hydrodynamic characteristics of the manifold. The major factors are (a) laminar flow (which produces a parabolic distortion of the initial boundaries), (b) axial diffusion, (c) radial diffusion, (d) radial mixing at confluence points (should the manifold contain these) and (e) secondary flow processes. The latter includes radial circulation induced by coiling of the flow conduits, vortex shedding caused by step changes in tube diameter, small regions of turbulent flow produced by sharp angle bends (if any) and surge in flow produced when the selection valve is switched. Although flow reversal is not a characteristic of the manifold, it is one of the most important factors governing zone penetration in sequential injection analysis.

The difficulties of describing these processes accurately are well recognized, and the design of manifolds are based on the expected trends in dispersion behaviour as a function of the various parameters over which there is some control. These include flow rate, volume injected, extend of coiling, use of packed reactors, etc.

The experimental conditions usually involved in FIA result in incomplete mixing of the injected sample plug with the carrier stream, with two important consequences.

(a) Mixing is time-dependent, and therefore occurs to different extends at different points along the flow line.

(b) The extent of mixing is highly reproducible from sample to sample.

Thus, the technique give rise to the creation of a time-dependant concentration gradient of sample within the carrier streams.

2.2 Transport

Despite the fact that early workers [17] assumed the need for turbulent flow to avoid cross-contamination between samples successively injected into the carrier stream, it was soon verified [18] that the Reynolds number is always much less than 2 000, so the transport of matter along the tubes takes place essentially by laminar flow.

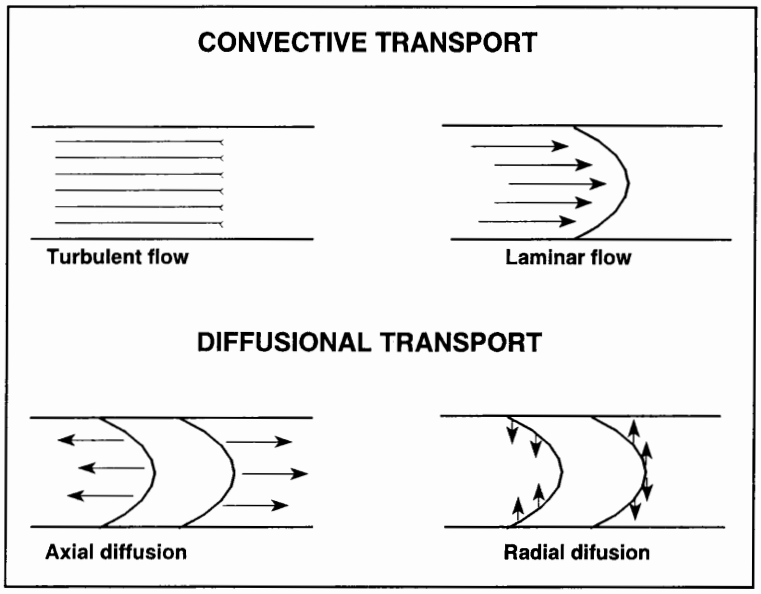

Fig. 2.1 General types of transport in closed tubes.

There are two mechanisms contributing to the dispersion of the injected sample (Fig. 2.1) [7]:

(i) Convective transport, occurring under laminar flow conditions. This yields a parabolic velocity profile with sample molecules at the tube walls having zero linear velocity and those at the centre of the tube having twice the average velocity. The effect of this is that convection, resultant from the concentration gradient between the sample and the surrounding carrier stream, has a large area over which to operate.

(ii) Diffusional transport, due to the presence of concentration gradients in the convective transport regime, gives rise to axial and radial diffusion. The former, due to horizontal concentration gradients at the leading and tailing edges of the injected sample zone contributes insignificantly to the overall dispersion, whereas the latter, resulting from concentration differences perpendicular to the direction of flow makes an important contribution to the overall dispersion in a flow injection system.

It is clear from Fig. 2.2 that transport of the injected zones in SIA occurs via laminar flow. During zone reversal a short period of turbulent flow occurs, but after a few seconds laminar flow is restored.

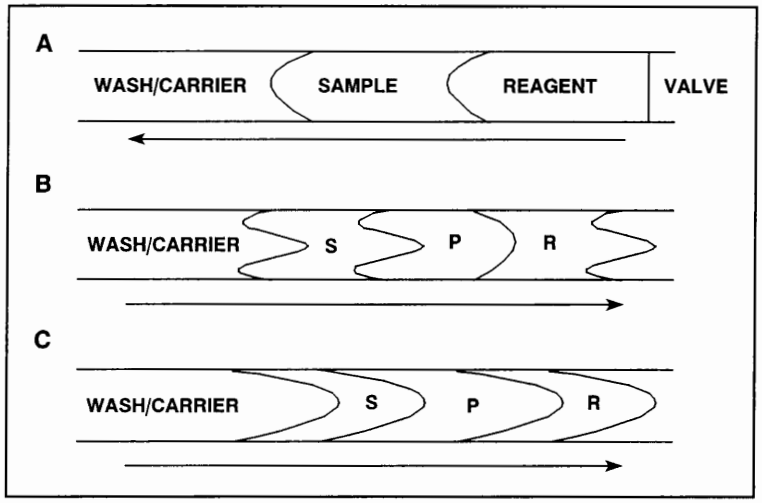

Fig. 2.2 Flow profiles of the sequenced (A) and injected zones (B - immediately after flow reversal and C - in reactor 2). S - sample, R - reagent and P - formed product zones.

It should be borne in mind that all the illustrations of zone profiles show atypically small volumes and concentration contours representing only the first few milliseconds of laminar flow.

2.3 Dispersion

Reproducible dispersion is the basis for analysis by flow injection methods. From the early days of FIA, dispersion was recognized as being fundamental to the optimum design and understanding of this approach to sample manipulation. Initially chemical engineering

hydraulic models were employed as predictive estimators of the flow-injection response curve. These models are limited to the description of dispersion in the manifold (resulting from laminar flow) and do not consider the contribution from the valve (injection valve in the case of FIA), mixing and connection components and detector flow cell. Furthermore, theoretical studies have been undertaken for systems where there is no chemical reaction and those where chemical reactions take place. A wide spectrum of models that have been applied to the dispersion phenomenon in flow-injection systems is reviewed by Valcarcel *et al* [7]. There is however, despite of the extensive efforts in the development of models, no uniformly acceptable understanding or description of dispersion available.

2.3.1 Theoretical models

First of all, it is salutary to explain the difficulties involved in the theoretical predictions of the behaviour of the injected sample or reagent plug in practical systems. It is not an easy task to define the contributions of elements such as the injection operation, connectors or geometry of the flow-cell to the dispersion. All the relations are therefore empirical in nature. Nevertheless, several models have been developed, for laminar conditions, to define the theoretical principles and derive mathematical expressions accounting for the physical behaviour of the injected plug. A number of these models are described in the following paragraphs. Table 1 gives a list of the symbols that will be used in the discussions.

TABLE 1. List of symbols

Sample/reagent		Reactor geometry	
C	= concentration (M)	L	= overall tube length (cm)
C^0	= initial concentration	l	= partial tube length (cm)
C^{max}	= concentration at signal maximum	R	= tube radius (mm)
		r	= partial tube radius (mm)
V_i	= injected volume ($\mu\ell$)	d	= tube diameter (mm)
		V_r	= volume of reactor/system (mℓ)
Hydrodynamic aspects		**FIA/SIA signal**	
q	= flow rate (mℓ.min^{-1})	D	= dispersion coefficient
u	= linear velocity (cm.sec^{-1})	t_a	= travel time (sec)
u_0	= maximum linear velocity (cm.sec^{-1})	Δt	= baseline-to-baseline time (sec)
$\bar{t}_r$	= mean residence time (sec)	T	= residence time

2.3.1.1 Taylor's model [7]

Taylor's model is applicable to Gaussian distribution defined by C = f(t) in a form which depends on the chosen parameters, namely

$$C = \frac{m}{4r^2\pi Dt} \exp\left[\frac{-(x - L)^2}{4Dt}\right] \quad \textbf{(1)}$$

and

$$C = \frac{C_0 V_i}{q\sigma(2\pi)^{1/2}} \exp \frac{(t - \bar{t}_r)^2}{2\sigma^2} \quad \textbf{(2)}$$

where m is the injected solute mass ($m = C^0V_i$), σ is the parameter corresponding to the standard deviation of a Gaussian distribution and x is the axial distance from the injection point.

This model is only applicable if the injected volume is practically neglible compared to the reactor volume ($V_i << V_r$). As this is not the case for SIA, where zone volumes are of the same order as reactor volumes [15], this model is not applicable to the sequential injection (SI) technique.

2.3.1.2 Tanks-in-series model

This model was first discussed in connection with FIA by Růžička and Hansen [8] and later by Betteridge [19]; and is analogous to the description of liquid chromatography in terms of theoretical plates. It relies on the assumption that the fluid flow passes sequentially through a large number (N) of minichambers in which stirring is perfect (instantaneous mixing). The mathematical expression derived from this model is [8]

$$C = \frac{1}{(\bar{t}_r)_N} \left[\frac{t}{(\bar{t}_r)_N}\right]^{N-1} \frac{1}{(N-1)!} \exp\left[\frac{-t}{(t_r)_N}\right] \qquad \textbf{(3)}$$

$(\bar{t}_r)_N$ being the mean residence time of an element of fluid in a given tank. The larger N, the more Gaussian the profiles of the C = f(t) curves become. Under these conditions, the variance is given by

$$\sigma^2 = N(\bar{t}_r)_N^2 = \frac{(\bar{t}_r)^2}{N} \quad \textbf{(4)}$$

since the overall mean residence time is $\bar{t}_r = N(\bar{t}_r)_N$. The random walk model (described later) uses a similar approach to explain mixing in SIA.

2.3.1.3 Mixing chamber model

This model is based on the model developed by Pardue and Fields [9, 10], which in turn was inspired by the tanks-in-series model. In 1979, Pungor *et al* [20] developed a mathematical model to describe the dispersion when there is a mixing minichamber positioned close to or in the reactor itself. The concentration of a substance in the mixing chamber can be described as a function of time by

$$\frac{d\Delta C_t}{dt} = \frac{V}{W}\left[\Delta(C_s)_t - \Delta C_t\right] \quad \textbf{(5)}$$

where t is the time (sec) from the moment of injection, $\Delta C_t = C_t - C_0$; C_t is the actual analyte concentration in the carrier stream on entry to the mixing chamber, C_0 is the analyte concentration before injection, V is the flow rate ($m\ell.min^{-1}$) and W is the volume of the mixing chamber. Mixing chambers are used in SIA mainly to dilute highly concentrated samples [27] or to ensure adequate mixing of the zones when more than three zones are involved [26].

2.3.1.4 General model [7]

The expression which takes strictly into account both convective and diffusional transport and therefore best describes the overall dispersion phenomena is

$$D[\frac{\delta^2 C}{\delta l^2} + \frac{\delta^2 C}{\delta r^2} + \frac{1}{r}\frac{\delta C}{\delta r}] = \frac{\delta C}{\delta t} + u_0(1 - \frac{r^2}{R^2})(\frac{\delta C}{\delta l}) \qquad \textbf{(6)}$$

This is derived by applying a mass balance to a differential element of volume in the fluid and takes into account axial and radial concentration gradients, as well as flow-profiles under a laminar flow regime. The left hand side corresponds to diffusional transport, the first term within the [] brackets accounting for axial diffusion (dependence of C on l) and the other two for radial diffusion (dependence of C on r). The first term on the right hand side corresponds to a build-up of matter, which only occurs in a non-steady regime, as in this case, and the second term accounts for the contribution from convective transport for which the velocity profile is parabolic in shape and given by

$$u = u_0(1 - \frac{r^2}{R^2}) \qquad \textbf{(7)}$$

The molecules at the tube walls (r = R) have zero velocity (u = 0), whereas those at the centre (r = 0) have the maximum velocity ($u = u_0$).

2.3.2 Practical definition of dispersion

The dispersion or dilution of a sample injected into a carrier stream, is given by the position and shape of the analyte signal band. Therefore, in practice it is the parameters characterizing the transient signal which are chosen to define the dispersion. An FIA and SIA peak is characterized, at least qualitatively, by

(a) its position, as defined by the travel time, t_a,

(b) its bandwidth, characterized by the baseline-to-baseline time, Δt, and

(c) the co-ordinates of the band maximum (T, C^{max}).

Bearing in mind the general theoretical considerations and the description of the different models used to define dispersion, it is easy to understand the difficulty involved in relating them to the experimental observations in a straightforward way. Only one of the various approaches proposed for this purpose is discussed below.

2.3.2.1 Růžička's dispersion coefficient

Růžička and Hansen [4] defined the conceptually simple and practically useful dispersion coefficient, $D = C^0/C$, where C^0 is the concentration of the sample material before the dispersion process begins and C is the concentration of the sample, after the dispersion process, in the element of fluid that yields the analytical readout. Thus each peak is characterised by an infinite number of D_s values ranging from infinity at the beginning of the peak, falling to a minimum at the peak maximum and rising to infinity again at the end of the peak (each point on the signal record has therefore a corresponding dispersion

coefficient). At the signal maximum,

$$D^{max} = \frac{C^0}{C^{max}} \quad \textbf{(8)}$$

Since there is generally a direct relationship between the property used for detection, the magnitude of the transduced signal recorded and the concentration of the sample or its reaction product, the dispersion coefficient can be determined from the ratio of the height of the signal found in the absence of dispersion to that of the FIA or SIA signal. Thus

$$D^{max} = \frac{k_0 h^0}{k_1 h^{max}} = \frac{h^0}{h^{max}} \quad \textbf{(9)}$$

where k_0 and k_1 are proportionally constants, identical if the signal height is linear related to the concentration over the range considered. Hence, the dispersion coefficient can often be taken as the signal height ratio.

Subscripts indicating whether the dispersion coefficient refers to sample or reagent are also frequently used. It is important to remember that the dispersion coefficient (D) only considers the physical process of dispersion and not the ensuing chemical reactions. The use of this simple relationship has dominated experimental design and the development of the technique. The dispersion coefficient, D_s, has been defined as the ratio of the concentration of the sample material before (C_s^0) and after (C_s) the dispersion process has taken place, C_s being the concentration in that element of fluid from which the readout is being taken, i.e., D_s =

C_s^0/C_s. Similarly, reagent dispersion, D_r, has been defined so that $D_r = C_r^0/C_r$. These simple relations allow estimation of the concentrations of reacting components in the relevant element of the dispersed sample zone.

2.3.3 Influence of geometric and hydrodynamic aspects on dispersion

Ramsing and co-workers [21] have proposed the following expression for dispersion coefficient of an elementary FIA system, which relates it to the geometric characteristics of the reactor (L, R), some hydrodynamic aspects (u, $\bar{t}_r$) and the injected sample volume (V_i):

$$D = \frac{2\pi^{3/2}R^2(Lu\delta\bar{t}_r)^{1/2}}{V_i} \qquad \textbf{(10)}$$

where the longitudinal dispersion number, δ, is defined by Levenspiel and Smith [22] for a non-Gaussian curve as

$$\sigma^2 = 8\delta^2 + 2\delta \qquad \textbf{(11)}$$

or

$$\delta = \frac{1}{8}[8(\sigma^2 + 1)^{1/2} - 1] \qquad \textbf{(12)}$$

σ^2 being the variance of their equation for dispersion in a flowing system. This expression establishes that there is an interesting relationship between D^{max}, which describes the peak height, and σ, which provides a measure of the peak width; this is clearly plausible since the greater the variance (σ^2), the greater the dispersion.

2.3.3.1 Hydrodynamic factors

2.3.3.1.1 Flow rate

From Vanderslice's expression [7], the flow rate, q, can be related to the travel and baseline-to-baseline times through

$$t_a = \frac{k}{q^{0.125}} \qquad \textbf{(13)}$$

and

$$\Delta t = \frac{k'}{q^{0.64}} \qquad \textbf{(14)}$$

SIA peaks obtained (Fig. 5.5, p 160) with the experimental arrangement depicted in Fig. 5.4 show that this results are applicable to SIA systems. This results (t_a and Δt increase with decreasing flow rate) show that the dispersion coefficient decreases with increasing flow rate, resulting in better sensitivity of the method.

Although it is possible to write equations for most of the hydrodynamic regimes when considered individually, it is not possible to produce useful equations for any given reaction zone which incorporates different types of flow. This is especially true for SIA where flow reversal causes a small region of turbulent flow.

2.3.3.2 Geometric factors

This section deals with the influence of the reactor shape (open, coiled, packed) and its dimensions on the dispersion.

2.3.3.2.1 Straight tubes

Straight tubes represents the simplest situation. As it can be seen from equations 15 and 16, t_a and Δt increase with reactor length according to Vanderslice's predictions [7].

$$t_a = kL^{1.025} \quad \textbf{(15)}$$

and

$$\Delta t = k'L^{0.64} \quad \textbf{(16)}$$

It is also clear that t_a and Δt are directly related to the diameter (R = d/2), in agreement with Vanderslice's predictions [7]

$$t_a = kd^2 \quad \textbf{(17)}$$

and

$$\Delta t = k'd^2 \quad \textbf{(18)}$$

The residence time and the dispersion coefficient increase therefore linearly with the tube diameter [7].

2.3.3.2.2 Coils

When the reactor tube is coiled helically the centrifugal force originating from the circulation of fluid through the tube results in radial-type flow. At low flow rates, the centrifugal force is not very great and the velocity profile is practically parabolic. At high flow rates the profile is completely different since molecules at the tube walls travel at a higher velocity than those at the centre of the tube (Fig. 2.3) [7]. Both situations result in a split circulation, symmetrically with respect to the ideal central plane of the tube. This circulation, especially fast at high flow rates, has been termed 'secondary flow' by Tijssen [23]; it has the same effect than radial diffusion, thus tending to decrease the dilution or dispersion of the injected plug.

Coiling is qualitatively defined by the relation

λ = coil tube diameter : tube diameter

For $\lambda = 10$, the dispersion is one-fourth of that for the uncoiled tube [7]. It can thus be observed that the smaller the coil diameter, the smaller the dispersion.

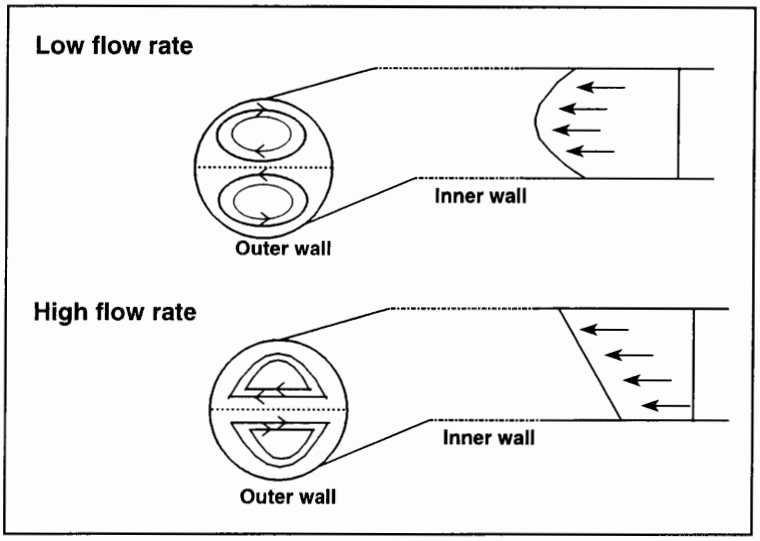

Fig. 2.3 Fluid dynamics corresponding to variations in flow rate.

The coil radius is usually not small enough for this effect to be significant.

2.3.3.2.3 Knitted reactors

If a length of flexible tubing is knotted from end to end, the dispersion is drastically decreased. This may be due to the intensifying of the dispersion-reducing effect introduced by coiling, since in effect the knots are very tight coils.

2.3.3.2.4 Normal packed tubes

The behaviour of packed reactors is well known in chromatography. The ratio

τ = tube diameter : particle diameter

is a useful parameter to describe dispersion. For $5 < \tau < 50$ the axial dispersion is directly related to the particle size: the smaller the particle diameter, the smaller the dispersion.

2.3.3.2.5 Single bead string reactors

The chief effect of the beads is to increase radial dispersion, which reduces the dilution and therefore decreases dispersion.

2.3.4 Influence of chemical reactions on the dispersion

In analogy with conventional flow injection analysis (FIA) [7], the dispersion of the sample zone has to be adjusted to suit the requirement of the intended measurement. Thus, for pH or conductivity measurement, limited dispersion ($D \rightarrow 1$) is required. For reagent-based chemistries such as colorimetry, fluorescence, or chemiluminescence, sample and reagent zones must mix in a suitable proportion and therefore medium dispersion ($D = 2 - 10$) has to be achieved. And for extensive sample dilution large dispersion ($D > 10$) may be necessary.

Although Růžička and Hansen always recognized the limitations of their approach to theoretical modelling with respect to the influence of chemical reactions [8], it was not until 1981 that the kinetic implications of a chemical reaction were included in the theoretical models by Pardue and Fields [9, 10] and Painton and Mottola [11, 12].

Betteridge *et al* [13] took a different approach by developing a model which operates on individual molecules. The so called random walk model was chosen because it is well suited to investigating sample size, chemical kinetics and the combination of reaction rate and physical dispersion. This model successfully predicted many observations made with real flow-injection systems, furthermore, conceptually it is easier than theories based on a series of imaginary tanks [8, 19]. Most important for this investigation into SIA the random walk model suggested that mixing, the fundamental requirement for both FIA and SIA, could take place with no nett displacement of the sample. It is thus possible to have $D > 1$ without traversing a manifold of length, L. This important concept is discussed in more detail in the next paragraphs and is the foundation on which SIA is built.

2.4 From flow injection to sequential injection via the random walk model [2, 5]

Flow injection analysis relies on the injection of a well defined sample zone into a moving carrier stream and the subsequent detection of the signal which has been modulated by a combination of physical and chemical interactions between the analyte and reactive surfaces or reagents. Until recently, this technique relied on a constant monotonous flow rate. A dramatic decrease in reagent consumption and the design of more effective flow-injection systems has resulted from the introduction of flow programming, first as stopped flow, then flow reversal and most recently as sinusoidal flow [1].

The successful operation of any injection analyzer requires that the sample and reagents are brought together, mixed and allowed to react in a perfectly reproducible manner. So as to

obviate the need for frequent recalibration, it is necessary to maintain reproducible flow conditions for extended periods of operation. This has led to the practice of using unidirectional monotonous flow, because as long as a constant flow rate is maintained the sample may be injected into the system at any time. In this way, what happens to one sample happens in exactly the same way to any other sample, regardless of when the sample is injected into the carrier stream. Obviously to fulfil these criteria, strict control of the flow rate must be maintained throughout the entire analysis period.

A theoretical description of the zone dispersion processes in the analyzer channel is a central issue in FIA and, as it is a random process, it can be described by the random walk model. Each molecule in their simulated sample plug is represents by x, y and z co-ordinates constrained within the boundaries of the hypothetical tube in such a fashion as to give a uniform number of molecules per unit volume. The molecules were moved so as to simulate both random dispersion (Δd) and longitudinal transport by laminar flow (Δf). Thus for each cycle, $(x_i, y_i, z_i)_{new} = (x_i, y_i, z_i)_{old} + \Delta d + \Delta f$. Without flow, random dispersion causes the initial rectangular injection to become Gaussian. In the presence of laminar flow, the resultant sample peak become skewed Gaussian as it is frequently observed in flow-injection profiles. The random walk model allows one to view the element of fluid as being displaced during the dispersion process in any direction by a step of fixed length. The direction of the step is determined entirely by chance. If the change of moving in any direction is equal, then the random walk is symmetrical. As all molecules within a said element of fluid cannot be expected to move through the same step of fixed length (their movement is erratic), the length of a fixed step must be taken as the average length of the actual displacement (*viz.*, its square root). Thus, if a large number of molecules start together on a random walk of

many steps, the standard deviation, σ, of the resulting (Gaussian) concentration profile is

$$\sigma = \ell n^{1/2} \qquad \textbf{(19)}$$

where ℓ is the fixed step length and n is the number of steps taken. It is noteworthy that the spread of the zone and resulting degree of mixing with the surrounding carrier stream are proportional to the individual step length, ℓ, which is easy to understand as the final displacement of the molecule from the origin depends on step length in any direction. The final zone displacement increases, however, only with the square root of the number of steps, n, taken. This is to be expected as a cancellation effect must be considered in which the molecule is equally likely to move in the opposite direction to the original replacement. If several random walks occur simultaneously or consecutively, as they do in FIA, the final displacement of any given molecule is determined by the sum of the displacements in all directions. Therefore,

$$\sigma^2 = \ell^2 n_1 + \ell^2 n_2 + \ldots = \sigma_1^2 + \sigma_2^2 + \ldots \qquad \textbf{(20)}$$

so that components of the process (variances, σ^2) are additive.

There are two driving forces which cause the molecules to move and the zone to spread: an internal one which is symmetrical and caused by molecular diffusion, and an external one caused by the flow imposed on the liquid which transport the zone through the system. If the flow is unidirectional and if the molecular diffusion and/or radial mass transfer (caused by coiling or packing the tubing) does not compensate for the asymmetry resulting from

Poiseuille flow, the resulting concentration profile is asymmetric. Consequently, the result of such a random process is asymmetric. The accumulated distance of migration, L, imposed by the flow, can be traversed in many ways, each of which constitutes a different number of random steps depending on the flow geometry. This relationship has been expressed in chromatography by means of the height equivalent to a theoretical plate, $H = \sigma^2/L$, which in fact is a measure of the generation of variance per unit length of a column travelled by the dispersing zone. Clearly the zone spreading increases with the square root of the distance (L) travelled, while separation of the components increases with the number of theoretical plates (N) unidirectionally traversed, and therefore linearly with distance travelled (as $NH = L$ for uniform plate dimension). Resolution, which is the key issue in chromatography, is satisfactory only when the gap between component zones centres become outdistance by zone spreading. This situation happens sooner for lower H values and higher L values. As no separation is achieved otherwise, unidirectional monotonous flow is an absolute condition for chromatography [3].

The use of an unidirectional monotonous flow rate has been the prevailed practice in FIA, which unlike chromatography, does not aim at separation of the analyte components, but rather at their effective chemical conversion into detectional species. Therefore, the key issue in FIA is the reproducible dispersion of the injected zone into the carrier stream and timing of the arrival of the reacted zone at the detector.

The random walk model is useful for visualization of the degree of mixing, since the transition of the original square input, through skewed peaks, and finally to Gaussian-shaped peaks is indicative of the degree of mixing of the reacting species. As it is well known that

the skewness of the peak is due to initial acceleration and is further amplified by Poiseuille flow, the value of the symmetrical random walk is that it leads to the conclusion that efficient mixing of the reacting components can be achieved without actually travelling any nett distance, L. By moving the injected zone forward and back in several steps (n) of sufficient length (ℓ) an efficient mixing of sample zone and carrier stream components may be achieved through a combination of external and internal forces (eqn. 19) (although this movement is not strictly random, the same principles hold). By selecting the step length (ℓ) and number of flow reversals (n), any degree of mixing and desired length of reaction time can be conveniently obtained simply through flow reversal. The need to travel the length of a channel in one direction in classical flow injection systems is only necessary because the sample zone has to be transported from the injector, past a mixing point (where confluence of reagent and sample zone bearing carrier stream occurs), through the reaction coil and detector to waste. Hence, it is the physical size of the system and configuration of its components (pump → injector → confluence point → reactor → detector → waste) which require a nett flow of the carrier stream larger than the minimum volume required by the reacting species. As forward flow is used to promote mutual dispersion of reacting species, the consumption of liquid is mainly determined by the flow channel dimensions and flow rates. The required volume is therefore much larger than if a nett zero flow took place. On the other hand, as flow reversal yields a zero nett flow, a very high linear flow velocity can be imposed on the selected elements of fluid and thus turbulent flow may be achieved if necessary.

Use of a flow pattern, rather than constant monotonous flow, requires synchronization of sample zone injection with the start of each flow cycle. Therefore, a system configuration

must be conceived which will allow sample zone injection, reagent addition, mixing, measurement and ejection of reacted mixture by a combination of forward and reversal flow steps. It follows from the length, duration and speed provided that they always follow the same pattern. There are clearly many possible combinations of the step length (ℓ) and step number (n) and also of the resulting nett flow, yet if the pattern is strictly repeatable in each measuring cycle, the sample zone dispersion, being composed of individual variances, will always be the same (eqn. 20) and so will the reaction time. To achieve an absolute zero nett flow is, of course, not practical. Sample and reagent consumption can however be reduced drastically and the flow system streamlined if mutual dispersion of the sample and reagent zones and detection of the formed reaction products occur within the same section of flow conduit.

2.5 Approach to sequential injection analysis

Homogeneous reactions require reproducible mixing of reactants to allow the chemical reaction to occur. The classical batch approach is to obtain a homogeneous mixture and then either measure the reaction rate or wait until equilibrium has been reached. The flow injection method exploits the formation of reproducible concentration gradients and transient measurement of the resulting products. It is important to note that neither approach is adaptable to sequential injection, where homogeneous mixing of reagents will be attainable by replacing the reactor coil with a mixing chamber and by allowing the chemical reactions to reach equilibrium. This approach is, however, more complex and time consuming than the flow injection mode.

2.6 Basic SI methodology

To explain features such as zone overlap and the influence of sample volume on zone penetration, experiments using a nonreactive blue dye were carried out. The concentration of the nonreactive dye (bromothymol blue, BTB) was 0.02 g.ℓ^{-1} in a 0.01 mol.ℓ^{-1} borax buffer, using water as carrier/wash stream [6]. The absorbance of the BTB solution was measured at 620 nm.

It is at this stage well known that the measuring cycle of the sequential injection (SI) technique (Fig. 2.4) comprises the following operations: (i) aspiration of carrier/wash solution with the selector valve in position 1, while the piston makes a large reverse step, (ii) aspiration of sample solution with the selector valve in position 3, while the piston makes a small reverse step, (iii) aspiration of reagent solution with the valve in position 4, using a small piston reverse step, (iv) a forward piston move with the valve in position 5, with the stroke length adjusted such that a preselected section of the interdispersed sample/reagent zone is injected through the reactor into the detector, (v) a stopped flow period of reaction rate monitoring and (vi) forward large piston stroke, which expels all sample and reagent as well as the majority of the carrier/wash solutions from the valve and from the flow channel. When the chemical reaction is fast and when the peak height is measured rather than reaction rates, step (v) is omitted. If two reagents are used, the optional port 2 and appropriate flow programming is used to introduce the second reagent. When using a peristaltic pump instead of a piston pump step (i) is omitted.

It follows from the foregoing that zone sequencing and mutual dispersion of the zones are the key operations. These have to be carried out in such a manner that a desired degree of penetration of sample and reagent zones will be achieved, within an adequate residence time, while yielding a satisfactory sample frequency.

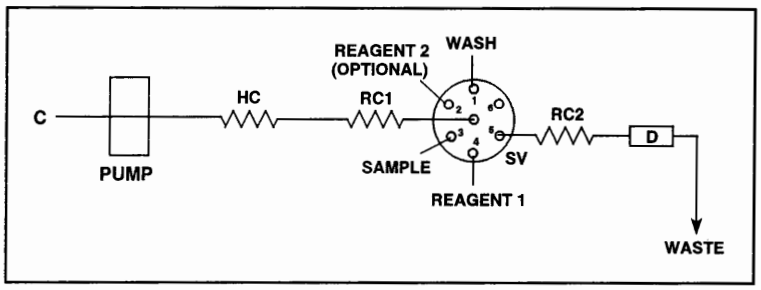

Fig. 2.4 Sequential injection system. HC - holding coil, RC - reaction coil, SV - selection valve, C - carrier and D - detector.

2.7 Zone overlap

Although Růžička and Gübeli [25] stated that 'for a rational design of the sequential injection analyzer, the degree of sample dispersion must be considered as the main design guideline', zone penetration, related to dispersion, is found to be the key parameter, the control of which is essential to a successful execution of sequential injection [6]. The importance of zone penetration can be ascribed to the fact that this influence has a dramatic impact on the surface area over which a concentration gradient exist and therefore over which axial mixing takes place. It follows from the foregoing that, for reagent-based chemistries, a region of mutually interdispersed sample and reagent zones must be identified, within which D_s is larger than 2, and where at the same time sufficient excess of reagent is present. For single reagent chemistries, merging of sample and reagent zones is sufficient, whereas for two reagent

chemistries merging of three sequentially staked zones will be required. Obviously, a parameter describing the degree of mutual zone penetration has to be established in order to identify a time interval within which a meaningful readout, such as peak height or peak area, can be obtained.

In formal analogy with the definition of resolution as used in chromatography, the concept of zone penetration is introduced here (Fig. 2.5). By defining

$$P = 2W_0(W_s + W_r) \qquad (21)$$

a complete zone overlap is obtained for P = 1, zero zone overlap would be at P = 0, and partial zone overlaps will attain values between these two extremes.

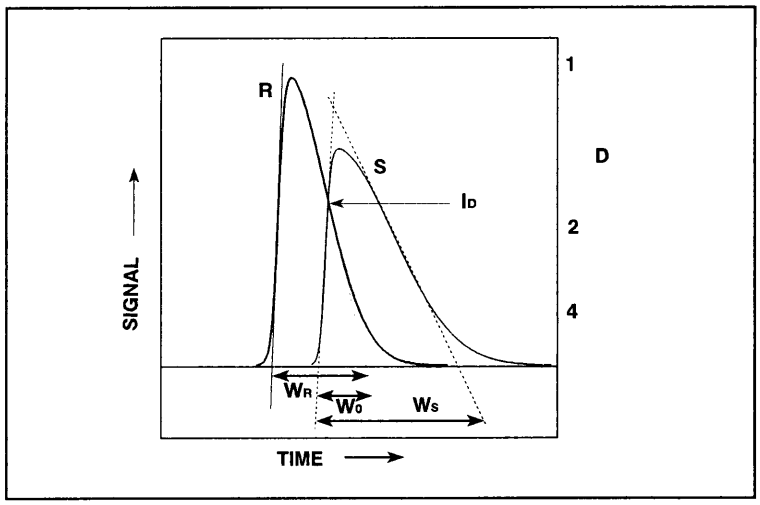

Fig. 2.5 Zone penetration. S - sample zone, R - reagent zone, I_D - isodispersion point, W_R, W_O and W_S are the respective widths of the reagent, overlap and sample zones and D - dispersion coefficient.

It should further be noted that in the absence of complete zone overlap, an isodispersion point, I_D, is observed where the dispersions of the sample and reagent zones are identical. This isodispersion point is independent of concentration. In the element of fluid corresponding to I_D, the ratio of sample and reagent concentrations is the same as their ratio prior to injection ($C_s/C_r = C_s^0/C_r^0$), since they are equally dispersed.

In case of a complete reaction and equal (equivalent) input of sample and reagent concentrations, a maximum of product concentration will be observed at the isodispersion point. If the product is detected, the peak maximum will appear at time, t, of the isodispersion point (I_D). Since C_r^0/C_s^0 is usually much larger than 1 due to an excess of reagent normally used, the position of the peak maximum will move from the I_D point towards the centre of the sample zone. This shift continues until the reagent gradient causes the value of C_r to drop to the point where the equivalent sample concentration exceeds it, and the concentration of the monitored product no longer increases, but decreases. Again, this simplification does not take reaction kinetics into consideration and therefore, the position of I_D along the time axis can serve only as a guide for system design and to estimate how changes of reagent concentration will affect the effective zone overlap and sensitivity of the determination.

Zone penetration was studied as a function of relative volumes of sample and reagent zones [6, 25]. Studies were all made by injecting zones of the same nonreactive dye into a colourless carrier stream in two different experimental runs and by recording separately the injected dye zone as a "sample" and then a "reagent" peak. In this way two concentration profiles were recorded, one for the reagent zone (R) and the other for the sample zone (S),

allowing their mutual overlap to be visualized. In all experiments, the reagent zone was less dispersed than the sample zone, since it was stacked as the second zone and, being closer to the valve, was subjected to less flow reversal and travelled a shorter distance than the sample zone.

It was found by Gübeli *et al* [6] that when increasing zone volumes at equal volume ratios zone overlap decreased from nearly a complete overlap (P = 0.796) to a partial one (P = 0.498). This was the result of a 10-fold increasing in zone volumes. This phenomenon is schematically represented in Figs. 2.6 and 2.7.

It follows from these experiments that when the injected volumes of sample and reagent are increased in the same proportion, above one $S_{1/2}$ value, the increase in peak height is achieved through substantial increase in the consumption of sample, reagent, wash solution and time. It can thus be concluded that a simultaneous increase in sample and reagent volumes above one $S_{1/2}$ value is not an effective way to increase peak height and sensitivity of a measurement.

Complete overlap (Fig. 2.8) results in conditions which are closest to a conventional flow injection technique, as traditionally performed by stream confluence: all elements of the dispersed sample zone are mixed with an adequate amount of reagent solution. At these conditions, peak height and peak area measurements will yield comparable results, and the influence of kinetics of chemical reactions will be minimized.

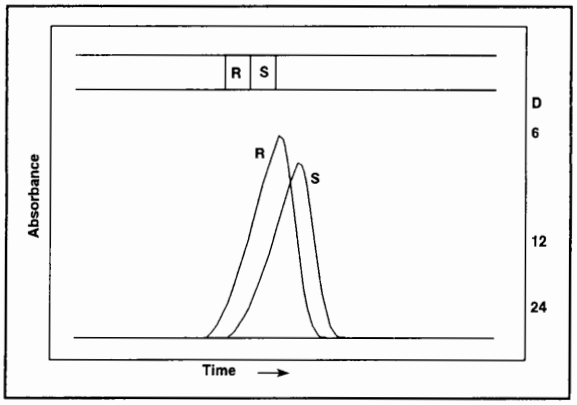

Fig. 2.6 Penetration of sample (S) and reagent (R) zones for $R_v = S_v = 0.25S_{1/2}$.

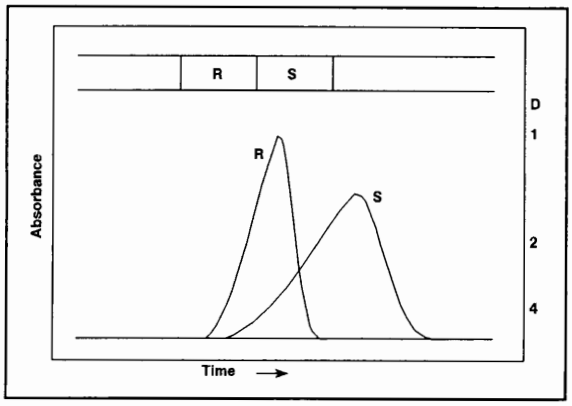

Fig. 2.7 Penetration of sample (S) and reagent (R) zones for $R_v = S_v = 2.5S_{1/2}$.

Partial overlap (Fig. 2.9), having a low P value, yields only a limited range of time slices (situated in front of I_D towards the reagent zone) at which the vertical readout will yield a meaningful result. The part of the response curve past I_D is starved for reagent and the very end of the zone is devoid of it. The peak maximum will be located (in case of complete chemical reactions) within that element of fluid where sample and reagent components are equivalent, and this equivalence of reagent and analyte will make peak height measurements more prone to irreproducibilities caused by flow pulsations or irregularities of the injection process. Yet, the partially overlapped zones offer a wider range of information: not only can analyte readouts be obtained within a desired time span, but a sample blank is also accessible at the tail of the sample zone.

It can be concluded from Figs. 2.8 and 2.9 that injecting at least twice as large reagent zone volume as sample zone volume, while keeping the sample zone less than or equal to 0.5 $S_{1/2}$, the optimum conditions for sequential injection single reagent based chemistry is to be met.

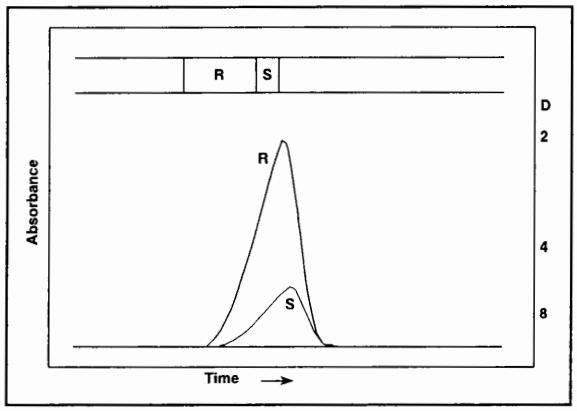

Fig. 2.8 Penetration of sample (S) and larger reagent (R) zone.

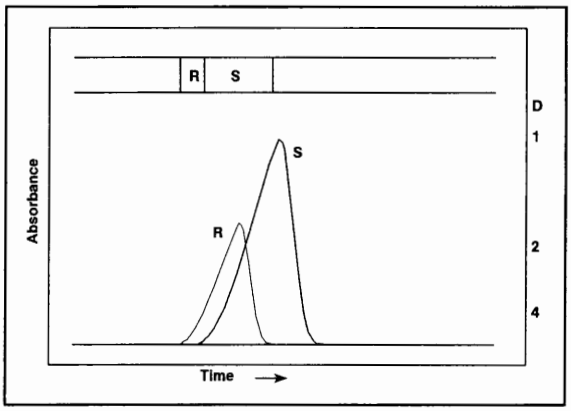

Fig. 2.9 Penetration of sample (S) and smaller reagent (R) zone.

For a chemical reaction to take place, elements of sample fluid must come into intimate contact with elements of reagent fluid. For manifolds where no reaction takes place, zone penetration and band broadening must be kept to minimum. With the emphasis on zone penetration, radial influences should not be overlooked as it is these that ensure contact between the reacting components. In most cases, this is best achieved by mechanical means, but then only once one zone has significantly penetrated the next.

2.8 Three-zone penetration

A third zone can be introduced into the sequential system by two mechanisms [6]: by introducing this zone into the stack of sequenced zones or staking two zones, mixing them, and then add a third zone to the mixture. Obviously, the second mechanism will closely resemble the two zone mixing discussed above.

The same experimental setup as before (2.7 Zone overlap, p 40) was used to illustrate the influence of the third zone on the mixing. Two zones of the nonreactive BTB dye were injected, in equal volumes, into a colourless carrier stream in two different experimental runs and the absorbance of the injected dye zone (first as sample and then as reagent peak) was recorded separately. A "spacer", Sp, representing a third zone, was inserted in the experimental runs as a colourless carrier stream between the sample and the reagent zones. In this way, two concentration profiles were recorded, one for the reagent zone (R) and one for the sample zone (S), allowing their mutual overlap in the presence of a spacer to be visualized. The spacer remains invisible, but its presence is apparent by an increasing gap as the spacer volume increases. Again, in these experiments the sample zone is progressively more dispersed, since it has been stacked behind the increasingly larger zone of spacer, becoming thus subjected to larger flow reversal and travelling a longer distance than the reagent zone. As one would expect, increasing the volume of the spacer zone separates the marginal zones further, causing the outside zone overlap to decrease dramatically from a partial one ($P = 0.571$) (Fig. 2.10a) to a minimized one ($P \rightarrow 0$) (Fig. 2.10b).

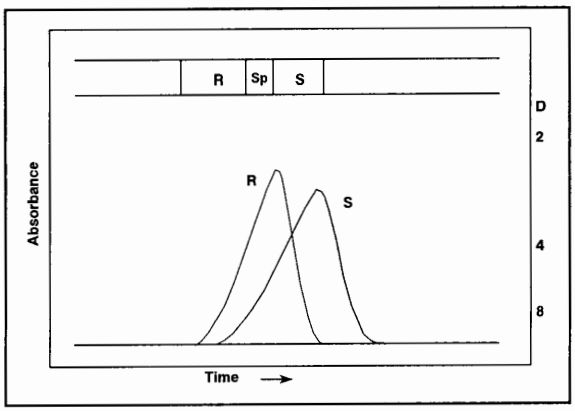

Fig. 10a Penetration of sample (S), reagent (R) and spacer (Sp) zones (P = 0.571).

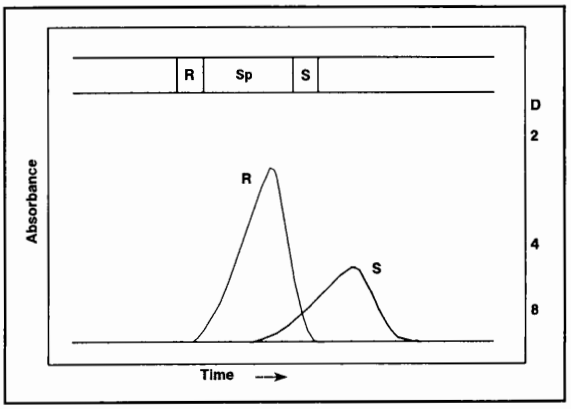

Fig. 2.10b Penetration of sample (S), reagent (R) zones with a large spacer (Sp) zone between the sample and reagent zones (P → 0).

It follows from these experiments that two reagent chemistry (three zones) becomes feasible in the following way. When the sample zone is sequenced in the spacer position and the two complementing reagents are sequenced as R and S zones (Fig. 10a) the sequentially stacked and injected zones will sufficiently overlap to form a product peak which will yield a meaningful readout. The peak maximum will be close to the I_D point, provided that the original concentrations of injected reagents (C_{r1}^0 and C_{r2}^0) are much higher than the concentration of the sample material (C_s^0). Only under these conditions will the sample zone be supplied with sufficient excess of both reagents. Since lack of reagent will affect the peak maximum first, the calibration curve based on peak height measurements will not be linear, while measurement of peak areas may be influenced to a lesser extent. The reagent deficiency, however, may be corrected by increasing the reagent concentrations or by decreasing S_v.

It can be concluded that two-reagent chemistry can be accommodated in the sequential injection system, provided that the sample volume is kept as small as possible (below the $S_{1/2}$

value) and that the concentrations of injected reagents are sufficiently high. The conclusion that the sample zone must be surrounded by the reagent zones [25] is however only partially true. As it is seen from the results in Chapters 4, 5, 7 and 8, the order in which the reagents and sample are injected into the SI system depends very much on the chemistry of the reaction present. This phenomenon is also described in a number of papers [6, 14 - 15]. The authors showed that the order in which the zones are stacked in the holding coil depends on the type of chemistry being utilized. It is however necessary to keep the volume of the "spacer" (middle) zone as small as possible. Increasing the "spacer" volume can however be used to dilute very concentrated samples to the extent of the linear range of the specific determination, as it is described in Chapter 6.

2.9 Flow reversal

It follows from the random walk model that effective mixing is obtained by a suitable combination of a number of steps (reversals), n, of length ℓ. This translates into a relationship between the stroke length, number of flow reversals and reagent zone volumes. Whereas increasing the number of shorter (periodic) pulses will result in increased zone penetration and more thorough mixing, the total stroke volume for the measurement cycle will limit the various volumes in the system to allow an appropriate wash of the sampling conduit, reaction coil and holding conduit.

Flow reversal effectively promotes zone penetration. It is the length of the step, ℓ, which causes zone broadening more effective than the number of steps, n. This can be observed in all the above mentioned experiments where all stacked zones have undergo a single flow

reversal but experienced different step lengths, due to the insertion of spacers and reagent zones of different volumes. It was clear from all the experiments that the sample zone was more dispersed than the reagent zone and this trend increases with the combined length of the imposed step. Gübeli *et al* [6] investigated the effect of the number of flow reversals at a constant step length and zone sequence composition. For this purpose a three zone sequence, similar to that shown in Fig. 2.10a was stacked and then injected into reactor 2 (RC2). The flow was then reversed to return the mixed zones into reactor 1 (RC1) and was reversed again to inject the zones through RC2 into the detector. During this cycle the composite zone experienced three reversals (n = 3). In contrast to previous experiments, the penetration of all three zones was recorded in a single double-humped curve for each cycle (Fig. 2.11). As expected, increasing the number of flow reversals indeed increases mutual zone penetration (P = 0.383 for a single reversal (curve A), while P = 0.738 for five flow reversals (curve C)). The top arrow in Fig. 2.11 indicates the stacking direction, the additional arrows indicate the number of flow reversals and their direction.

It is, however, the first flow reversal and its length which is most effective in providing mutual zone penetration, and since multiple flow reversals increase overall dispersion (and time to complete a measuring cycle) their use will remain restricted for difficult solution handling tasks, such as mixing of zones of very different viscosities.

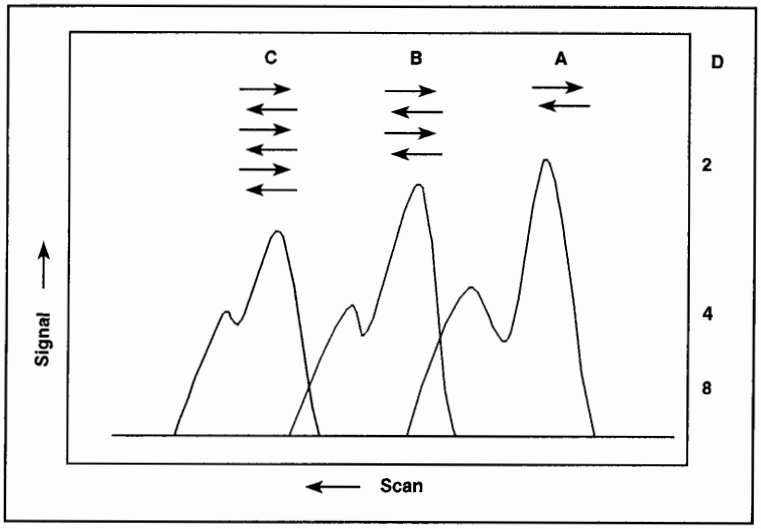

Fig. 2.11 Influence of repeated flow reversals on the mutual penetration of sample and reagent zones.

This is best understood by considering a schematic representation of the dispersion profiles of the zones just before the first zone reversal (Fig. 2.2A). It can be seen that the element of sample fluid with the highest concentration is well placed just prior to the first reversal to penetrate the trailing zone (Fig. 2.2B) in a similar fashion to the leading edge during uptake.

2.10 Sample volume

Selection of the injected sample volume is the main tool for optimizing readout in conventional flow injection and therefore this parameter is considered here as well. The injected sample zone can be viewed originally as a rectangular block input function, transformed during the passage through the flow channel, which is visualized as consisting of a number of mixing stages (N). For a single mixing stage [4]

$$\frac{C^{max}}{C^0} = 1 - \exp\left(\frac{-0.693\ S_v}{S_{1/2}}\right) \qquad (22)$$

where S_v is the injected sample volume and $S_{1/2}$ the volume necessary to reach $D^{max} = 2$. D^{max} is the dispersion in the element of fluid corresponding to the peak maximum. Table 2 shows the injected sample volumes and their corresponding D^{max} values.

TABLE 2. Injected sample volumes and their corresponding D^{max} values

Sample volume	D^{max}
160 $\mu\ell$ (2 s)	2.37
230 $\mu\ell$ (3 s)	1.87
310 $\mu\ell$ (4 s)	1.66
390 $\mu\ell$ (5 s)	1.51
470 $\mu\ell$ (6 s)	1.42
550 $\mu\ell$ (7 s)	1.36
620 $\mu\ell$ (8 s)	1.30

The pumpspeed was 4.70 $m\ell.min^{-1}$. The time the sample was injected is given in brackets. The D^{max} values were calculated as follows: A number of runs using only the carrier/wash solution were recorded to estimate the background value. This was followed by a number of runs using only BTB-dye solution (undispersed). A number of runs injecting the sample zone into the carrier/wash solution were then recorded. Using the equation

$$D^{max} = \frac{h^0}{h^{max}} \qquad (23)$$

where h^0 is the value of the absorbance of the undispersed BTB-dye solution minus the background value ($h^0 = h_{BTB} - h_{background}$) and h^{max} corresponds to the peak maximum. It is clear from Table 2 that the dispersion coefficient decreases with increasing sample volume. D and V_i are inversely proportional to each other ($D = k/V_i$).

For an increasing number of mixing stages, the skewness of the flow injection response curve decreases and at N = 10 approaches a Gaussian shape [6]. Therefore, for large values of N eqn. 22 is replaced by an error function [4], which for $S_v = S_{1/2}$ leads to

$$S_{1/2} = \frac{V_r}{2} \left(\frac{N}{2\pi}\right)^{1/2} \quad \textbf{(24)}$$

where V_r is the reactor volume.

Gübeli *et al* [6] showed that since values of N equal to 1 - 10 described dispersion within a full range of nearly all conceivable flow injection systems, the peak height (C/C^0) increases linear with injected sample volume. More importantly, it follows from eqn. 22 and 24 that $S_{1/2}$ is the parameter which describes dispersion of the zone in any flow injection system, regardless of its geometry and type of flow. This is because the dispersion is tied to the variance, which describes zone broadening, via the N value. Note that

$$\sigma^2 = N\ell^2 \quad \textbf{(25)}$$

where σ^2 is the variance of the peak width, ℓ is the length of the mixing step and N the number of steps [3]. Fig. 2.13 shows that the peak height increases with the injected sample volume, in the same way as described for conventional flow injection. By plotting the maximum absorbance for each peak (A^{max}) against the injected sample volume (S_v), the $S_{1/2}$ value whose ordinate is one-half of the initial absorbance (A^0) can readily be obtained. As predicted by theory (equations 26 and 27) [24], a plot of S_v versus log (1 - A^{max}/A^0) yields a straight line (Fig. 2.12).

$$\frac{A^{max}}{A^0} = 1 - \exp\ (0.693[\frac{S_v}{S_{1/2}}]) \qquad \textbf{(26)}$$

Equation 26 can be rearrange to give

$$-\log(1 - \frac{A^{max}}{A^0}) = \frac{0.693\ S_v}{2.303\ S_{1/2}} \qquad \textbf{(27)}$$

Therefore, the slope of this plot can also be used to calculate $S_{1/2}$.

It may be concluded that changing the injected sample volume is an effective way to change the sensitivity of the measurement (Fig. 2.13). While dilution of concentrated sample material is best achieved by reducing the injected sample volume (see Chapter 6), an increase in sensitivity of the measurement will be possible only when sufficient reagent excess is available in the element of fluid situated at the peak maximum. It is also clear that when large sample and/or reagent zones are used, low overlap figures are obtained (Fig. 2.7). This

demonstrates the uneconomical use of reagent and/or sample, but gives a false impression of the degree of overlap [15].

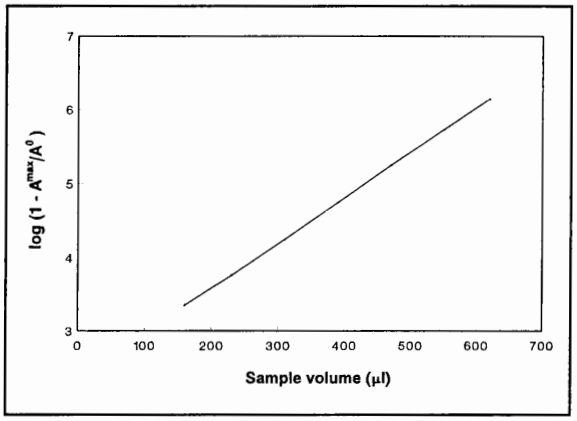

Fig. 2.12 Influence of the injected sample volume on the dispersion coefficient.

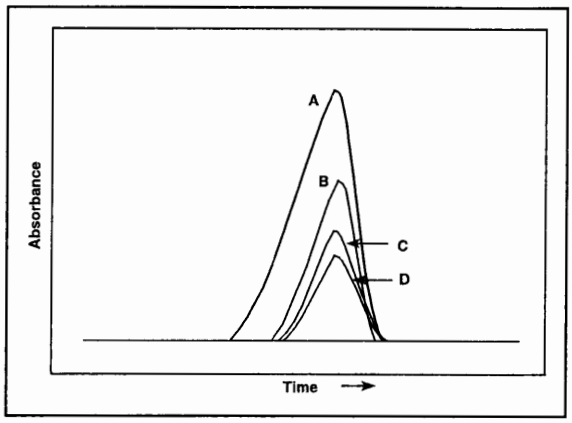

Fig. 2.13 Schematic representation of the influence of injected sample volume on sensitivity (A - 8 $\mu\ell$, B - 24 $\mu\ell$, C - 47 $\mu\ell$ and D - 95 $\mu\ell$).

Once suitable volumes have been established, the reproducibility of dispersion and the residence time in the analyzer can be determined.

2.11 Conclusions

Reproducibility of zone dispersion is a central issue in FIA and is equally important in SIA, although for SIA, a different, though not unrelated parameter, was found to be more useful. For a technique which operates on a stack of well defined sample and reagent zones, the concept of zone penetration was identified as being of fundamental importance. The importance of zone penetration can be ascribed to the fact that this influence has a dramatic impact on the surface area over which a concentration gradient exists and therefore over which axial mixing takes place. It is further established that a region of mutual interdispersed

sample and reagent zones must be identified, within which D_s is larger than 2 and where at the same time sufficient excess of reagent is present. Hence, whereas an adequate excess of reagent exists, even if the original injected concentrations of reagent and sample were equal ($C_A^0 = C_B^0$) an excess of reagent cannot be maintained, owing to insufficient penetration of the reagent zone. Indeed, the leading edge of the sample zone will always remain reagent free and the tailing edge of the reagent zone will remain sample free. An increasing number of flow reversals of sufficient amplitude, ℓ, will eventually lead to compensation of the initial peak skewness and, more important, thorough mixing of sample and reagent at their adjacent interfaces. The concentration gradient obtained by multiple flow reversals is similar to that obtained with unidirectional flow in a flow injection manifold. Although an increasing zone penetration is observed with increasing number of flow reversals, it follows from these injection profiles that a single flow reversal produces a section of mutually penetrated zones, where a reaction product will be monitored with sufficient reproducibility. It also follows that it is futile to increase the sample volume, with a view to increase the peak height, beyond the minimum volume required to ensure adequate zone overlap.

2.12 References

1. J. Růžička, G. D. Marshall and G. D. Christian, **Anal. Chem.**, **62** (1990) 1861.
2. G. D. Marshall, **Sequential-injection Analysis**, PhD-Thesis, University of Pretoria, 1994.
3. J. C. Giddings, **Dynamics of Chromatography**, Marcel Decker, New York, 1965.
4. J. Růžička and E.H. Hansen, **Flow Injection Analysis**, Wiley, New York, 2nd ed., 1988.
5. J. Růžička and G. D. Marshall, **Anal. Chim. Acta.**, **237** (1990) 329.
6. T. Gübeli, G. D. Christian and J. Růžička, **Anal. Chem.**, **63** (1991) 2407.
7. M. Valcarcel and M. D. Luque de Castro, **Flow Injection Analysis - Principles and Applications**, Horwood, Chichester, 1987.
8. J. Růžička and E. H. Hansen, **Anal. Chim. Acta.**, **99** (1978) 37.
9. H. L. Pardue and B. Fields, **Anal. Chim. Acta.**, **124** (1981) 39.
10. H. L. Pardue and B. Fields, **Anal. Chim. Acta.**, **124** (1981) 65.
11. C. C. Painton and H. A. Mottola, **Anal. Chem.**, **53** (1981) 1715.
12. C. C. Painton and H. A. Mottola, **Anal. Chim. Acta.**, **154** (1983) 1.
13. D. Betteridge, C. Z. Marczewski and A. P. Wade, **Anal. Chim. Acta.**, **165** (1984) 227.
14. D. J. Tucker, B. Toivola, C. H. Pollema, J. Růžička and G. D. Christian, **Analyst**, **119** (1994) 975.
15. G. D. Marshall and J. F. van Staden, **Process Control and Quality**, **3** (1992) 251.
16. B. Karlberg, **Anal. Chim. Acta.**, **180** (1986) 16.
17. J. Růžička and E. H. Hansen, **Anal. Chim. Acta.**, **78** (1975) 145.

18. J. Růžička, E. H. Hansen and E. A. Zagatto, **Anal. Chim. Acta.**, **88** (1977) 1.

19. D. Betteridge, **Anal. Chem.**, **50** (1987) 832A.

20. E. Pungor, Z. Fehér, G. Nagy, K. Tóth, G. Horvai and M. Gratzl, **Anal. Chim. Acta.**, **109** (1979) 1.

21. A. U. Ramsing, J. Růžička and E. H. Hansen, **Anal. Chim. Acta.**, **129** (1981) 1.

22. O. Levenspiel and W. H. Smith, **Chem. Eng. Sci.**, **6** (1957) 227.

23. A. Tijssen, **Anal. Chim. Acta.**, **114** (1980) 71.

24. A. Cladera, C. Tomás, E. Gómez, J. M. Estela and V. Cerdà, **Anal. Chim. Acta.**, **302** (1995) 297.

25. J. Růžička and T. Gübeli, **Anal. Chem.**, **63** (1991) 1680.

26. M. Guzman and B. J. Compton, **Talanta**, **40** (12) (1993) 1943.

27. A. Baron, M. Guzman, J. Růžička and G. D. Christian, **Analyst**, **117** (1992) 1839.

CHAPTER 3

Rules that Govern the Design of the Sequential Injection Manifold

3.1 Introduction

Both flow injection (FI) and sequential injection (SI) systems operate on identical underlying principles: sample injection, controlled dispersion and reproducible timing. Therefore, the design of the sequential injection system also follows the established rules [11, 16] for providing limited, medium and high dispersion of the injected sample and reagent zones. As discussed in Chapter 2 the dispersion of sample and reagent(s) have to be carefully considered when developing an assay. Hence, once designed, the SI system, in contrast to the FI system, does not need to be physically reconfigurated, even if the essential parameters such as flow rates, sample and reagent volumes, reactant ratios and reaction times are to be altered. All these changes can be made from a computer keyboard. Therefore, SI may well become the preferred tool for exploratory computer-optimized research into reagent based chemistries.

Whereas many detectors and computers used for current FI applications are suitable for SI, the properties of the software, valves and pumps must be carefully considered. Apart from selectivity, acceptable reproducibility is a key parameter of any instrumental method.

3.2 Instrumental set-up

Figure 3.1 depicts a typical sequential injection instrumental set-up. The manifold consists of the three main components plumbed with narrow-bore tubing. These three components are the pump (peristaltic or syringe pumps are used), the selection valve and the detector.

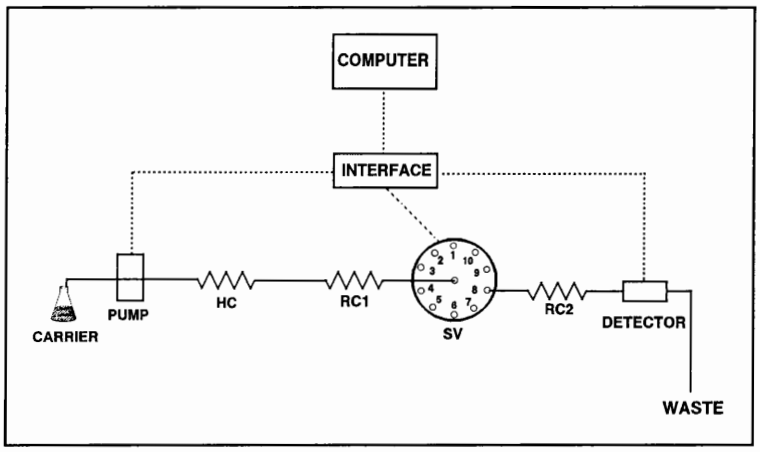

Fig. 3.1 Representation of a typical SI instrumental set-up. HC - holding coil, RC - reaction coil and SV - selection valve.

3.2.1 Pumps

Whereas FI uses a multichannel pump and unidirectional (forward) flow, SI uses a single-channel pump to propel the column of liquid in reverse and forward steps through the channel, which consist of a holding coil, multiposition selection valve and detector. Note that in the SI mode the sampling cycle equals the residence time that the injected zone spends while travelling from the injector throughout the system to the detector. As only one pump is used to propel the composite zone through a tortuous path (resulted from the complexity

of the system) the sampling frequency of SI will always be lower than that of the corresponding FI method.

Sample injection in SI systems depends critically on the reproducible aspiration of small volumes of liquid. As the same drive must also provide efficient washing of the entire flow channel, and as typical SI systems require the wash-to-sample ratio to be as large as 100 : 1, a liquid drive delivering 2 000 $\mu\ell.min^{-1}$ must also be capable of delivering 20 $\mu\ell$ with acceptable reproducibility [1% relative standard deviation (RSD)], which translates into a 1 : 10^4 repeatability of the piston position when piston pumps (Fig. 3.2) are used [1].

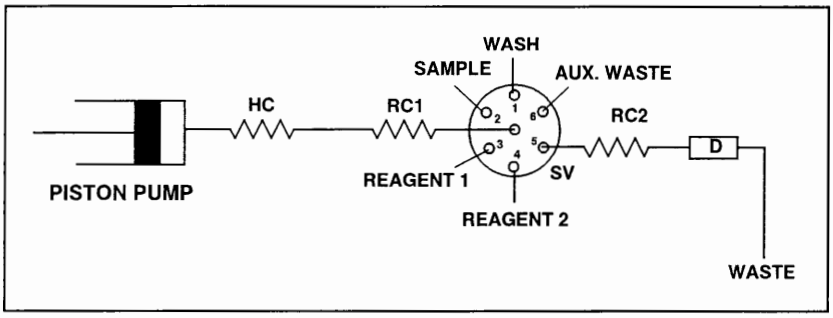

Fig. 3.2 SIA manifold using a piston pump as liquid drive. HC - holding coil, RC - reaction coil, SV - selection valve and D - detector.

As it was doubtful that such stringent requirement would be met by a peristaltic pump (Fig. 3.3) Ivaska and Růžička [1] did a study comparing the performance of a peristaltic pump with that of a piston pump. They found that as the angle of the pump head rotation increases, the reproducibility improves, and when rotation approaches one full (360°) revolution of the pump head to aspire the dye zone, a RSD of 0.5% is reached. Hence the smallest injected volume becomes a function of the tube diameter used. Aspiration of less than one pump head

revolution decreases the reproducibility owing to the random initial positions of the rollers on the pump tubing. Riley *et al* [8] recommended to start sampling with the same roller at the same angle for optimum precision. It is conceivable that by synchronizing the initial roller and belt position the injected volume can be further decreased. It is however questionable if this is a justified direction as with eight rollers on the pump head the use of an angle of a turn smaller than 90° would be questionable. Therefore, decreasing injected volumes is best achieved by using a pump tube of smaller inner diameter.

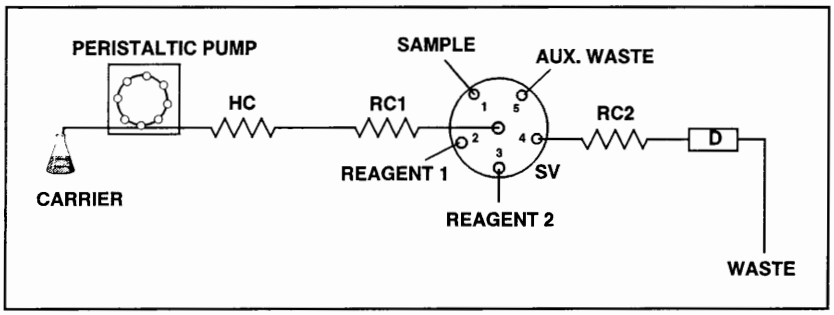

Fig. 3.3 SIA manifold using a peristaltic pump as liquid drive. HC - holding coil, RC - reaction coil, SV - selection valve and D - detector.

It was further found by Ivaska and Růžička [1] that the repeatability of the piston pump is superior to that of the peristaltic pump. This is because initial wear of the elastomer tubing (Tygon and Norprene pump tubing was used) leads to its stretching, which results in a gradual decrease in the flow rate. Fortunately, this initial wear levels off after about ten injections. The thick-walled Norprene tubing is favoured compared to Tygon pump tubing, because the regular Tygon tubing was found to be less stable and durable.

Mechanical stability and durability over prolonged periods are clear advantages of the piston

pump. The sinusoidal flow pump used [2, 3] routinely withstands several months of daily operation without the need of replacing the syringe or piston. In contrast, even the toughest elastomer tubing does not last more than two weeks [1]. Also, when not in use, and being released from the compression belt, tubes tend to contract, thus undergoing a partial recovery and consequently needing secondary restretching for the flow to stabilize fully.

It has been well established that all components of an FI system must be non-elastic, as elements such as air bubbles or unsecured sections of plastic tubing absorb and release mechanical energy, resulting in uncontrolled flow pulsations [1]. Whereas this requirement is less critical for continuous flow techniques, it is imperative for stopped flow FI and SI. The obvious differences between the piston and peristaltic pump propulsion is the way in which the liquid is propelled: the piston and barrel of the syringe pump are rigid, and therefore do not deform during prolonged use. Ivaska and Růžička [1] were surprised to observe that the elastic, deformable peristaltic pump tubing fulfilled the strict requirements set for SI. This is a valuable observation, as there are several advantages to the use of a peristaltic pump for SI: (i) the sampling cycle is considered shorter as there is no need for wash solution aspiration; (ii) the system is easier to configurate and simpler to design, initiate and operate; and (iii) peristaltic pumps are easy to handle and widely available.

In addition, as sequential injection requires only one channel and as the pump propels only pure solvent (usually water), the pump components are not exposed to corrosion, being insulated from the reagent-and-sampling-handling part of the system by a column of water or other inert liquid. Hence, for laboratory and portable instruments, a peristaltic pump is useful even for SI methodology. For process control, where sample frequency and system

versatility are of secondary importance compared with long-term stability and low maintenance, the piston pump will undoubtly remain the preferred liquid drive.

Autoburettes actuated by a stepper motor were used by Cladera *et al* [4] in order to simplify SI operation. In addition to being easier to operate and more widely available, autoburettes have longer lifetimes than peristaltic pump tubing and provide more precise results than PTFE tubes. In addition, an autoburette frees one of the channels of the selection valve as it can be loaded with carrier using its own two-position valve.

Although the piston pump seems to be the preferred pump for SIA in the first few papers published on sequential injection analysis an unique cam-driven pump specially designed for SIA has been used [2, 3, 5 - 7]. This pump generates a variable flow that can be calculated from the equation $Q = 2R\pi^2r^2\nu\sin\alpha$. The flow rate, Q, is therefore dependant upon the radius of the cam, R, the radius of the piston, r, the frequency of the pump in hertz, ν, and the angle of rotation [3]. Throughout this study a Gilson minipuls peristaltic pump (Model M312, Gilson, Villiers-le-Bel, France) was used to propel the zones forward and backwards in the sequential injection manifold.

Included in the specifications for the ideal pump are the following [12]:

(i) robust - able to withstand continual use for extended periods of time with little or no scheduled maintenance,

(ii) all wetted parts must be able to withstand corrosive solutions and organic solvents,

(iii) not prone to blockage,

(iv) be easily controlled using transistor-transistor-logic (TTL) or switch controls (forward, reverse and stop),

(v) device actions should be rapid and without significant inertia,

(vi) flow rates in the range 0.5 to 15 $m\ell.min^{-1}$,

(vii) constant flow rates over extended periods,

(viii) smooth, reproducible and pulseless flow,

(ix) pressures up to 700 kPa,

(x) small and compact in size,

(xi) multiple pumping channels (not necessary for SIA systems),

(xii) the pump should not be adversely affected if it runs dry. It should be self priming,

(xiii) low power consumption, and

(xiv) have the option of inherent safety.

The ability to control the pump speed via an analog input is seen as a desirable thought though not an essential option. In this regard, the option of having a high or normal pump speed may be adequate. A pump which satisfy all of these criteria is still to be developed. It is unlikely that all requirements will be satisfied in a single pump, rather it is expected that a range of pumps will cover the various desired features.

3.2.1.1 Pump tubing

The pump tubes are made of various materials, the properties of which make them suitable for use with a specific range of fluids [11]. Table 1 lists several classes of liquids and

solutions, both organic and inorganic, and the most suitable tubing material with each of them. Attack of the tubing by certain solutions may render it unsuitable for some purposes. For example, PVC, "Solvaflex"™, "Tygon"™ and silicone rubber tubing are not suitable with very acidic solutions or pure organic solvents and "Acidflex"™ tubing are especially unsuitable with ketones.

TABLE 1. Suitable tubing material to use with various organic and inorganic solutions

Classes of liquids and solutions	Tubing materials (Trade names)
Aqueous solutions	PVC, Tygon
Dilute ethanol solutions	PVC, Tygon
Dilute acids and bases	PVC, Tygon
Concentrated acids and bases	Fluoroplasts ("Acidflex" from Technicon)
Alcohols	Modified PVC ("Solvaflex" from Technicon)
Lower alcohols	Silicone rubber
Formaldehyde, acetaldehyde	PVC, Tygon
Acetone	Silicone rubber
Acetic acid and anhydride	Silicone rubber
Aliphatic hydrocarbons	Modified PVC ("Solvaflex" from Technicon)
Aromatic hydrocarbons	Fluoroplasts ("Acidflex" from Technicon)
Chloroform	Fluoroplasts ("Acidflex" from Technicon)
Carbon tetrachloride	Modified PVC ("Solvaflex" from Technicon)

3.2.1.2 Pump speed

In considering the pump speed (when using a piston pump), a measuring cycle may be split into two periods. The first is the period during which the wash solution is drawn up. The second is the period in which the sample and reagent zones are drawn up, one or more flow

reversals are carried out, and the detectable species are expelled through the flow-cell of the detector. The first period lengthen the reaction time and is constituted a disadvantage of SIA compared to FIA. There is no reason why this should not be carried out at a higher speed, provided that the pump will allow this. Future improvement to the pump and controlling software should allow the loading of the wash solution at accelerated speeds without cavitation.

Of greater importance in the consideration of pump speed is the effect of pump speed on back-pressure. At excessively high pump speeds, the back-pressure becomes too high. A balance must be obtained between pump speed, speed of analysis and reagent consumption.

3.2.1.3 Flow rate

Flow rate is, of course, proportional to the pump speed and the range of flow rates employed can be varied by changing the pump speed. The effect of pump speed on zone penetration and sensitivity is discussed below.

The same non-reactive blue dye used in Chapter 2 was used here to illustrate the influence of the flow rate on zone penetration and precision. The blue dye simply reflects the dispersion process taking place in the manifold and does not reflect any chemistry that might occur in a real system. Two measurements were carried out for each variation in flow rate. In the first, the dye was selected first and a buffer solution second. The dye solution represented the sample zone. This sequence was changed for the next measurement (the buffer solution first and the dye solution second). Here the dye solution represented the

reagent zone.

Fig. 3.4 shows that the relative peak height of the sample zone increase with increasing flow rate. The expected decrease in the dispersion of the sample zone is also illustrated. This is in correlation with the Vanderslice's expression, $D = k'q^{1/2}$, where q is the flow rate in $m\ell.min^{-1}$. The dispersion coefficient decreases with increasing flow rate because the residence time decreases, in a non-linear fashion, with increasing flow rate [11]. Fig. 3.5 shows that the same results are obtained for the reagent zone. Note that the sample zone is more dispersed (lower relative peak height) than the reagent zone (Figs. 3.4 and 3.5) and the residence time for the sample is longer than for the reagent zone.

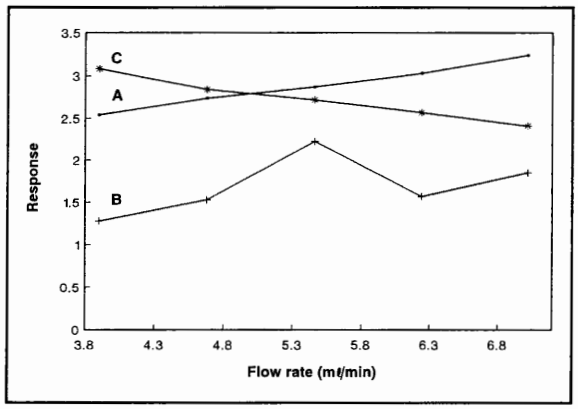

Fig. 3.4 Influence of flow rate on the sample zone (A - relative peak height, B - %RSD and C - D^{max}).

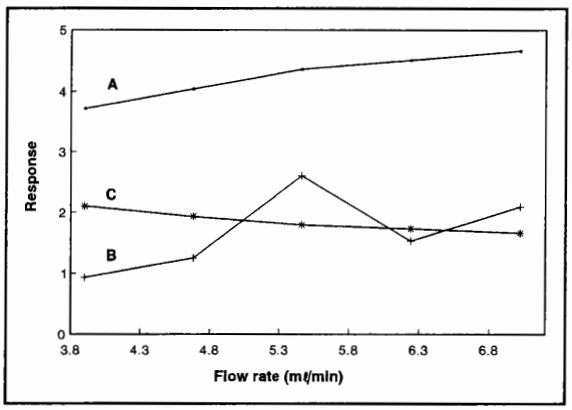

Fig. 3.5 Influence of flow rate on the reagent zone (A - relative peak height, B - %RSD and C - D^{max}).

Fig. 3.6 shows the results of the combination of the sample and reagent peaks, thus the zone overlap (or the relative peak height of the formed "product" zone). These results show the same tendency in relative peak height for increased flow rates and reagent zones. Fig. 3.7 shows the variation in sensitivity and, more importantly, the band broadening due to larger

dispersion at low flow rates of the formed barium sulphate product in the determination of sulphate (Chapter 5). The %RSD showed the same tendency for all three zones (sample, reagent and product) (Figs. 3.4 - 3.6). A slight decrease in precision at 4.0 - 5.5 $m\ell.min^{-1}$ was observed. Flow rates greater than 6.5 $m\ell.min^{-1}$ also showed a decrease in precision.

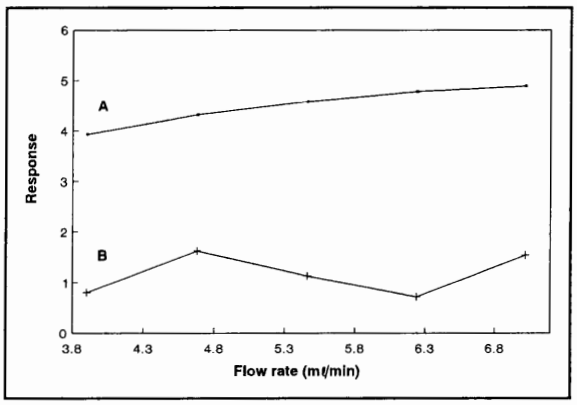

Fig.3.6 Influence of flow rate on zone overlap (A - relative peak height and B - %RSD).

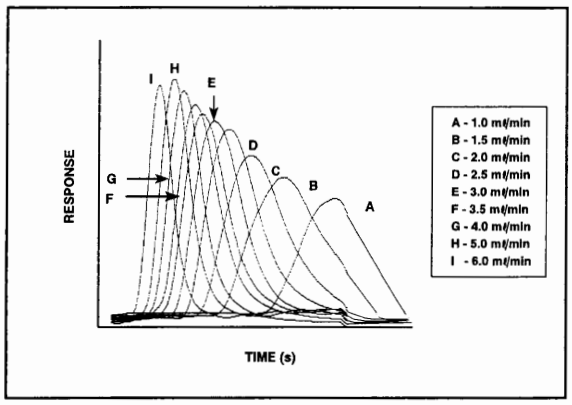

Fig. 3.7 Variation in sensitivity and band broadening due to variation in flow rate.

3.2.1.4 Sample and reagent volumes

Because the sample and reagent volumes are determined by the pump speed and the time the pump is drawing up solution from a selected stream, this section is included here. Theory would suggest that the volume drawn up can be kept constant by adjusting the times for sucking to compensate for the altered pump speed employed. In practice this is not the case. This is probably due to the imperfect flow dynamics of the pump, i.e. start up and stopping are not instantaneous. If a simple inverse ratio of time to pump speed is used, reduced volumes are obtained for higher pump speeds [9].

Gübeli *et al* [10] have conducted an in depth study on the effect of sample and reagent volume on zone penetration and sensitivity. This effects are also discussed in detail in Chapter 2. The conclusions can be summarized in three rules:

1) Changing the injected sample volume is an effective way to change the sensitivity of the measurement. Dilution of concentrated sample material is best achieved by reducing the injected sample volume.

2) Injecting at least twice as large reagent zone volume as sample zone volume, while keeping the volume of the sample zone less than or equal to 0.5 $S_{1/2}$, allows the optimum conditions for single based chemistries to be met. ($S_{1/2}$ is defined as the sample volume that yields a dispersion factor of two in the manifold).

3) Two reagent chemistries can be accommodate provided that the sample volume is kept below the $S_{1/2}$ value, that the sample zone is surrounded by the reagent zones and that the concentration of the injected reagents are sufficiently high.

It is shown in Chapter 2 that greater zone penetration occurs when smaller volumes are used (Figs. 2.6 and 2.7). This is however not that straightforward as it can be seen from Figs. 3.6 and 3.7. The relative peak height of the formed product zone (thus the zone overlap) increase with increasing flow rate. However, the respective volumes of the sample and reagents also increase with increasing flow rate as the time of drawing up these solutions was fixed. It is clear from the results in Chapter 5 that this increase of relative peak height with increasing flow rate is only valid up to 6.0 $m\ell.min^{-1}$ whereafter further increase in flow rate results in

a decrease in relative peak height (Table 3, p 160). Here the increased sample and reagent volumes tend to decrease the dispersion of the respective zones and therefore the zone overlap.

The fact that the injected sample volume is controlled by the time being drawn up is a great advantage of SIA. This results in flexibility in selecting the injected volume, in contrary to valve injection (FIA), where the sample volume can be changed only by reconfiguration of the sample loop.

3.2.2 Selection valve

In contrary to the injection valve used in FIA, a selection valve with 4 - 10 ports is used in SIA. Each of these ports can be connected respectively to the port in the middle of the valve, allowing reagents, samples or products to be propelled, in the correct order, through the manifold. Throughout this study a 10-port electrically actuated valve (Model ECSD10P; Valco Instruments, Houston, TX, USA) was used. Instead of the LOAD and INJECT commands of the injection valve (FIA), the selection valve is moved from one position to another by HOME and STEP commands. These commands can either be given manually or via the computer keyboard.

When the STEP command is given, the valve moves counter clockwise from position 1 to position 2. The valve only moves in one direction. It is therefore necessary to arrange the wash, sample and reagent solutions in an optimum sequence around the valve. In Chapters 4, 7 and 8 two measuring cycles were used on one complete cycle of the 10-port valve. This

was done to utilise the full available capacity of the valve.

When the HOME command is given the valve will go to HOME (position 1). As the valve moves towards HOME it sequences through each position, allowing the possibility that sample may flow briefly as each position is made. Care must be taken to prevent possible sample loss or contamination [15]. It should be emphasized that in order to perform sequential injection successfully, it is necessary to turn the valve only when the flow has been stopped (to avoid pressure build-up and cross-contamination). This is accomplished by including a 1 second stop period while the valve is turned.

Included in the specifications for the ideal valve are the following [12]:

(i) Continuous maintenance free operations for periods of weeks are necessary for process applications.

(ii) Flow paths should have a minimal effect on dispersion.

(iii) Various path options should be available, including dead stop, flow through individual and flow through to common.

(iv) All wetted parts must be resistant to a broad range of solvents and acids. It is unlikely that a single material would be able to satisfy all requirements for inertness and therefore two or three option should be available.

(v) Valve ports should match the dimensions of the flow manifold and should not include torturous paths.

(vi) Remote control via transistor-transistor-logic (TTL) or switch contacts should enable random selection of ports. The ability to sequentially step through ports should also be available. Some means of feed back indicating the present valve

position is required.

(vii) Power requirements should be low enabling the valve to be incorporated in portable systems. It would be desirable to offer a 12 V version.

(viii) Back-pressures of up to 700 kPa must be accommodated. For some applications 2 000 kPa would be desirable.

(ix) Connection to typical 0.5 mm, 0.8 mm and 1.5 mm id tubing should be by means of standard fittings.

(x) An intrinsically safe option would be required for certain applications.

(xi) Physical size should be kept as small as possible.

3.2.3 Detector

There is a dangerous tendency to simply move reliable laboratory detectors onto the process environment. This practice often fails. A superior approach is to develop a whole new range of detectors which are based on proven analytical concepts used in laboratory analyzers. These detectors should be designed with process conditions in mind with a minimum vulnerable parts and required neglible scheduled maintenance. Because these detectors can be configurated for a specific analyte, it is often possible to simplify their design. One of the most important components in any flow injection detector is the flow-cell. Time spent in ensuring a sound design is well spent. In this regard, strong guiding principles are [12]:

(i) minimized dead volume,

(ii) simplify flow paths,

(iii) avoid bubble traps, and

(iv) ensure convenient maintenance schedule.

To date most detectors are single channel devices. The most widely used detectors currently in SIA are those for measuring molecular absorption, i.e. measuring the absorbance of light (radial energy) by a coloured solution. Fluorescence detection was used by Růžička and Gübeli [3] and chemiluminescence detection by Tucker *et al* [14]. Only two papers report use of diode array spectrophotometers [4, 23]. Diode array spectrophotometers (uv, vis and ir regions) and electrode arrays for electrochemical detectors promise to be important detectors in future multi-component analyzers.

The detector can be placed either between the valve and the pump (Fig. 3.8A) or downstream from the selection valve (Fig. 3.8B). In the first published work [2], the detector was placed between the valve and the syringe pump. In this position a double peak results. The first peak is registered when the detectable species passes through the detector on their way to the pump. The second results when these same products, now somewhat more dispersed, are expelled through the detector and valve to waste. An exception to this case, as demonstrated in the first publication [2], occurs when the chemistry is contained within the detector, i.e. the so-called sensor injection.

Subsequent experimentation showed that a more desirable position for the detector is downstream from the valve in the waste line [9]. In this position, the familiar FIA response profile results. Also, and more importantly, the reaction products are moving under positive pressure through the detector. In the former position, the first peak is obtained under negative pressure. The chance of bubbles passing through the detector under these conditions is far greater than in the latter position. Bubble formation occurs when the pressure in the system drops below the partial pressure of the dissolved gasses in the wash/carrier, sample

or reagent solutions. Degassing of these solutions before use will minimize this problem.

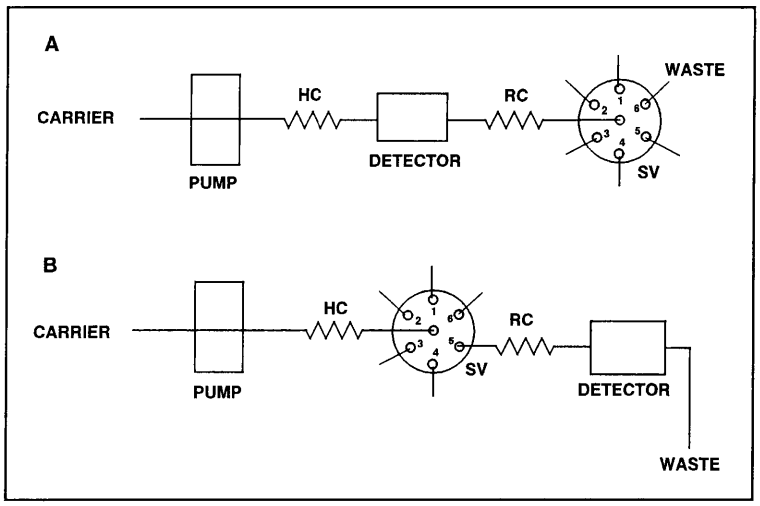

Fig. 3.8 Some variations in manifold arrangements (HC - holding coil, RC - reaction coil and SV - selection valve).

One consideration for the second position is that for half the experiment, the solution in the flow-cell is stationary, while the wash, reagent and sample solutions are drawn up. Usually this has no effect on the detector. An exception is discussed below.

Attention has to be given to avoid sample carry-over from one measurement to the next. The carry-over results from the sample solutions in the short length of tubing between the sampling point or reservoir and the selection valve. Several measurements to overcome this problem have been proposed [3] including the following:

(i) A portion of the wash solution is expelled via the sample line before a fresh sample is drawn up. This method can be used if there is a large reservoir of sample solution.

(ii) A large enough sample volume can be drawn up so that the contaminated

leading aliquot does not come into contact with the reagent during penetration of the reagent zone.

(iii) The contaminated sample zone can be expelled through an auxiliary waste line.

3.2.3.1 Calibration

Most detectors used in flow-based analysis require regular calibration. The mechanical system used should be as simple as possible, probably dependant on a multi-position selection valve. Of greater importance, the calibration algorithms and strategies require careful thought and attention. Some options which should be handled by the controlling software include the ability to [12]:

(i) Interdisperse calibration measurements with sample measurements.

(ii) Average replicate measurements after sensible outlier rejection.

(iii) Select number of calibrants.

(iv) Apply one of several curve fitting algorithms and even multi-variable calibration techniques. This option will become important as there is a move towards multi-element techniques based on detector arrays.

(v) Periodically check the validity of the calibration.

(vi) Ignore calibration if previous calibration is still valid.

(vii) Include statistical measures to establish the goodness of fit of the calibration curve.

3.3 Computerized control and data acquisition

Automated control of FIA manifolds is not mandatory, since many manual systems have been used successfully in a wide variety of applications. This is not the case for SIA. Because the sample and reagent volumes are determined by the time that the pump is drawing up solution from a selected stream, reproducible timing is imperative. This kind of accuracy can only be achieved by microprocessor-based control. This has been identified as a disadvantage of SIA [10], but it can be offset against the simplicity of the manifold, particularly because suitable software and hardware are available.

In the design of a device control and data acquisition system, the main consideration should be versatility. The ability to easily swop devices and detectors and program the device events in a conventional fashion is of paramount importance.

The rate of change of the detector response is such that a rate of 10 sec^{-1} per channel is more than adequate. Some redundancy to allow for statistical smoothing of the data is desirable, though not essential. There is a need to allow for different input voltages from the detector. A reliable amplifier and facility for offset adjustment are quite adequate.

Devices may require either transistor-transistor-logic (TTL) or switch control and both options should be available. Analyzer diagnostic systems often rely on digital inputs. These requirements have been adequately addressed in the FlowTEK™ software package [12, 13] obtainable from MINTEK, Randburg, South Africa.

3.3.1 Data output

While most process control systems have sophisticated calculation capabilities, it is most advantageous to carry out all calculations at the process analyzer itself and only release final concentration data (for samples and where required, calibrants) to the process control system [12].

Using the FlowTEK package, the acquired data are processed to yield peak height, area, time of peak maximum, width at a set height and concentration. These data, as well as the peak profiles, are stored on a suitable medium [9].

The continuum of information can be used in three different ways, best described from the pictorial presentation obtained from the analogue signal [24].

(i) Peak height: Using this procedure and having established a baseline or zero determinant response, calibration and sample values are obtained from an identification of the maximum signal relative to the baseline produced by each standard or sample on its passage through the detector/monitoring system.

Peak height measurements can however be limited by high determinant concentration depleting the reagents to generate a non-linear response. A similar effect can also arise consequent of other chemical reactions occurring during the analytical procedure. It is however, not essential

that peak maximum is used as the reference point of measurement; any point on the rising or falling profiles can be chosen.

Peak height is the most commonly used technique. The precision and accuracy achieved will be affected by the speed of response of the detector to the changes in the flowing stream and extent to which the profiles from such changes have reproducible symmetry.

(ii) Peak area: Having established the baseline or zero determinant response, the area relative to that baseline and enclosed by values produced as each standard or sample passes through the detector/measuring system is obtained. Comparisons are then made as in (i).

Peak area is more dependant upon the flow rate than peak height and suffers the same linearity problems. It offers little advantage and is less commonly used.

(iii) Peak width: Least used and relevant only when the chemistry involved reaches a precise reproducible and identifiable event, i.e. a given redox potential in titrations. It is not necessary for the signal to have a linear relationship with concentration.

The choice of procedure to be adopted for a particular analysis can be at the analyst's discretion, but will be determined by:

(i) the application involved,

(ii) the equipment to be used - all commercial available equipment provide peak height; peak area and peak width are not always available, and

(iii) the accuracy and precision required from the results.

Precision is measured by determining the relative standard deviation (%RSD) of 10 measurements at a given concentration. It is surprising that such good precision is attained in SIA measurements (even when peristaltic pumps are used), since the reaction takes place at an interface with steep concentration gradients. It was stated by Marshall [12] that in experimental work to date, good precision has been obtained if peak height is measured. The peak area and peak width measurements, however, give poorer precision. This observation is confirmed in this study, thus only the results obtained and calculated from peak height measurements are given in the experimental section (Chapters 4 - 8).

3.3.2 Interface board

A general-purpose analog and digital input/output interface board (PC-30B from Eagle Electric, Cape Town, South Africa) was used to interface the computer to the analytical instrumentation. The minimum specifications of this board is set out in Table 2 [12].

TABLE 2. Minimum specifications for the FlowTEK interface board

Specification	
Analog input channels	4 single ended (12 unused by the program) 12-bit resolution Input range (0 - 10 V) Input impedance (> 100 kΩ/100 p) Acquisition rate (3 x 10^4 sec^{-1} variable)
Digital I/O	24 in 3 ports programmable as Input or Output Transistor-transistor-logic (TTL) compatible
Required power	100 mA at ± 5V
PC connection	Uses a fully bussed full length 8-bit slot of an 80 x 86 computer

Facilities are provided for the connection of up to eight user-definable devices (e.g. pumps, valves, on/off switches to digital output points). Four digital input points are configurated to enable a measure of instrumental diagnostics (e.g. to test whether the reagent reservoir is empty) or other diagnostic signals to software. Four analog input ports allow for a maximum of four detectors or other analog devices to be sampled by the FlowTEK program. Fig. 3.1 illustrates the relationship between the computer and analytical apparatus for SIA.

3.4 Manifold dimensions and geometry

3.4.1 Tubing

The tubes, connecting the main components of the SIA system (pump, valve and detector), are made of various materials. In order to achieve an appropriate degree of mixing, without undue carry-over between successive analyses, the tubing is constructed from a non-wettable plastic, often polytetrafluoroethylene (PTFE), and has a bore of about 0.5 mm [24]. The

materials used to make the tubing should be chemically inert and insensitive to temperature change over a broad range of temperatures. Teflon, polyethylene and polypropylene are most commonly used, but they are rather permeable to oxygen. This creates a problem especially when strong reductants are used [11]. Polyethylene tubing readily deteriorates when subjected to temperatures of about 80 °C for a few hours [25].

The length of tubing is dictated by the experimental requirements. Different pieces of tubing are connected to one another as well as to the different components of the system by means of connectors. Particular care should be taken, in making connections, to avoid dead volumes, leakage or the introduction of air bubbles [11].

Tygon and Teflon tubing are commonly used for the holding and reaction coils. Tubing of this kind is relatively inexpensive, readily available and easy flanged for making low dead volume connections. Throughout this study Tygon tubing of various diameters was used.

3.4.2 Effect of tube diameter

Several factors should be born in mind when considering the optimum tube diameter. These include the resultant back-pressure in a length of tubing, the vulnerability to blockage and the degree of radial dispersion attainable.

Smaller diameter tubing gives rise to higher back-pressures. When the pressure in the reverse stroke drops below the partial pressure of the dissolved gasses, bubbles can lead to spurious signals from the detector. The back-pressure is also related to the pump speed, and so for

the smaller diameter tubing, some trade-off against pump speed may be necessary to overcome this problem. When the pump is forced to work under conditions of high back-pressure, it starts to labour, and poor precision results [9].

The narrower the tubing, the more it becomes prone to blockage. With suitable choice of wash solution and adequate sample filtering, this problem can be minimized.

The ratio of the inside surface area to inner diameter of the tubing decreases as the diameter increases. Therefore, the frictional effect of the tubing walls decreases with increasing tube diameter. This reduces axial dispersion and narrow peaks are obtained. This has a negative influence on zone penetration.

3.4.3 Effect of reaction tube geometry

Various geometries have been proposed for reactors consisting of lengths of tubing [11, 16]. As may be expected from what has been observed in FIA, straight tubes result in greater axial dispersion. A coiled reactor gives less axial dispersion and a knitted reactor gives the least axial dispersion. The coil radius is usually not small enough for this effect to be significant. Coiling is therefore merely used to streamline the manifold. Whereas with FIA it was desirable to minimize axial dilution of the injected plug, in SIA axial dispersion promotes zone penetration and straight reactors are therefore more desirable [9].

Of course, once zone penetration has taken place, it is desirable to promote radial mixing in order for the reaction to take place. For this reason, a short length of coiled or knitted coil

just prior to detection is usually incorporated in the manifold [12].

3.4.4 Holding coil

The holding coil should be large enough to prevent the stack of sample and reagents from entering the syringe barrel (when a syringe pump is used) or the pump tubing (in the case of a peristaltic pump). The diameter of the holding coil can also be larger, provided that the reaction products do not penetrate this coil [9]. This prerequisite is necessary because, when the stack of zones enters the pump conduit, deformation of the zones takes place and this results in a decrease in zone penetration, and therefore sensitivity and precision. Another reason is to ensure that organic or other corrosive solvents do not come into contact with the vulnerable pump components. The holding coil used by Růžička and Gübeli [3] had a volume of about 1.4 mℓ. The authors stated that this apparently large volume was needed, since even prior to flow reversal the combined stack of sample and reagents zones, might (due to the parabolic profile of the injected zones) occupy twice as much space as the originally injected volumes.

That the holding coil mainly acts as a reservoir [2, 12], is illustrated in Figs. 3.9 - 3.14. The line length (Fig. 3.9 - 3.11) of the holding coil (after established the required length to prevent the stack of zones from entering the pump conduit) did not have any effect on the sensitivity of the sequential injection system, but did have a influence on the precision of the method. This is clearly visible in Figs. 3.9 and 3.10 that longer tubes resulted in better reproducibility. The same tendency is observed in Figs. 3.12 - 3.14. These figures show that although the tube diameter of the holding coil did not have any influence on the sensitivity,

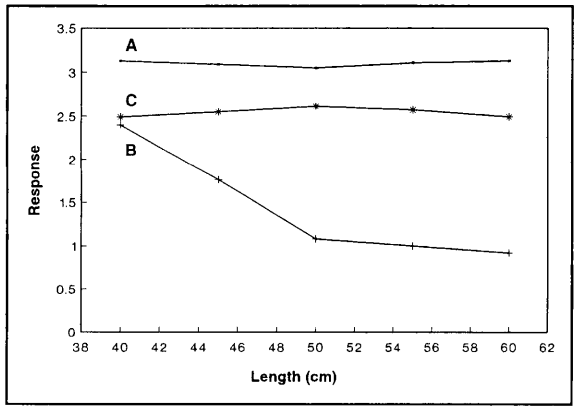

Fig. 3.9 Influence of holding coil length on the sample zone (A - relative peak height, B - %RSD and C - D^{max}).

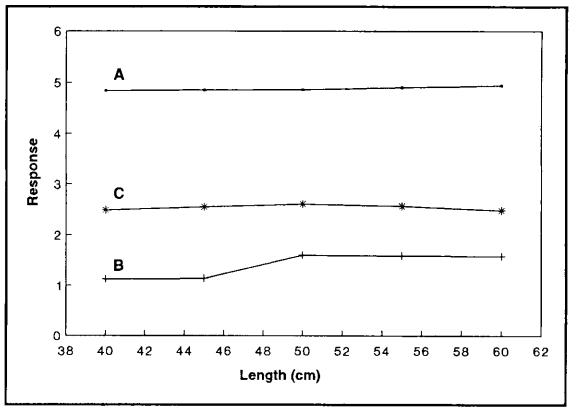

Fig. 3.10 Influence of holding coil length on the reagent zone (A - relative peak height, B - %RSD and C - D^{max}).

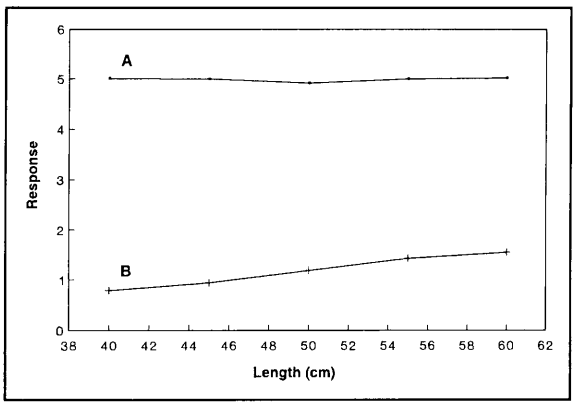

Fig. 3.11 Influence of holding coil length on zone penetration (A - relative peak height and B - %RSD).

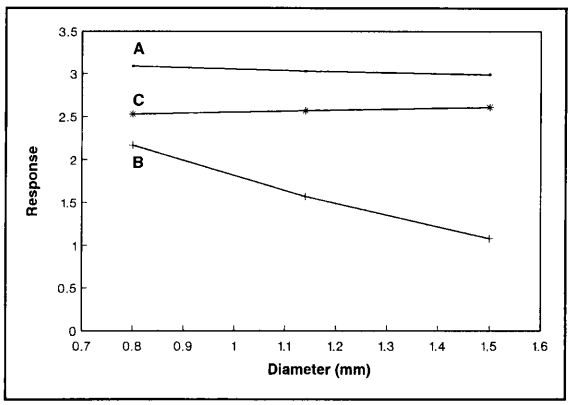

Fig. 3.12 Influence of HC diameter on the sample zone (A - relative peak height, B - %RSD and C - D^{max}).

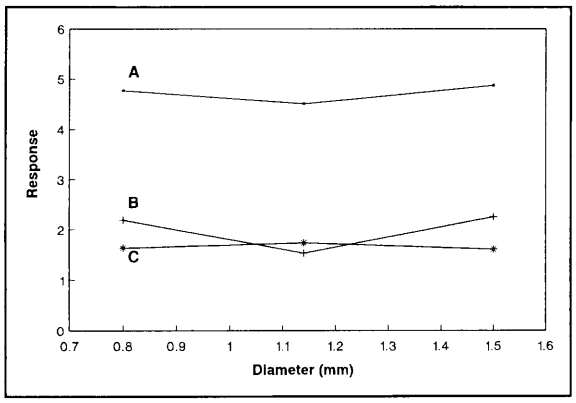

Fig. 3.13 Influence of holding coil diameter on the reagent zone (A - relative peak height, B - %RSD and C - D^{max}).

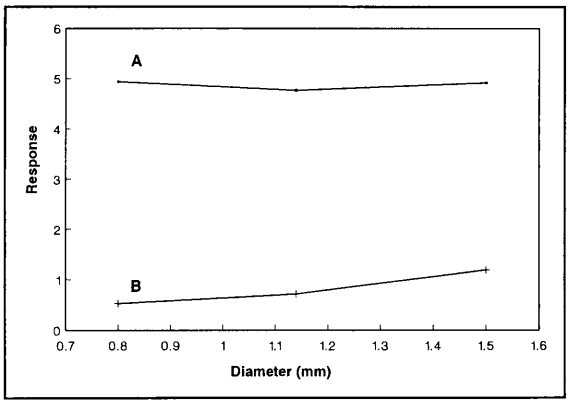

Fig 3.14 Influence of holding coil diameter on zone penetration (A - relative peak height and B - %RSD).

it clearly affects the precision of the method. It can therefore be concluded that larger diameter tubing must be used in construction of the holding coil. Wider tubing results in better axial dispersion which is essential for zone penetration.

Although the holding coil geometry did not have a marked effect on the sensitivity and precision (Table 3) straight coils are usually used, due to their promotion of axial dispersion. An exception is the sorbent extraction used by Marshall [12] where a knitted holding coil was used. This was done because zone penetration was undesirable in the application.

TABLE 3. Influence of holding coil geometry on sensitivity and precision

Configuration	Sample zone		Reagent zone		Product zone	
	RPH*	%RSD	RPH*	%RSD	RPH*	%RSD
Straight	3.38	1.02	4.86	1.48	4.99	4.53
Coiled	3.31	1.32	4.79	1.59	4.84	1.81
Knitted	3.27	1.36	4.64	1.80	4.80	2.07

RPH* - relative peak height

3.4.5 Reaction coils

The reaction coils should not exceed one-third of the wash solution volume, thereby ensuring that the manifold is adequately flushed during each experiment. When using a peristaltic pump this prerequisite falls away, because in methods where peristaltic pumps are used, the step of aspiring wash solution into the system is excluded.

The first reaction coil (RC1) (Figs. 3.1 - 3.3) connects the holding coil with the selection

valve. As the stack of sample and reagent solutions are propelled through reaction coil 1, they penetrate each other to a certain degree depending on the dimensions of the coil [17]. Although some researchers [18 - 22] incorporate this reaction coil in the holding coil (resulting in one long holding coil), the configuration with both a holding coil and reaction coil (RC1) between the pump and valve is frequently used [3, 10, 12, 17]. The reaction coil (RC1) is designed to accommodate the entire reagent zone and the non-cross-contaminated sample zone [3].

According to Figs. 3.16 and 3.17 it is clear that wider tubing is favoured, although the diameter of RC1 did not have a major influence on sensitivity and precision. Contrary to this observation, Fig. 3.15 shows that smaller diameter tubing gave the best results for the sample zone. This is surprisingly, since it would be expected that larger tubing would be favoured due to its promotion of axial dispersion. Shorter reaction coils is favoured for both the sample (Fig. 3.18) and reagent (Fig. 3.19) zones. Figs. 3.18 and 3.20 show that the precision become unacceptably high for tubing longer than 1.0 m. It can therefore be concluded that the major amount of axial dispersion takes place in the holding coil. In the first reaction coil reacting species already starts to interact and less dispersion is necessary.

Three types of tube geometry *viz.* coiled, straight and knitted were studied for reactor 1. The differences in zone penetration (relative peak height) and precision between the coiled and straight reactors were not significant which means that the axial dispersion for samples and reagents was more or less the same for these two geometries. The knitted reactor gave the least desirable sensitivity and precision.

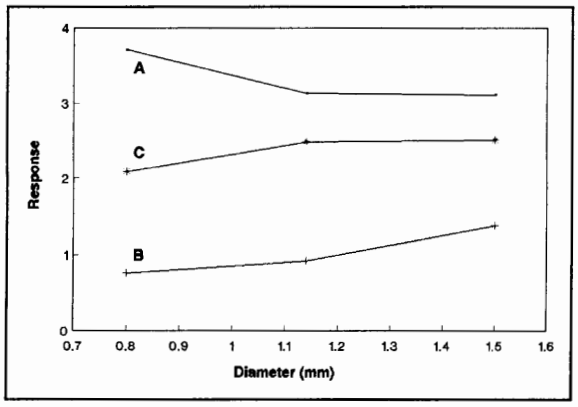

Fig. 3.15 Influence of RC1 diameter on the sample zone (A - relative peak height, B - %RSD and C - D^{max}).

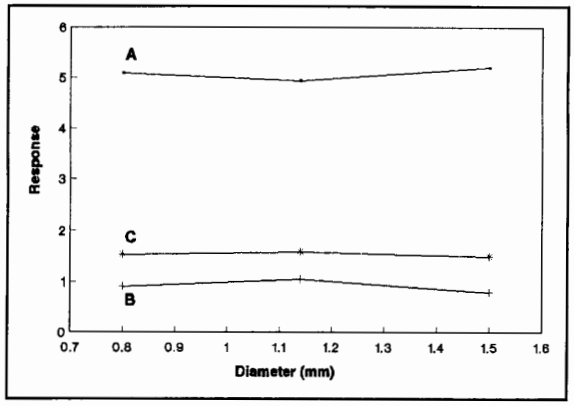

Fig. 3.16 Influence of RC1 diameter on the reagent zone (A - relative peak height, B - %RSD and C - D^{max}).

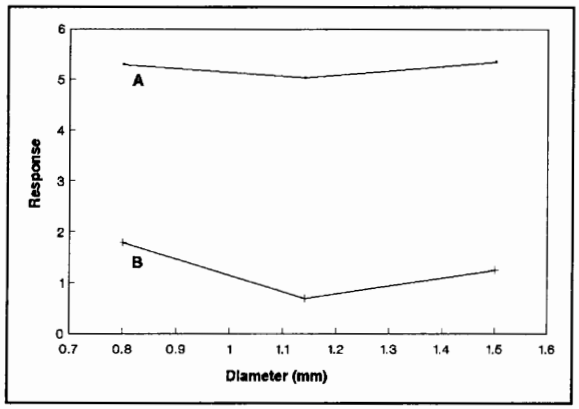

Fig. 3.17 Influence of RC1 diameter on zone penetration (A - relative peak height and B - %RSD).

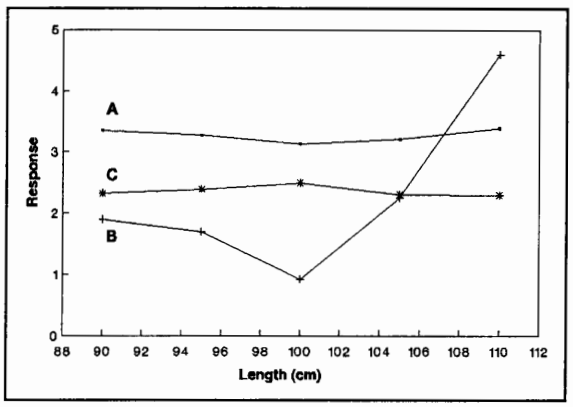

Fig. 3.18 Influence of RC1 length on the sample zone (A -relative peak height, B - %RSD and C - D^{max}).

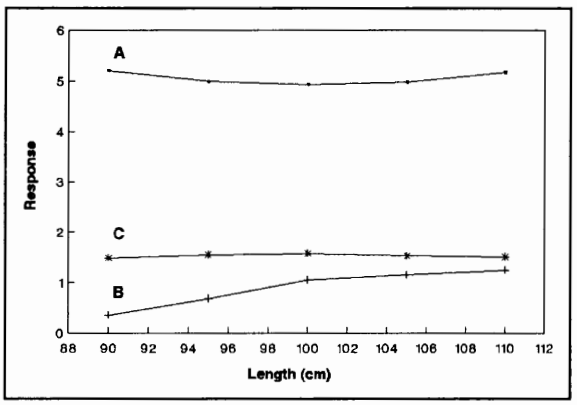

Fig. 3.19 Influence of RC1 length on the reagent zone (A - relative peak height, B - %RSD and C - D^{max}).

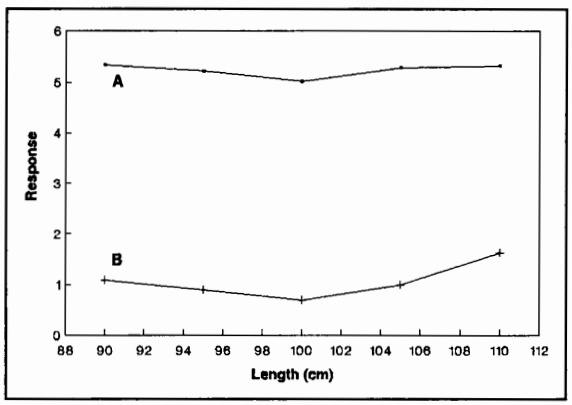

Fig. 3.20 Influence of RC1 length on zone penetration (A - relative peak height and B - %RSD).

The resulting merged zones from the first reaction coil are propelled forward by the peristaltic pump through the second reaction coil (RC2) on route to the flow-cell of the detector. Because this reactor connects the selection valve and detector its minimum length is determined by the physical distance between these two components. The length of this reactor does not have a large influence on the sensitivity of the method. It is however clear from Figs. 3.21 - 3.23 that shorter reaction coils will result in better sensitivity. This is easy to understand, since dispersion increase with increasing reactor length. To prevent unnecessary dilution of the formed product zone, it is best to use shorter lengths of tubing.

It is also feasible to use narrow tubing for the second reaction coil as it can be observed from Figs. 3.24 - 3.26. This is done to prevent axial dispersion and therefore dilution of the product as zone penetration is almost complete when the stack of zones reaches RC2. It is clear from these figures that the precision decreases unacceptably with increasing tube diameter.

For a reaction to take place, radial dispersion is promoted to ensure intimate contact between the reacting species. For this reason, a short length of coiled or knitted coil just prior to detection is usually incorporated in the manifold. A study of three different geometric configurations (straight, coiled and knitted) revealed that there was no significant difference between the respective geometries. This is expected, since the blue dye only reflects the physical dispersion process taking place and does not reflect any chemistry that might occur in a real system.

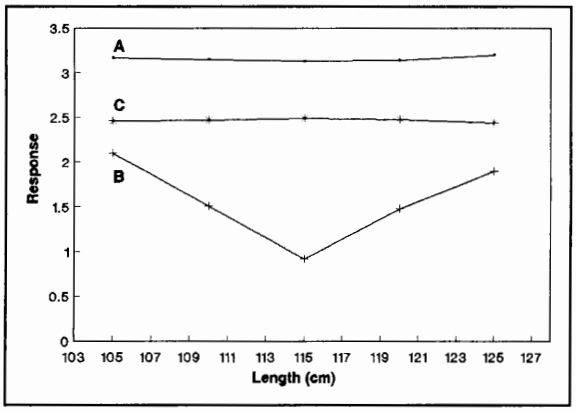

Fig. 3.21 Influence of RC2 length on the sample zone (A - relative peak height, B - %RSD and C D^{max}).

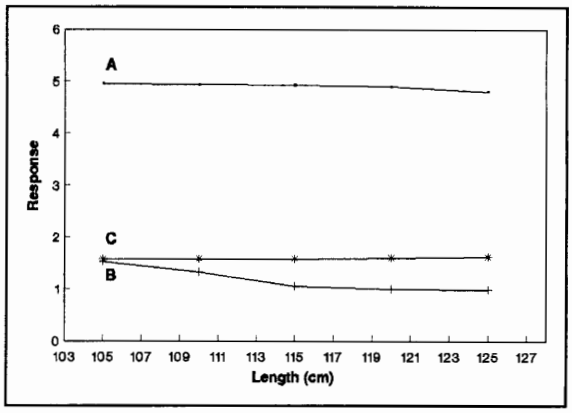

Fig. 3.22 Influence of RC2 length on the reagent zone (A - relative peak height, B - %RSD and C - D^{max}).

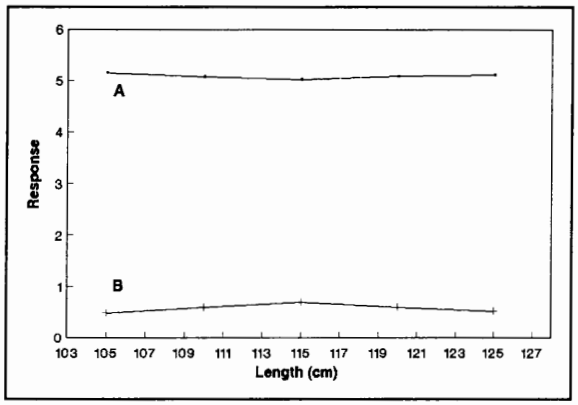

Fig. 3.23 Influence of RC2 length on zone penetration (A - relative peak height and B - %RSD).

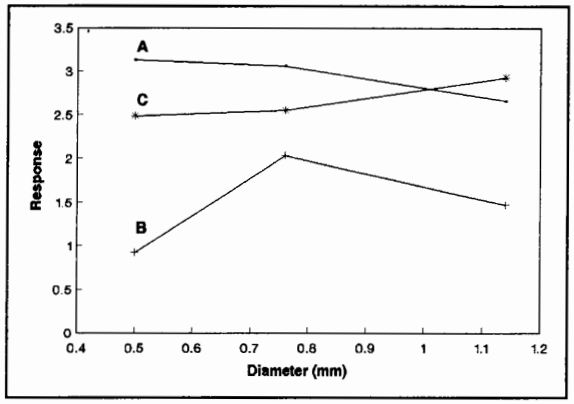

Fig. 3.24 Influence of RC2 diameter on the sample zone (A - relative peak height, B - %RSD and C - D^{max}).

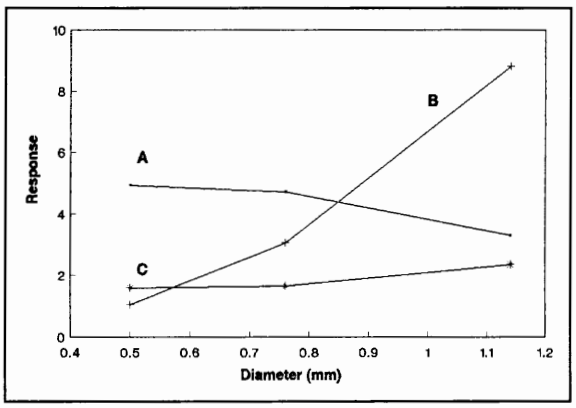

Fig. 3.25 Influence of RC2 diameter on the reagent zone (A - relative peak height, B - %RSD and C - D^{max}).

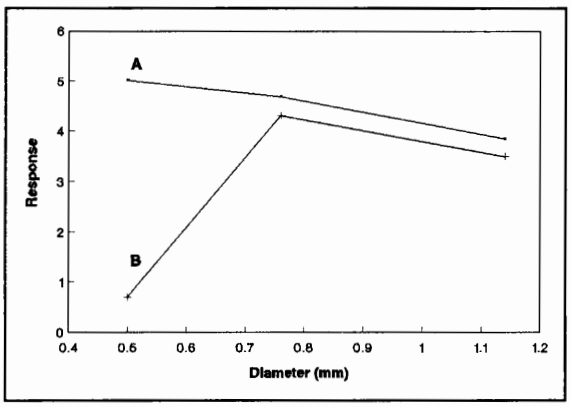

Fig. 3.26 Influence of RC2 diameter on zone penetration (A - relative peak height and B - %RSD).

3.4.6 Up-take tubes

The tubes leading to the selection valve for reagent lines should be as large as possible, in order to minimize the back-pressure caused by narrow tubing. The diameter of the sample line should however be kept to a minimum to reduce problems associated with carry-over.

3.4.7 Order of injection

In double-injection FIA, the order in which the sample and reagent zones are introduced has a minimal effect, as the volumes of the injection loops are usually much less than the system volume. The second zone therefore has a similar distance to travel as the first zone. In SIA, where at least one flow reversal takes place, and zone volumes are of the same order as reactor volumes, this is not the case. The dispersion of the first zone introduced is greater than that of the second. This can be seen in the difference in relative peak heights in Fig. 3.4 and 3.5. One must therefore decide which zone to introduce first. Clearly, the kind of application will dictate the order chosen. This phenomenon is also described in a number of papers [9 - 10, 14, 17]. These authors showed that the order in which the zones are stacked in the holding coil depends on the type of chemistry being utilized.

The following must be born in mind: when sensitivity is important, the reagent, at sufficient high concentration, should be introduced first and allowed to penetrate the sample zone, which will experience minimal dispersion. If buffering of the sample by the wash solution is required, the order must be reversed. If solubility considerations prevent the reagent concentration from being increased, sandwitching of the sample between reagent zones is an

option to be considered [9].

3.5 Housing

Some process analyzers are installed in specially constructed analyzer shelters and then the demands on the analyzer housing are fairly lenient. Where this is not the case, protection from the elements and plant environments is required. Generally, an IP55 coded housing is sufficient. In the choice of the analyzer housing material, careful cognisance of the plant environment is required. This is particularly important in corrosive environments. In explosive environments (Div 1 Class 1) where inherent safe instrumentation is required, it may be necessary to purge the analyzer housing and equipped the door of the housing with a cut off switch that powers the analyzer down when the housing is opened.

3.6 Conclusions

Further steps have been taken towards defining the parameters that affecting the design of the manifold for SIA. Decreasing the tube diameter results in increased back-pressures and prevents the miniaturization of flow conduits. Unlike FIA, where knitted reactors are preferred, in SIA straight reactors allow greater zone penetration through axial dispersion. The optimum arrangement for chemical reaction to occur is obtained by enhancing mixing of the penetrated zone just prior to detection using one or other mechanical means, e.g. a short length of knitted tubing. Pump speed is a complicated parameter to evaluate. This is particularly so when the effect of pump speed on zone penetration is investigated. When a constant-flow pump is used, the evaluation of this parameter is more meaningful. For

sinusoidal flow, the effect of pump speed on the back-pressure can be empirically monitored and optimized. Faster pump speeds are desirable when analysis time are to be minimized. The greater dispersion observed in the first zone selected must be considered in the design of an analysis procedure. Optimum use of the two dispersion patterns will ensure sensitivity and reproducible measurements. Sequential injection has reached the point where a manifold that does not need changing can be designed.

3.7 References

1. A. Ivaska and J. Růžička, **Analyst**, **118** (1993) 885.
2. J. Růžička and G. D. Marshall, **Anal. Chim. Acta.**, **237** (1990) 329.
3. J. Růžička and T. Gübeli, **Anal. Chem.**, **63** (1991) 1680.
4. A. Cladera, C. Tomàs, E. Gómez, J. M. Estela and V. Cerdá, **Anal. Chim. Acta.**, **302** (1995) 297.
5. J. Růžička, **Anal. Chim. Acta.**, **261** (1992) 3.
6. G. D. Christian and J. Růžička, **Anal. Chim. Acta.**, **261** (1992) 11.
7. J. L. P. Pavon, E. R. Gonzalo, G. D. Christian and J. Růžička, **Anal. Chem.**, **64** (1992) 923.
8. C. Riley, B. F. Rocks and R. A. Sherwood, **Anal. Chim. Acta.**, **179** (1986) 69.
9. G. D. Marshall and J. F. van Staden, **Process Control and Quality**, **3** (1992) 251.
10. T. Gübeli, G. D. Christian and J. Růžička, **Anal. Chem.**, **63** (1991) 2407.
11. M. Valcarcel and M. D. Luque de Castro, **Flow Injection Analysis. Principles and Applications**, Horwood, Chichester, 1987.
12. G. D. Marshall, **Sequential-Injection Analysis**, PhD-Thesis, University of Pretoria, 1994.
13. G. D. Marshall and J. F. van Staden, **Anal. Instrum.**, **20** (1992) 79.
14. D. J. Tucker, B. Toivola, C. H. Pollema, J. Růžička and G. D. Christian, **Analyst**, **119** (1994) 975.
15. **Multiposition Electric Actuator Instruction Manual**, Valco Instruments Co. Inc., Houston, TX, USA.
16. J. Růžička and E. H. Hansen, **Flow Injection Analysis**, Wiley, New York, 2nd. ed.,

1988.

17. J. F. van Staden and R. E. Taljaard, **Anal. Chim. Acta.**, In Press.

18. S. M. Sultan, F. E. O. Suliman and B.B. Saad, **Analyst**, **120** (1995) 561.

19. J. Růžička, C. H Pollema and K. M. Scudder, **Anal. Chem.**, **65** (1993) 3566.

20. C. H. Pollema and J. Růžička, **Anal. Chem.**, **66** (1994) 1825.

21. M. Guzman, C. H. Pollema, J. Růžička and G. D. Christian, **Talanta**, **40** (1) (1993) 81.

22. C. H. Pollema and J. Růžička, **Analyst**, **118** (1993) 1235.

23. E. Gómez, C. Tomás, A. Cladera, J. M. Estela and V. Cerdà, **Analyst**, **120** (1995) 1181.

24. **Flow Injection Analysis - An Essay Review and Analytical Methods.** Methods for the Examination of Waters and Associated Materials, HMSO, 1990.

25. H. Kagenow and A. Jensen, **Anal. Chim. Acta.**, **114** (1980) 227.

CHAPTER 4

Determination of Calcium by Sequential Injection Analysis

4.1 Introduction

Compounds of calcium have been known from ancient times though nothing was known of their chemical nature until the seventh century. The Romans used a mortar prepared from sand and lime (obtained by heating limestone, $CaCO_3$), because these lime mortars withstood the moist climate of Italy better than the Egyptian mortars based on partly dehydrated gypsum ($CaSO_4.2\ H_2O$). Gypsum had been used, for example, in the Great Pyramid of Gizech, and all plaster in Tutankhamun's tomb was based on gypsum [1].

Calcium is the fifth most abundant element in the earth's crust and hence the third most abundant metal after Al and Fe. Vast sedimentary deposits of $CaCO_3$, which represent the fossilized remains of earlier marine life, occur over large parts of the earth's surface. The deposits are of two main types - rhombohedral calcite, which is the more common, and orthorhombic aragonite, which sometimes forms in more temporate seas. Representative minerals of the first type are limestone itself, dolomite, marble, chalk and iceland spar. Extensive beds of the aragonite form of $CaCO_3$ make up the Bahamas, the Florida Keys and the Red Sea basin. Corals, sea shells and pearls consist also mainly of $CaCO_3$. Other important minerals are gypsum ($CaSO_4.2\ H_2O$), anhydrite ($CaSO_4$), fluorite (CaF_2: also blue

john and fluorspar) and apatite [$Ca_5(PO_4)_3F$].

Calcium is one of the basic components in many biological and industrial processes and plays a very important role in some pharmaceutical formulations. It also plays a key role in the environment and in surface waters.

4.2 Uses of calcium

Calcium is produced by electrolysis of fused $CaCl_2$ {obtained either as a byproduct of the Solvay process (the ammonia-soda process for Na_2CO_3) or by the action of HCl and $CaCO_3$}. It is less reactive than Sr or Ba, forming a protective oxide-nitride coating in air which enables it to be machined in a lathe or handled by other standard metallurgical techniques. Calcium metal is used mainly as an alloying agent to strengthen Al bearings, to control graphic C in cast iron and to remove Bi from Pb. Chemically it is used as a scavenger in the steel industry, to remove N_2 from argon and as a reducing agent in the production of other metals such as Cr, Zr, Th and U. Calcium also reacts directly with H_2 to give CaH_2, which is a useful source of H_2. World production of the metal is probably of the order of 1000 tonnes per year [1].

Lime is the largest tonnage chemical used in the treatment of potable and industrial water supplies. In conjunction with aluminium or iron salts it is used to coagulate suspended solids and remove turbidity. It is also used in water softening to remove temporary (bicarbonate) hardness. Typical reactions are:

$$Ca(HCO_3)_2 + Ca(OH)_2 \rightarrow 2\ CaCO_3\downarrow + 2\ H_2O$$

$$Mg(HCO_3)_2 + Ca(OH)_2 \rightarrow MgCO_3\downarrow + CaCO_3\downarrow + 2\ H_2O$$

$$MgCO_3 + Ca(OH)_2 \rightarrow Mg(OH)_2\downarrow + CaCO_3\downarrow$$

The neutralization of acid waters (and industrial wastes) and the maintenance of optimum pH for the biological oxidation of sewage are further applications.

The chemical industry uses lime in the manufacture of calcium carbide (for acetylene), cyanamide and numerous other chemicals. Glass manufacturing is also a major consumer, most common glasses having ~ 12% CaO in their formulation. The insecticide calcium arsenate, obtained by neutralizing arsenic acid with lime, is much used for controlling the cotton boll weevil, codling moth, tobacco worm and Colorado potato beetle. Lime-sulphur sprays and Bordeaux mixtures [($CuSO_4$/$Ca(OH)_2$] are important fungicides [1].

The paper and pulp industries consume large quantities of $Ca(OH)_2$ and precipitated (as distinct from naturally occurring) $CaCO_3$. The manufacture of high quality paper involves the extensive use of specially precipitated $CaCO_3$. This is formed by calcining limestone and collecting the CO_2 and CaO separately; the latter is then hydrated and recarbonated to give the desired product. $CaCO_3$ adds brightness, opacity, ink receptivity and smoothness to paper.

Because of stricter environmental requirements, paper mills are forced to recirculate their white water. This inevitably results in increased concentrations of dissolved and colloidal substances (DCS) in the water system. In integrated mechanical pulp and paper mills DCS

in the white water system originate mainly from the wood material used in the mechanical pulping process. DCS also include simple electrolytes such as Ca^{2+}, originating from the wood material, fillers (e.g., $CaCO_3$) and gypsum coated paper returned for repulping. The anions of soaps of fatty or resin acids, also found in DCS, exist as insoluble protonated acids in the acidic pH range. In neutral paper making processes, pH 7.0 - 7.5, these anions together with free calcium ions can give rise to deposits of sticky and insoluble metal soaps. These deposits have negative effects on both paper quality and the running of the paper machine. Due to these harmful effects, monitoring of calcium in white water is of interest [11].

Domestic and pharmaceutical uses of precipitated $CaCO_3$ include its direct use as an anti-acid, a mild abrasive in toothpastes, a source of Ca enrichments in diets, a constituent of chewing gum and a filler in cosmetics. Analysis of calcium in blood plasma, urine and tissue is routinely done in most hospitals and clinical laboratories.

In the dairy industry $CaCO_3$ finds many uses. Lime is often added to cream when separated from whole milk, in order to reduce its acidity prior to pasteurization and conversion to butter. The skimmed milk is then acidified to separate casein which is mixed with lime to produce calcium caseinate glue [1].

Likewise the sugar industry relies heavily on lime to precipitate calcium sucrate which permits purification from phosphatic and organic impurities [1].

4.3 Atomic and physical properties of calcium

Calcium is a silvery white, lustrous and relative soft metal. Tables 1 and 2 highlighted some of the atomic and physical properties of calcium [1].

TABLE 1. Atomic properties of calcium

Property	
Atomic number	20
Number of naturally occurring isotopes	6
Atomic weight	40.08 $g.mol^{-1}$
Electronic configuration	$[Ar]4s^2$
Ionization energies	589.6 $kJ.mol^{-1}$ 1145 $kJ.mol^{-1}$
Metal radius	197 pm
Ionic radius	100 pm
E^0 for $M^{2+}_{(aq)} + 2\ e^- \rightarrow M_{(s)}$	-2.87 V

TABLE 2. Physical properties of calcium

Property	
Melting point	839 °C
Boiling point	1497 °C
Density (20 °C)	1.55 $g.cm^{-3}$
$\triangle H_{fus}$	8.6 $kJ.mol^{-1}$
$\triangle H_{vap}$	155 $kJ.mol^{-1}$
Electronic resistivity (20 °C)	3.5 μohm.cm

4.4 Compounds

The predominant divalence of calcium can be interpreted in terms of its electronic configuration, ionization energies and size (Table 1). Further ionization to give simple salts of stoichiometry MX_3 is precluded by the magnitude of the ionization energy involved. The third stage ionization energy for calcium being 4 910 $kJ.mol^{-1}$.

Reasons for the absence of univalent compounds MX are less obvious. The first stage ionization energy for Ca is similar to that of Li (520.1 $kJ.mol^{-1}$) though the larger size of the hypothetical univalent ion, when compared to Li, would reduce the lattice energy somewhat. By making plausible assumptions about the ionic radius and structure the approximate enthalpy of formation of such compounds can be estimated and they are predicted to be stable with respect to the constituent elements. The non-existence of the univalent MX compounds is related to the much higher enthalpy of formation of the conventional MX_2 compounds, which leads to rapid and complete disproportionation [1].

4.5 Choice of analytical method

The following reagents are employed for detection and determination of calcium (Table 3) [2].

TABLE 3. Reagents and methods for detection and determination of calcium

Reagent	Method
Glyoxal bis(2-hydroxyanil)	Photometry
8-Hydroxyquinoline/n-butylamine	Photometry, separation
(Ethylenedinitrilo)tetraacetic acid disodium salt (Titriplex III)	Titrimetric analysis
Calcein (2,7-bis[bis(carboxymethylaminomethyl]fluorescein)	Photometry
Chloranilic acid (3,6-dichloro-2,5-dihydroxy-p-benzoquinone)	Photometry
Eriochrome black T	Photometry
Nuclear fast red	Qualitative detection
Murexide (ammonium purpurate)	Photometry

None of the above mentioned methods are automated and it seems very difficult to automate these methods since they involve several extractions and precipitation reactions (Chloranilic acid method). The latter method is unfavourable for automatization due to the possibility of blocking the system.

Using the chromogenic reagent 4-(2-pyridylazo)resorcinol (PAR), Gómez *et al* [3] determined Ca and Mg simultaneously with SIA. This reaction was previously used in batch [4] and FI methods [5] for the determination of the two alkaline earth metals in drinking and waste waters. This method is, however, not used in this study due to the severe interference of magnesium.

Calcium can be determined indirectly by using sodium phosphate solution. Calcium is separated from the sample solution as calcium oxalate and the oxalate is subsequently converted to calcium phosphate by reaction with sodium phosphate. The precipitate of

calcium phosphate is dissolved and the phosphate content of the resulting solution is determined. From this phosphate value the corresponding calcium concentration is calculated [19].

In 1960 a paper by Close and West [20] was published describing the synthesis, properties and some of the applications of a new reagent which is specific for calcium within the alkaline earth group. In strong alkaline solutions, pH 13, only calcium forms a coloured product with the reagent, *cyclo*-tris-7-(1-azo-8-hydroxynaphthalene-3:6-disulphonic acid) (Calcichrome). Neither magnesium nor the other two alkaline earths give a colour reaction with Calcichrome.

The metallochromic reagent 3,3'-dimethyl-5,5'-[N,N-di(carboxymethyl)aminomethyl]-phenolphthalein (o-cresolphthalein complexone CPC, metalphthalein, phthalein purpur or methylphthalexon) can be used in the determination of Ca^{2+}. Calcium and o-cresolphthalein complexone form a pink complex, with an absorbance maximum at 580 nm.

4.6 Principle of the reaction between calcium and CPC

The spectrophotometric method for the determination of calcium is based on the fast complexometric reaction between calcium as metal ion and cresolphthalein complexone (CPC) as metallochromic indicator using the correct pH conditions. Cresolphthalein complexone forms $Ca(CPC)^{4-}$, $CaH(CPC)^{3-}$ and $Ca_2(CPC)^{2-}$ complexes with Ca^{2+} (or Mg^{2+}) [6]. A weak absorbing complex $H_2(CPC)^{4-}$ is also formed. The concentration of these species is a function of pH, metal ion concentration and ionic surroundings (Fig. 4.1). The colour

formed by the CPC complex is the result of the formation of a lactone ring in the phthalein molecule.

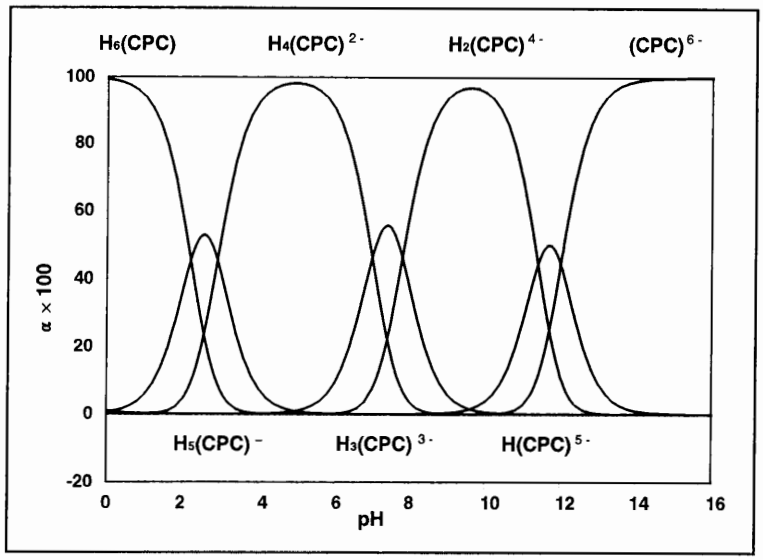

Fig. 4.1 The percentage of each ionic form of CPC present at different pH values.

The structural formula of CPC is shown in Fig. 4.2. It can be seen from this that the molecule might be expected to bind up to two metal ions per molecule via the two iminodiacetate groups. It would be anticipated that the nature of the bonding would be similar to that of the calcium-EDTA complex. This has been classically represented as six co-ordinate [22], the hexadentate EDTA ligand occupying all six metal co-ordination sites. Whilst this appears to be true for the complexes of smaller cations, such as cobalt, calcium is a relatively large ion (radius 100 pm compared with 71 pm for cobalt) and it is likely that it has a co-ordination number greater than six in this type of complex. X-ray crystallography of Ca[CaEDTA].7 H_2O has demonstrated that the chelated calcium is eight co-ordinated [23], the co-ordination sites not occupied by EDTA being filled by water molecules. From this it

is postulated that the calcium ion in the calcium-CPC complex is also eight co-ordinated.

When a calcium ion is bound by the iminodiacetate group, co-ordination can occur between the metal and two carboxylic oxygen atoms, the imino nitrogen and the phenolic oxygen. The interaction between the calcium ion and these atoms would be mainly electrostatic, so not disturbing any delocalisation in the electronic structure of the ligand system. It is known that when a calcium ion interacts with ligands containing ionisable hydrogen atoms it enhances their acidity; this is clearly shown by the marked fall in pH when a calcium salt is added to a neutral aqueous solution. The pK_a of water bounded to the calcium ion has been found to be 12.85 [24], indicating that the effect of the ion is to increase the acidity of the water by a factor of 14. The situation in the reagent mixture used in calcium analyses is such that when the calcium co-ordinates to the CPC it increases the acidity of the last two ionisable protons, causing their ionisation and the development of colour due to the generation of the extensively delocalised chromophore.

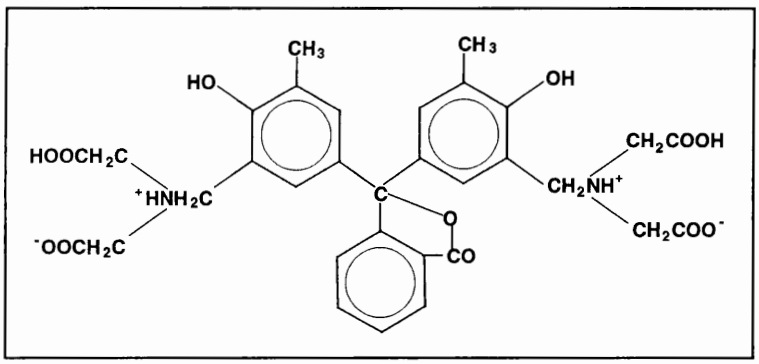

Fig. 4.2 The structural formula of CPC.

Representing the CPC molecule as H_6Z, the type of equilibria involved would be:

$$Ca(H_2O)_8^{2+} + H_2Z^{4-} \rightleftharpoons CaH_2Z(H_2O)_2^{2-} + 6\ H_2O,$$

with the ionisation of the compound so formed:

$$CaH_2Z(H_2O)_2^{2-} \rightleftharpoons CaHZ(H_2O)_2^{3-} + H^+_{(aq)}.$$

A further reaction could then occur between this complex and a second calcium ion:

$$Ca(H_2O)_8^{2+} + CaHZ(H_2O)_2^{3-} \rightleftharpoons Ca_2HZ(H_2O)_4^{-} + 6\ H_2O,$$

with subsequent ionisation to:

$$Ca_2HZ(H_2O)_4^{-} \rightleftharpoons Ca_2Z(H_2O)_4^{2-} + H^+_{(aq)}.$$

Anderegg *et al* [10] postulated that the formation of the coloured complex only occurred on binding of the second calcium ion, in the same way that full colour development of phenolphthalein only occurs on ionisation of the second phenolic hydrogen atom and formation of a quinoid structure. However, the HZ^{5-} ion is pale pink in colour, which implies that the $CaHZ(H_2O)_2^{3-}$ ion may also be coloured, although the $Ca_2Z(H_2O)_4^{2-}$ ion would be expected to be the major chromophore.

4.7 The determination of calcium with sequential injection analysis (SIA)

4.7.1 Experimental

4.7.1.1 Reagents and solutions

All reagents were prepared from analytical-reagent grade unless specified otherwise. All aqueous solutions were prepared with doubly distilled deionised water. All solutions were degassed before measurements with a vacuum pump system.

A stock standard calcium solution containing 1 000 mg.ℓ^{-1} was prepared as follows. 2.4980 g of calcium carbonate was carefully dissolved in approximately 0.50 mol.ℓ^{-1} hydrochloric acid solution by adding the hydrochloric acid dropwise until all of the calcium has just dissolved. The solution was carefully boiled for a few minutes in order to remove carbon dioxide. The calcium solution was neutralise with approximately 0.10 mol.ℓ^{-1} sodium hydroxide solution, adjusting the pH to about 6. The solution was diluted to 1 ℓ. Working standard calcium solutions were prepared by suitable dilution of the stock solution.

The cresolphthalein complexone reagent (CPC) was prepared by dissolving 0.10 g of cresolphthalein complexone, obtained from BDH, in 40 mℓ of 5.0 mol.ℓ^{-1} hydrochloric acid. 2.0 g of quinolin-8-ol was added and dissolved. The solution was quantitatively diluted to 2 ℓ with distilled water and filtered. The final solution was diluted to 50% (v/v) before used.

The 2-amino-2-methylpropan-1-ol (AMP) buffer solution was prepared by dissolving 140 g of 2-amino-2-methylpropan-1-ol in approximately 900 mℓ of distilled water. The pH of the solution was adjusted to 10.5 with diluted hydrochloric acid and the solution quantitatively diluted to 1 ℓ.

4.7.1.2 Apparatus

The sequential injection system depicted in Fig. 4.3 was constructed from the following components: a Gilson minipuls peristaltic pump; a 10-port electrically actuated selection valve (Model ECSD10P; Valco Instruments, Houston, TX, USA); and a Unicam 8625 UV-visible spectrophotometer equipped with a 10-mm Hellma type flow-through cell (volume: 80 μℓ) for absorbance measurements. The calcium-cresolphthalein complexone complex formed, was monitored by measuring the absorbance at 573 nm. Data acquisition and device control were achieved using a PC30-B interface board (Eagle Electric, Cape Town, South Africa) and an assembled distribution board (MINTEK, Randburg, South Africa). The *FlowTEK* [7] software package (obtainable from MINTEK, Randburg, South Africa) for computer-aided flow-analysis was used throughout for device control and data acquisition. Tygon tubing was used for the holding and reaction coils.

A Varian AA-1275 flame atomic absorption spectrometer was used as detector to compare the results obtained with the proposed sequential injection system. A Varian calcium hollow-cathode lamp, with a current of 3 mA, was used to give a monochromatic light ray in the detector. A wavelength of 422.7 nm and a 0.2 mm slit width was used. An N_2O-acetylene flame was used.

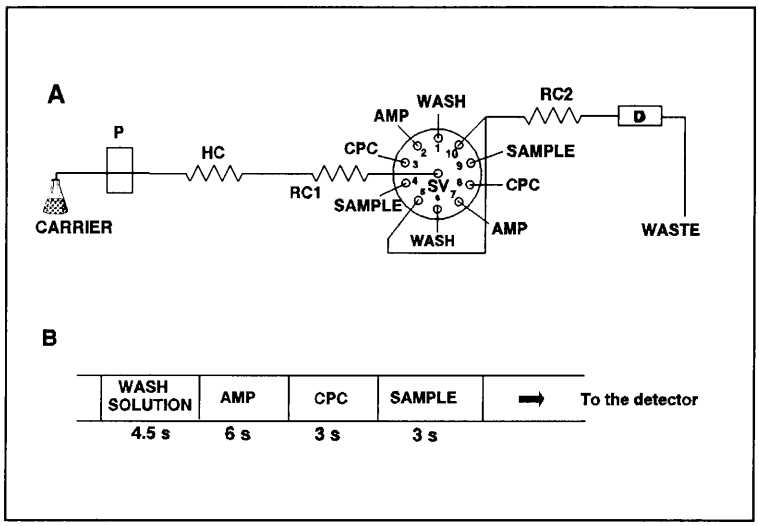

Fig. 4.3 **A**: A schematic diagram of the SIA system used for the determination of calcium. P - pump, HC - holding coil, RC - reaction coil, SV - selection valve and D - detector. **B**: Sequence of wash solution, AMP, CPC, sample and detection.

4.7.1.3 Procedure

The device sequence for the determination of calcium by sequential injection is given in Table 4. Two measurement cycles were used on one complete cycle of the 10-port selection valve (Fig. 4.3A). This was done to utilise the full available capacity of the 10-port Valco valve. As seen from the sequential injection system depicted in Fig. 4.3 the first cycle (wash, AMP, CPC, sample and flushed to the detector) involved ports 1 to 5 of the selection valve. This was followed by an identical cycle involving ports 6 - 10 after a waiting period of 2 sec.

TABLE 4. Device sequence for one cycle of the sequential injection system

Time (s)	Pump	Valve	Description
0	Off	Wash	Pump off, select wash solution
5.25	Reverse		Draw up wash solution
9.75	Off		Pump stop
10.5		AMP	Select AMP stream
12.3	Reverse		Draw up AMP solution
18.3	Off		Pump stop
19.8		CPC	Select CPC stream
21.8	Reverse		Draw up CPC solution
24.8	Off		Pump stop
26.3		Sample	Select sample stream
28.2	Reverse		Draw up sample solutions
31.2	Off		Pump stop
32.7		Detector	Select detector line
34	Forward		Pump stack of zones to detector
84.3	Off	Home	Return pump and valve to starting position

4.8 Method optimization

Determinations involving chromogenic reagents in sequential injection analysis (SIA) are more complicated than their batch [4] and flow injection (FI) [5] counterparts, as direct acquisition of the sample spectrum can be hindered by two effects. One arises from changes in the refractive index when the injected products reach the detector. These changes give rise to a non-spectral, sample dependant variation of the signal, but can be readily corrected for by subtracting the absorbance at a wavelength at which neither the reagents nor the products absorb (using a diode array spectrophotometer [3]). The other effect originates from the

absorbance of the chromogenic reagent and cannot be suppressed by instrumental zeroing (as in the case of FI) because the reagent is injected into a non-absorbing carrier and its absorption is variable.

It was clear from the initial experiments that the sequence of samples and reagents would be a limiting factor in employing the proposed system at a high degree of sensitivity, accuracy and precision. Although the reaction rate of the complexometric reaction between calcium as metal ion and cresolphthalein complexone (CPC) as metallochromic indicator was very fast [6, 8 - 10], the coloured background of the free indicator species as a blank background gave problems with the base-line of the proposed system in initial experiments. The same problem was experienced by Gómez *et al* [3]. Using a diode array spectrophotometer, they handled the problem as follows. After SI recordings for the sample have been acquired, spectra were corrected in order to avoid the effect of changes in the refractive index inside the sensing microcell and subtracted for the absorbance of the chromogenic reagent.

The PAR-calcium reaction was monitored via absorbance readings at 500 nm, from which are subtracted those at 650 nm, where no reactant or product absorb, in order to minimized the potential effects from differences in the refractive index [3]. Since PAR is a coloured reagent and absorbs in the same visible spectral region as its complexes with various metals, the peaks obtained will always be the summation of two contributions, *viz.*, that from the unreacted PAR and that from its complexes (Ca-PAR). Hence the actual peak height for each complex can be determined by subtracting the blank spectrum from that for an injected sample or standard. The amount of reacted PAR is assumed to be negligible relative to that of the unreacted reagent, which is plausible as the complexes formed are highly labile and

a large excess of reagent is used.

4.8.1 Physical parameters

Sensitivity (degree of zone penetration) and precision (reproducibility of zone penetration) were used to evaluate the influence of the following physical parameters, *viz.* pump speed, holding coil (tube diameter, tube length and coil configuration), reaction coil 1 (tube diameter, tube length and coil configuration) and reaction coil 2 (tube diameter, tube length and coil configuration). Particular attention was given before [12] to considerations required in system design such as the influence of tube diameter, reaction coil geometry, pump speed and selection order. A blue dye was used [12] to carry out a study of the effect of different parameters on zone penetration and precision, a syringe pump was used and only one reaction coil was used. In this study real samples and reagents were used which changed the situation.

4.8.1.1 Pump speed

Two measurement cycles were used on one complete cycle of the 10-port selection valve as outlined in Fig. 4.3A; the first measurement cycle from port 1 to port 5 and the second identical measurement cycle from port 6 to port 10. The different steps followed in one of the measurement cycles is given in Table 4. Movement of the pump occurred during the following periods (or sequences) as illustrated in Fig. 4.3B: Pump in reverse; (i) wash solution was drawn up for 4.5 sec, (ii) AMP was drawn up for 6 sec, (iii) CPC was drawn up for 3 sec and (iv) sample was drawn up for 3 sec. Pump forward; (v) the stack of well-

defined zones was flushed via reaction coil 2 for mutually dispersion and penetration before detection in the flow through cell of the detector. This step took 50.3 sec for penetration and final reaction. The pump speed during the different sequences was the same. Table 5 shows the results obtained with different pump speeds given as flow rates (The flow rates obtained was directly proportional to the pump speed.).

TABLE 5. Effect of flow rate (pump speed) on sensitivity and precision

Flow rate ($m\ell.min^{-1}$)	3.12	3.90	4.68	5.46	6.24
Mean relative peak height	7.19	7.57	8.19	8.46	8.75
% RSD	1.06	1.03	0.87	2.90	2.50

The results revealed a slight increase in zone penetration and therefore sensitivity with an increase in flow rate. Optimum reproducibility in zone penetration was obtained with a flow rate of 4.68 $m\ell.min^{-1}$ where the best relative standard deviation of 0.87% was reached. As previously reported [12] at excessively high pump speeds, the back-pressure became too high which resulted in a deterioration of precision as it is visible from Fig 4.4. Low flow rates gave a larger zone penetration, but at a certain point a further decrease in the flow rate also gave a decrease in sensitivity.

Nyman and Ivaska [11] studied the influence of the flow rate on the linearity of the detector response. At the maximum pump speed a flow rate of 3.5 $m\ell.min^{-1}$ was achieved with a 1.0 mm id Tygon pump tubing. They found that good linearity of the detector response was obtained only with flow rates above 3.0 $m\ell.min^{-1}$. A decrease in the flow rate of 10 - 15%, within the ranges 3.0 - 3.5 $m\ell.min^{-1}$, can be accepted without any significant loss of linearity

of the response. Changes of this magnitude easily take place as the tubing wears.

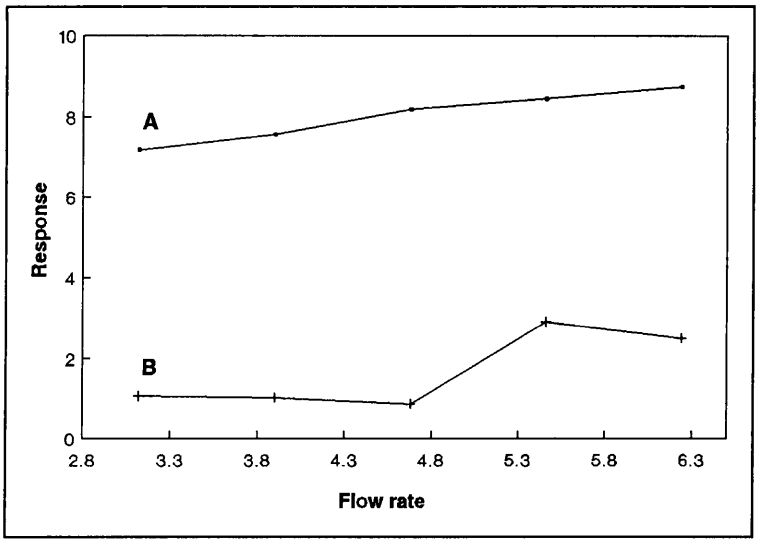

Fig. 4.4 Influence of flow rate on sensitivity and precision (A - relative peak height and B - %RSD).

4.8.1.2 Holding coil

The holding coil serves as a reservoir [13, 14] which prevents the stack of zones from entering the conduit of the pump tubing of the peristaltic pump where deformation could take place. As zone movement into the holding coil takes place, it may also contributes to zone penetration and the dimensions (tube diameter and length) and geometry of the holding coil on sensitivity and precision were therefore evaluated.

4.8.1.2.1 Tube diameter

The influence of holding coil tube diameter on sensitivity and precision was studied for tube diameters between 0.5 and 1.6 mm id. It was found that the tube diameter did not have a

large influence on the sensitivity, but did have a marginal effect on the precision. A marginally poorer precision was obtained with narrow-bore tubing. A slight decrease in relative peak height is also visible for the narrow-bore tubing (Fig. 4.5). The best results were obtained with a tube diameter of 1.6 mm and this was chosen for the proposed SIA system.

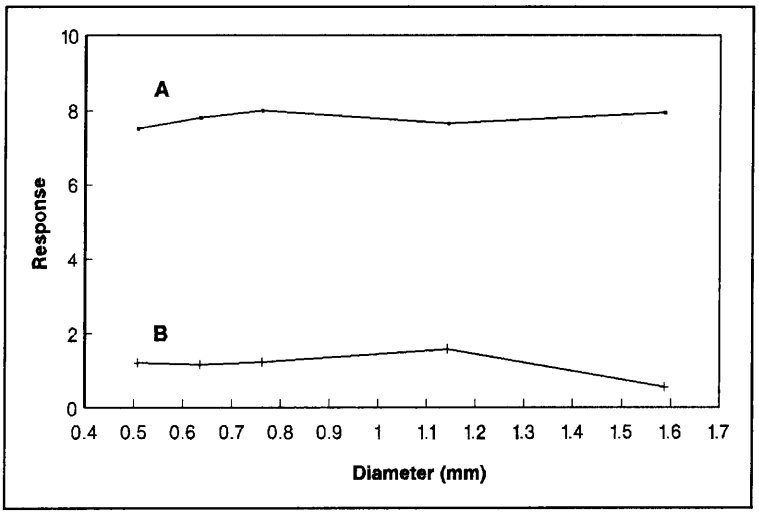

Fig. 4.5 Effect of holding coil tube diameter on sensitivity and precision (A - relative peak height and B - %RSD).

4.8.1.2.2 Holding coil length

Line lengths between 50 and 70 cm were evaluated for the holding coil. As expected did the line length of the holding coil not have any effect on the sensitivity of the sequential injection system, but did have an influence on the precision of the proposed method. A holding coil length of 50 cm gave the best precision and was chosen as optimum holding coil length. With holding coil lengths less than 50 cm, the stack of zones was drawn into the pump tubing of

the peristaltic pump. This resulted in a drastical decrease in precision due to deformation effects originating in the pump tubing.

4.8.1.2.3 Holding coil geometry

The geometry of the holding coil was also investigated. Three types of geometry *viz.* coiled, straight and knitted were studied and the results obtained are given in Table 6.

TABLE 6. Influence of holding coil geometry on sensitivity and precision.

Geometry	Coiled	Straight	Knitted
Mean relative peak height	7.48	7.39	7.76
% RSD	1.22	0.85	1.28

It was obvious from the results that the holding coil mainly served as a reservoir and that the geometry did not really effect the relative peak height. A straight holding coil was used for the proposed system due to the best precision obtained.

4.8.1.3 Reaction coil 1

As the stack of sample and reagent solutions are propelled through reaction coil 1, they penetrate each other resulting in a certain degree of penetration which depends on the dimensions of the reaction coil. The tube diameter, line length and geometry of the first reaction coil were therefore evaluated in order to obtain the best reaction conditions in terms of degree of zone penetration (sensitivity) and precision for the proposed sequential injection

system.

4.8.1.3.1 Tube diameter

Smaller diameter tubing gives rise to higher back-pressures and is also more vulnerable to blockage [12, 14]. However just like FIA smaller diameter tubing is responsible for sharper peaks as illustrated by Table 7. Fig. 4.6 shows however that marginally poorer precision was obtained when narrow-bore tubing was used. The best precision was obtained with a tube diameter of 1.1 mm for reaction coil 1 and this was used in the proposed SIA system.

TABLE 7. Effect of tube diameter of reaction coil 1 on sensitivity and precision

Diameter (mm)	0.6	0.8	1.1	1.6
Mean relative peak height	8.93	8.94	8.36	7.33
% RSD	1.89	1.47	0.56	0.61

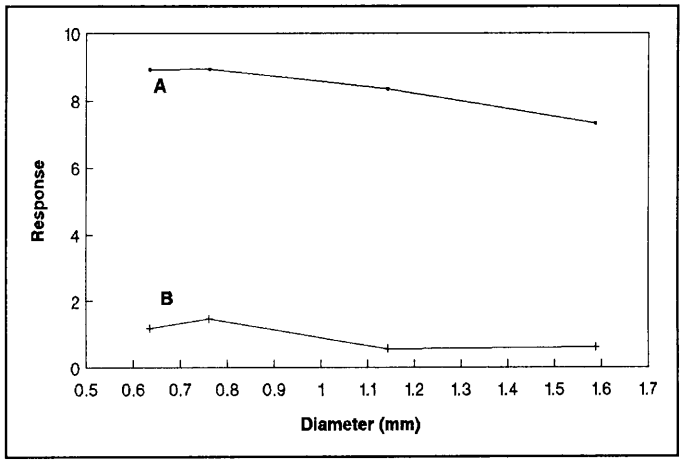

Fig. 4.6 Effect of tube diameter of reaction coil 1 on zone penetration and precision (A - relative peak height and B - %RSD).

4.8.1.3.2 Length of reaction coil 1

The complexation reaction between Ca^{2+} and CPC takes place immediately when the zones start to mix. The length of the reaction coil affects the degree of dispersion and therefore the linear range of the response signal. Lengths of between 90 and 110 cm were evaluated in final experiments. The results obtained, are summarised in Table 8.

TABLE 8. Effect of the length of reactor 1 on zone penetration and precision.

Length (cm)	90	95	100	105	110
Mean relative peak height	8.44	8.25	7.74	7.59	7.63
% RSD	0.69	0.63	1.49	0.80	1.04

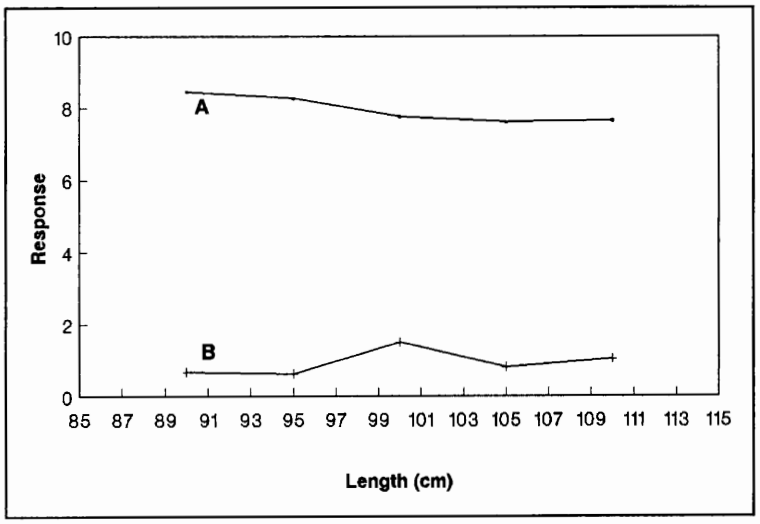

Fig. 4.7 Effect of the length of reactor 1 on zone penetration and precision (A - relative peak height and B - %RSD).

It is obvious from Fig. 4.7 that zone penetration decreased when the length of reactor 1 increased from 90 to 100 cm before stabilising. The best precision was obtained between 90 and 95 cm before the precision deteriorated which confirmed previous results [12, 14] that the length of the reaction coil should be kept as short as possible to avoid problems associated with back-pressures. A length of 90 cm gave the highest relative peak height, was among the best precision and was chosen for reaction coil 1 in the proposed SIA system. The precision tended to decrease with a tube length less than 90 cm and it is not advisable to use lengths shorter than 90 cm.

4.8.1.3.3 Reactor 1 geometry

Three types of geometry *viz.* coiled, straight and knitted were studied for reactor 1. The differences in zone penetration (mean relative peak height of 7.7) and precision (%RSD = 0.75) between the coiled and straight reactor geometry were not significant which means that the axial dispersion for the sample and reagents in the determination of calcium is more or less the same for these two geometries. Although the knitted geometry gave the largest zone penetration (mean relative peak height of 8.1) for this application, a marginally poorer precision (%RSD = 0.98) was obtained ruling this geometry out for the proposed SIA system. The coiled geometry was selected.

4.8.1.4 Reaction coil 2

The resulting merged zones from the first reaction coil are propelled forward by the peristaltic pump through the second reaction coil on route to the flow-through cell of the

detector. The stack of zones is pump for a relatively long period through the second reaction coil when compared to the other sequences in the determination of calcium. Optimisation of this coil therefore forms a very important part in obtaining maximum sensitivity and precision. Tube diameter, line length and geometry of reaction coil 2 were thus also evaluated for the best conditions for the proposed sequential injection system.

8.4.1.4.1 Tube diameter

The results for the various diameters studied are shown in Fig. 4.8. There was a tendency for a slight increase in sensitivity when the tube diameter increased from 0.5 mm to 0.6 mm before the expected decrease in relative peak height. The best relative peak height was obtained with a tube diameter of 0.6 mm, which also gave the best precision and this was chosen for further work.

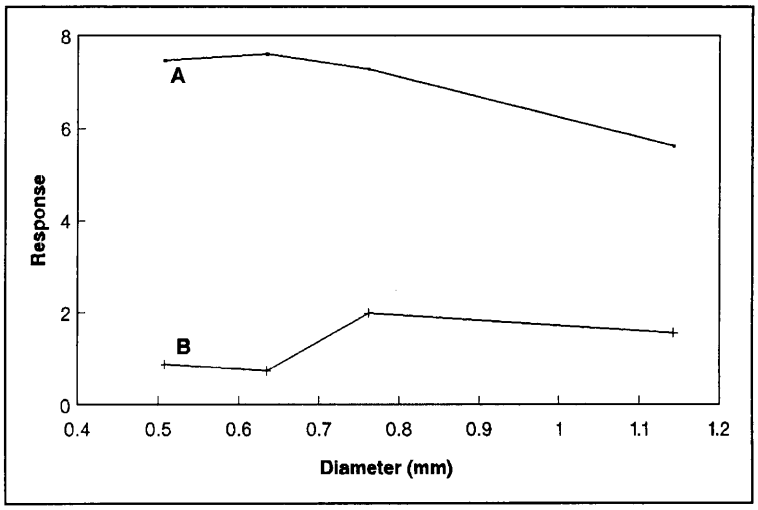

Fig. 4.8 Influence of tube diameter of reactor 2 on relative peak height and precision (A - relative peak height and B - %RSD).

4.8.1.4.2 Line length of reactor 2

Line lengths between 105 and 125 cm were finally evaluated and the results are highlighted in Table 9. The highest reproducibility was obtained with a line length of 115 cm, which means that the axial dispersion was the best controlled under these conditions. The decrease in precision with line lengths less than 115 cm is presumably due to a pulsation effect from the valve system, and the decrease in precision with line lengths longer than 115 cm is probably due to a deterioration in the core of the zone penetration stacks. A line length of 115 cm for reactor 2 was therefore chosen for the proposed system.

TABLE 9. Effect of line length of reactor 2 on sensitivity and precision.

Length (cm)	105	110	115	120	125
Mean relative peak height	7.62	7.11	7.60	7.59	7.48
% RSD	0.67	0.97	0.22	0.97	0.78

It was found by Nyman and Ivaska [11] that the reproducibility of the signal did not depend much on the length of the reaction coil. This result is confirmed in Table 9.

4.8.1.4.3 Reaction coil 2 geometry

Coiled, straight and knitted geometric configurations were also studied for reactor 2. The differences in zone penetration (mean relative peak height of 7.5) and precision (%RSD = 0.61) between the straight and coiled reactor geometry were not significant which means that the axial dispersion for the different stacks of zones remains more or less the same for these

two geometries. The coiled geometry gave the largest zone penetration (mean relative peak height of 7.7) and precision (%RSD = 0.48) and was selected.

4.8.1.5 Uptake tubes

Although the dimensions of the uptake tubes for the wash solution, reagents and samples are not so critical, the different solutions must get to the different ports at a certain fixed time. During the whole measuring cycle, the peristaltic pump operates at a certain pump speed and the dimensions of these tubes need to be optimised for optimum performance. The uptake tubes were all 45 cm long. Narrow-bore tubing gave however rise to higher back-pressures [12, 14] which normally resulted in poorer precision. The uptake tube diameters were therefore evaluated and the results obtained for two diameters are given in Table 10.

TABLE 10. Influence of uptake tube diameter on SIA performance

Diameter	0.8 mm	1.1 mm
Mean relative peak height	7.70	8.04
% RSD	0.63	0.51

An uptake diameter of 1.1 mm gave the best sensitivity and precision and was chosen for all uptake tubes. Uptake tubes with a larger diameter are subjected to less back-pressure and therefore gave a higher precision. However, for the specific selection valve used, Tygon tubing with a diameter larger than 1.1 mm leaks at the connection point between Tygon tubing and Teflon tubing from the valve ports and could not be used.

4.8.2 Chemical parameters

Initial experiments revealed that when the sequence of CPC, sample and then AMP was used, no distinction was found between concentrations. However, when the sequence was changed to AMP, CPC and then sample a distinction was obtained. It seems that the zone penetration of CPC and AMP first had to take place before penetration with the sample. Presumably the sequence AMP, CPC provided the correct pH for the reaction to occur. Zone overlap and penetration would be necessary for significant reaction of AMP, CPC and sample [15, 16].

In the spectrophotometric determination of calcium with CPC, the free indicator is also coloured [6] at certain pH values and although the $Ca_2(CPC)^{2-}$ ion would be expected to be the major chromophore, the presence of free indicator tends to give a background colour. The choice of the correct SIA conditions is therefore crucial in order to minimise the background caused by the coloured free indicator species.

4.8.2.1 Choice of buffer

Preliminary experiments indicated that the optimum detection of the calcium-cresolphthalein complexone (CPC) complex, for the determination of calcium, was in the region of a pH between 10 and 11. A buffer that should maintain pH in this region was therefore required. AMP and NH_3/NH_4Cl was compared as buffers at a pH of 10.5 by scanning solutions containing similar amounts of the free CPC indicator with both buffers in the SIA system at maximum sensitivity. This was repeated with similar CPC indicator solutions containing the same amounts of calcium. The results are depicted in Fig. 4.9. It was clear that the signal

(4) with calcium to background (3) without calcium ratio was by far better for the AMP-buffer (11.4 : 1) as illustrated in Fig. 4.9 than the signal (2) with calcium to background (1) without calcium ratio of 3.6 : 1 for the NH_3/NH_4Cl-buffer. AMP was therefore selected as buffer.

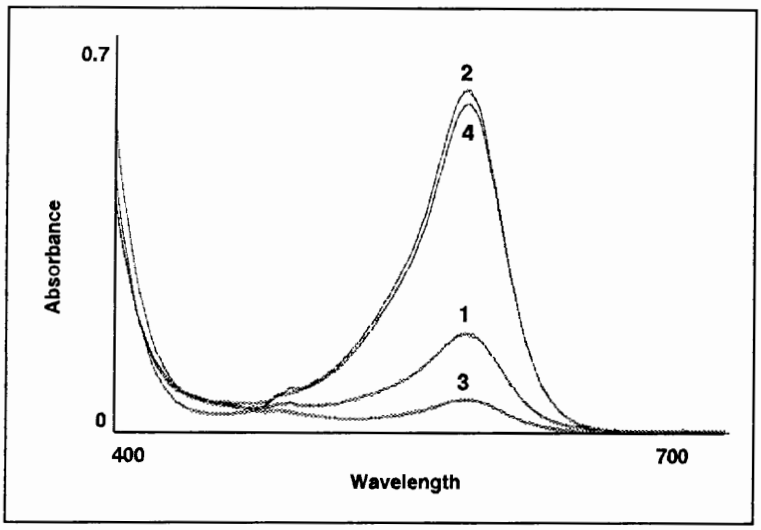

Fig. 4.9 Absorption spectra for the AMP- and NH_3/NH_4Cl buffer solutions at pH 10.5 illustrating the signal obtained with calcium and without calcium in each case.

Nyman and Ivaska [11] also used AMP as buffer solution in the determination of calcium. Other buffers that could be used to maintain a pH of 10.5 is either carbonates or phosphates. These buffers are however unsuitable for this determination because insoluble complexes with calcium are likely to form ($CaCO_3$:- K_{sp} - 2.5×10^{-14} and $Ca_3(PO_4)_2$:- K_{sp} - 1.0×10^{-25}) [17]. An organic base is usually used to provide the necessary alkaline conditions because inorganic alkalis tend to cause high blanks [21].

4.8.2.2 pH of the AMP solution

The optimum pH for the AMP buffer solution was determined by comparing the signal to background ratio at different pH values between 9.55 and 13.6. This was done by scanning solutions containing similar amounts of the free CPC indicator and buffer solution at different pH values, in the SIA system at maximum sensitivity. The experiments were repeated with similar CPC indicator solutions containing the same amounts of calcium at the corresponding pH values. The results are depicted in Table 11.

TABLE 11. Absorption values of the signal with calcium to the background signal without calcium.

pH	Background absorption (b)	Absorption signal with calcium (s)	Ratio (b:s)
13.6	0.263	0.766	1 : 2.9
12.5	0.258	0.758	1 : 2.9
12.0	0.159	0.708	1 : 4.5
11.5	0.124	0.688	1 : 5.5
11.0	0.100	0.669	1 : 6.69
10.5	0.055	0.627	1 : 11.4
10.0	0.023	0.276	1 : 12
9.55	0.023	0.103	1 : 4.5

Although the signal with calcium to background (without calcium) ratio was larger at a pH of 10 than at a pH of 10.5, the buffer capacity of the AMP solution was better at pH 10.5 and pH 10.5 was therefore selected for further work. It was also found by Nyman and Ivaska [11] that the optimum reaction pH was 10.5 as it was suggested by Bishop [8].

4.8.2.3 Concentration of AMP

The main function of the AMP-buffer was to stabilise the pH of the reaction mixture. AMP concentrations of 35, 70 and 140 g.ℓ^{-1} were evaluated in order to find the optimum buffer concentration. The results are summarised in Table 12.

TABLE 12. Effect of AMP concentration on SIA performance

Concentration (g.ℓ^{-1})	35	70	140
Mean relative peak height	4.82	5.20	7.26
% RSD	1.16	0.78	0.82

It is obvious from Table 12 that an AMP concentration of 140 g.ℓ^{-1} gave the best relative peak height and it was selected for further work. With AMP concentrations greater than 140 g.ℓ^{-1} there was a deterioration in precision, mainly due to insufficient mixing (due to the relatively large viscosity of the AMP solution). The background signal also increased presumably due to a colour increase of the AMP solution. The curve representing the mean relative peak height against AMP concentration also tended to flatten with AMP concentrations above 140 g.ℓ^{-1}.

4.8.2.4 Volume of the AMP

Gübeli *et al* [18] and Tucker *et al* [16] have conducted an in-depth study of the effect of reagent volume on zone penetration and sensitivity. The first prerequisite was that a certain amount of AMP buffer solution was necessary in the centroid of the stack of zones to

produce an optimal buffer capacity at a pH of 10.5. Gübeli *et al* [18] and Tucker *et al* [16] reported that for an optimised region of mutually interdispersed sample and reagent zones, with a high precision, the reagent volume should be at least twice that of the sample volume. The following volumes were investigated for AMP. The results are summarised in Table 13.

TABLE 13. Effect of the volume of AMP on SIA performance

Volume (mℓ)	0.31	0.47	0.62
Mean relative peak height	7.27	7.67	7.40
% RSD	0.82	0.19	2.83

As seen from the results a volume of 0.47 mℓ AMP buffer solution gave the best sensitivity and precision which confirmed the results obtained by the abovenamed authors when the ratio of AMP zone volume to sample zone volume (0.23 mℓ) was compared. A volume of 0.47 mℓ was therefore chosen for the SIA system.

4.8.2.5 pH of the CPC

As previously mentioned a coloured background originating from the unreacted chromogenic reagent occurs at every sample/standard peak. This complicated situation is illustrated in Fig. 4.10 where values of pCa corresponding to various metal-indicator complexes of metalphthalein (phthalein complexone) are plotted as a function of pH. The formation of CaI (I ≡ CPC) affects the equilibrium as seen in the figure. The optimum pH range is between 10.5 and 11. At pH values above 12 the colour is always red (purple) and at pH values from 8 to 10.5 the colour change is not very distinct, since the formation of the pink-coloured

complex $CaHI^{3-}$ spread the colour-change interval [8].

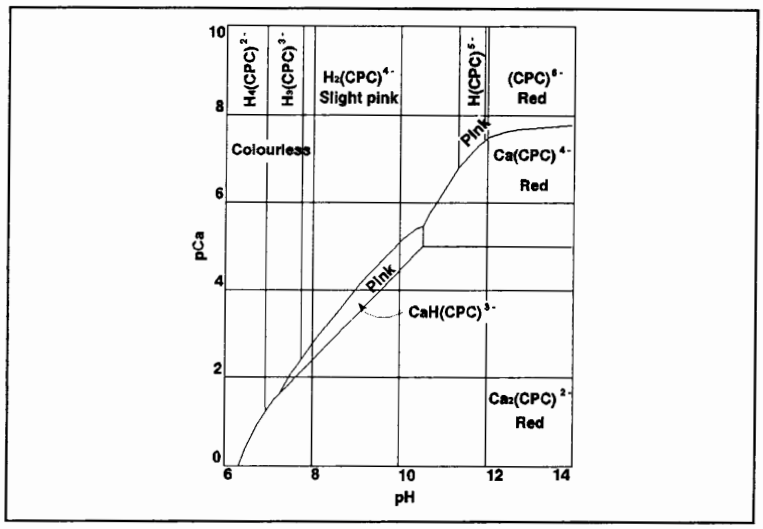

Fig. 4.10 The variation of the colour of the indicator metalphthalein with the calcium and hydrogen ion concentration.

The metallochromic indicator (CPC) solution was subjected to a number of different pH values in order to find a solution which gives the maximum sensitivity. The results of pH values of 1.9 and 3.67 are graphically presented in Fig. 4.11. The signal with calcium to background (without calcium) ratio was used as criteria. A signal to background ratio of 11.4:1 was obtained with a CPC solution where the pH was adjusted to 1.9 (signal 2 with calcium compared with signal 1 as background without calcium) compared to a ratio of 3.125:1 for a CPC solution with a pH of 3.67 (signal 4 with calcium compared with signal 3 as background without calcium). It is clear from the graphical representation that a CPC solution with a pH of 1.9 was the best choice.

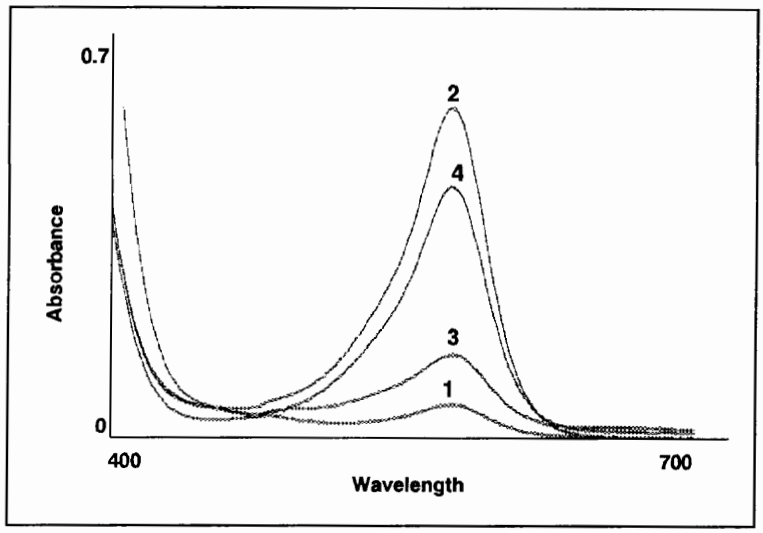

Fig. 4.11 Absorption spectra of the CPC solutions at different pH values illustrating the signal with calcium and without calcium in each case.

4.8.2.6 Volume of the CPC

In their in-depth study on the effect of sample and reagent volume on zone penetration and sensitivity Gübeli *et al* [18] reported that at least twice as large a reagent zone volume as a sample zone volume should be "injected". The conclusion from this was that the volume of CPC colour reagent should be twice that of the sample. As complexation between calcium and CPC occurs in the ratio of two calcium ions for every one CPC-molecule [6], the same volumes should be used for the CPC and sample solutions. This was evaluated and compared. Larger volumes of CPC solution increased the relative peak height, but also had a dramatic effect on the background signal resulting in poor results. The volume of the CPC solution was therefore chosen as 0.23 mℓ.

4.8.2.7 Concentration of CPC

Nyman and Ivaska [11] studied the influence of the concentration on the linearity of the response of the SIA method. During this study the concentration of the masking agent (8-hydroxyquinoline) was kept constant. They found that the response of the blank was not affected by the CPC concentration. With a CPC concentration of 0.24 mmol.ℓ^{-1} they obtained a linear response up to 500 mg.ℓ^{-1} calcium.

It was found in this study that the detection limit of the determination was affected by the CPC concentration. An increase in CPC concentration lowers the corresponding relative peak heights as the number of Ca^{2+} ions needed to form the Ca_2I species, increase with increased CPC concentration. This phenomenon is shown in Table 14.

TABLE 14. Influence of CPC concentration on sensitivity and precision

Concentration	0.05 g.ℓ^{-1}	0.10 g.ℓ^{-1}	0.15 g.ℓ^{-1}	0.20 g.ℓ^{-1}
Mean relative peak height	5.43	6.89	6.21	5.74
%RSD	0.81	0.84	0.92	0.98

Lower CPC concentrations resulting in smaller linear ranges. The 50 mg.ℓ^{-1} calcium standard used in the optimization studies was "too concentrated" for the 0.05 g.ℓ^{-1} CPC solution. This concentration already fell into the flattened part of the calibration curve.

4.8.2.8 Volume of the sample

As SIA is based on the same theories as FIA, the optimal sample volume of the system can be determined as proposed in theory [18] by determining the $S_{1/2}$ value (sample volume necessary to reach 50% of the steady-state value, corresponding to D = 2) for the system. Different sample volumes were investigated. The results are summarised in Table 15.

TABLE 15. Effect of sample volume on sensitivity and precision

Volume (mℓ)	0.12	0.23	0.47
Mean relative peak height	2.37	7.47	7.70
% RSD	2.01	0.87	1.0

It is necessary for proper colour development that two calcium ions complexes with a CPC molecule [6]. Although a sample volume of 0.47 mℓ gave the best zone penetration and sensitivity, a sample volume of 0.23 mℓ revealed the best reproducibility for zone penetration and the latter was selected for optimum working conditions.

4.8.2.9 Carrier stream

AMP buffer solution was originally used as carrier stream. This resulted in the formation of a broad negative signal after the formation of each peak. Doubly distilled deionised water was used to replace the buffer solution. This change had no influence on the sensitivity of the method. Nyman and Ivaska [11] also used distilled, deionized water (Millipore) as carrier.

4.8.2.10 Wash solution

The function of a wash solution between sample cycles is to prevent carry-over between samples [12, 15]. Results showed that a volume of 0.31 mℓ doubly distilled deionised water as wash solution between samples was sufficient enough to prevent any sample interaction.

4.8.2.11 Temperature

The impact of temperature of the sample on the detector signal was studied by Nyman and Ivaska [11]. The room temperature in their laboratory (25 °C) was chosen as reference temperature, while standard solutions at different temperatures up to 50 °C were used. An increase in temperature was found to have no significant effect on the detector signal.

4.9 Evaluation of the SI method

The proposed SIA system was critically evaluated with regard to accuracy, precision, detection limit, dynamic range, sample interaction, interferences and sample frequency.

4.9.1 Linearity

The linearity of the proposed SIA system for the spectrophotometric determination of calcium was evaluated under optimum running conditions. The calibration curve is linear for calcium ion concentrations between 0 and 20 mg.ℓ^{-1} (Fig. 4.12) with a linear relationship between relative peak height and calcium ion concentration given by:

$$y = 0.1031x + 2.7991; \quad r = 0.9941$$

where y = relative peak height and x = calcium ion concentration in mg.ℓ^{-1}.

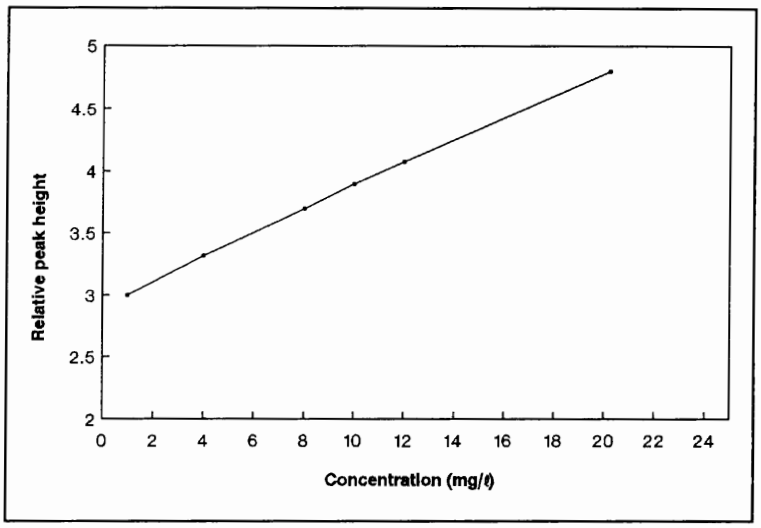

Fig. 4.12 Calibration curve for standard calcium solutions in the range 0 - 20 mg.ℓ^{-1}.

In the method used by Nyman and Ivaska [11] the ascending part of the signal was studied in order to find the optimum time for calibration. This was done by measuring the absorbance in the time interval 4.0 - 6.0 s after the flow reversal. The best linearity was found at 4.8 s. At this point the ratio between standard and reagent is an optimum and gave a linear response over a range of 10 - 500 mg.ℓ^{-1} Ca^{2+}. This way of calibration was used because the traditional way of calibrating, i.e. plotting peak height vs. concentration, would have resulted in a non-linear response.

Reasons for the non-linear response: At low calcium concentrations the 1:1 (Ca : CPC) complex predominates; as this has a lower extinction than the 2:1 complex, the calibration

curve is non-linear at low calcium levels. Regardless the strength of the CPC reagent used, linearity is only achieved over a range of calcium : CPC ratios. At higher calcium : CPC ratios the calibration curve flattens out as the amount of available CPC falls. The final ionisation step, whether induced by increasing pH or by binding calcium, leads to the major change in absorbance. At this stage the absorbance change is linearly related to calcium concentration until the reagent concentration becomes limiting [21].

4.9.2 Accuracy

The accuracy of the proposed SIA system was evaluated by comparing the results of the SIA system with the results obtained by using a standard atomic absorption procedure. Samples in the range of 0 - 20 mg.ℓ^{-1} (water, control sample and urine) was analyzed directly. Above this range samples had to be diluted. Calcium-Sandoz Forte effervescent tablets (from Sandoz Products, Randburg, South Africa) providing 500 mg elemental calcium per tablet as calcium lactate-gluconate and calcium carbonate were prepared as follows. An effervescent tablet was quantitatively dissolved in 1 ℓ doubly distilled deionised water. A portion of this solution was diluted 100 times before analyses. The results as shown in Table 16 revealed an excellent correlation between the two methods. The control sample containing 3.5 mg.ℓ^{-1} calcium also shows excellent agreement with the result of 3.6 mg.ℓ^{-1} calcium obtained by the proposed SIA system. The value of 566 mg/tablet Ca^{2+} for the effervescent tablet compare well with the value of 500 mg/tablet given by the pharmaceutical company.

Table 16. Comparison of results of a number of samples as determined with the SIA system and a standard atomic absorption method.

Sample	SIA	AAS
Effervescent tablet	566 mg/tablet	575 mg/tablet
Tap water	26.8 mg.ℓ^{-1}	25.8 mg.ℓ^{-1}
Control sample	3.6 mg.ℓ^{-1}	3.9 mg.ℓ^{-1}
Urine sample	3.1 mg.ℓ^{-1}	3.2 mg.ℓ^{-1}

4.9.3 Standard addition

A method of standard additions was also used to determine the concentration of calcium in the effervescent tablet. This was done to confirm the value obtained by the SIA procedure. Effervescent solutions were spiked with a range of standard calcium solutions, by suitable dilution of a concentrated stock solution with the dissolved effervescent tablet solution. A normal calibration procedure was followed. A linear calibration curve was obtained and the concentration of calcium in the effervescent tablet solution read as the negative of the x-axis intercept (Fig. 4.13). The concentration of the calcium in the tablet was calculated as 585 mg of Ca^{2+} per tablet which compared excellently with both the SIA and standard AAS methods.

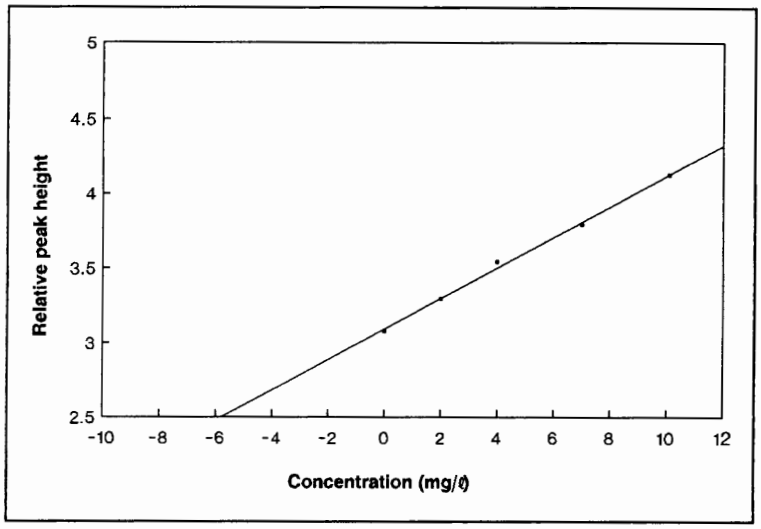

Fig. 4.13 Calibration curve for employing a standard addition method.

4.9.4 Precision

The precision of the proposed SIA system was determined through 10 repetition analyses of a number of standard calcium solutions and samples as indicated in Table 17.

Table 17. Precision of the proposed SIA system

Standard/Sample	% RSD
1 mg.ℓ^{-1}	0.71
8 mg.ℓ^{-1}	0.66
15 mg.ℓ^{-1}	0.85
20.2 mg.ℓ^{-1}	0.82
Effervescent tablet	1.36
Tap water	0.31
Control sample	1.37
Urine	0.27

A precision of less than 1.4% RSD was obtained. The shoulder peak caused by the unreacted CPC is highly reproducible and did not have any influence on the peak height of standards and samples, and therefore on accuracy and precision. No base-line drift was experienced as it can be seen from Fig. 4.14.

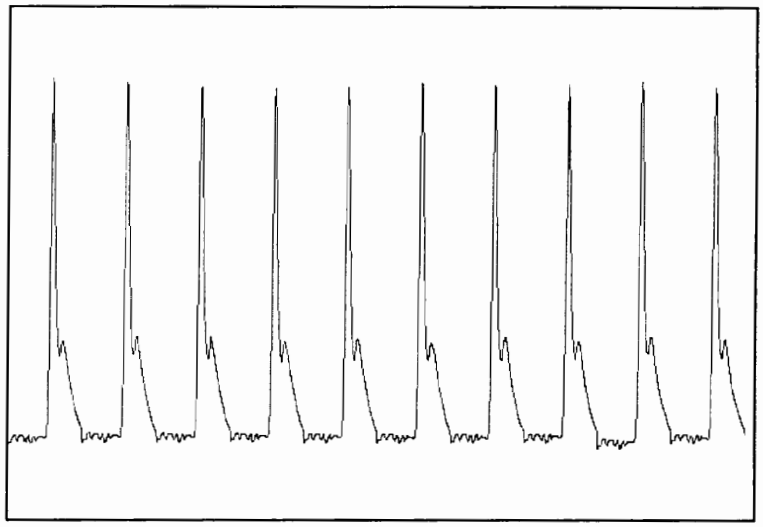

Fig. 4.14 A typical run of the proposed SIA system for a 15 mg.ℓ^{-1} calcium standard showing the reproducibility.

4.9.5 Detection limit

The detection limit of the proposed SIA system was calculated using the formula

$$Detection\ limit = \frac{3 \times S_k}{100} \times K$$

where $S_k = 0.71$ is the relative standard deviation of the lowest concentration of the method and $K = 2.66$ is the average signal value of the corresponding lowest concentration. A

25% safety factor was also used to calculate the final detection limit. The detection limit was calculated to be 0.06 mg.ℓ^{-1}.

4.9.6 Sample interaction

The sample interaction (carry-over effect) between consecutive samples was determined by analysing a sample with a low analyte concentration (1 mg.ℓ^{-1} of calcium) followed by one with a high analyte concentration (10 mg.ℓ^{-1} of calcium) which was again followed by a sample with a low analyte concentration (1 mg.ℓ^{-1} of calcium).

The sample interaction between samples was then calculated using the following formula

$$Sample\ Interaction = \frac{(A_3 - A_1)}{A_2} \times 100$$

where

A_1 = relative peak height of a sample containing 1 mg.ℓ^{-1} of calcium followed by

A_2 = relative peak height of a sample containing 10 mg.ℓ^{-1} of calcium followed by

A_3 = relative peak height of a sample containing the same amount of calcium as A_1. The relative peak heights of A_1, A_2 and A_3 were respectively 2.45, 3.93 and 2.46. The sample interaction between samples as calculated was 0.25% which is neglible.

4.9.7 Interferences

A wide variety of inorganic and organic species can form soluble complexes with calcium, e.g. colloidal calcium oxalate. Aggegration between Ca^{2+} and DSC (dissolved and colloidal substances) from mechanical pulp has been reported. These aggregates did not have any interferences in the developed method [11].

The complexation reaction between Ca^{2+} and CPC is severely interfered by magnesium owing to its strong complexation ability with o-cresolphthalein complexone. The stability constant of the Mg-CPC complex ($K_{MgL} = 10^{8.9}$, where L represents CPC) is of about the same order of magnitude as the stability constant for the Ca-CPC complex ($K_{CaL} = 10^{7.8}$) [11]. Mg^{2+} started to interfere at a concentration of 50 mg.ℓ^{-1} with a decrease in relative peak height of 4.02% The interference of magnesium may to a certain extent be diminished by masking Mg^{2+} with 8-hydroxyquinoline. In the normal application of 8-hydroxyquinoline, calcium does not react with the reagent. It is nevertheless able to form several complexes which is soluble in chloroform and can be extracted under suitable conditions in the alkaline range [2].

When determining Ca^{2+} in the range 0 - 100 mg.ℓ^{-1} with conventional FIA, the maximum tolerable Mg^{2+} concentration has been reported to be 10 mg.ℓ^{-1}. The reason for the increased masking effect in SIA (maximum tolerable Mg^{2+} concentration: 50 mg.ℓ^{-1}, for the range 0 - 20 mg.ℓ^{-1} calcium) is due to the fact that the measurement in this application is done at a point where the CPC, 8-hydroxyquinoline and sample zones overlap in the most favourable way. This shows one of the advantages of SIA, where the zone overlap can easily be

manipulated [11].

Barium, strontium, zinc and copper may be possible interferences in the samples analyzed and these interferences were evaluated. Ba^{2+} and Sr^{2+} started to interfere at a concentration of 100 mg.ℓ^{-1}. The interference was however very small, as this concentration only lower the relative peak height by 0.51%. Zn^{2+} and Cu^{2+} started to interfere at a concentration of 70 mg.ℓ^{-1} which resulted at a decrease in relative peak height of 3.94%. Gómez *et al* [3] found that the maximum tolerated concentrations for Cu^{2+} and Zn^{2+} were 0.05 mg/ℓ^{-1} and 0.1 mg.ℓ^{-1} respectively.

4.9.8 Sample frequency

It took 84.3 sec to complete one sampling cycle which gave a sample frequency of about 43 per hour.

4.10 Conclusion

The methodology developed during this study demonstrates the suitability of sequential injection analysis for the spectrophotometric determination of calcium in water, urine and pharmaceutical formulations. It was possible by using an optimised sequence of sample and reagents to eliminate any background originating from coloured free indicator species. The proposed system is fully computerised and is able to monitor calcium in samples at a frequency of 43 samples per hour with a relative standard deviation of better than 1.4%. The calibration curve is linear between 0 and 20 mg.ℓ^{-1}. The detection limit is 0.06 mg.ℓ^{-1}.

4.11 References

1. N. N. Greenwood and A. Earnshaw, **Chemistry of the Elements**, Chapter 5, pp 117 - 155, Pergamon Press, 1986.
2. J. Fries and H. Getrost, **Organic Reagents for Trace Analysis**, E. Merck, Dramstadt, 1977.
3. E. Gómez, C. Tomás, A. Cladera, J. M. Estela and V. Cerdà, **Analyst**, **120** (1995) 1181.
4. E. Gómez, J. M. Estela and V. Cerdà, **Anal. Chim. Acta.**, **249** (1991) 513.
5. A. Cladera, E. Gómez, J. M. Estela, V. Cerdà, A. Alvarez Ossorio, F. Rioncón and F. Salvà, **Int. J. Environ. Anal. Chem.**, **45** (1991) 143.
6. J. F. van Staden and A. van Rensburg, **Analyst**, **115** (1990) 605.
7. G. D. Marshall and J. F. van Staden, **Analytical Instrumentation**, **20** (1992) 79.
8. E. Bishop, **Indicators**, Pergamon Press, Oxford, 1972.
9. A. Ringbom, **Complexation in Analytical Chemistry**, Interscience Publishers, New York, 1979.
10. G. Anderegg, H. Flaschka, R. Sallman and G. Schwarzenbach, **Helv. Chim. Acta.**, **37** (1954) 113.
11. J. Nyman and A. Ivaska, **Anal. Chim. Acta.**, **308** (1995) 286.
12. G. D. Marshall and J. F. van Staden, **Process Control and Quality**, **3** (1992) 251.
13. J. Růžička and G. D. Marshall, **Anal. Chim. Acta.**, **237** (1990) 329.
14. G. D. Marshall, **Sequential-Injection Analysis**, PhD-Thesis, University of Pretoria, 1994.
15. J. Růžička and T. Gübeli, **Anal. Chem.**, **63** (1991) 1680.

16. D. J. Tucker, B. Toivola, C. H. Pollema, J. Růžička and G. D. Christian, **Analyst**, **119** (1994) 975.

17. L. W. Potts, **Quantitative Analysis. Theory and Practice**, Harper and Row, New York, 1987.

18. T. Gübeli, G. D. Christian and J. Růžička, **Anal. Chem.**, **63** (1991) 2407.

19. L. C. Thomas and G. C. Chamberlin, **Colorimetric Chemical Analytical Methods**, 8th Ed., The Tintometer Ltd., Salisbury, England, 1974, pp 123 - 128.

20. R. A. Close and T. S. West, **Talanta**, **5** (1960) 221.

21. C. M. Corns and C. J. Ludman, **Ann. Clin. Biochem.**, **24** (1987) 345.

22. F. L. Garvan in F. P. Dwyer and D. P. Meller (eds.), **Chelating Agents and Metal Chelates**, Academic Press, New York, 1965, p 290.

23. B. L. Barnett and V. A. Uchtman, **Inorg. Chem.**, **18** (1979) 2674.

24. C. F. Baes and R. E. Messmer, **Hydrolysis of Cations**, Wiley-Interscience, London, 1976.

CHAPTER 5

Turbidimetric Determination of Sulphate by Sequential Injection Analysis

5.1 Introduction

Sulphur is widely distributed in nature but it is seldom concentrated enough to justify economic mining. Its ubiquitity is probably related to its occurrence in nature in both inorganic and organic compounds and to the fact that it can occur in at least five oxidation states: -2 (sulphides, H_2S and organosulphur compounds), -1 (disulphides, S_2^{2-}), 0 (elemental sulphur), +4 (SO_2) and +6 (sulphates). Elemental sulphur in the caprock of salt domes was almost certainly produced by the anaerobic bacterial reduction of sedimentary sulphate deposits (mainly anhydride or gypsum). An interesting discovery recently made is that sulphur, together with H_2SO_4, forms a major component of the atmosphere of the planet Venus [25].

Sulphur occurs in many localities as the sulphates of electropositive elements and to a lesser extent as sulphates of Al, Fe, Cu and Pb. Gypsum ($CaSO_4.2\ H_2O$) and anhydride ($CaSO_4$) are particularly notable. Similarly, by far the largest untapped source of sulphur is in the oceans as the dissolved sulphates of Mg, Ca and K. It has been calculated that there are some 1.5×10^9 cubic km of water in the oceans of the world and that 1 cubic km of sea-water

contains approximately 1 million tonnes of sulphur combined as sulphate [25].

The quality of water, especially drinking water is very important to human life. In a country, like South Africa with its periodic periods of drought, water is a relative scares commodity. Furthermore, the recent drought in our country resulted in a dramatic decrease in our natural water resources. This inevitably results in an increase in the concentration of substances in the water system. The limited available water resources therefore automatically lead to stricter environmental requirements. In this circumstances the quality of available water becomes a factor to be seriously considered within water supplies. Pollution of the fresh water sources is therefore a main concern as it will determine the quality of the final water product. Water purification and recycling is nowadays a major industry. The method of treatment depends upon the source of the water, the use envisaged and the volume required. Table 1 lists the World Health Organization's drinking water standards.

TABLE 1. World Health Organization drinking-water standards

Material	Maximum desirable [ ] in mg.ℓ^{-1}	Maximum permissible [ ] in mg.ℓ^{-1}
Total dissolved solids	500	1500
Mg	30	150
Ca	75	200
Chlorides	20	60
Sulphates	200	400

There is thus an increasing need for process analyzers to monitor natural water streams and industrial effluents. It is clear from Table 1 that the sulphate ion is one of the components that need monitoring.

5.2 Preparation, properties and uses of sulphate

Anhydrous sulphuric acid (Fig. 5.1) is a dense, viscous liquid which is readily miscible with water in all proportions: the reaction is extremely exothermic ($\sim$ 880 $kJ.mol^{-1}$ at infinite dilution) and can result in explosive spattering of the mixture if the water is added to the acid.

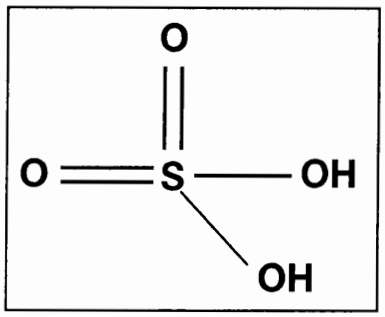

Fig. 5.1 Sulphuric acid.

Sulphuric acid is the world's most important industrial chemical and is the cheapest bulk acid available in every country in the world. Current usage of H_2SO_4 is dominated by fertilizer production (65%) followed by chemical manufacture, metallurgical uses, petroleum refining, paints, pigments and dyestuff intermediates, soaps and detergents and natural and manmade fibres [25].

Sulphuric acid forms salts (sulphates and hydrogen sulphates) with many metals. These are frequently very stable and, indeed, they are the most important mineral compounds of several of the more electropositive elements. Sulphates can be prepared by [25]:

(a) dissolution of metals in aqueous H_2SO_4 (e.g. Fe);

(b) neutralization of aqueous H_2SO_4 with metal oxides or hydroxides (e.g. MOX);

(c) decomposition of salts of volatile acids (e.g. carbonates) with aqueous H_2SO_4;

(d) metathesis between a soluble sulphate and a soluble salt of the metal whose (insoluble) salt is required;

(e) oxidation of metal sulphides or sulphites.

The sulphate ion is tetrahedral (S-O 149 pm) (Fig. 5.2A) and can act as a monodentate, bidentate (chelating) or bridging ligand. Examples are given in Fig. 5.2. Vibrational spectroscopy is a useful diagnostic, as the progressive reduction in local symmetry of the SO_4 group from T_d to C_{3v} and eventually C_{2v} increases the number of infrared active modes from 2 to 6 and 8 respectively and the number of Raman active modes from 4 to 6 and 9. Pairs of corner-shared SO_4 tetrahedra are found in disulphates, $S_2O_7^{2-}$ (S-O_μ-S 124°, S-O_μ 164,5 pm, S-O_t 144 pm); they are made by thermal dehydration of $MHSO_4$. Likewise the trisulphate ion, $S_3O_{10}^{2-}$, is known and also the pentasulphate ion, $S_5O_{16}^{2-}$, whose structure indicates an alternation of S-O interatomic distances and very long O-S distances to the almost planar terminal SO_3 groups [25].

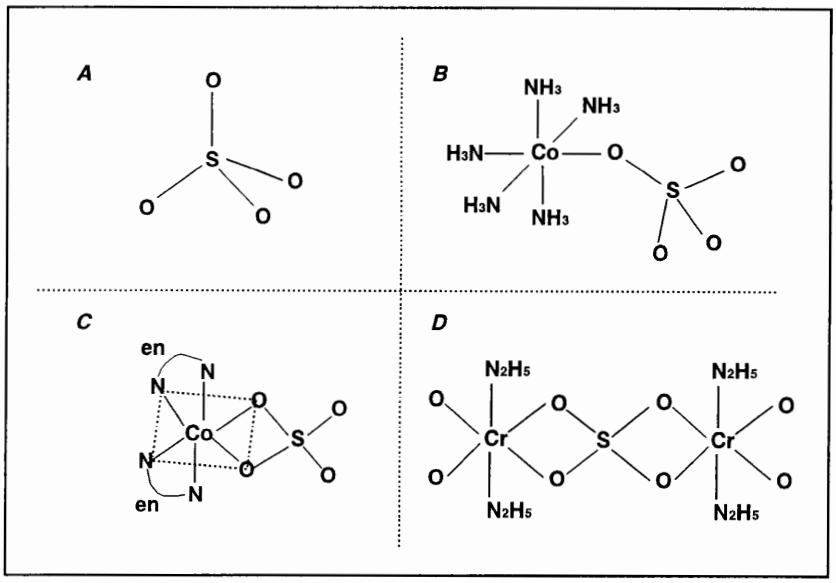

Fig. 5.2 SO_4^{2-} as ligand. A - uncoordinated (T_d), B - monodentate (C_{3v}), C - bidentate (C_{2v}) and D - bridging.

An interesting phenomenon is the occurrence of monomeric neutral SO_4. This can be obtained by reaction of SO_3 and atomic oxygen; photolysis of SO_3/ozone mixtures also yields monomeric SO_4, which can be isolated by inert-gas matrix techniques at low temperatures (15 - 78 K). Vibration spectroscopy indicates either an open peroxo C_s structure (Fig. 5.3A) or a closed peroxo C_{2v} (Fig. 5.3B) structure, the former being preferred by the most recent study, on the basis of agreement between observed and calculated frequencies and reasonable values for the force constants [26].

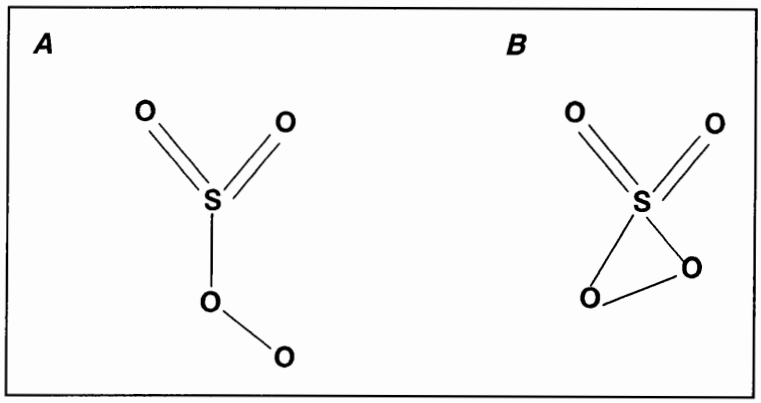

Fig. 5.3 Open peroxo structure (C_s) (A) and closed peroxo structure (C_{2v}) (B) of the monomeric neutral SO_4.

The compounds decomposes spontaneously below room temperature.

5.2.1 Uses of sulphate

Salt cake (Na_2SO_4) is a byproduct of HCl production, using H_2SO_4, and is also the end product of hundreds of industrial operations in which H_2SO_4, using for processing, is neutralized by NaOH. For an extended period of time it had few uses, but now it is the mainstay of the paper industry, being a key chemical in the kraft process for making brown wrapping paper and corrugated boxes. Digestion of wood chips or saw-mill waste in very hot alkaline solutions of Na_2SO_4 dissolves the lignin (the brown resinous component of wood which cements the fibres together) and liberates the cellulose fibres as pulp which then goes to the paper making screens. The remaining solution is evaporated until it can be burned, thereby producing steam for the plant and heat for the evaporation: the fused Na_2SO_4 and NaOH survive the flames and can be reused. Most of the Na_2SO_4 produced is used in the paper industry and smaller amounts are used in glass manufacture and detergents [25].

Calcium sulphate usually occurs as the dihydrate (gypsum) though anhydride ($CaSO_4$) is also mined. Alabaster is a compact, massive, fine-grained form of $CaSO_4.2\ H_2O$ resembling marble. When gypsum is calcinated at 150 - 165 °C it looses approximately three-quarters of its water of crystallization to give the hemihydrate $CaSO_4.1/2\ H_2O$, also known as plaster of Paris because it was originally obtained from gypsum quarried at Montmartre. Heating at higher temperatures yields various anhydrous forms:

$$CaSO_4.2\ H_2O \xrightarrow{\sim 150\ ^\circ C} CaSO_4.1/2\ H_2O \xrightarrow{200\ ^\circ C} \tau\text{-}CaSO_4 \xrightarrow{\sim 600\ ^\circ C} \beta\text{-}CaSO_4 \xrightarrow{\sim 1100\ ^\circ C} CaO + SO_3$$

Gypsum, though not mined on the same scale as limestone, is nevertheless still a major industrial mineral. Most of the gypsum is for Portland cement or agricultural purposes. In the absence of a retarder, cement reacts rapidly with water giving a sharp rise in temperature and a "flash set" during which the various calcium aluminate hydrates precipitate and congeal into an unmanageable mass. This can be avoided by grinding in 2 - 5% of gypsum with the cement clinker; this reacts rapidly with dissolved aluminates in the presence of $Ca(OH)_2$ to give the calcium sulfatoaluminate, $3\ CaO.Al_2O_3.3\ CaSO_4.31\ H_2O$, which is much less soluble than the hydrated calcium aluminates and therefore preferentially precipitates and prevents the premature congealing. Of calcinated gypsum, virtually all (95%) is used for prefabricated products, mainly wall board, and the rest is for industrial and building plasters.

Products of the reaction between H_2SO_4 and calcium oxides can be used as oxidising agents and bleaches [25]:

$$CaO_2 + H_2SO_{4(aq)} \rightarrow CaSO_{4\,(s)} + H_2O_{2\,(aq)}$$

$$Ca(O_2)_2 + H_2SO_{4\,(aq)} \rightarrow CaSO_{4\,(s)} + H_2O_{2\,(aq)} + O_{2\,(g)}$$

Treatment of SnO_2 with hot diluted H_2SO_4 yields the hygroscopic dihydrate $Sn(SO_4)_2.2\,H_2O$. In the Sn^{2+} series $SnSO_4$ is a stable, colourless compound which is probably the most convenient laboratory source of Sn^{2+} uncontaminated by Sn^{4+}. $SnSO_4$ was at a time thought to be isostructural with $BaSO_4$ but this seems unlikely in view of the very different sizes of the cations. $PbSO_4$ is also stable when dry and can be made by the action of concentrated H_2SO_4 on $Pb(OAc)_4$ or by electrolysis of strong H_2SO_4 between Pb electrodes. $PbSO_4$ is familiar as a precipitate for the gravimetric determination of sulphate (solubility 4.25 mg per 100 mℓ at 25 °C) [25].

Sulphate is the cheapest salt of Fe^{3+} and forms no less than six different hydrates (12, 10, 9, 7, 6 and 3 mols of water of which 9 H_2O is the most common); it is widely used as a coagulant in the treatment not only of potable water but also sewage and industrial effluents. Addition of $Fe_2(SO_4)_3$ produces flocs of $Fe(OH)_3$ that can be filtered off.

Ammonia and CO_2 can be passed through a gypsum slurry to give ammonium sulphate for use in fertilizers:

$$CaSO_4 + (NH_4)_2CO_3 \rightarrow CaCO_3 + (NH_4)_2SO_4.$$

K_2SO_4 is also used in fertilizers [25].

Reduction of a sulphate with carbon yield a sulphide ($Na_2SO_4 + 4\ C \rightarrow Na_2S + 4\ CO$). Sulphides and hydrogen sulphides are moderately strong reducing agents and are oxidized either to dithionate or sulphate. The reaction with iodine is quantitative and is used in volumetric analysis:

$$HSO_3^- + I_2 + H_2O \rightarrow HSO_4^- + 2\ H^+ + 2\ I^-.$$

Sulphur dioxide is made commercially on a large scale either by combustion of sulphur or H_2S or by roasting sulphide ores (particularly pyrite, FeS_2) in air. It is also produced as a noxious and undesirable byproduct during the combustion of coal and fuel oil. The ensuing environmental problems and the urgent need to control this pollution are matters of considerable concern and activity. The detection of SO_2 in the atmosphere has become a refined analytical procedure. Several techniques are available. Some of these are based on sulphate determinations.

Rapid and accurate determination of sulphate in rain and river water is used by Nakashima *et al* [15] to provide information on acid precipitation studies.

5.3 Choice of analytical method

Several approaches have already been described for the determination of sulphate ions in various materials. The existing manual methods, for example the standard gravimetric method [1] and the titrimetric methods [2, 3, 34], including the potentiometric methods with ion-selective electrodes, which usually involve precipitation titrations with lead(II) solution and a lead sensitive electrode [3 - 8] are all cumbersome, tedious and time-consuming.

Accordingly, a number of spectrophotometric methods for determining sulphate have been developed. The three methods that appear to be used most frequently are the barium chloroanilate method [9, 10, 34], the methylthymol blue method [11] and the barium sulphate turbidimetric procedure [12]. A number of methods have also been adapted to flow-injection analysis for the determination of sulphate. The spectrophotometric methods include the methylthymol blue method [13], the dimethylsulphonazo-III-(sulhonazo-III) procedure [14, 15], the barium chloroanilate method [16] and the barium sulphate turbidimetric method [17 - 19].

Madsen and Murphy [13] reported a FIA procedure for the determination of sulphate in rain water using the automated methylthymol blue (MTB) method. Samples were drawn through a cation-exchange column in the sample line in order to eliminate interferences from some cations. The procedure is sensitive with a detection limit of 0.1 mg.ℓ^{-1}, but has a narrow linear range (0.1 to 6.0 mg.ℓ^{-1}) and samples with higher sulphate values had to be diluted manually before analysis. The method is not very precise (RSD of 4.1%) and with a rate of 20 samples h^{-1}, the throughput is rather low, when compared with a normal sample capacity for FIA of about 40 to 60 samples h^{-1}.

This method [13] is based on the indirect determination of sulphate. The indirect method based on competitive reaction of sulphate and MTB with the barium in solution can be accomplished by measurement of absorbance due to either uncomplexed MTB or the MTB-barium complex. Absorbance at 460 nm due to uncomplexed MTB will increase while absorbance due to the MTB-barium complex (at 608 nm) will decrease as sulphate concentrations increase. The complexation reaction of barium with MTB occurs only at high

pH. pH must therefore be controlled to an extent which ensures that all barium which does not react with sulphate will complex with MTB.

Jones [35, 36] described a method for sulphate determination, where sulphate catalyses the reaction between zirconium and methylthymol blue to form a complex measured at 586 nm. Certain anions, like sulphate, phosphate and fluoride, form labile complexes with zirconium that can react more rapidly with the ligand (MTB) than the polymerized zirconyl species that normally persist in weakly acidic solutions.

Reijnders *et al* [14] was the first group to report on the sensitive determination of sulphate in environmental samples by FIA using the barium chelate of dimethylsulphonazo-III (DMSA) as indicator. Interfering cations were also eliminated by using a cation-exchange column in the sample line. The procedure, furthermore, still uses a bubble pattern in the manifold system. Although the method is very sensitive with a detection limit of about 0.25 $mg.\ell^{-1}$ of sulphate, the precision at this limit was poor (24%). The same concept was also used by Kondo *et al* [20] for the sensitive determination of sulphate in river water, but without the air segmentation. This method is more precise as the above mentioned one, but suffers from a relatively low sample throughput (30 samples h^{-1}). The procedure also has a limited calibration range (0 to 30 $mg.\ell^{-1}$).

The method that appears to be used almost universally is the barium sulphate turbidimetric procedure. Krug *et al* [21] first adapted the turbidimetric sulphate procedure to FIA using various types of flow systems with more than one reagent or carrier stream. A sampling rate of 180 samples h^{-1} was achieved, the concentration range was extended to 140 $mg.\ell^{-1}$ with

a good precision (0.85%). Basson and van Staden [22] improved on the 40 samples h^{-1} for the segmented barium sulphate turbidimetric procedure. The sampling rate was increased to about 200 samples h^{-1} and the flow diagram simplified to a single carrier reagent stream. The precision was however unacceptable (3.9%).

5.4 Principle of the turbidimetric determination

The turbidimetric determination of sulphate is based on the following reaction:

$$SO_4^{2-}{}_{(aq)} + BaCl_{2(aq)} \rightarrow BaSO_4\downarrow + 2\ Cl^-_{(aq)}$$

A colloidal barium sulphate suspension, which is pH dependant, is formed. The turbidity of this suspension is measured at 420 [17 - 19, 21] or 540 nm [39]. The accuracy and precision therefore depend critically on the crystalline form and size distribution of the light-scattering particles in the suspension. The degree of suspension is controlled by several factors and therefore the concentrations related to reagents and precautions preparing the reagents must be strictly followed.

Polyvinyl alcohol [21] and gelatine [22] have been used to stabilise the barium sulphate suspension in order to obtain a relatively good precision. Thymol is added to the reagent to prevent bacterial growth [23].

5.4.1 Colloidal suspensions

A colloidal state exists when particles with sizes in the range of 1 - 250 nm are dispersed in a medium [37]. Because turbidimetric determinations rely on the formation of stable colloids it is essential to find conditions favouring the formation of colloidal suspensions. To produce this type of suspension it is necessary that a large number of small nuclei must form immediately when the reagents are mixed together.

Although the exact mechanism by which nuclei form depends on the characteristics of each particular system, there are two models which are appealing in their simplicity. According to the first, nuclei can form "homogeneously" within the liquid phase. Local concentration fluctuations in solutions bring together aggregates of ion pairs. Crystals form around these aggregates. According to the second model, nuclei are formed "heterogeneously" around foreign particles, such as dust, present in the solution.

Once a nucleus has been formed, a crystal can grow by a two-step process involving *diffusion* of solute ions to the nucleus surface and their subsequent *deposition*. The rate of growth can be limited by either process. The rate of diffusion depends on the concentration of the ions near the surface and in the bulk of the solution and the temperature, whereas the rate of deposition depends on the nature of the surface and the pattern of crystal growth [37].

Because a large number of small nuclei is needed for a colloidal suspension, nuclei formation is accelerated by addition of gelatine as 'seed crystals'. When a large number of nuclei form very fast the dissolved solute is used up so quickly that the nuclei cannot grow very large,

resulting in the large number of small nuclei needed for a colloidal suspension.

The turbidimetric determination is based on the optical properties of the colloidal suspension. A true solution of ions is said to be "optically empty", because when a beam of light is shone through the solution no light is scattered at right angles to the light path. If, however, particles larger than about 10 nm are dispersed in a solvent, light is scattered at right angles at high intensity (the Tyndall effect) [37].

5.5 Determination of sulphate with sequential injection analysis

5.5.1 Experimental

5.5.1.1 Reagents and solutions

All reagents were prepared from analytical-reagent grade unless specified otherwise. All aqueous solutions were prepared with doubly distilled deionised water. All solutions were degassed before measurements with a vacuum pump system.

Standard sulphate solutions: A stock solution containing 5 000 mg.ℓ^{-1} of sulphate was prepared by dissolving 16.7715 g $Na_2SO_4.10\ H_2O$ in distilled water and diluting it to 1 ℓ. Working solutions in the range of 1 - 500 mg.ℓ^{-1} were prepared by suitable dilution of the stock solution.

Buffer solution: 40 g of EDTA (disodium salt), 7 g of ammonium chloride and 57 mℓ concentrated ammonia (sp. gr. 0.88) were dissolved in 500 mℓ distilled water and diluted to 1 ℓ.

Barium chloride solution: A potassium hydrogen phthalate - hydrochloric acid buffer at pH 2.5 was prepared by adding 388 mℓ of a 0.1 mol.ℓ^{-1} HCl solution to 500 mℓ of a 0.1 mol.ℓ^{-1} potassium hydrogen phthalate solution. 10 g of $BaCl_2.2\ H_2O$, 1.0 g thymol and 0.62 g gelatine were dissolved in this buffer and the solution was diluted to 1 ℓ. The reagent was filtered through a Millipore membrane (type HA) (45 μm).

5.5.1.2 Apparatus

The sequential injection system depicted in Figure 5.4 were constructed from the following components: a Gilson minipuls peristaltic pump; a 10-port electrically actuated selection valve (Model ECSD10P; Valco Instruments, Houston, TX, USA); and a Unicam 8625 UV-visible spectrophotometer equipped with a 10-mm Hellma type flow-through cell (volume: 80 μl) for absorbance measurements. The barium sulphate suspension formed, was monitored by measuring the absorbance at 540 nm. Data acquisition and device control were achieved using a PC30-B interface board (Eagle Electric, Cape Town, South Africa) and an assembled distribution board (MINTEK, Randburg, South Africa). The *FlowTEK* [24] software package (obtainable from MINTEK, Randburg, South Africa) for computer-aided flow-analysis was used throughout for device control and data acquisition.

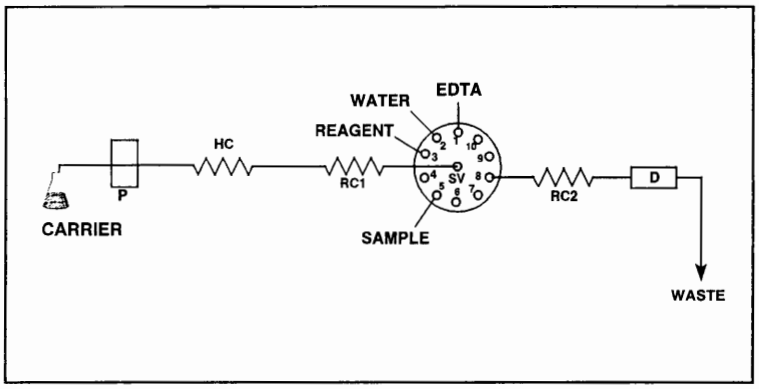

Fig. 5.4 A schematic diagram of the SIA system used for the determination of sulphate. P - pump, HC - holding coil, RC - reaction coil, SV - selection valve and D - detector.

5.4.1.3 Manifold

The components of the SIA system were arranged as illustrated in Fig. 5.4. The holding coil was made of 2.8 m x 1.02 mm id coiled Tygon tubing, reaction coil 1 of 1.3 m x 1.02 mm id straight Tygon tubing and reactor 2 of 1.0 m x 0.65 mm id straight Tygon tubing. The flow rate used was 5.0 $m\ell.min^{-1}$.

5.4.1.4 Procedure

The device sequence for the determination of sulphate is given in Table 2.

TABLE 2. Device sequence of the sequential injection system

Time (s)	Pump	Valve	Description
0	Off	Off	Pump off
1		Detector	Select detector line
7	Forward		Pump wash solution through detector
51.5	Off		Pump stop
53.5		EDTA	Select EDTA (wash) stream
57.5	Reverse		Draw up EDTA solution
62.5	Off		Pump stop
63.5		Water	Select water stream
65	Reverse		Draw up water
80	Off		Pump stop
82		$BaCl_2$	Select $BaCl_2$ stream
83	Reverse		Draw up $BaCl_2$-solution
86	Off		Pump stop
87		Sample	Select sample stream
88.5	Reverse		Draw up sample/standard solutions
97.5	Off		Pump stop
98.5		Detector	Select detector line
101	Forward		Pump stack of zones to detector
138	Off		Return pump and valve to starting position

5.5.2 Method optimisation

5.5.2.1 Physical parameters

The conditions for the determination of sulphate were optimised by studying the influence of various parameters such as flow rate and the dimensions of the different coils (tube

diameter, tube length and coil configuration). The response, given by the degree of zone penetration, and precision, given by the reproducibility of zone penetration, were used as indicators in the optimisation of the sequential injection system.

5.5.2.1.1 Flow rate

The formation of the barium sulphate suspension to the correct measurable conditions from Ba^{2+} and SO_4^{2-} is a relatively slow process. The flow rate during the different sequences is therefore a very important parameter to be optimised because it regulates the volume of the sample and reaction zones and the flow of the zones through the system. Movement of the pump occurred during the following periods (or sequences). Pump forward; (i) wash solution was pumped through the detector for 44.5 sec. Pump in reverse; (ii) EDTA solution was drawn up for 5 sec., (iii) water was drawn up for 15 sec., (iv) barium chloride solution was drawn up for 3 sec., (v) sample/standard solutions were drawn up for 9 sec. Pump forward; (vi) the stack of well-defined zones flushed via a reaction coil for mutually dispersion and penetration before detection in the flow-cell of the detector. This step took 37 sec. for penetration and final reaction. The flow rate during the different sequences was the same. The effect of the flow rate on the sensitivity, precision and linearity of detector response was studied. The results obtained, are listed in Table 3 and illustrated in Fig. 5.5.

TABLE 3. Effect of flow rate (pump speed) on sensitivity and precision

Flow rates (mℓ.min^{-1})	Mean relative peak height	% RSD
1.0	2.24	2.51
1.5	2.60	1.33
2.0	2.95	0.63
2.5	3.37	1.40
3.0	3.43	2.08
3.5	3.61	1.09
4.0	3.75	1.55
5.0	3.97	0.79
6.0	4.17	2.28
7.8	4.06	3.08

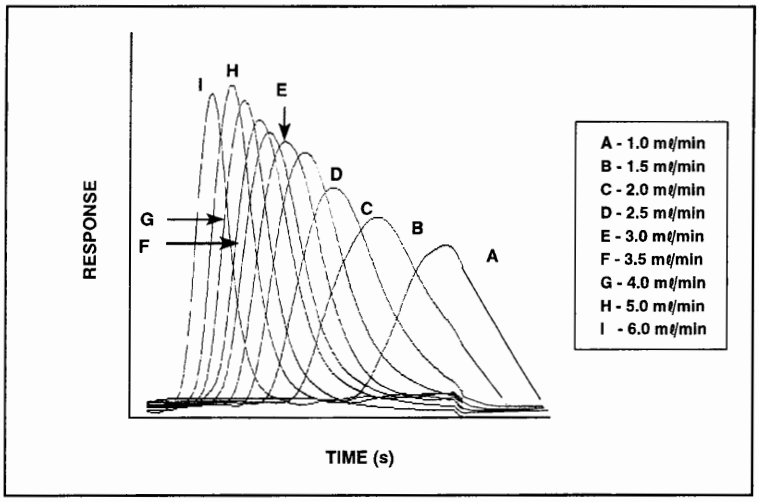

Fig. 5.5 Schematic representation of the influence of flow rate on sensitivity and band broadening of the SIA response.

The results showed an increase in the mean relative peak height (sensitivity) from a value of 2.2 at a flow rate of 1.0 mℓ.min^{-1} to a value of 4.2 at a flow rate of 6.0 mℓ.min^{-1} due to an increase in zone penetration when the flow rate increases. Optimum precision in zone

penetration was obtained with a flow rate of 5.0 $m\ell.min^{-1}$ where the best RSD of 0.79% was reached.

5.5.2.1.2 Holding coil

The main function of the holding coil is to serve as a reservoir [27] preventing the stack of zones from entering the conduit of the pump tubing of the peristaltic pump where deformation could take place. As zone movement into the holding coil takes place, it may also contributes to zone penetration and the dimensions (tube diameter and length) and geometry of the holding coil on sensitivity and precision was therefore evaluated.

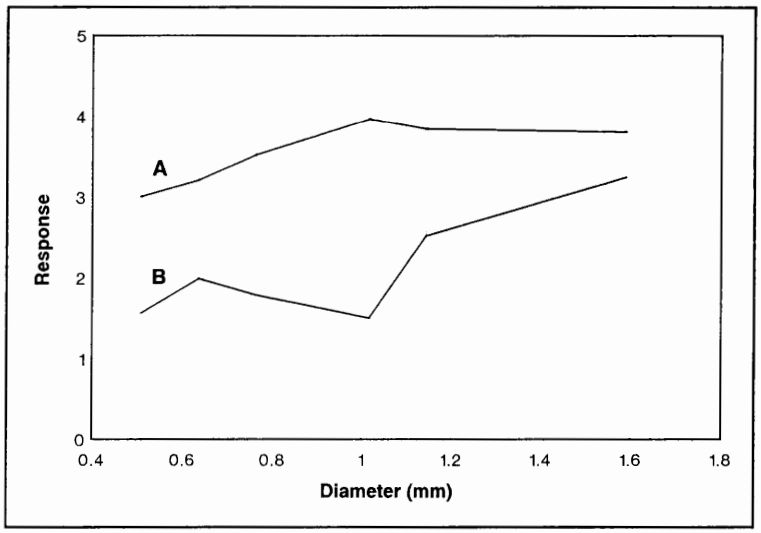

Fig. 5.6 Influence of holding coil tube diameter on sensitivity and precision (A - relative peak height and B - %RSD).

Tube diameter is responsible for the distance travelled by a zone. The tube inner diameter is normally an inverse of the zone length for a specific zone volume. The smaller the tube

diameter the longer the zone length. The effect of holding coil tube diameter on sensitivity and precision (Fig. 5.6) was studied for tube diameters between 0.51 and 1.59 mm. There is a slight increase in peak height with an increase in tube diameter. This is due to a decrease in zone length with a consequent better zone penetration. Zone penetration reached an optimum (mean relative peak height = 3.97) at a tube diameter of 1.02 mm with the best precision (%RSD = 1.50) and this diameter was chosen.

Various holding coil lengths between 2.0 and 2.8 m were evaluated. As expected the holding coil length did not have any influence on the response of the sequential injection system, but had an effect on the reproducibility of zone penetration where line lengths of between 2.4 and 2.8 m gave the best results (Table 4). A holding coil length of 2.8 m was selected for the proposed SIA analyzer, because of its lower %RSD of 0.42. The main prerequisite is that the holding coil must be long enough to accommodate the stack of zones pumped into it. It is therefore not really necessary to optimise the holding coil length - only the diameter and geometry [28].

TABLE 4. Effect of holding coil length on sensitivity and precision

Length (m)	Mean relative peak height	% RSD
2.0	4.09	1.26
2.2	3.90	1.00
2.4	4.05	0.69
2.6	4.03	0.74
2.8	3.81	0.42

The following configurations for the holding coil were examined: Coiled, straight and knitted. The results (Table 5) confirmed expectations that the holding coil geometry did not really effect the peak height and precision. Any of the three geometries investigated will suit the proposed system. A coiled holding coil was however used for the proposed system mainly due to the lower RSD of 0.52% obtained. Coiling of the holding coil made the manifold more streamline.

TABLE 5. Influence of holding coil geometry on sensitivity and precision

Geometry	Mean relative peak height	% RSD
Coiled	3.92	0.96
Straight	3.78	0.62
Knitted	3.74	0.72

5.5.2.1.3 Reaction coil 1

A certain degree of penetration, depending on the dimensions of the reaction coil, occurs as the stack of sample and reagent solutions are transported through reaction coil 1. The tube diameter, line length and geometry of the reaction coil were therefore evaluated in order to obtain the best reaction conditions in terms of degree of zone penetration (sensitivity) and precision for the proposed system.

The tube bore in reaction coil 1 is mainly responsible for two physical parameters; the movement of a zone through the tube and the length of the zone within the tube. It is a well-known fact from FIA that smaller diameter tubing is responsible for sharper peaks mainly

due to the faster movement of a zone through the tubing [29 - 31]. The length of a zone within a tube also has an influence on the peak shape and longer zone lengths result in broader peaks. The tube inner diameter is normally an inverse of the zone length for a specific zone volume and the smaller the tube diameter the longer the zone length. In SIA the degree of zone penetration mainly determines the shape of the peak obtained [28, 32 - 43].

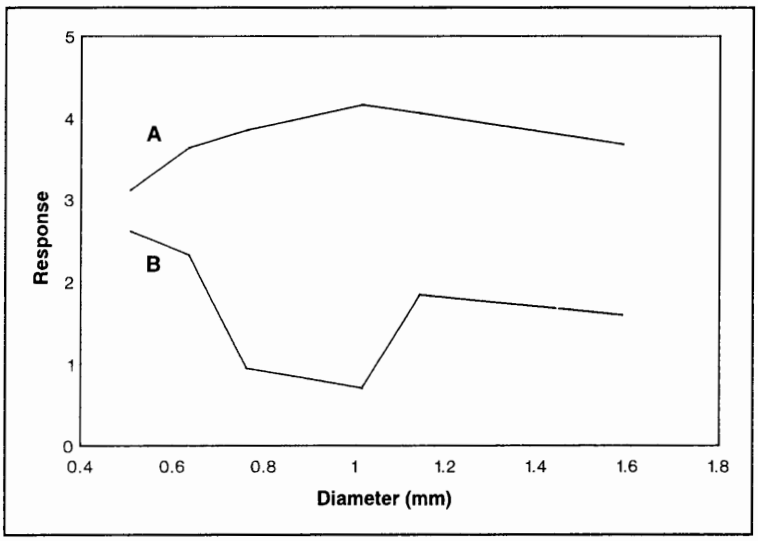

Fig. 5.7 Effect of tube diameter of reaction coil 1 on zone penetration and precision (A - relative peak height and B - %RSD).

The influence of reaction coil 1 tube diameter on the response and precision was studied for tube diameters between 0.51 and 1.59 mm. The results (Fig. 5.7) reveal that the mean relative peak height decreases with an increase in tube diameter. It is obvious that a decrease in zone length of a particular zone with an increase in tube diameter created the conditions for better zone penetration. Zone penetration reaches an optimum at a tube diameter of 1.02 mm. It is also clear from the results that the reproducibility of zone penetration was poorer

when narrow-bore tubing was used, but improved with tubing diameters of 0.76 and 1.02 mm with the best precision (RSD = 0.71%) obtained for 1.02 mm. There was a deterioration in zone penetration with tube diameters of 1.14 mm and larger which was expected since the zone length of a particular zone decreases to such an extend that the degree of zone penetration was not reliable anymore [27 - 28]. The optimum diameter was chosen as 1.02 mm.

Lengths of between 1.1 and 1.9 m were investigated. According to Marshall and van Staden [28] the length of the first reaction coil should not exceed one-third of the volume of the wash solution, thereby ensuring that the whole manifold is adequately flushed during every experiment. The result was confirmed. It was however clear (Table 6) that the degree of zone penetration for reaction coil lengths between 1.1 and 1.9 m did not differ significantly. It was however difficult to get an optimum reproducible degree of zone penetration for the formed barium sulphate suspension. The optimum length was chosen as 1.3 m due to the best precision (RSD = 1.03%) obtained.

TABLE 6. Effect of the length of reactor 1 on zone penetration and precision

Length (m)	Mean relative peak height	% RSD
1.1	3.69	1.14
1.3	3.69	1.03
1.5	3.75	1.50
1.7	3.72	2.55
1.9	3.83	1.54

The following geometries for reactor 1 were examined: Coiled, straight and knitted. It is clear from the results obtained (Table 7) that the degree of zone penetration did not alter very much with the type of geometry used and that any of the three geometries investigated will suit the proposed system. A straight reactor coil was however used for the system due to the precision of 0.89% obtained.

TABLE 7. Influence of reactor 1 geometry on zone penetration and precision

Geometry	Mean relative peak height	% RSD
Coiled	3.67	1.67
Straight	3.77	0.89
Knitted	3.94	1.06

5.5.2.1.4 Reaction coil 2

In the final stage of the sequential analyzer merging zones from the first reaction coil are propelled forward by the peristaltic pump through the second reaction coil to the flow-cell of the detector. Maximum peak response and precision are obtained when the dimensions of this reactor coil are well-defined. Tube diameter, line length and geometry of the second reaction coil were thus evaluated for the best conditions for the system.

A number of tube diameters (0.51 - 1.59 mm) were evaluated. There was a general tendency for the formed penetrated product zone of barium sulphate suspension to disperse more in the tubing when the diameter increases from 0.51 to 1.59 mm resulting in a decrease in peak height (Fig. 5.8). The reproducibility of the product zone was also difficult to define, but a

tube diameter of 0.64 gave the best mean relative peak height and precision and was chosen for the proposed system.

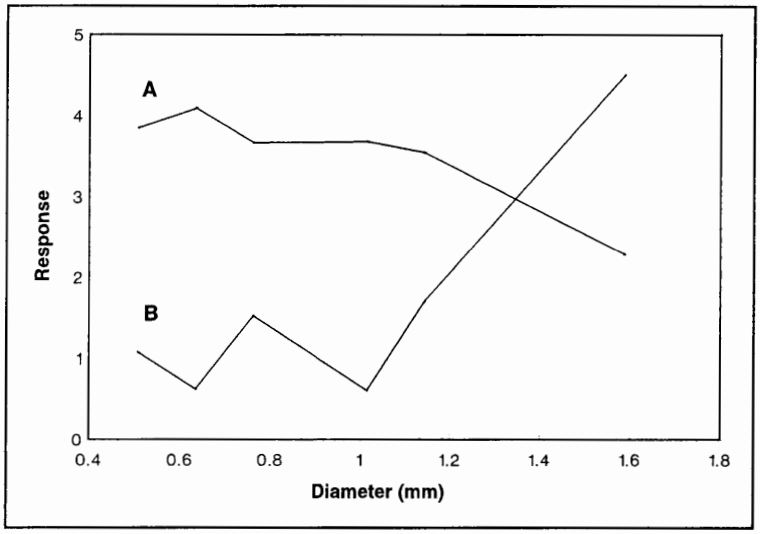

Fig. 5.8 Influence of tube diameter of reactor 2 on relative peak height (A) and precision (B - %RSD).

Line lengths between 0.6 and 1.4 m were evaluated for reactor 2. The differences in mean relative peak height for line lengths between 0.6 and 1.4 m were not significant (Table 8) which means that the overall dispersion of the formed product zone of barium sulphate suspension did not alter very much for this range of length. The best precision for the proposed system were obtained between 0.8 and 1.2 m and the worst for line lengths shorter than 0.6 m and longer than 1.4 m. The optimum length was chosen as 1.0 m.

TABLE 8. Effect of line length of reactor 2 on sensitivity and precision

Length (m)	Mean relative peak height	% RSD
0.6	3.90	1.05
0.8	3.92	0.69
1.0	4.04	0.74
1.2	3.86	0.69
1.4	3.74	1.24

Three types of geometry *viz.* coiled, straight and knitted were studied for reactor 2. There are no significant differences between the mean relative peak heights of the three types of geometries (Table 9). The straight configuration propelled the formed product zone with the lowest RSD of 0.91% and was selected as optimum for the proposed system.

TABLE 9. Effect of the geometry of reactor 2 on sensitivity and precision

Geometry	Mean relative peak height	% RSD
Coiled	4.02	1.94
Straight	4.06	0.91
Knitted	4.10	2.22

5.5.2.2 Chemical parameters

5.5.2.2.1 Optimisation of the barium chloride reagent

The formation of the correct barium sulphate suspension in the conduits of the sequential injection system was of critical importance in the precision of the proposed process analyzer.

This was achieved by the optimization of the barium chloride reagent solution. The following solutions was used in the optimization process.

Solution (i) [17 - 19]: 0.2 g Thymol crystals were dissolved in 500 mℓ of 0.005 mol.ℓ^{-1} HCl at a temperature of about 80 °C. The solution was cooled to 40 °C and 1.5 mℓ of 0.005 mol.ℓ^{-1} HCl was added. 4 g of gelatine was added very slowly and the solution was stirred until dissolved. When dissolved, 20 g of $BaCl_2.2\ H_2O$ was added. Preparation of this solution resulted in a white solution due to sulphate impurities in the gelatine reagent. This gave rise to a relatively high background value. This method was not sensitive enough to discriminate between the signals obtained for the background, 1 mg.ℓ^{-1} and 10 mg.ℓ^{-1} sulphate solutions. The difference between the signals obtained for the background, 100 and 200 mg.ℓ^{-1} sulphate solutions were however significant, as a difference of almost 2 units (on a measuring scale of 7 units) on the data system was obtained. It seems that this reagent was ruled out for samples with sulphate contents lower than 100 mg.ℓ^{-1}.

Solution (ii): 10 g of $BaCl_2.2\ H_2O$ was dissolved in distilled water and diluted to 1 ℓ.
The use of this solution resulted in very small peaks and it was obvious that a system containing this reagent solution was neither sensitive nor precise. However, a preliminary evaluation of the solution indicated that when the solution was acidified, the results improved with an increase in sensitivity.

The influence of pH on the absorbance of a 200 mg.ℓ^{-1} standard sulphate solution for both barium chloride solutions (*i* and *ii*) was therefore evaluated at two different wavelengths and the results obtained, are outlined in Table 10.

TABLE 10. Effect of pH on the absorbance of a 200 mg.ℓ^{-1} standard sulphate solution at different wavelengths

Sample pH	Abs. of $BaSO_4$ (*i*) at 420 nm	Abs. of $BaSO_4$ (*i*) at 540 nm	Abs. of $BaSO_4$ (*ii*) at 420 nm	Abs. of $BaSO_4$ (*ii*) at 540 nm
1	0.428	0.521	0.163	0.403
2	0.449	0.522	0.388	0.418
2.5	0.850	0.966	0.392	0.420
3	0.665	0.659	0.793	0.536
4	0.450	0.524	0.706	0.779
5	0.433	0.458	0.659	0.633
7.69	0.434	0.378	0.532	0.549

It is obvious from Fig. 5.9 that the barium chloride solution (*i*) with a pH of 2.5 gave the best sensitivity. As the pH of the samples varied, the results obtained were however not consistent, the precision was poor and it was therefore necessary to use a buffer of pH 2.5 to prepare the reagent.

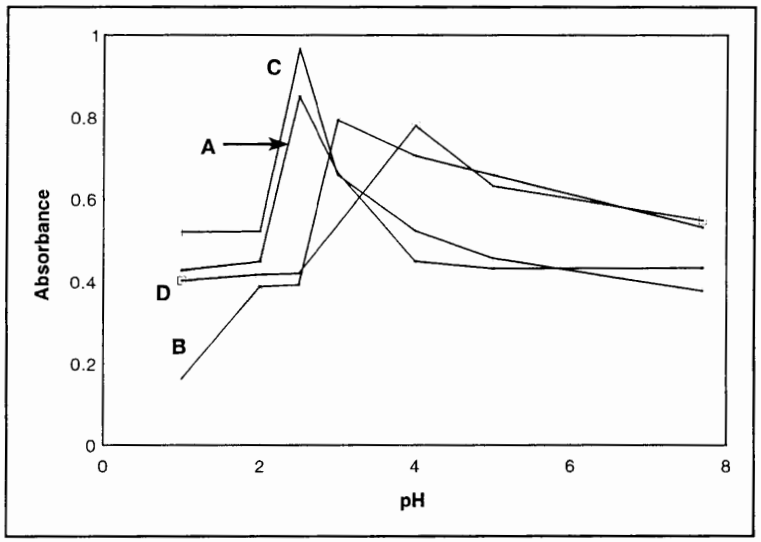

Fig. 5.9 Influence of $BaCl_2$-reagent on the absorbance of the $BaSO_4$ suspension. (A - absorbance at 420 nm using reagent *i*, B - absorbance at 420 nm using reagent *ii*, C - absorbance at 540 nm using reagent *i* and D - absorbance at 540 nm using reagent *ii*.)

Solution (iii): From the results obtained for solutions (*i* and *ii*) solution *iii* was prepared. A barium chloride solution containing a potassium hydrogen phthalate - hydrochloric acid buffer at pH 2.5 was prepared by adding 388 mℓ of a 0.1 mol.ℓ^{-1} HCl solution to 500 mℓ of a 0.1 mol.ℓ^{-1} potassium hydrogen phthalate solution. $BaCl_2.2\ H_2O$ (10 g) was dissolved in this buffer and the solution was diluted to 1 ℓ. The same results were obtained with this reagent (*iii*) as obtained with the reagent without the buffer (*ii*). The precision still remained poor with an RSD of 7.7%. Another problem experienced with this solution was that the potassium hydrogen phthalate precipitated when it was left overnight and had to be redissolved every morning. Addition of 0.062 g gelatine per 100 mℓ improved both the sensitivity and the reproducibility remarkedly. The problem with the overnight precipitation of potassium hydrogen phthalate was also solved as it seemed as if the gelatine stabilized the solution. The addition of gelatine however gave rise to a background value (due to sulphate impurities in the gelatine), but this value was very small compared to the analyte peak and the reproducibility was very good. The reagent was filtered through a Millipore membrane (type HA) (45 μm). This reduced the background value completely. This reagent solution was stable for up to six months. To prevent bacterial growth, 0.1 g thymol per 100 mℓ solution was added.

5.5.2.2.2 Sequences of sample and reagents

It was clear from initial experiments that the proposed sequential injection system would need a sequence of four stacks of zones *viz.* an alkaline buffer-EDTA, water, barium chloride reagent and sample to obtain a high degree of sensitivity, accuracy and precision. The order in which the different sequences of reagents and sample are drawn up and propelled into the

detector is very important in SIA. The results obtained, revealed that the alkaline buffer-EDTA solution had to be separated from the acidified barium chloride reagent solution by a water zone. There were therefore only two zones that need to be properly mixed. The sample zone was initially placed between the water and barium chloride reagent zones, but that gave a mean relative peak height of 4.13 with an RSD of 0.92%. When the zones were changed and the barium chloride reagent zone was placed between the water and the sample, better results were obtained, with a mean relative peak height of 4.93 and an RSD of 0.89%. The optimum zone order is shown schematically in Fig. 5.10.

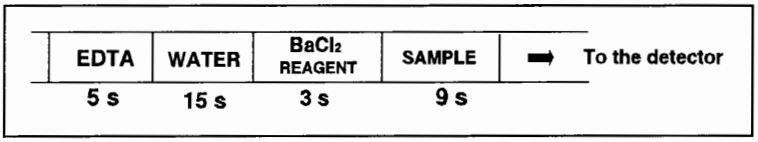

Fig. 5.10 Sequence of EDTA (wash solution), water, $BaCl_2$-reagent, sample and detection.

5.5.2.2.3 Volume of the barium chloride reagent solution

The volume of the barium chloride reagent solution is a function of both the flow rate as well as the period the reagent is drawn up. The influence of a number of reagent volumes on sensitivity and precision were evaluated by changing the period in which the reagent was drawn up. The results obtained, are summarised in Table 10.

TABLE 10. Effect of reagent volume on sensitivity and precision

Volume (μl)	Mean relative peak height	% RSD
83.3	4.46	2.47
166.7	4.83	2.62
250	4.94	1.43
333.3	4.85	1.45
416.7	4.92	2.07
500	4.84	4.02

The reagent volume of 250 μl gave the best sensitivity and precision and was chosen for the proposed SI analyzer.

5.5.2.2.4 Sample volume

The sample volume also depends on the flow rate as well as the period the sample is drawn up. Various volumes were examined and the results are summarised in Fig. 5.11.

A sample volume of 750 μl was selected for the proposed system due to the best sensitivity and precision. It seems that larger volumes ($>$ 750 μl) will result in better sensitivity. This is however not the case. When the sample zone became too large a decrease in zone overlap was observed.

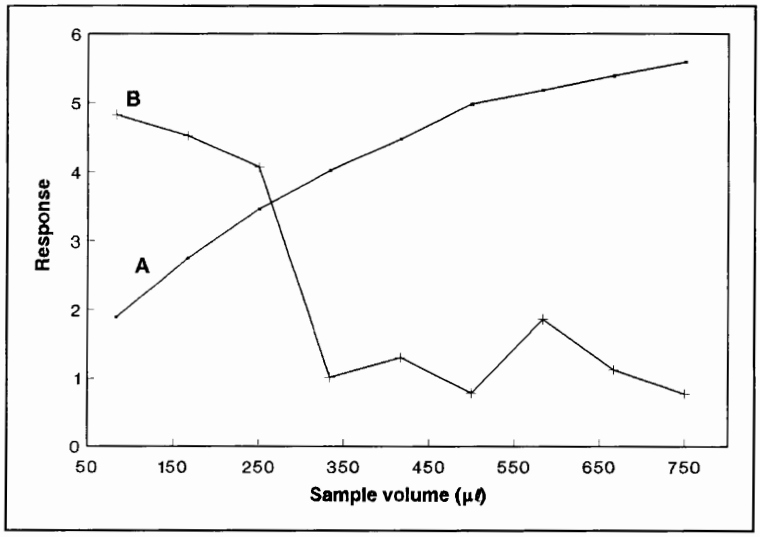

Fig. 5.11 Influence of sample volume on zone penetration (A) and precision (B - %RSD).

5.5.3 Method evaluation

The proposed sequential injection analyzer was evaluated with regard to linearity, accuracy, precision, detection limit, sample interaction (carry-over), interferences and sampling rate.

5.5.3.1 Linearity

The linearity of the proposed SIA system for the turbidimetric determination of sulphate was evaluated under optimum running conditions. The relationship obtained for relative peak height versus sulphate ion concentration was:

$$y = 0.0278x + 0.5195; \quad r = 0.9982$$

where y = relative peak height and x = sulphate ion concentration in mg.ℓ^{-1}. The correlation coefficient (r) indicated that the method was linear for an analyte concentration ranging between 10 and 200 mg.ℓ^{-1}.

5.5.3.2 Accuracy

Real samples were analyzed with the SIA system. The accuracy of the proposed SIA analyzer was evaluated by comparing the results obtained from the real samples with the SIA system with the values obtained by ion chromatography (results obtained from MINTEK, Randburg South Africa) and with values obtained with an AutoAnalyser (results obtained from the Institute for Water Quality Studies, Pretoria, South Africa). The results as shown in Table 11 and 12 revealed a good correlation between the SIA system and the values obtained by ion chromatography and the AutoAnalyzer respectively.

TABLE 11. Comparison of results of a number of samples as determined with the proposed SIA system and ion chromatography

Sample	SIA ([ ] in mg.ℓ^{-1})	Ion chromatography ([ ] in mg.ℓ^{-1})
Sample A	13.6	15.1
Sample B	49.4	46.7
Tap water	35.2	33.6
D32W	189.5	202

TABLE 12. Comparison of results of a number of samples as determined with the SIA system and an AutoAnalyser

Sample	SIA ([ ] in mg.ℓ^{-1})	AutoAnalyser ([ ] in mg.ℓ^{-1})
95730825	45.2	45.1
95730862	73.9	75.1
95730886	8.6	10.1
95730904	19.1	18.6
95730916	179.3	188.9
95730930	112.8	121.9
95730990	18.6	22.2
95731003	120.5	115.8
95731015	140.7	136.8
95731027	31.9	35.9
95731039	30.0	34.4
95731064	121.6	125.1
95731088	157.8	152.5
95731118	46.6	49.6
95731155	141.1	148.0

A method of standard addition was also used to determine the concentration in one of the samples obtained from the Institute for Water Quality (Sample 95730825). This was done to confirm the value obtained by the SIA procedure. A linear calibration curve was obtained ($r = 0.9995$) and the concentration of sulphate in the sample was calculated as 45.2 mg.ℓ^{-1} which compared well with both the SIA and AutoAnalyser methods.

5.5.3.3 Precision

The precision of the method was determined by 10 repetitions of each standard solution in the linear range of the specific method as well as 10 repetitions of each sample within the range. The results of some of these repetitions are listed in Table 13.

TABLE 13. Precision of the proposed SIA system

Standard/Sample ([ ] in mg.ℓ^{-1})	% RSD
10	1.22
20	2.81
50	2.57
100	1.10
150	2.44
200	1.43
Sample A	3.05
Sample B	0.67
Tap water	3.81
D32W	1.36

A precision of less than 3.9% RSD was obtained.

In order to ensure high sensitivity and reproducibility Nakashima *et al* [15] found that it was necessary to saturate the carrier solution with barium sulphate and to fill the reaction coil with ethanol-water (1 : 1) when not in use. It was however not necessary to saturate the reagent solution with barium sulphate.

5.5.3.4 Detection limit

The detection limit is both a function of sensitivity and noise. The detection limit of the method was calculated using the formula

$$Detection\ limit = \frac{3 \times S_k}{100} \times K$$

where $S_k = 1.22$ is the relative standard deviation of the lowest concentration of the specific method and K = 10 mg.ℓ^{-1} is the lowest standard concentration for this method. The detection limit was calculated to be 0.37 mg.ℓ^{-1}. There is however reason to doubt the validity of this theoretical detection limit, for the dynamic range for this method is 10 - 200 mg.ℓ^{-1}. Madsen and Murphy [13] stated that barium sulphate turbidimetric methods have been successful only when sulphate concentrations in the sample of interest are above 10 mg.ℓ^{-1}. The detection limit is therefore taken as 10 mg.ℓ^{-1}.

The detection limit is instrument dependant below 10 mg.ℓ^{-1} sulphate [39]. It is suggested that if concentrations of below 10 mg.ℓ^{-1} need to be determined, either another method (e.g. methylthymol blue method) or sample preconcentration should be used depending on the instrument design.

5.5.3.5 Sample interaction

One of the problems associated with the barium sulphate turbidimetric procedure, is the built-up of barium sulphate precipitate in the flow system which tends to settle in the flow-cell. This leads to low precision and ultimately blocks the manifold. The addition of an alkaline buffer-EDTA solution to redissolve the accumulated barium sulphate precipitate is one way of overcoming the problem.

Baban *et al* [38] used a carrier solution of barium(II) ions with an excess of EDTA in alkaline medium (pH 10) to dissolve any accumulated precipitate. Precipitation occurs under the very acidic conditions of the well-defined zone (pH 1.5 - 2.5) in the analytical manifold where a pH-gradient in the sampling zone is established. The precipitate is, however, redissolved outside this zone by the self-cleansing action of the excess alkaline-EDTA carrier solution. By using pH-gradients and alkaline-EDTA a sufficiently stable barium sulphate suspension is obtained, which obviates the use of protective colloids such as polyvinyl alcohol or thymol gelatine.

Van Staden [17] used a different approach by utilising 60 $\mu\ell$ water samples from one loop of a two position sampling valve alternating with an alkaline buffer-EDTA solution (100 $\mu\ell$) from the second loop which was injected into a barium sulphate-thymol-gelatine single line carrier stream. This ensures that the residual precipitate, coating the walls of the flow-cell, is redissolved and the system kept clean.

Sample interaction was determined using the equation:

$$Interaction = \frac{(A_3 - A_1)}{A_2} \times 100$$

where

A_1 = the true peak height of a sample with a low analyte concentration (10 mg.ℓ^{-1}),

A_2 = the true peak height of a sample containing ten times more analyte (100 mg.ℓ^{-1}), and

A_3 = the peak height for an interacted sample containing the same amount of analyte as A_1.

The relative peak heights of A_1, A_2 and A_3 were respectively 0.45, 3.57 and 0.47. The sample interaction between samples as calculated was 0.56% which is neglible. Sample interaction is reduced effectively by the EDTA-solution that rinse the system after every experiment.

5.5.3.6 Sample frequency

The sampling rate is calculated by dividing 3600 s (1 h) through the time (in seconds) needed to complete one experiment. It took 138 sec to complete one sampling cycle which gave a sample frequency of about 26 per hour.

5.5.3.7 Interferences

There are a number of ions that may be possible interferences in the samples analyzed and these interferences were evaluated. An industrial effluent (D32W) with the values of ions present in the sample is given in Table 14. The concentrations of the various ions were obtained with ion chromatography by MINTEK. Table 14 also listed the concentration where these ions started to interfere.

TABLE 14. Effect of some interfering ions on the determination of sulphate

Ion	Concentration present in sample D32W ($mg.\ell^{-1}$)	Concentration where interference start ($mg.\ell^{-1}$)	Effect
Ca^{2+}	78	10 50	Decrease in relative peak height by 0.9967% Increase in relative peak height by 1.2477%
Mg^{2+}	30	10 100	Decrease in relative peak height by 0.5979% Increase in relative peak height by 1.7020%
Zn^{2+}	0.40	200	Decrease in relative peak height by 3.5353%
Mn^{2+}	1.5	10	Decrease in relative peak height by 7.5457%
Co^{2+}	< 0.05	200	Decrease in relative peak height by 6.7605%
Na^{+}	85	200	No interference
K^{+}	15	200	No interference
Cl^{-}	65	200	Decrease in relative peak height by 9.9471%

Of all the cations only calcium was present in concentrations that would interfere with the determination of sulphate in the proposed SIA analyzer. Nakashima *et al* [15] stated that the

'calcium ion in river water severely interferes with the determination of sulphate'. The interferences by calcium was eliminated by a cation-exchange column in the sampling line. The influence of the calcium interference with and without a cation-exchange column is shown in Fig. 5.12.

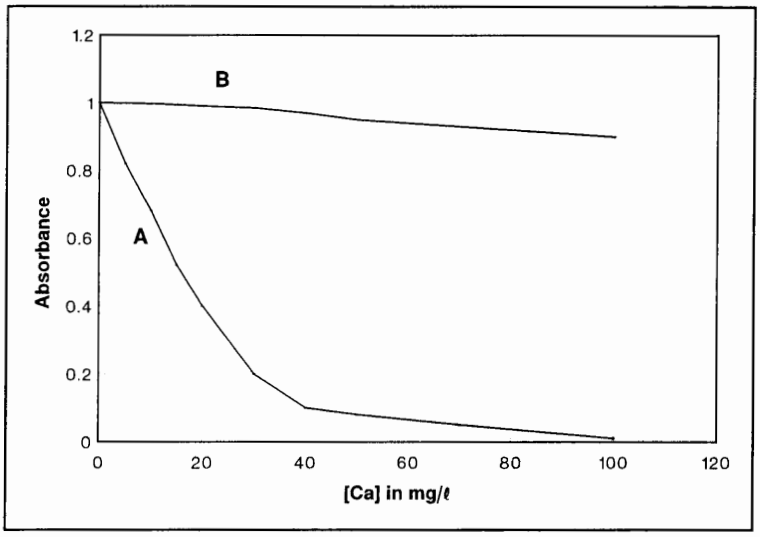

Fig. 5.12 Effect of calcium on the determination of sulphate with (B) and without (A) the cation-exchange column.

A number of the cations, as well as anions, interfere in the determination of sulphate. The addition of the cations to the sulphate standard seemed to change the ionic environment. This change results in a change in the conditions effecting particle formation. This effect is called a salt error, where high concentrations of ions not common to a reaction increase the overall ionic strength of the solution and so change the solubility of salts and equilibria of complex formation. Most of the complexes formed between the cations and sulphate are soluble in water and are not suppose to interfere by forming a precipitate.

The main interfering substances, bicarbonate, carbonate (alkalinity) and chloride, are all present at levels not usually found in raw and potable waters. The interferences, apart of that of carbonate, are probably due to physical rather than chemical effects; viscosity and refractive index differences between sample and carrier can cause mixing boundaries. The alkalinity interference is probably due to consumption of the acid in the reagent.

Bismuth, iron, cerium, manganese, antimony, selenium, tin, tellurium, thorium and vanadium interfere in the determination of sulphate. These interferences can be eliminated by cation exchange. Interferences due to fluoride and phosphate can be removed by pretreatment with magnesium oxide [36]. Hydrochloric acid is added to the barium chloride solution to prevent the formation of precipitates of carbonate, chromate, sulphite, phosphate and oxalate of barium which may interfere [19]. Nakashima *et al* [15] found however that Mg^{2+} and NH_4^+ (30 mg.ℓ^{-1}), Na^+ (50 mg.ℓ^{-1}), K^+ (80 mg.ℓ^{-1}) and Cl^-, NO_3^-, PO_4^{3-}, HCO_3^- and SiO_3^{2-} (100 mg.ℓ^{-1}) do not interfere with the sulphate determination at levels which are normally present in natural waters. Jones [36] found that amounts of sodium up to a maximum concentration of 4 g.ℓ^{-1} had no effect on the recovery of sulphate. At low pH levels $Fe_2(SO_4)_3$ hydrates precipitates and interferes in the determination of sulphate [25].

Nakashima *et al* [15] used an ion exchange column (3 mm id x 8 cm) packed with Amberlite IR-120B (H-form, particle size: 20 - 50 mesh) cation-exchange resins. They also found that when placing the cation-exchange column in the flow line better results were obtained compare to the placing of the column in the sample line [14, 20]. The latter position is the only position possible to use in SIA, because only a single flow line manifold is used. The life time of the cation-exchange column was found to be at least two months when regularly

used. Madsen and Murphy [13] used a 22 x 0.32 cm pretreated column packed with Dowex 50 x 8 (20 - 50 mesh) cation-exchange resin in the hydrogen form to separate the interfering ions from the sample.

The other problems associated with the procedure are suspended solids, the presence of organic substances and colour in samples which interfere at 420 or 540 nm. Van Staden [18] solved this problem by using a similar automated method previously described [17] together with automated pre-valve sample filtration in a packed carbon tube as part of the sample line. This method was improved by switching to active carbon filter paper [18]. This ensures a great improvement in accuracy of some water samples with no loss in other features.

5.6 Conclusions

A sequential injection analyzer was developed to monitor the sulphate ion concentration in the effluents of chemical process industries as well as the natural waters downstream. Incorporation of an alkaline buffer-EDTA solution in the correct sequence of the system redissolved accumulated barium sulphate precipitate to give a high degree of sensitivity, accuracy and precision. The proposed system is fully computerised and is able to monitor sulphate in samples at a frequency of 26 samples per hour with a relative standard deviation of 3.9%. The calibration curve is linear between 10 and 200 mg.ℓ^{-1}.

5.7 References

1. American Society for Testing and Materials, **'1973 Book of ASTM Standards. Part 23. Water: Atmospheric Analysis'**, ASTM. Philadelphia, 1973, pp. 425 - 431.
2. W. C. Schroeder, **Ind. Eng. Chem.**, **5** (1933) 403.
3. J. W. Ross and M. S. Frant, **Anal. Chem.**, **41** (1969) 967.
4. **Orion Res. Newsl.**, **2** (1970) 21.
5. A. Hulanicki, R. Lewandowski and A. Lewenstam, **Analyst**, **101** (1976) 939.
6. E. P. Scheide and R. A. Durst, **Anal. Lett.**, **10** (1977) 55.
7. M. Trojanowics and A. Hulanicki, **Chem. Anal.** (Warsaw), **22** (1977) 615.
8. J. Vesely, **Collect. Czech. Chem. Commun.**, **46** (1977) 368.
9. R. J. Bertolacini and J. E. Barney, **Anal. Chem.**, **29** (1957) 281.
10. J. Agterdenbos and N. Martnius, **Talanta**, **11** (1964) 875.
11. A. L. Lazrus, K. C. Hill and J. P. Lodge, **'A New Colorimetric Microdetermination of Sulphate Ion'**, Technicon Symposia 1965, Automation in Analytical Chemistry, Mediad Inc., New York, 1966, p. 291.
12. R. T. Sheen, H. L. Kahler, E. M. Ross, W. H. Betz and L. D. Betz, **Chem. Anal. Ed.**, **7** (1935) 262.
13. B. C. Madsen and R. J. Murphy, **Anal. Chem.**, **53** (1981) 1924.
14. H. F. R. Reijnders, J. J. van Staden and B. Griepink, **Fresenius' Z. Anal. Chem.**, **295** (1979) 410.
15. S. Nakashima, M. Yagi, M. Zenki, M. Doi and K. Toei, **Fresenius' Z. Anal. Chem.**, **317** (1984) 29.
16. K. Yakata, F. Sagara, I. Yoshida and K. Ueno, **Anal. Sciences**, **6** (1990) 711.

17. J. F. van Staden, **Fresenius' Z. Anal. Chem.**, **310** (1982) 239.

18. J. F. van Staden, **Fresenius' Z. Anal. Chem.**, **312** (1982) 438.

19. J. F. van Staden, **Water S A**, **12** (1986) 43.

20. O. Kondo, H. Miyata and K. Tóei, **Anal. Chim. Acta.**, **134** (1982) 353.

21. F. J. Krug, F. H. Bergamin, E. A. G. Zagatto and S. S. Jorgensen, **Analyst**, **102** (1977) 503.

22. W. D. Basson and J. F. van Staden, **Lab. Practice**, **25** (1978) 863.

23. W. D. Basson and J. F. van Staden, **Water Research**, **15** (1981) 333.

24. G. D. Marshall and J. F. van Staden, **Analytical Instrumentation**, **20**(1) (1992) 79.

25. N. N. Greenwood and A. Earnshaw, **Chemistry of the Elements**, Pergamon Press, 1986.

26. P. La Bonville, R. Kugel and J. R. Ferraro, **J. Chem. Phys.**, **67** (1977) 1477.

27. G. D. Marshall, **Sequential-Injection Analysis**, PhD-Thesis, University of Pretoria, 1994.

28. G. D. Marshall and J. F. van Staden, **Process control and Quality**, **3** (1992) 251.

29. J. F. van Staden, **S. A. J. Chem.**, **48** (1995) 8.

30. M. Valcarcel and M. D. Luque de Castro, **Flow Injection Analysis. Principles and Applications**, Ellis Horwood, Chichester, 1987.

31. J. Růžička and E. H. Hansen, **Flow Injection analysis**, 2nd ed, John Wiley & Sons, New York, 1988.

32. T. Gűbeli, G. D. Christian and J. Růžička, **Anal. Chem.**, **63** (1991) 2407.

33. D. J. Tucker, B. Toivola, C. H. Pollema, J. Růžička and G. D. Christian, **Analyst**, **119** (1994) 975.

34. J. Fries and H. Getrost, **Organic Reagents for Trace Analysis**, E. Merck,

Darmstadt, 1977.

35. E. A. Jones, **Anal. Chim. Acta.**, **156** (1984) 313.

36. E. A. Jones, **MINTEK report M111**, 1983, pp 7 - 10.

37. L. W. Potts, **Quantitative Analysis. Theory and Practice**, Harper and Row, New York, 1987.

38. S. Baban, D. Beetlestone, D. Betteridge and P. Sweet, **Anal. Chim. Acta.**, **114** (1980) 319.

39. **Sulphate in Waters, Effluents and Solids.** Methods for the Examination of Waters and Associated Materials, 2nd ed, London, HMSO, 1988.

CHAPTER 6

On-line Dilution performed by Sequential Injection Analysis

6.1 Introduction

One of the prerequisites of an on-line process analyzer or monitoring system for industrial effluents is the capability to monitor the content of certain components over a wide concentration range including highly concentrated solutions. A practical drawback of most instrumentation is the narrow linear response range of the detection system. For some samples the analyte concentration may be too high for direct measurement and analysis may require extensive dilution as an essential step in sample pretreatment. For example, industrial processes and effluents where sulphate is involved, contain sulphate ranging from near zero up to about 5 000 mg.ℓ^{-1} and even more. Manual dilution of samples is often necessary prior to performing analysis, but these are time consuming, tedious, expensive and operator intensive when used in routine analysis and cannot be applied in on-line monitoring systems. Furthermore, manual dilution of samples is often a source for experimental errors. Most commercial diluters and robots operate batch-wise and are designed to produce diluted, homogeneous solutions where equilibrium prevails. These techniques are however also time- and solvent-consuming sample pretreatment methods.

So far flow injection analysis (FIA) was accepted as an alternative analytical technique which is suitable to perform automated dilution under non-equilibrium conditions of sample solutions which are too concentrated for direct measurement. Various approaches have been used for automated on-line dilutions in FIA. These include, increase of the dispersion coefficient by decreasing the sample volume or by increasing the radius or length of the flow system tubing [1], by automated prevalve dilution before sample injection [2], by utilizing gradient dilution [3], by gradient chamber-based single-line dilution [1, 4, 5], merging streams [6], zone sampling [7], cascade dilution [8], gradient chamber-based zone sampling [9, 10], split zone sampling [11], dialysis [12 - 14] and mixing chambers [26]. Among the various FIA on-line dilution systems reported, the zone penetration (originally termed the sequential injection) approach [15] was shown to be one of the most versatile and routinely applied techniques for on-line dilution [16, 17]. A fundamental characteristic of sequential injection analysis (SIA) [18 - 22] is zone penetration with which controlled, precise sample manipulations can be automated. A single standard calibration and dilution method employing a dilution conduit for storing a concentration gradient of an injected analyte utilizing SIA was described [23].

This chapter describes an on-line dilution SIA system where the concept of zone penetration is exploited in an automated in-line dilution step in a system for monitoring sulphate in industrial effluents.

6.2 Experimental

6.2.1 Reagents and solutions

All reagents were prepared from an analytical-reagent grade unless specified otherwise. All aqueous solutions were prepared with doubly distilled deionised water. All solutions were degassed before measurements with a vacuum pump system.

A stock standard sulphate solution containing 5 000 mg.ℓ^{-1} of sulphate was prepared by dissolving 16.7715 g $Na_2SO_4 \cdot 10\ H_2O$ in distilled water and diluting it to 1 ℓ. Working solutions in the range of 1 - 5 000 mg.ℓ^{-1} was prepared by suitable dilution of the stock solution.

A buffer solution containing, 40 g of EDTA (disodium salt), 7 g of ammonium chloride and 57 mℓ concentrated ammonia (sp. gr. 0.88), was prepared by dissolving the different chemicals in succession in 600 mℓ of distilled water and diluting to 1 ℓ.

A barium chloride reagent solution containing a potassium hydrogen phthalate - hydrochloric acid buffer at pH 2.5 was prepared by adding 388 mℓ of a 0.1 mol.ℓ^{-1} HCl solution to 500 mℓ of a 0.1 mol.ℓ^{-1} potassium hydrogen phthalate solution. 10 g of $BaCl_2 \cdot 2\ H_2O$, 1.0 g thymol and 0.62 g gelatine were dissolved in this buffer and the solution was diluted to 1 ℓ. The reagent was filtered through a Millipore membrane (type HA) (45 μm).

6.2.2 Apparatus

The sequential injection system used in this work was constructed from the following components: a Gilson minipuls peristaltic pump (Model M312, Gilson, Villiers-le-Bel, France); a 10-port electrically actuated selection valve (Model ECSD10P; Valco Instruments, Houston, TX, USA); and a Unicam 8625 UV-visible spectrophotometer equipped with a 10-mm Hellma (Hellma GmbH & Co., Mülheim/Baden, Germany) type flow-through cell (volume: 80 $\mu\ell$) for absorbance measurements. The barium sulphate suspension formed, was monitored by measuring the absorbance at 540 nm. Data acquisition and device control were achieved using a PC30-B interface board (Eagle Electric, Cape Town, South Africa) and an assembled distribution board (MINTEK, Randburg, South Africa). The *FlowTEK* [22] software package (obtainable from MINTEK, Randburg, South Africa) for computer-aided flow-analysis was used throughout for device control and data acquisition. Tygon tubing was used for the holding and reaction coils.

6.2.3 Manifold

Two manifold SIA systems were evaluated; a system including a dilution step and one with a dilution coil in the manifold conduits. The components of the SIA system including a dilution step were arranged as illustrated in Fig. 6.1A. The holding coil was made of 2.8 m x 1.02 mm id coiled Tygon tubing, reaction coil 1 of 1.3 m x 1.02 mm id straight Tygon tubing and reaction coil 2 of 1.0 m x 0.64 mm id straight Tygon tubing. The sampling, standard and reagent lines were made of 45 cm x 1.1 mm id Tygon tubing. The flow rate used, was 5.0 $m\ell.min^{-1}$. The optimum zone order is shown in Fig. 6.1B. Dilution is done

by the well-defined water zone between the barium chloride reagent zone and the sample zone. The degree of dilution obtained, depended on the timing sequence allowed for the dilution step. A timing sequence between 0 and 15 seconds was used.

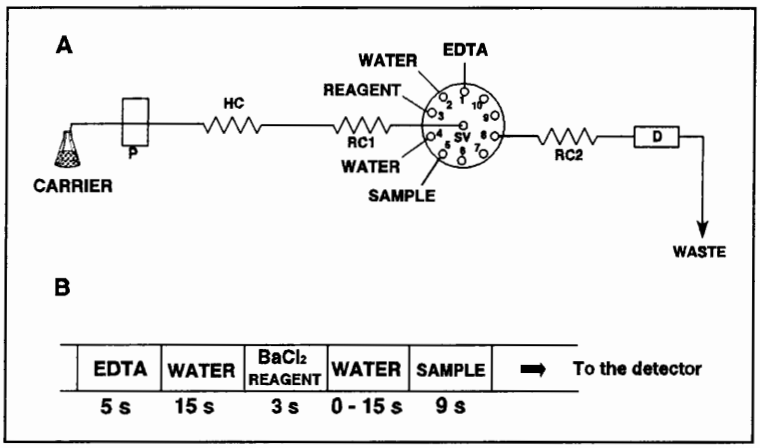

Fig. 6.1 A schematic diagram of the SIA analyzer (A) using a dilution step as timing sequence to monitor sulphate in industrial effluents. P - pump, HC - holding coil, RC - reaction coil, SV - selection valve and D - detector. (B) Sequence of zones.

The components of the SIA system using a dilution coil were arranged as outlined in Fig. 6.2A. The holding coil was made of 2.8 m x 1.02 mm id coiled Tygon tubing, reaction coil 1 of 1.3 m x 1.02 mm id straight Tygon tubing, reaction coil 2 of 1.0 m x 0.64 mm id straight Tygon tubing and the dilution coil of 1.24 m x 0.76 mm id coiled Tygon tubing. The sampling, standard and reagent lines were made of 45 cm x 1.1 mm id Tygon tubing. The flow rate used, was 5.0 $m\ell.min^{-1}$. The optimum zone order is shown in Fig. 6.2B.

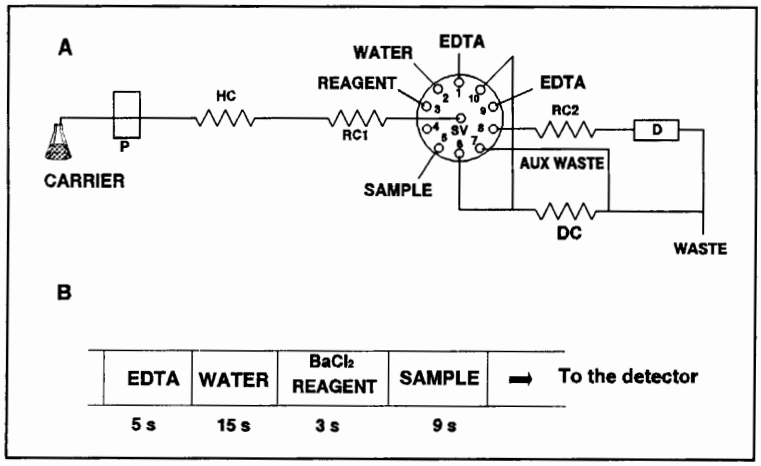

Fig. 6.2 A schematic diagram of the SIA analyzer using a dilution coil (A) to monitor sulphate in industrial effluents. P - pump, HC - holding coil, RC - reaction coil, SV - selection valve, DC - dilution coil and D - detector. (B) Sequence of zones.

6.2.4 Procedure

The device sequence used for dilution, with a dilution coil, is given in Table 1 and the device sequence for dilution, with a dilution step between the sample and reagent zones, in Table 2. This sequence is for a dilution step of 6.5 s.

TABLE 1. Device sequence of the sequential injection system with a dilution coil

Time (s)	Pump	Valve	Description
0	Off	Off	Pump off
1		Detector	Select detector line
7	Forward		Pump wash solution through detector
46	Off		Pump stop
47.5		EDTA	Select EDTA (wash) stream
49.5	Reverse		Draw up EDTA solution
54.5	Off		Pump stop
56		Dilution coil	Select line to dilution coil
57	Forward		Pump wash solution through dilution coil
77	Off		Pump stop
78.5		EDTA	Select EDTA stream
80.5	Reverse		Draw up EDTA solution
85.5	Off		Pump stop
86.5		Water	Select water stream
88	Reverse		Draw up water
103	Off		Pump stop
104.5		$BaCl_2$	Select $BaCl_2$ stream
105.5	Reverse		Draw up $BaCl_2$-solution
108.5	Off		Pump stop
109.5		Sample	Select sample stream
111.5	Reverse		Draw up sample/standard solutions
120.5	Off		Pump stop
122		Dilution coil	Select line to dilution coil
124	Forward		Pump stack of zones to dilution coil
139	Off		Pump stop
140	Reverse		Draw up a part from the formed $BaSO_4$
148	Off		Pump off
150		Detector	Select detector line
152.5	Forward		Pump stack of zones to detector
182.5	Off		Return pump and valve to starting position

TABLE 2. Device sequence of the sequential injection system using a dilution step

Time (s)	Pump	Valve	Description
0	Off	Off	Pump off
1		Detector	Select detector line
7	Forward		Pump wash solution through detector
51.5	Off		Pump stop
53.5		EDTA	Select EDTA (wash) solution
57.5	Reverse		Draw up EDTA solution
62.5	Off		Pump stop
63.5		Water	Select water stream
65	Reverse		Draw up water
80	Off		Pump stop
82		$BaCl_2$	Select $BaCl_2$ stream
83	Reverse		Draw up $BaCl_2$-solution
86	Off		Pump stop
87		Water	Select water stream
88.5	Reverse		Draw up water (dilution step)
95	Off		Pump stop
96		Sample	Select sample stream
98	Reverse		Draw up sample/standard solutions
107	Off		Pump stop
108		Detector	Select detector line
110.5	Forward		Pump stack of zones to detector
147	Off		Return pump and valve to starting position

6.3 Parameters effecting the magnitude of dilution

6.3.1 SIA system with dilution coil

This method of dilution describes a system where one port on the multiposition valve is dedicated to holding a dilution conduit, a tube where a concentration gradient of the analyte is stored. This gradient is then used to generate a set of diluted standard aliquots. When the formed product zone is transferred into the dilution conduit, it generates a concentration gradient along the physical length of the dilution conduit (Fig. 6.3). Aspiration of a fixed volume from the dilution conduit back into the holding coil, and then propelling it to the detector, effectively takes a slice of the concentration profile established in the dilution conduit.

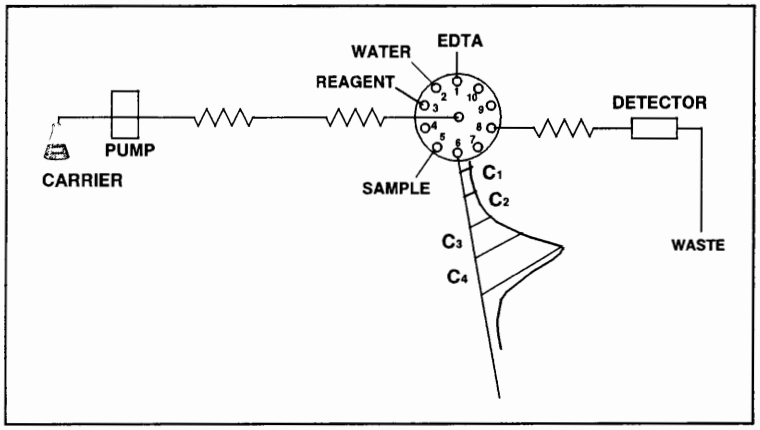

Fig. 6.3 Generation and storage of the concentration gradient of the formed product zone in the dilution conduit. C_x - fixed volumes to generate different magnitudes of dilution.

Control over the magnitude and range of dilution for a particular conduit is effected by four volume parameters. These parameters are:

(1) The sample volume (V_s)

(2) The reagent volume (V_r)

(3) The transfer volume (V_t)

(4) The analysis volume (V_a)

(1) Sample volume

The sample volume (V_s) is the amount of sample or standard which is withdrawn into the holding coil via the sample port. The influence of the sample volume on the magnitude of dilution was determined and the results are shown in Fig. 6.4. It is clear from Fig. 6.4 that the higher the sample volume, the higher the relative peak height. It may therefore be concluded that changing the injected sample volume is an effected way to change the sensitivity of the measurement. Dilution of concentrated sample material is best achieved by reducing the injected sample volume [25].

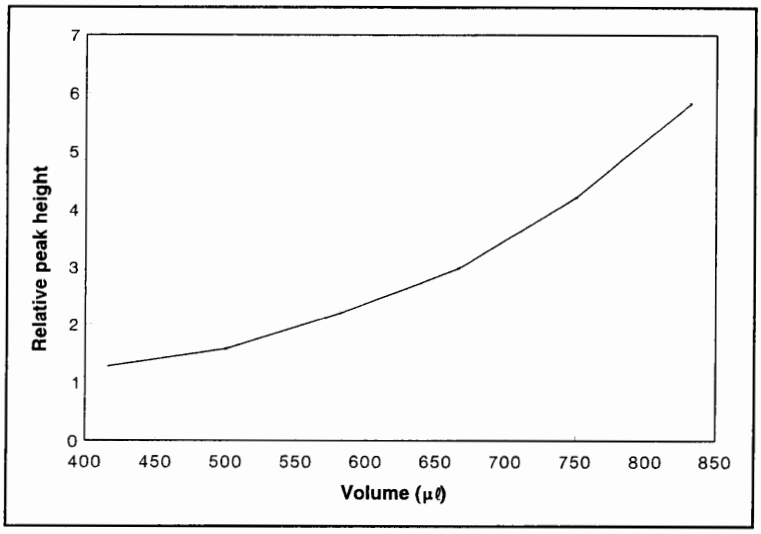

Fig. 6.4 Influence of the sample volume on the magnitude of dilution using a dilution coil.

(2) Reagent volume

The reagent volume (V_r) is the amount of reagent which is withdrawn into the holding coil via the reagent port. The influence of the reagent volume on dilution is schematically shown in Fig. 6.5. It can be seen from Fig. 6.5 that the relative peak height increases with increasing reagent volume until it reaches a point where an increase in reagent volume no longer gives rise to higher relative peak heights.

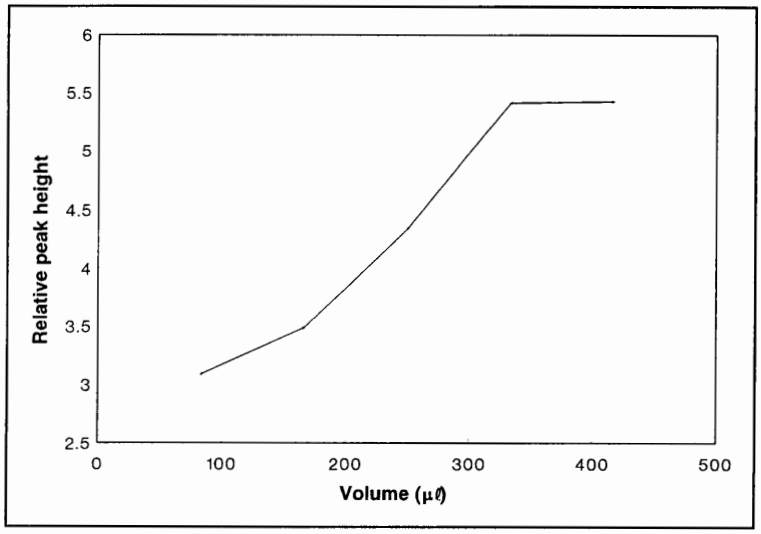

Fig. 6.5 Influence of reagent volume on the magnitude of dilution using a dilution coil.

(3) Transfer volume

The transfer volume (V_t) describes the volume of formed product plus the accompanying sample, reagent and wash solution in the holding coil and tubing which are transferred into the dilution conduit from the holding coil. The effect of the transfer volume is shown in Fig. 6.6. A 3 000 mg.ℓ^{-1} sulphate standard was used to illustrate the influence of the transfer volume. The sample volume (250 $\mu\ell$), reagent volume (750 $\mu\ell$) and analysis volume (670 $\mu\ell$) were kept constant throughout the measurements. It is clear from Fig. 6.6 that a larger transfer volume results in smaller dilution.

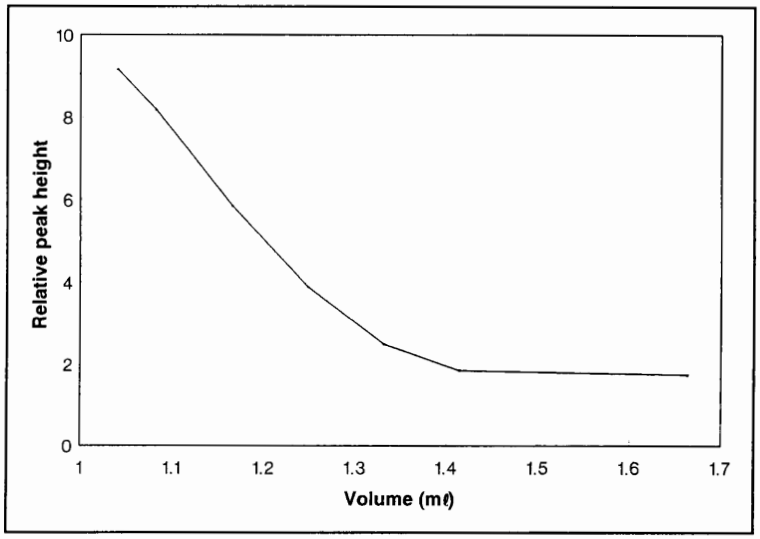

Fig. 6.6 Influence of the transfer volume on the magnitude of dilution.

(4) Analysis volume

The analysis volume (V_a) is the volume of the aliquot taken from the dilution conduit to the holding coil and then propelled to the detector, via the holding coil. The effect of the analysis volume was determined the same way as the transfer volume. The transfer volume was kept constant at 1.248 mℓ. The results of these determinations are shown in Fig. 6.7.

It is clear from Fig. 6.7 that an increase in analysis volume results in an increase in sensitivity of the measurements.

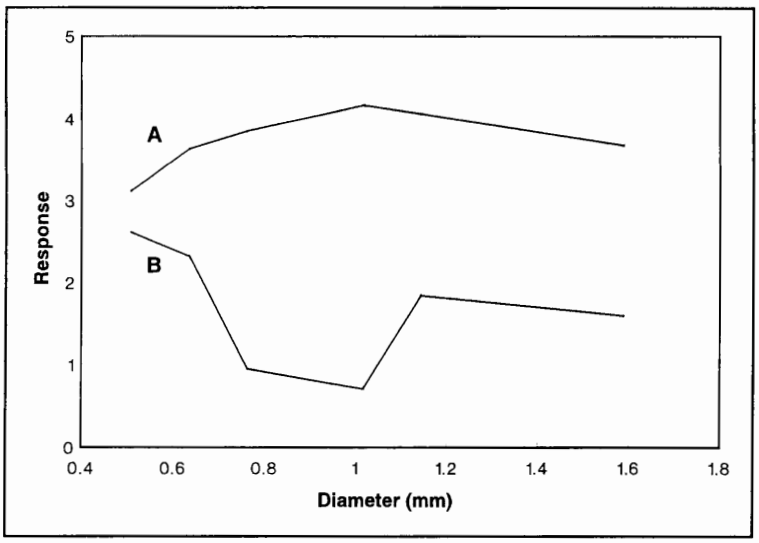

Fig. 6.7 Influence of the analyses volume on the magnitude of dilution.

6.3.2 SIA system with dilution step

In this method of dilution, a dilution zone (step) is incorporated into the procedure between the sample and reagent zones. Distilled, deionized water is used for this step. Control over the magnitude and range of dilution for this particular conduit is effected by three volume parameters: sample volume, (V_s), reagent volume, (V_r), and dilution step volume, (V_d). The zones as they appear in the holding coil is shown schematically in Fig. 6.2B.

(1) Sample volume

As in the previous dilution method the sample volume is the amount of sample or standard which is withdrawn into the holding coil via the sample port. The effect of the sample volume is determined and the results are outlined in Fig. 6.8.

The same results were obtained as in the dilution method with the dilution coil: smaller injected sample volume resulted in lower sensitivity. This confirm the conclusion that reduction of the sample volume is an effective dilution method.

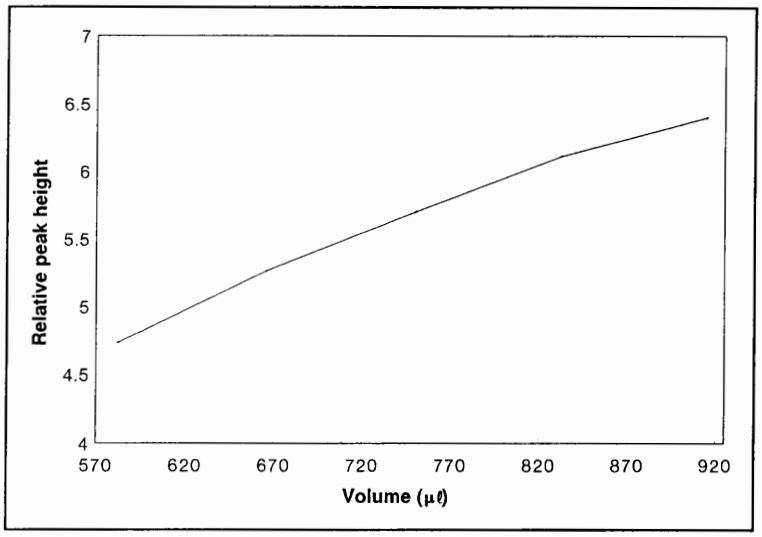

Fig. 6.8 Influence of the sample volume on the magnitude of dilution using a dilution step of 6.5 sec.

(2) Reagent volume

The effect of the reagent volume on the dilution is represented in Fig. 6.9. As in the case of dilution using a dilution coil, the relative peak height increases with increasing reagent volume. With reagent volumes higher than 350 $\mu\ell$ no further increase in relative peak height is observed. This is because the larger volume results in smaller axial dispersion and therefore smaller zone overlap.

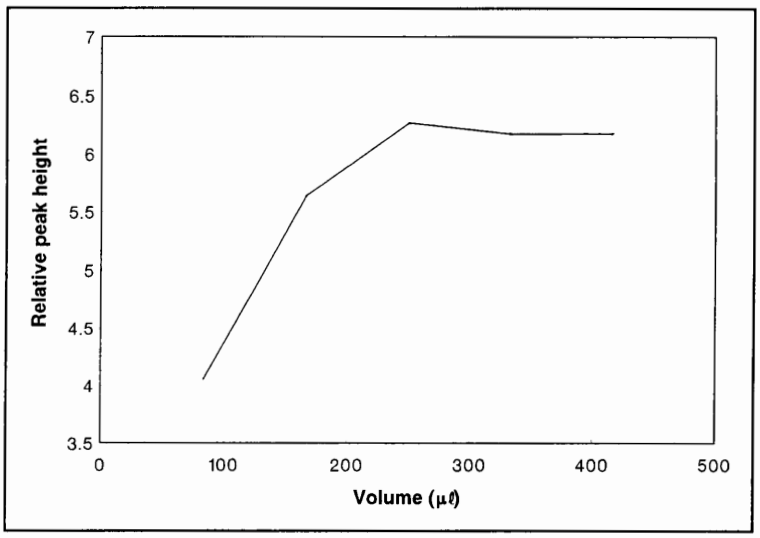

Fig. 6.9 Influence of the reagent volume on the magnitude of dilution using a dilution step of 6.5 sec.

(3) Dilution volume

The dilution step represents the water zone incorporated between the sample and reagent zone. This zone fulfils the same function as the "spacer" zone described by Gübeli *et al* [25]. The longer the dilution step (greater volume), the larger is the dilution effect. This effect is illustrated in Fig. 6.10.

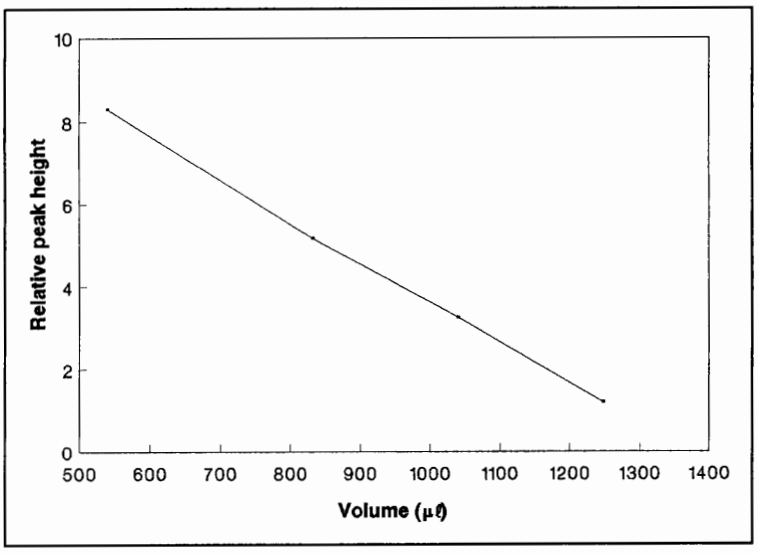

Fig. 6.10 Influence of the dilution step volume on the magnitude of dilution.

6.4 Method evaluation

The performance of the proposed two SIA dilution systems for the on-line determination of sulphate was evaluated under optimum running conditions with regard to linearity, dynamic range, accuracy, precision, detection limit, sample interaction and sample frequency. The linear regions of the two dilution systems are outlined in Figs. 6.11 and 6.12 for systems with the dilution coil and dilution step respectively. The linear relationship between relative peak height and concentration is given in Table 3.

TABLE 3. Linear relationship between relative peak height and concentration for the proposed SIA system with a dilution coil and a dilution step.

DILUTION COIL		
Linear range ([] as mg.ℓ^{-1})		**Linear equation***
50 - 5 000		y = 0.0015x + 0.7576; r = 0.9985
50 - 500		y = 0.0023x + 0.5337; r = 0.9979
500 - 5 000		y = 0.0015x + 0.9860; r = 0.9999
DILUTION STEP		
Timing sequence	**Linear range ([] as mg.ℓ^{-1})**	**Linear equation***
6.5 seconds	50 - 250	y = 0.0089x + 0.2463; r = 0.9911
	2 000 - 5 000	y = 0.00082x + 4.9911; r = 0.9968
10 seconds	150 - 750	y = 0.0034x + 0.1093; r = 0.9920
	750 - 2 000	y = 0.0011x + 1.7266; r = 0.9993
	2 000 - 5 000	y = 0.00062x + 2.7797; r = 0.9955
12.5 seconds	500 - 1000	y = 0.0019x - 0.2087; r = 0.9979
	1 000 - 5 000	y = 0.00051x + 1.3489; r = 0.9770
15 seconds	750 - 5 000	y = 0.00056x - 0.0679; r = 0.9998

* y = relative peak height, x = sulphate concentration in mg.ℓ^{-1} and r = correlation coefficient

A linear calibration curve between 50 and 5 000 mg.ℓ^{-1} is obtained for the proposed SIA system where a dilution coil is involved (Fig. 6.11). This calibration curve is suitable for process analyzers where only an approximate value is needed. There is however a break in the slope of the curve at 500 mg.ℓ^{-1} and for more accurate values enlargements of the linear curves as shown in Fig. 6.11A for the linear range between 50 and 500 mg.ℓ^{-1} and Fig. 6.11B for the linear range between 500 and 5 000 mg.ℓ^{-1} should be applied. For the proposed SIA system where a dilution step is used, the degree of dilution obtained, and therefore the linear working range, depended on the timing sequence allowed for the dilution step.

Different timing sequences for the dilution steps were evaluated and the calibration curves associated with the different linear regions are illustrated in Fig. 6.12. It is clear from the calibration curves (Fig. 6.12) that a linear calibration curve (Fig. 6.12D) with a very good correlation coefficient (r = 0.9998, Table 3) between 750 and 5 000 mg.ℓ^{-1} was obtained with a timing sequence of 15 seconds. A timing sequence of 6.5 seconds gave a calibration curve between 50 and 1 000 mg.ℓ^{-1} that was not linear but which can be used for calibration (Fig. 6.12A). This curve flattened for concentrations > 1 000 mg.ℓ^{-1} with a slope that was not suitable for calibration. Although several linear regions were possible for curves at other timing sequences as shown in Table 3 and illustrated in Fig. 6.12, no one was suitable for measurement over the full concentration range, which made it a major drawback for this type of SIA system as process analyzer.

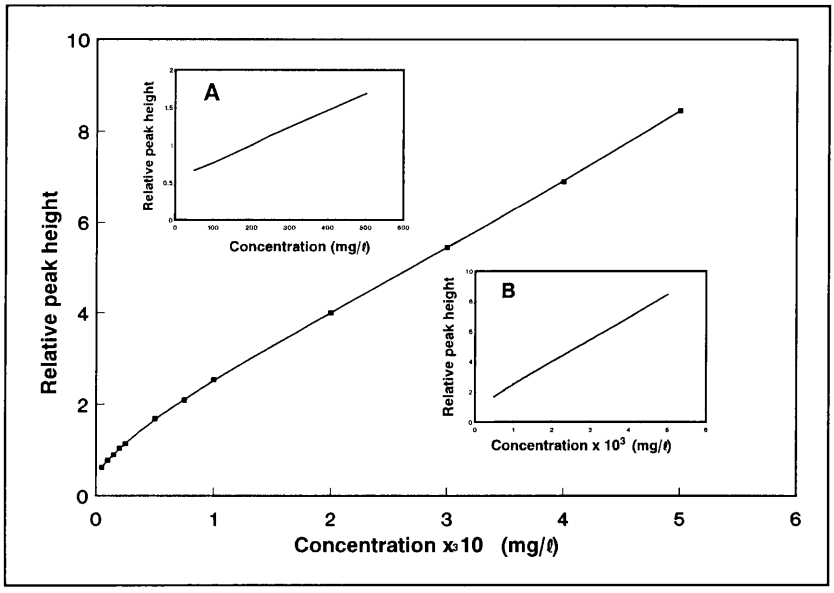

Fig. 6.11 Calibration curve: 50 - 5 000 mg/ℓ sulphate. Enlargements of A: the range 50 - 500 mg/ℓ and B: the range 500 - 5 000 mg/ℓ.

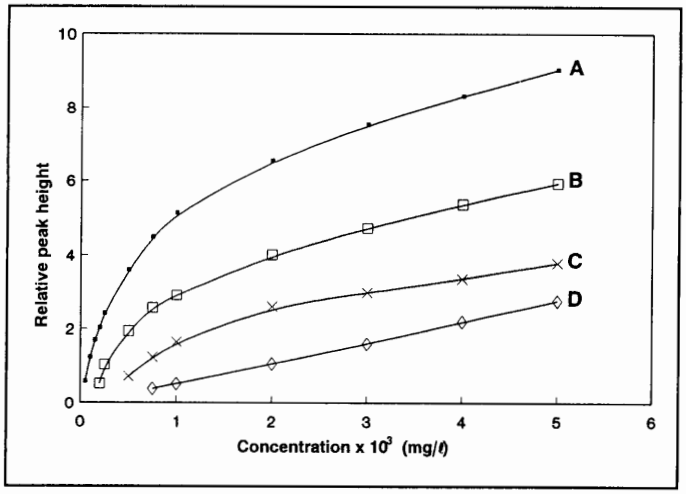

Fig. 6.12 Calibration curves for standard sulphate solutions using a dilution step between the sample and reagent zones. (A) The range 50 - 5 000 mg.ℓ^{-1} using a dilution step of 6.5 s, (B) the range 150 - 5 000 mg.ℓ^{-1} using a dilution step of 10 s, (C) the range 750 - 5 000 mg.ℓ^{-1} using a dilution step of 12.5 s and (D) the range 750 - 5 000 mg.ℓ^{-1} using a dilution step of 15 s.

The accuracy of both proposed SIA systems (a dilution coil and dilution step) was tested by comparing the results of a number of samples with those obtained by a standard automated segmented method where the samples were manually diluted before analysis. Results compared favourably as can be seen from Table 4.

TABLE 4. Comparison of results of a number of samples between the proposed SIA systems (dilution coil and dilution step) and a standard automated segmented method

Sample No.	**Proposed SIA system ([] as mg/ℓ)**		**Standard automated segmented method ([] as mg/ℓ)**
	Dilution coil	**Dilution step**	
0837	951	953	924
0862	239	239	247
1052	275	281	309

The precision of both proposed SIA systems (a dilution coil and dilution step) was tested on a number of standard sulphate solutions and samples and the results are given in Table 5.

TABLE 5. Precision of both proposed SIA systems (dilution coil and dilution step)

Sample/Standard ([] as mg.ℓ^{-1})	**DILUTION COIL**	**DILUTION STEP**			
	%RSD*	**%RSD (6.5 s)***	**%RSD (10 s)***	**%RSD (12.5 s)***	**%RSD (15 s)***
50	4.41	2.93			
100	3.71	2.55			
150	3.05	1.76	3.51		
200	3.05	1.84	2.84		
250	3.05	1.70	2.34		
500	3.05	1.12	2.41	4.25	
750	2.81	0.41	2.17	4.02	4.40
1 000	2.53	1.04	2.65	3.71	2.8
2 000	2.77	1.42	1.43	3.60	2.22
3 000	2.32	1.05	1.90	3.25	1.69
4 000	2.23	1.90	1.01	2.08	1.29
5 000	2.03	1.65	0.33	1.28	1.17
S0837	2.53		1.79		
S0862	3.12		2.75		
S2052	3.91		1.90		

* n = 10

Although the precision for the SIA system without dilution (Chapter 5) was better, a precision of less than 4.5% was obtained for both SIA systems (a dilution coil and dilution step). The precision was better for the more concentrated standards and for the smaller dilution steps.

Because sample carry-over is a problem in the turbidimetric determination of sulphate, due to the precipitation of barium sulphate in the manifold and flow-cell, the sample interaction was calculated for every dilution system (dilution coil and dilution steps). The results are summarised in Table 6.

TABLE 6. Carry-over effect for the various dilution systems

Dilution system	Sample interaction
Dilution coil	0.15%
Dilution step: 6.5 s	0.03%
Dilution step: 10 s	0.02%
Dilution step: 12.5 s	0.03%
Dilution step: 15 s	0.004%

The carry-over effect is smaller than 0.03% for the respective dilution steps and less than 0.15% for the dilution system using the dilution coil and had therefore no effect on the analysis.

There is without controversy reason to doubt the detection limits (Table 7) calculated by the equation

$$Detection\ limit = \frac{3 \times S_k}{100} \times K$$

where S_k is the relative standard deviation of the lowest concentration of the specific method and K is the corresponding lowest concentration for this method. It is stated by Madson and Murphy [24] that the turbidimetric determination of sulphate is only valid for sulphate concentrations higher than 10 mg.ℓ^{-1}. It is further highly unlikely that a peak would be measured for a sample with a sulphate content of 6.61 mg.ℓ^{-1} (detection limit for SIA method with dilution coil) as the relative peak height for a standard sulphate solution containing 50 mg.ℓ^{-1} sulphate is only 0.62 absorbance units.

TABLE 7. Detection limits for the various dilution systems

Dilution system	Lowest concentration (K) ([ ] in mg.ℓ^{-1})	%RSD (S_k)	Theoretical detection limit ([ ] in mg.ℓ^{-1})
Dilution coil	50	4.41	6.61
Dilution step: 6.5 s	50	2.93	4.39
Dilution step: 10 s	150	3.51	15.80
Dilution step: 12.5 s	500	4.25	63.79
Dilution step: 15 s	750	4.40	98.93

There is therefore no reason to calculate the theoretical detection limits for the various dilution systems and it is advised that the lowest concentration for the specific method (K) is used as detection limit.

The incorporation of either the dilution coil or various dilution steps lengthen the analysis time and has a large influence on the sample frequency of the proposed methods. Shorter analysis time favoured the dilution with the dilution step, but the limited linear range is a large drawback. The sample frequencies of the various dilution systems is listed in Table 8.

TABLE 8. Sample frequencies for the various dilution systems

Dilution system	Time per experiment (s)	Sample frequency (h^{-1})
Dilution coil	182.5	20
Dilution step: 6.5 s	147	24
Dilution step: 10 s	150.5	24
Dilution step: 12.5 s	153	23
Dilution step: 15 s	155.5	23

6.5 Conclusion

The use of a dilution conduit in the SIA mode allows for easy and rapid dilution of concentrated samples. The method is versatile, suitable for different detection schemes and equally valid for single and multizone analyses. In addition the method is independent of the events which follow the dilution step, thus making it suitable for analyses which involved stopped-flow or steps for matrix removal. This dilution technique can greatly extent the

working range of an analysis that has a limited response range.

On-line dilution with sequential injection analysis have been evaluated for sulphate monitoring in industrial effluents using a dilution coil in the conduits of the manifold system and a dilution step as part of the timing sequence. The manifold of the SIA system with the dilution coil is more complex than the system including the dilution step. The former method needs more complicated programming as well. Shorter analysis time favoured the dilution with the dilution step, but the limited linear range of this method is a large drawback. The large linear range of the SIA system with dilution coil makes it very suitable to be used as a process analyzer. The proposed SIA system is suitable to monitor sulphate in industrial effluents in the range 50 - 5 000 mg.ℓ^{-1} with a dilution coil, in the range 50 - 1 000 mg.ℓ^{-1} with a timing sequence of 6.5 seconds and in the range 750 - 5 000 mg.ℓ^{-1} with a timing sequence of 15 seconds using a dilution step; al three ranges with a RSD $< 4.5\%$.

6.6 References

1. J. Růžička and E. H. Hansen, **Anal. Chim. Acta.**, **99** (1978) 37.
2. J. F. van Staden, **Fresenius' Z Anal. Chem.**, **322** (1985) 36.
3. S. Olsen, J. Růžička and E. H. Hansen, **Anal. Chim. Acta.**, **136** (1982) 101.
4. K. K. Stewart and A. G. Rosenfeld, **Anal. Chem.**, **54** (1982) 2368.
5. M. Gisin, C. Thommen and K. F. Mansfield, **Anal. Chim. Acta.**, **179** (1986) 149.
6. J. Růžička and E. H. Hansen, **Anal. Chim. Acta.**, **87** (1976) 353.
7. B. F. Reis, J. Jacintho, J. Moratatti, F. J. Krug, E. A. G. Zagatto, F. H. Bergamin and L. C. R. Pessenda, **Anal. Chim. Acta.**, **123** (1981) 221.
8. D. A. Whitman and G. D. Christian, **Talanta**, **36** (1989) 205.
9. J. Toei, **Anal. Lett**, **21** (1988) 1633.
10. M. B. Garn, M. Gisin, H. Gross, P. King, W. Schmidt and C. Thommen, **Anal. Chim. Acta.**, **207** (1988) 225.
11. G. D. Clark, J. Růžička and G. D. Christian, **Anal. Chem.**, **61** (1989) 1773.
12. J. F. van Staden, **Water SA**, **12** (1986) 43.
13. J. F. van Staden, **Anal. Lett.**, **19** (1986) 1407.
14. J. F. van Staden, **Fresenius J. Anal. Chem.**, **340** (1991) 415.
15. E. A. G. Zagatto, M. F. Gine, E. A. N. Fernandes, B. F. Reis and F. J. Krug, **Anal. Chim. Acta.**, **173** (1985) 289.
16. Z. Fang, M. Sperling and B. Welz, **Anal. Chim. Acta.**, **269** (1992) 9.
17. S. Xu and Z. Fang, **Microchemical Journal**, **50** (1994) 145.
18. J. Růžička and G. D. Marshall, **Anal. Chim. Acta.**, **237** (1990) 329.
19. J. Růžička, G. D. Marshall and G. D. Christian GD, **Anal. Chem.**, **62** (1990) 1861.

20. G. D. Marshall, **Sequential-Injection Analysis**, PhD-thesis, University of Pretoria, 1994.

21. G. D. Marshall and J. F. van Staden, **Process Control and Quality**, **3** (1992) 251.

22. G. D. Marshall and J. F. van Staden, **Analytical Instrumentation**, **20** (1992) 79.

23. A. Baron, M. Guzman, J. Růžička and G. D. Christian, **Analyst**, **117** (1992) 1839.

24. B. C. Madsen and R. J. Murphy, **Anal. Chem.**, **53** (1981) 1924.

25. T. Gübeli, G. D. Christian and J. Růžička, **Anal. Chem.**, **63** (1991) 2407.

26. J. C. Mansini, P. J. Baxter, K. R. Detwiler and G. D. Christian, **Analyst**, **120** (1995) 1583.

CHAPTER 7

Determination of Phosphate with Sequential Injection Analysis

7.1. Introduction

Phosphorus is the eleventh element in order of abundance in crustal rocks of earth and it occurs there to the extent of ~ 1120 $mg.g^{-1}$ (cf. H ~ 1520 $mg.g^{-1}$, Mn ~ 1060 $mg.g^{-1}$). All its known terrestrial minerals are orthophosphates though the reduced phosphite mineral schriebersite $(Fe, Ni)_3P$ occurs in most iron meteorites. Some 200 crystalline phosphate minerals have been described, but by far the major amount of P occurs in a single mineral family, the apatites, and these are the only ores of industrial importance, the others being rare curiosities. Apatites have the idealized general formula $3Ca_3(PO_4)_2.CaX_2$, that is $Ca_{10}(PO_4)_6X_2$, and common members are fluoroapatite $Ca_5(PO_4)_3F$, chloroapatite $Ca_5(PO_4)_3Cl$ and hydroxyapatite $Ca_5(PO_4)_3(OH)$. In addition, there are vast deposits of amorphous phosphate rock, phosphorite, which approximates in composition to fluoroapatite. These deposits are widely spread throughout the world [1].

Phosphorus also occurs in all living things and the phosphate cycle, including the massive use of phosphatic fertilizers, is of great interest. The movement of phosphorus through the environment differs from that of the other non-metals essential to life (H, C, N, O and S)

because it has no volatile compounds that can circulate via the atmosphere. Instead, it circulates via two rapid biological cycles (weeks and years) superimposed on a much slower primary inorganic cycle (millions of years) as shown schematically in Fig. 7.1 [2].

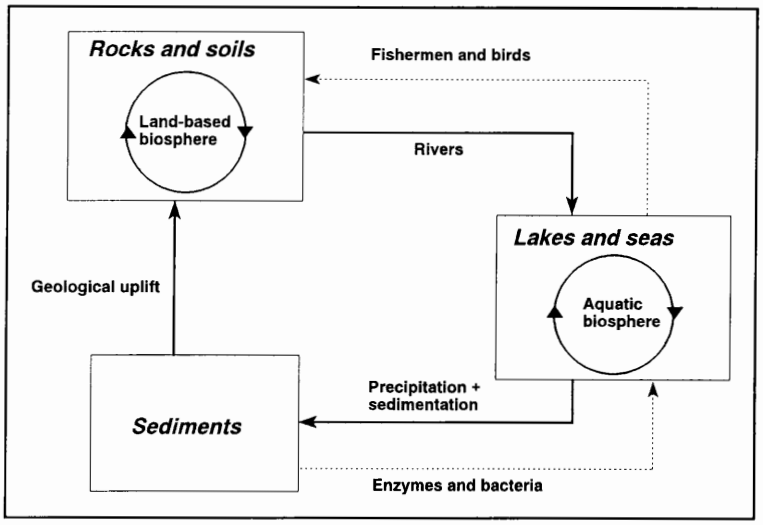

Fig. 7.1 The phosphate cycle.
— Primary inorganic cycle ~ millions of years.

In the inorganic cycle, phosphates are slowly leached from the igneous or sedimentary rocks by weathering, and transported by rivers to the lakes and seas where they are precipitated as insoluble metal phosphates or incorporated into the aquatic food chain.

The secondary biological cycles stern from the crucial roles that phosphates and particularly organophosphates play in all life processes. Thus organophosphates are incorporated into the backbone structures of DNA and RNA which regulate the reproductive processes of cells, and they are also involved in many metabolic and energy transfer processes either as adenosine triphosphate (ATP) or other such compounds. Another role, restricted to higher forms of life, is the structural use of calcium phosphates as bones and teeth.

The land-based phosphate cycle is shown in Fig. 7.2. The amount of phosphate in untilled soil is normally quite small and remains fairly stable because it is present as the insoluble salts of Ca^{2+}, Fe^{3+} and Al^{3+}. To be used by plants, the phosphate must be released as the soluble $H_2PO_4^-$ anion, in which form it can be taken up by plant roots. Although acidic soil conditions will facilitate phosphate absorption, phosphorus is the nutrient which is often in shortest supply for the growing plant. Most mined phosphate is thus destined for use in fertilizers and this accounts for up to 75% of phosphate rock in technologically advanced countries and over 90% in less advanced (more agriculturally based) countries [1].

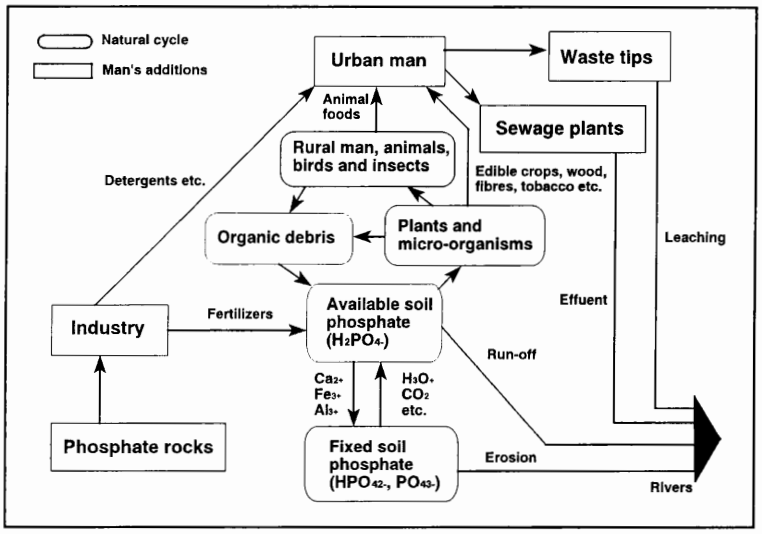

Fig. 7.2 The land-based phosphate cycle.

Moderation in all things, however: excessive fertilization of natural waters due to detergents and untreated sewage in run-off water can lead to heavy overgrowth of algae and higher plants, thus starving the water of dissolved oxygen, killing fish and other aquatic life and preventing the lakes and dams for recreation.

As just implied, the land based phosphorus cycle is connected to the water based cycle via

the rivers and sewers. It has been estimated that on a global scale about 2 million tonnes of phosphate are washed into the seas annually from natural processes and rather more than this amount is dumped from human activities. Details of the subsequent water based phosphate cycle are shown schematically in Fig. 7.3. The water based cycle is the most rapid of the three phosphate cycles and can be completed within weeks (or even days).

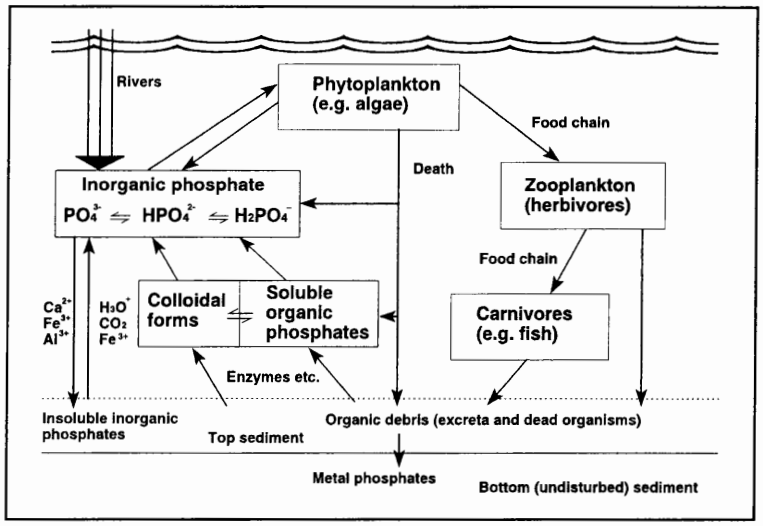

Fig. 7.3 The water-based phosphate cycle.

7.1.1 Why do we need to determine phosphate?

Phosphorus are used in an astonishing variety of domestic and industrial applications but their ubiquitous presence and substantial impact on everyday life is frequently overlooked. The most widely used compounds are the various phosphate salts of Na, K, NH_4 and Ca.

Na_3PO_4 is strongly alkaline in aqueous solutions and is thus a valuable constituent of scouring powders, paint strippers and grease saponifiers. Its complex with NaOCl

[$(Na_3PO_4.11H_2O)_4.NaOCl$], is also strongly alkaline (a 1% solution has pH 11.8) and in addition it releases active chlorine when wetted; this combination of scouring, bleaching and bacterial action makes the adduct valuable in formulations of automatic dishwashing powders [1].

Na_2HPO_4 is widely used as a buffer component. The use of the dihydrate (~ 2% concentration) as an emulsifier in the manufacture of pasteurized processed cheese was patented by J. L. Kraft in 1916 and is still used. It is also used to maintain the correct Ca^{2+}/PO_4^{3-} balance in evaporated milk and to prevent gelation of the milk powder to a mush [1].

NaH_2PO_4 is a solid, water soluble acid and its property finds use in effervescent laxative tablets and in the pH adjustment of boiler waters. It is also used as a mild phosphatizing agent for steel surfaces and as a constituent in the undercoat for metal paints [1].

K_3PO_4 (like Na_3PO_4) is strongly alkaline in aqueous solution and is used to absorb H_2S from gas streams; the solution can be regenerated simply by heating. K_3PO_4 is also used as a regulating electrolyte to control the stability of synthetic latex during the polymerization of styrene butadiene rubbers. The buffering action of K_2HPO_4 is the reason for its addition as a corrosion inhibitor to car-radiator coolants which otherwise tend to become acidic due to slow oxidation of the glycol antifreeze. KH_2PO_4 is a piezoelectric and finds use in submarine sonar systems [1].

$(NH_4)_2HPO_4$ and $(NH_4)H_2PO_4$ can be used interchangeably as specialist fertilizers and

nutrients in fermentation broths. Ammonium phosphates are also much used as flame retardants for cellulosic materials. Their action probably depends on their ready dissociation into NH_3 and H_3PO_4 on heating; the H_3PO_4 then catalyses the decomposition of cellulose to a slow burning char (carbon) and this together with the suppression of flammable volatiles, smothers the flame [1].

Calcium phosphates have a broad range of applications both in the food industry and as bulk fertilizers. The crucial importance of Ca^{2+} and PO_4^{3-} as nutrient supplements for the healthy growth of bones, teeth, muscle and nerve cells has long been recognized. The non-cellular bone structure of an average adult human consist of ~ 60% of some form of tricalcium phosphate [$Ca_5(PO_4)_3OH$]; teeth likewise comprise ~ 70% and the average person carries 3.5 kg of this material in his body. Phosphates in the body are replenished by a continuous cycle and used P is carried by the blood to the kidneys and then excreted in urine, mainly as $Na(NH_4)HPO_4$. An average adult eliminates 3 - 4 g of PO_4^{3-} equivalent daily [1].

The former paragraphs highlighted some of the uses of phosphates. Fig. 7.4 is a schematic representation of the uses of phosphate. Phosphates are however not always wanted and need to be determined in waste and other effluent waters. The first members of the food chain are the algae and experiments with radioactive ^{32}P have shown that, within minutes of entering an aquatic environment, inorganic phosphate is absorbed by algae and bacteria (50% uptake in 1 minute, 80% in 3 minutes) [1]. Thus the discharge of raw or treated wastewater, agricultural drainage, or certain industrial wastes to water may stimulate the growth of photosynthetic aquatic micro- and macro organisms in nuisance quantities.

Phosphorus is also found in ferrous metallurgical products because of the occurrence of phosphates in iron ore and in the limestone used as flux. High concentrations of phosphorus in steel causes embrittlement and it is therefore necessary to determine the amount of phosphate present [4].

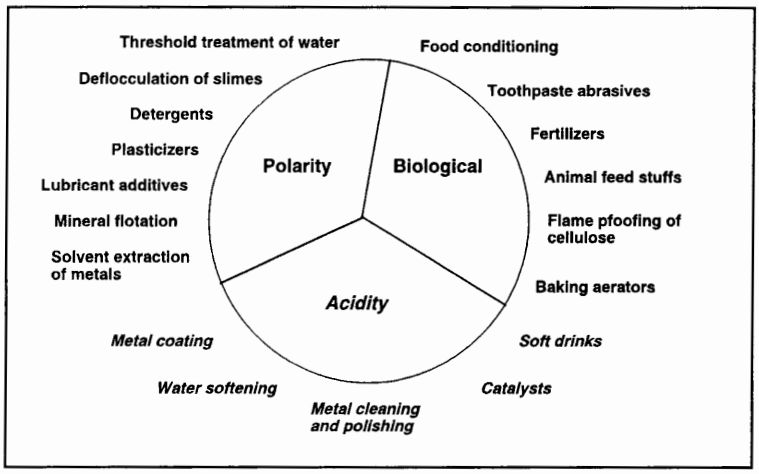

Fig. 7.4 Applications of phosphoric acid and its derivates.

Phosphorus is involved in all phases of cellular metabolism. Growth, limited by phosphate, has been used for the production of alkaloids in plant cell structures. Proteins, such as interferons, have also been produced in yeast and bacteria fermentations. In *Saccharomyces cerevisae* fermentations, phosphate has been used to control the expression of heterologous proteins (whose genes are linked to promoters of acid phosphatases). Media with a high phosphate concentration repress the expression of heterologous proteins, whereas in media with low levels of phosphate, the production of acid phosphatases and related heterologous proteins is enhanced [25].

7.1.2 Methods to determine phosphate

Phosphorus may be present in water, effluent and sewage in a variety of physical and chemical forms. In the past soluble (or dissolved) reactive (free) phosphate (often considered to be orthophosphate) was the most frequently required determinant. Polyphosphates can however readily convert into orthophosphate; substituted phosphates, phosphonates and phosphonium compounds can oxidise or hydrolyse (even if only slowly) and insoluble or encapsulated compounds can be solubilized. Hence, total phosphorus determinations are becoming important. Occasionally, especially when study sources of pollution, a knowledge of the speciation is required.

7.1.2.1 Pretreatment [3]

Phosphorus in natural (including saline) and waste waters will almost invariably be present in one or more of the following forms:

(a) orthophosphate (the commonest form found);

(b) condensed phosphates (eg. pyro and polyphosphates), these are often referred to as hydrolysable phosphates;

(c) organophosphorus, mainly phosphate esters, but also compounds in which phosphorus is directly bonded to carbon (eg. aminophosphonic acids).

Phosphorus in suspended matter may be present as phosphate minerals (such as apatite), be absorbed onto other solids or be contained in the microbiota. Even free phosphorus has been

found following pollution. The separation of phosphorus into its various forms is defined analytically. Filtration through a 0.45 μm membrane filter separates dissolved from suspended forms of phosphorus. The fact that no separation of this nature can be truly complete is reflected in the use of the terms 'filterable' and 'particulate'. The filtration is merely a convenient and replicable analytical technique designed to make a gross separation. Fig. 7.5 shows a schematic diagram of the various forms of phosphorus and how they are obtained.

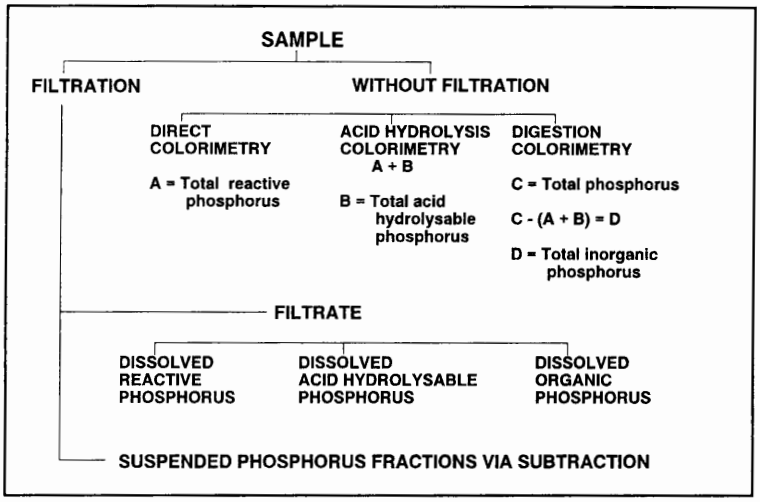

Fig. 7.5 Schematic representation of the various forms of phosphates and an indication of how they are obtained.

Of the three groups listed above (a - c), only (a) will respond directly to spectrophotometric procedures. The condensed phosphates of group (b) require hydrolysis by boiling in the presence of diluted sulphuric acid to convert them to orthophosphate. Similarly, the organic forms of group (c) must first be broken down by suitable techniques such as oxidation by persulphate. While spectrophotometric procedures will measure the orthophosphate content of the sample, the acidic conditions present may concurrently bring about partial hydrolysis

of some group (b) compounds, or even the conversion of the more labile group (c) forms if these are present. For this reason some analysts choose to refer to all the species responding to the molybdenum blue procedure (described later) as 'reactive phosphate phosphorus' instead of orthophosphate.

In some cases when very polluted water were analyzed it is necessary to include a preliminary filtration through an appropriate porosity ashless cellulose filter paper as an initial step. Great care is needed if filtering off biota not to rupture cells as this may greatly increase the apparent soluble phosphate value.

7.1.2.2 The different methods of phosphate analysis

There are numerous methods available for the determination of phosphate. They range from the classical molybdenum blue method where orthophosphate reacts with molybdate ions in acidic solution to form molybdophosphoric acid, which upon selective reduction produces a molybdenum blue complex [5] (maximum absorbance at 650-700 nm) to laser induced thermal lensing colorimetry that can be used to analyze phosphate at the parts per trillion (1.61×10^{-10} mol.dm^{-3}) level.

The two most commonly used colorimetric methods available for phosphate determination are either the yellow-coloured vanadomolybdate for relatively high phosphate concentrations or the molybdenum blue procedure for relatively low phosphate concentrations [26]. The latter method makes use of phosphomolybdenum blue complexes which rely on the initial formation of heteropolymolybdic acids prior to reduction to the blue complex. There are a

large number of poly- and heteropolyacids, formed by molybdates and tungstates with phosphorus(V), arsenic(V), silicon(IV), germanium(IV), titanium(IV) and also with cobalt(II) and (III), nickel(II) and (IV) and vanadium(V). Which acid is formed is highly dependant on the particular molybdate (or tungstate) used (paramolybdate $Mo_7O_{24}^{6-}$ is the one usually used for analysis), on the molybdenum concentration and acidity of the solution, the other ions present (such as tartrate or oxalate) and in some instances on the temperature and reaction time.

Molybdenum and other metals such as tungsten, vanadium, titanium and iron form Berthollides (a non-stoichiometric series of compounds), all highly coloured, in which some of the metal atoms in the complex lattice are one valency below (or above) the others, the strong colour being due to the electron transfer phenomenon [1]. As molybdenum can form almost continuous series of berthollides from 6 valent to 4 valent, with varying colours and solubilities, it is equally essential for reliable analysis that both the conditions for the initial heteropoly acid formation and the reduction are fully controlled.

7.1.3 Principle of the reaction between phosphate and molybdenum

The analytical method is based on the following reactions: [6]

$$H_3PO_4 + 12\ H_2MoO_4 \rightarrow H_3P(MoO_{40}) + 12\ H_2O$$

reducing agent

Mo(VI) → → → → → → Mo(V) reduction

slowly

There is however reason to doubt the stoichiometry of the reactions because of the different heteropolyanions that can be formed between Mo and PO_4^{3-}.

In 1826 J. J. Berzelius found that acidification of solutions containing both molybdate and phosphate produced a yellow crystalline precipitate [7]. This was the first example of a heteropolyanion and it contains the phosphomolybdate ion, $[PMo_{12}O_{40}]^{3-}$, which is used in the quantitative estimation of phosphate.

In these ions the heteroatoms are situated inside "cavities" or "baskets" formed by MoO_6 octahedra and are bonded to oxygen atoms of the adjacent MoO_6 octahedra. The stereochemistry of the heteroatom is determined by the shape of the cavity which in turn depends on the ratio of the number of heteroatoms to parent atoms. Four major classes are found:

1 : 12, tetrahedral: These occur with small heteroatoms such as P^V, (As^V, Si^V and Ti^V) which yield tetrahedral oxoanions.

2 : 18, tetrahedral: If solutions of the 1 : 12 anions $[X^VM_{12}O_{40}]^{3-}$ (X = P, As; M = Mo) are allowed to stand, the 2 : 18 $[X_2M_{18}O_{62}]^{6-}$ ions are gradually produced. The ion is best considered to be formed from two 1 : 12

anions, each of which loses three MO_6 octahedra.

1 : 6, octahedral: These are formed with larger heteroatoms such as Te^{VI}, I^{VII}, Co^{III} and Al^{III} which coordinate to 6 edge-sharing MoO_6 octahedra in the form of a hexagon around the central XO_6 octahedron.

1 : 9, octahedral: The structures of these ions are based solely on edge sharing MoO_6 octahedra.

Mild reduction of 1 : 12 and 2 : 18 heteropolymolybdates produces characteristic and very intense blue colours ("heteropoly blues"). The reductions are most commonly of 2 electron equivalents but may be up to 6 electron equivalents. The reduction evidently occurs on individual Mo atoms, producing a proportion of Mo^{V} ions. Transfer from Mo^{V} to Mo^{VI} is then responsible for the intense "charge transfer" absorption.

7.2 The determination of phosphate with sequential injection analysis

7.2.1 Experimental

7.2.1.1 Reagents and solutions

All reagents were prepared from analytical-reagent grade unless specified otherwise. All aqueous solutions were prepared with doubly distilled deionised water. All solutions were degassed, before measurements, with a vacuum pump system.

(a) Standard phosphate solutions: A stock solution containing 1 000 mg.ℓ^{-1} of phosphate was prepared by dissolving 1.3905 g $(NH_4)_2HPO_4$ in distilled water and diluting it to 1 litre. Working solutions in the range 1 - 200 mg.ℓ^{-1} were prepared by suitable dilution of the stock solution.

(b) Molybdenum reagent: 12.3586 g $(NH_4)_6Mo_7O_{24}.4\ H_2O$ were dissolved in almost 900 mℓ water. The pH of the reagent was adjusted to 0.9 with hydrochloric acid (concentrated) and the solution quantitatively diluted to 1 litre.

(c) Ascorbic acid reagent: A 0.64% (m/v) ascorbic acid solution was prepared. 1% (m/v) glycerine was added to the solution. The solution was made up with a potassium hydrogen phthalate - hydrochloric acid buffer of pH 2.5.

7.2.1.2 Apparatus

The sequential injection system depicted in Fig. 7.6 were constructed of the following components: a Gilson minipuls peristaltic pump; a 10-port electrically actuated selection valve (Model ECSD10P; Valco Instruments, Houston, TX, USA); and a Unicam 8625 UV-visible spectrophotometer equipped with a 10-mm Hellma type flow-through cell (volume: 80 μl) for absorbance measurements. The reduced blue molybdenum complex was monitored by measuring the absorbance at 865 nm. Data acquisition and device control were achieved using a PC30-B interface board (Eagle Electric, Cape Town, South Africa) and an assembled distribution board (MINTEK, Randburg, South Africa). The *FlowTEK* [8] software package (obtainable from MINTEK, Randburg, South Africa) for computer-aided flow-analysis was

used throughout for device control and data acquisition. Tygon tubing was used for the holding and reaction coils.

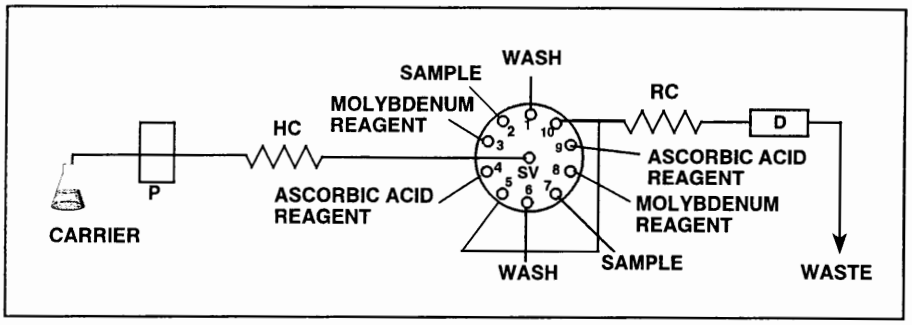

Fig. 7.6 Sequential injection system used in the determination of phosphate. HC - holding coil, RC - reaction coil, P - pump, SV - selection valve and D - detector.

7.2.1.3 Procedure

The device sequence for the determination of phosphate by sequential injection is given in Table 1. Two measurement cycles were used on one complete cycle of the 10-port selection valve (Fig. 7.6). This was done to utilise the full available capacity of the 10-port Valco valve. As seen from the sequential injection system depicted in Fig. 7.6 the first cycle (wash, sample, molybdenum reagent, ascorbic acid reagent and flushed to the detector) involved ports 1 to 5 of the selection valve. This was followed by an identical cycle involving ports 6 to 10.

In all operations, the peristaltic pump was programmed to be stopped while the multi-position valve was rotating, in order to avoid cross-contamination problems as well as bubble formation and pressure surges.

TABLE 1. Device sequence for one cycle of the sequential injection system

Time (s)	Pump	Valve	Description
0	Off	Off	Pump and valve off
1		Wash	Select wash solution
5.5	Reverse		Draw up wash solution
10.5	Off		Pump stop
11.5		Sample	Select sample solution
13	Reverse		Draw up sample solutions
18.6	Off		Pump stop
19.6		Molybdenum reagent	Select molybdenum reagent
20.6	Reverse		Draw up reagent
23.2	Off		Pump stop
23.8		Ascorbic acid reagent	Select ascorbic acid reagent
25.3	Reverse		Draw up reagent
32.9	Off		Pump stop
33.9		Detector	Select detector line
35.4	Forward		Pump stack of zones forward to penetrate each other
40.4	Off		Pump stop, flow is stopped to give the reaction time to develop
160.4	Forward		Pump formed product to the detector
205	Off	Off	Return pump and valve to starting position

7.3 Optimization

7.3.1 Chemical parameters

The formation of the heteropoly acid between Mo and PO_4^{3-} is very fast, while reduction of this heteropoly acid with ascorbic acid could take up to 10 minutes to take place. The reduction of the heteropoly acid was therefore the rate determining step. The formation of the heteropoly acid is acid catalyzed and it was therefore necessary to optimise the pH of the molybdenum reagent. Since the molybdate is incompatible, on storage, with reductants such as ascorbic acid, two separate reagents must be sequentially used. In the three-zone configuration the 'spacer' (the zone in the middle) volume and reagent concentrations are critical parameters [14].

7.3.1.1 pH of molybdenum reagent

Initially no acid was added to the molybdenum reagent. The pH of this solution was 4.802. At this pH it took almost ten minutes for the blue colour to develop. With addition of concentrated HCl the pH of the reagent was decreased and the results are represented in the Fig. 7.7.

It is clear (from Fig. 7.7) that the reaction time was dependant on the pH of the solution. A pH of 0.974 gave a reaction time of 5 seconds. The reaction rate was measured by adding the reagents and sample into a cuvette (in the same ratio used in the SIA method) and measuring the time for the blue colour to develop with a stop watch. The reagents and

sample in the cuvette was well mixed and therefore the results of this measurements only serve as an indication of the reaction time.

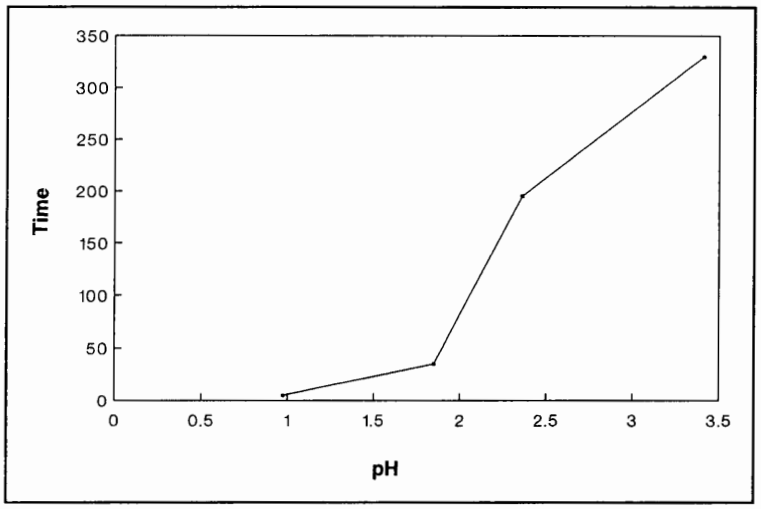

Fig. 7.7 Graphical representation of the influence of the pH of the molybdenum reagent on the reaction time.

According to Greenwood and Earnshaw [1] the first major polyanion formed when the pH of an aqueous molybdate solution is reduced below about 6 is the heptamolybdate $[Mo_7O_{24}]^{6-}$, traditionally known as the paramolybdate (in this determination the paramolybdate is used as reagent). Anions with 8 and 36 Mo atoms are also formed before the increasing acidity suffices to precipitate the hydrous oxide. The formation of these isopolyanions may be represented by the net equations:

$$7\ [MoO_4]^{2-} + 8\ H^+ \rightarrow [Mo_7O_{24}]^{6-} + 4\ H_2O$$

$$8\ [MoO_4]^{2-} + 12\ H^+ \rightarrow [Mo_8O_{26}]^{4-} + 6\ H_2O$$

$$36\ [MoO_4]^{2-} + 64\ H^+ \rightarrow [Mo_{36}O_{112}]^{8-} + 32\ H_2O$$

Of course many intermediate reactions occur: in particular hydration (which raises the coordination number of the molybdenum from 4 to 6) and protonation (which reduces the high charges on some of the ions).

The precipitation of the hydrous oxide by increased acidification, becomes visible as a white precipitate on the bottom of the reagent container. This together with self-reduction which Mo undergoes, is the reason why the molybdenum reagent has to be replaced every fourteen days.

Careful adjustment of acidity can produce mixtures of polyanions, but amongst the distinct species which have been characterized are: the dimolybdate, $[Mo_2O_7]^{2-}$; the hexamolybdate, $[Mo_6O_{19}]^{2-}$ and the decamolybdate, $[Mo_{10}O_{23}]^{8-}$. As noted in the equations above, the condensation of MoO_6 and MoO_4 polyhedra to produce larger anions requires large quantities of strong acid, as the supernumerary oxygen atoms are removed in the form of water molecules. These large anions produce the "cavities" where the heteroatoms are situated before reduction.

7.3.1.2. Concentration of molybdenum reagent

In the original Murphy and Riley procedure [9], the H^+ and molybdenum concentrations in the final solution were 0.4 mol.ℓ^{-1} and 5.438 mmol.ℓ^{-1}, respectively, corresponding to an $[H^+]$:[Mo] ratio of ca. 74. Going and Eisenreich [11] studied the influence of the $[H^+]$:[Mo]

ratio on the absorbance of the phosphoantimonylmolybdenum blue species. They found that the optimum range for the ratios lies between 60 and 80. Above this level, colour formation is incomplete, whereas below it the molybdate ion undergoes self-reduction even in the absence of phosphate.

In the procedure used for phosphate determination as described in this chapter no antimony or other catalyst were used. The $[H^+]$:[Mo] as described above is therefore not applicable on this method. As noted in paragraph 7.3.1.1 a pH of 0.974 is used which corresponds to a $[H^+]$ of 0.106 mol.ℓ^{-1}. Various molybdenum concentrations were investigated. The results are summarised in Table 2 and schematically represented in Fig. 7.8.

TABLE 2. Influence of molybdenum concentration on relative peak height and precision

Concentration (mol.ℓ^{-1})	Relative peak height	%RSD
5.00×10^{-4}	1.00	2.85
1.00×10^{-3}	1.96	1.83
2.00×10^{-3}	3.21	1.19
5.00×10^{-3}	4.64	1.08
1.00×10^{-2}	5.47	0.72

The sensitivity increases as the Mo concentration increases. It seemed from Fig. 7.8 that higher concentrations of molybdenum would result in higher sensitivities. Concentrations from 1.00×10^{-1} mol.ℓ^{-1} are however partly insoluble and by addition of HCl a white precipitate were formed which are insoluble. (After stirring and heating for about 10 minutes the precipitate starts to dissolve.) No background value was obtained for a molybdenum concentration of 1.00×10^{-2} mol.ℓ^{-1} and it was therefore selected for further studies.

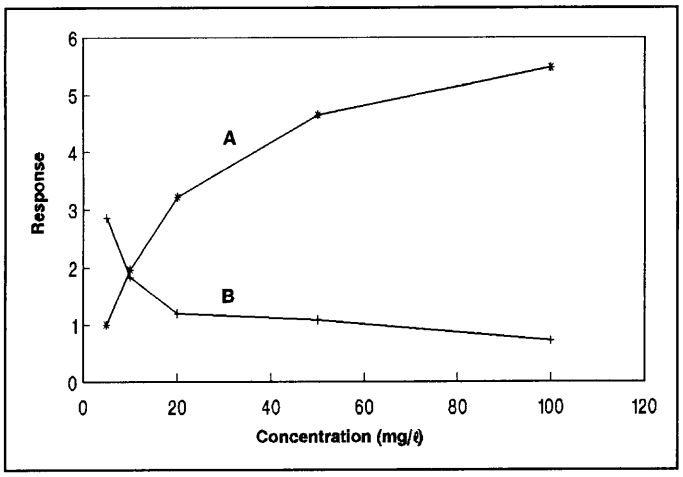

Fig. 7.8 Influence of the molybdenum concentration on relative peak height (A) and precision (B).

The $[H^+]$:[Mo] ratio for the uncatalized reaction was found to be 10.6 : 1. No self-reduction of the molybdenum reagent took place as it could be seen from the absence of background values.

7.3.1.3 Reaction time

Unfortunately, Going and Eisereich [11] did not study the effect of variations in the $[H^+]$:[Mo] ratio on the reaction rate. A knowledge of the kinetics of the reaction is of particular value when adapting the process to sequential injection analysis (SIA), since the time spend by the sample in the manifold is too short for complete colour development. Complete colour development can take up to 10 minutes to occur. These times would be inconveniently long for flow-injection analysis and would mean that much potential sensitivity might be sacrificed. In SIA, however, the flow can easily been stopped for a certain amount of time to give the reaction time to develop. A waiting period was incorporated into the

system after all the reagents were drawn up. The stack of zones was pumped forward to penetrate each other whereafter the flow was stopped. The results of the various lengths of waiting periods are summarised in Table 3 and represented in Fig. 7.9.

Masini *et al* [25] used 30 second stopped-flow periods permitting the reaction to occur to a greater extent than in the continuous-flow mode. This stopped-flow period took place as soon as the reaction product reach the detector (after a delay time of 20 seconds and at a flow rate of 1.2 $m\ell.min^{-1}$).

TABLE 3. Influence of waiting period on sensitivity and precision

Waiting period (s)	Relative peak height	%RSD
5	1.72	2.71
10	1.82	1.98
15	2.01	1.74
20	2.18	1.71
25	2.21	1.65
30	2.36	1.42
60	2.98	1.28
90	3.14	1.16
120	3.40	0.83
150	3.33	0.86
180	3.26	0.94
210	3.18	1.08
240	3.06	1.15

A waiting period of two minutes seems to be long enough for the reaction to develop completely. After two minutes no further reaction took place and the formed product zone began to disperse (dilute).

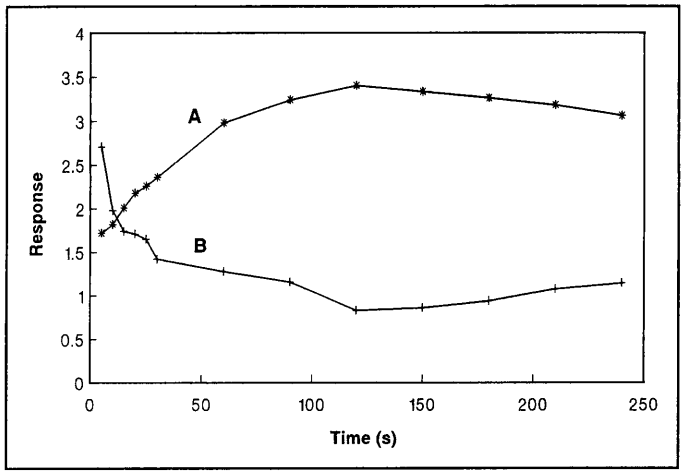

Fig. 7.9 Influence of the waiting period on sensitivity (A) and precision (B).

7.3.1.4 Reducing agent

A number of reducing agents are available from which tin(II)chloride [12] and ascorbic acid [10] are the most important. For the following reasons ascorbic acid is generally chosen [6]:

a) a more stable reduction product is formed than with tin(II)chloride

b) a smaller salt correction is necessary

c) the reproducibility with ascorbic acid is better than with tin(II)chloride

d) tin(II)chloride is unstable because it is easily oxidised by atmospheric oxygen. This results in base line drifts, that are not experienced with ascorbic acid.

7.3.1.5 pH of ascorbic acid reagent

As in the case of the molybdenum reagent the pH of the ascorbic acid also plays a role in the sensitivity of the method. Although not a major role, the influence of the pH can undoubtly be seen in Table 4 and schematically in Fig. 7.10.

TABLE 4. Influence of pH of the ascorbic acid reagent on the sensitivity and precision

pH	Relative peak height	%RSD
0.94	2.83	1.08
1.74	3.26	0.97
2.54	3.35	0.93
3.21	3.12	0.91
4.15	3.06	1.21

The higher the pH of the ascorbic acid solution, the more stable the baseline becomes. The sensitivity increase with increasing pH, but from pH 2.54 a slight decrease in sensitivity is visible.

As the addition of the buffer resulted in better reproducibility, a potassium hydrogen phthalate - hydrochloric acid buffer of pH 2.5 was used to prepare the ascorbic acid solution.

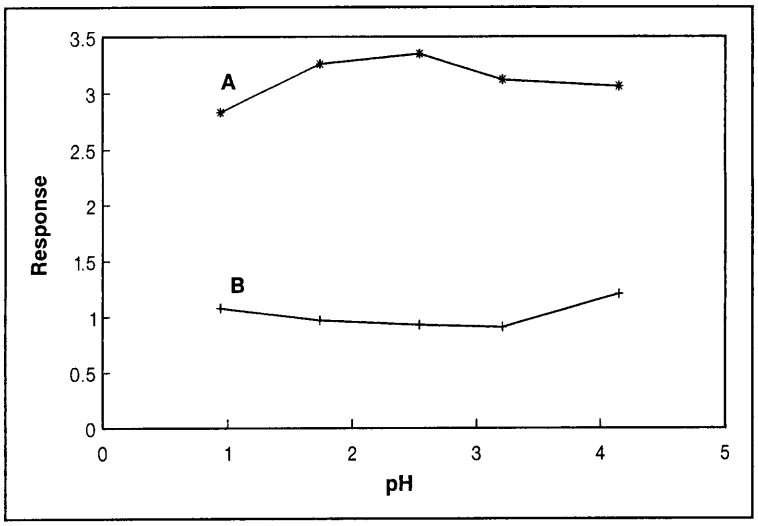

Fig. 7.10 Influence of the pH of the ascorbic acid reagent on sensitivity (A) and precision (B).

7.3.1.6 Concentration of the ascorbic acid reagent

Carroll and Tyson [5] used a 0.16% ascorbic acid solution as reducing agent. The ascorbic acid concentration was varied and the results are summarised in Table 5 and shown in Fig. 7.11.

TABLE 5. Influence of ascorbic acid concentration on sensitivity and precision

Concentration (%)	Relative peak height	%RSD
0.04	4.44	1.58
0.08	5.07	1.41
0.16	5.29	0.68
0.32	6.13	0.70
0.64	6.69	0.64
1.28	8.13	0.82

An increase in ascorbic acid concentration resulted in an increase in sensitivity. It is clear from Fig. 7.11 that 1.28% (or even higher concentrations) gave the best sensitivity. A hugh background value with relative peak height of 1.42 units was however formed. This is probably due to the reduction of the molybdenum reagent (without phosphate) by the ascorbic acid. An 0.64% ascorbic acid solution gave a stable baseline and was therefore chosen as optimum concentration.

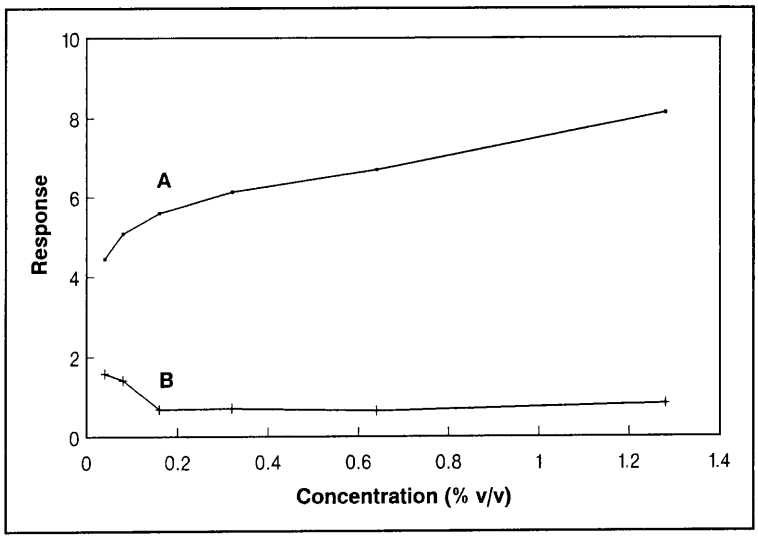

Fig. 7.11 Influence of the ascorbic acid concentration on sensitivity (A) and precision (B).

7.3.1.7 Concentration of the glycerine in the ascorbic acid reagent

The addition of glycerine to the ascorbic acid solution stabilised the solution and lead to better reproducibility day after day. A number of glycerine concentrations were evaluated and the results are shown in Table 6.

TABLE 6. Influence of glycerine (concentration) on the sensitivity and precision of the method.

Concentration (%)	Day 1 Relative peak height	Day 1 %RSD	Day 2 Relative peak height	Day 2 %RSD
0	6.85	1.11	5.81	1.83
1	6.88	0.66	6.83	0.78
2	6.92	0.86	6.04	0.97
5	7.42	1.21	5.90	1.53

The addition of 1% glycerine clearly stabilised the reagent. At day 3 the 0%, 2% and 5% solutions decreased further, while the 1% solution maintain a relative peak height of 6.84 (%RSD - 0.76). The ascorbic acid is stable for up to six weeks whereafter it turned yellow and had to be discharged. Masini *et al* [25] used 10% glycerine in the ascorbic acid reagent. The addition of glycerine is to prevent the precipitation of the reaction products.

7.3.1.8 Sequences of sample and reagents

The order in which the different sequences of reagents and samples are drawn up and propelled through the detector are very important in SIA. Initially the following order of sample and reagents was used (as suggested in [14]): first the molybdenum reagent, followed by the sample and last the ascorbic acid reagent. The relative peak height was 7.07 and the %RSD 0.52. The order was changed and the results are highlighted in Table 7.

TABLE 7. Influence of order of reagents and sample on zone overlap and precision

Order	Relative peak height	%RSD
MSA*	7.08	0.52
ASM*	7.64	0.69
SMA*	8.63	1.20
SAM*	7.44	0.69
MAS*	8.26	1.36
AMS*	9.95	0.59

* M = molybdenum reagent
S = sample
A = ascorbic acid reagent

From Table 7 it is clear that the order ascorbic acid reagent, molybdenum reagent and then the sample produced the best sensitivity as well as the best precision. Unfortunately, it also produced the "best" background value. This could be explained when one consider the time that the molybdenum reagent and ascorbic acid have to react with each other (and reduce the molybdenum) before and while the sample is drawn up. Almost the same situation occur in the order molybdenum reagent, ascorbic acid and then the sample where a relatively large background value occur. The order sample, molybdenum reagent and last the ascorbic acid reagent gave no background value. The phosphate already started to react with the molybdenum reagent whilst the ascorbic acid reagent was drawn up and there was therefore less time for the ascorbic acid to reduce the molybdenum reagent.

7.3.1.9 Temperature

The determination of phosphate as described in this chapter was done at room temperature. The reagents (molybdenum and ascorbic acid) as well as the samples were store at room temperature. This was done due to the purpose this method was developed for. The complete system (manifold, reagents, detector and computer) have to fit into a small "box" and place near a river, dam or in the effluent water of an industrial site. The system must operate for a certain period of time (24 hours a day) in the field and it was therefore necessary to know what the lifetimes of the reagents were at room temperature and how good the proposed system would operate at that temperature. Cooling of the reagents was therefore not done and heating of the manifold to speed up the reaction was ignored.

Temperature however plays an important role in the development of the reaction. According to Pauer [6] increase the sensitivity with increasing temperature. The maximum sensitivity was found at 59 °C, but above 45 °C bubbles were formed which interfere in the determination. Pauer found that 39 °C produced a satisfactory sensitivity, whilst Pai et al [10] settle for 70 °C.

7.3.1.10 Catalysts

Potassium antimony tartrate [3] or vanadium (ammonium metavandate) [3] are generally used to catalyze the reaction between the molybdenum and phosphate. A phosphoantimonylmolybdenum blue complex and phosphovanadomolybdenum blue complex formed respectively. These complexes were reduced by a suitable reducing agent, such as

ascorbic acid, to form the blue colour.

No catalyst was used in this determination and it should be considered a hugh shortcoming, for a catalyst could speed up the reaction and a higher sample frequency could be obtained.

7.3.2 Physical parameters

Instead of using the univariate optimization (Appendix B) as in the case of the chemical parameters, simplex optimization (Appendix A) was used to optimise the physical parameters. Simplex optimization was not used for the chemical parameters, because of the background values that were obtained in some cases. This problem does not arise in flow-injection analysis because the detector is zeroed on the 'background value' and it therefore does not contribute to the final peak profile.

The following parameters were optimized by simplex optimization:

1) Holding coil diameter

2) Reaction coil 1 diameter

3) Reaction coil 2 diameter

4) Pump speed (flow rate)

5) Sample volume

6) Molybdenum reagent volume

7) Ascorbic acid reagent volume

During the optimization the lengths of the holding coil, reaction coil 1 and reaction coil 2 were held on 2.1 m, 1.8 m and 1 m respectively. These parameters were not included into the simplex because of their almost fixed nature (as described later).

Simplex optimization was restarted twice. The first simplex was terminated because the response obtained with the 200 mg.ℓ^{-1} phosphate standard became to high to measure and a new simplex was started using a 50 mg.ℓ^{-1} phosphate standard. The results are summarised in Tables 8 and 9.

The same vertex number of the old simplex was used for the new simplex. The interaction between the different parameters is illustrated in Table 9. The influence of the difference in flow rate and differences in tube diameter of the holding and reaction coils is illustrated by the differences in response. The volumes of the reagents and samples varied only slightly at the different vertexes.

The second simplex was terminated because almost every new simplex move resulted in a poorer vertex and was rejected in a following move. It was clear that an optimum was reached and that any further move was reflecting a poorer result. Vertex 22 gave the best response and the best precision (%RSD - 0.54) and was taken as the optimum.

TABLE 8. Simplex optimization of selected physical parameters using a 200 mg.ℓ^{-1} phosphate standard

Vertex	HC diameter (mm)	RC 1 diameter (mm)	RC 2 diameter (mm)	Flow rate (mℓ/min)	Sample volume ($\mu\ell$)	Reagent 1 volume ($\mu\ell$)	Reagent 2 volume ($\mu\ell$)	Response	Result
1	1.02	1.02	0.64	3.9	325	130	325	7.91	R_{15}
2	1.02	1.02	0.64	4.7	157	390	390	3.99	R_1
3	1.02	1.02	0.64	3.1	260	260	260	6.02	R_4
4	1.02	1.02	0.64	2.3	76	76	76	4.61	R_2
5	1.02	1.02	0.64	3.1	155	155	155	6.30	R_5
6	1.02	1.02	1.14	3.1	207	103	207	6.34	R_9
7	1.14	1.14	0.51	3.9	260	130	260	7.89	R_{14}
8	1.02	0.76	0.51	3.9	130	130	130	6.39	R_{10}
9	1.02	1.02	1.76	2.0	170	17	71	2.50	R_3
10	1.02	1.02	0.76	4.3	433	194	371	8.79	
11	1.14	1.02	0.76	5.2	274	420	513	5.57	R_6
12	1.14	1.02	0.76	4.7	218	39	260	4.44	R_7
13	1.14	1.02	0.76	5.1	400	134	460	8.22	
14	1.14	1.02	0.76	3.0	250	60	120	4.89	R_8
15	1.02	1.02	0.76	3.1	310	173	240	7.82	R_{12}

TABLE 8. continue

Vertex	HC diameter (mm)	RC 1 diameter (mm)	RC 2 diameter (mm)	Flow rate (mℓl/min)	Sample volume ($\mu\ell$)	Reagent 1 volume ($\mu\ell$)	Reagent 2 volume ($\mu\ell$)	Response	Result
16	1.02	1.02	0.76	4.8	330	260	500	7.70	R_{11}
17	1.14	1.02	0.51	5.2	429	240	454	5.56	
18	1.14	1.14	0.76	4.8	400	240	656	8.48	
19	1.14	1.14	0.76	3.9	390	110	520	6.37	R_{13}
20	1.14	1.14	0.64	5.7	380	123	760	9.85	
21	1.02	1.02	0.51	5.5	330	248	330	9.08	
22	1.02	1.02	0.76	5.9	550	256	747	9.60	
23	1.14	1.14	0.76	6.5	498	303	801	8.76	

R_x - rejected vertex
HC - holding coil
RC - Reaction coil
Reagent 1 - molybdenum reagent
Reagent 2 - ascorbic acid reagent

TABLE 9. Simplex optimization of selected physical parameters using a 50 mg.ℓ^{-1} phosphate standard

Vertex	HC diameter (mm)	RC 1 diameter (mm)	RC 2 diameter (mm)	Flow rate (mℓ/min)	Sample volume ($\mu\ell$)	Reagent 1 volume ($\mu\ell$)	Reagent 2 volume ($\mu\ell$)	Response	Result
10	1.02	1.02	0.76	4.3	425	192	368	5.13	R_5
13	1.14	1.02	0.76	5.1	403	137	463	5.26	
17	1.14	1.02	0.51	5.1	429	240	454	5.56	
18	1.14	1.14	0.76	4.8	397	238	634	4.43	R_1
20	1.14	1.14	0.64	5.7	382	124	764	4.73	R_2
21	1.02	1.02	0.51	5.5	328	246	328	5.47	
22	1.02	1.02	0.76	5.9	550	260	750	5.93	
23	1.14	1.14	0.76	6.5	496	302	798	4.91	R_3
24	1.02	1.02	0.76	6.2	472	184	410	5.74	
25	1.02	1.02	0.76	5.3	509	307	263	4.53	R_4
26	1.02	1.02	0.64	4.2	379	154	168	5.42	
27	1.14	1.02	0.64	5.1	357	94	561	4.39	R_6
28	1.14	1.02	0.51	6.4	384	75	747	4.35	R_7
29	1.02	1.02	0.64	5.9	492	305	334	5.27	

The optimum physical parameters were as followed:

1) Holding coil diameter : 1.02 mm

2) Reaction coil 1 diameter: 1.02 mm

3) Reaction coil 2 diameter: 0.76 mm

4) Flow rate: 5.9 $m\ell.min^{-1}$

5) Sample volume: 550 $\mu\ell$

6) Molybdenum reagent volume: 260 $\mu\ell$

7) Ascorbic acid reagent: 750 $\mu\ell$

The configurations of the holding coil and reaction coils were determined by univariate optimization (Appendix B). In all the cases the following configurations were examined: coiled, straight and knitted. The results are summarised in Tables 10, 11 and 12.

(a) Holding coil (Table 10)

TABLE 10. Effect of the geometry of the holding coil on sensitivity and precision

Configuration	Relative peak height	%RSD
Coiled	5.63	0.99
Straight	5.73	0.75
Knitted	5.70	0.96

As expected did the holding coil geometry not really affect the relative peak height or the precision. A straight holding coil was however used for the system due to the slightly better peak height and precision.

(b) Reaction coil 1 (Table 11)

TABLE 11. Effect of the first reaction coil geometry on zone penetration and precision

Configuration	Relative peak height	%RSD
Coiled	5.44	1.12
Straight	5.73	0.73
Knitted	5.42	1.43

As seen from the results, the degree of zone penetration did not alter very much with the type of geometry used and any of the three geometries will suit the proposed system. A straight reactor coil was however used for the system due to better relative peak height and precision.

(c) Reactor coil 2 (Table 12)

TABLE 12. Effect of the geometry of reactor 2 on sensitivity and precision

Geometry	Relative peak height	%RSD
Coiled	6.09	0.71
Straight	5.73	0.73
Knitted	5.95	0.90

There were no significant difference between the three geometries, but a coiled reaction coil was used to connect the valve with the detector due to the slightly better peak height and precision.

These results confirm the results obtained by Marshall [13] that straight reactors are more desirable in SIA because it promotes axial dispersion, which on its turn promotes zone penetration. Radial dispersion is promoted after zone penetration took place in order for the reaction to take place, therefore a short length of knitted or coiled reactor is usually incorporated just prior to detection.

As seen from the results the holding coil and first reaction coil is of the same diameter and configuration. This reduces the holding and reaction coils to only a long holding coil. As previously mentioned, the lengths of the holding coil and reaction coil are almost fixed. The holding coil acts as a reservoir [15] and must therefore be long enough to accommodate the stack of zones drawn up through the valve. To determine the length of the holding coil a blue dye was drawn up through all the ports of the valve. As the holding coil must be long enough to prevent the dye of entering the pump conduit, a length of 3.5 m was required.

The second (or in this case only) reaction coil connect the valve with the detector. Because of its coiled geometry a minimum length of 1 m was required. Longer reaction coils did not improve the sensitivity or precision which showed that the reaction was complete and there was no need for a longer reaction coil.

7.4 Evaluation of the SIA method

The proposed sequential injection system was evaluated with regard to linearity, accuracy, precision, detection limit, sample interaction, sampling rate and interferences.

7.4.1 Linearity

The linearity of the SIA system was evaluated under optimum running conditions. It is clear from Fig. 7.12 that Beer's law was obeyed for 0 - 70 mg.ℓ^{-1} phosphate. The relationship for relative peak height versus phosphate concentration was:

$$y = 0.0967x + 0.839;\ r = 0.99987$$

where y = relative peak height and x = phosphate concentration in mg.ℓ^{-1}. The flattening of the calibration curve at concentrations above 70 mg.ℓ^{-1} is due to the small amount of molybdenum reagent available (only 260 $\mu\ell$). At phosphate concentrations higher than 70 mg.ℓ^{-1} the "cavities", where the heteroatoms are located, tend to become fully occupied and the ratio of Mo : P changed. On-line dilution (as described in Chapter 6) would be ideal to dilute more concentrated samples to the extent of the linear range of the method.

Because the real samples, obtained from the Institute for Water Quality Studies, Pretoria, were preserved with 2 mg.ℓ^{-1} $HgCl_2$ a calibration curve was constructed using phosphate standards with 2 mg.ℓ^{-1} $HgCl_2$. The calibration curve was linear between 0 and 70 mg.ℓ^{-1} phosphate. The relationship obtained for relative peak height versus phosphate concentration was:

$$y = 0.0793x + 1.168;\ r = 0.9995$$

where y and x are the same as previously described. From the above equation it is clear that the relative peak height was slightly higher in the presence of $HgCl_2$ (see 7.4.7 Interferences).

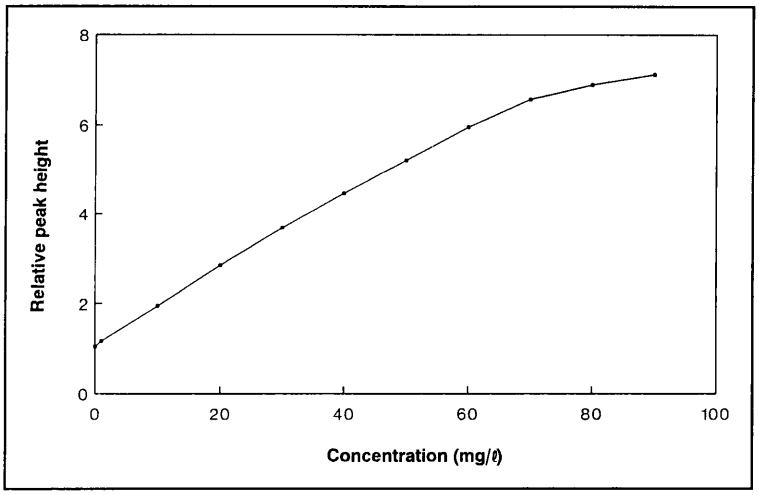

Fig. 7.12 The calibration curve was linear between 0 and 70 mg.ℓ^{-1} phosphate.

It is possible to enlarge the dynamic range by using small volumes of standard. For more precise results, a syringe pump should be used at these volumes (see Chapter 3). Larger volumes improve however the sensitivity, accuracy and precision.

It should be noted that the higher phosphate concentrations could, in principle, be determined without the need of dilution, if unreduced molybdophosphoric acid had been measured, as the absorptivity of the unreduced form (at 400 nm) is about 3400 ℓ/mol.cm, one seventh of that of the reduced form at 660 nm [25].

7.4.2 Accuracy

Real samples (water from rivers across South Africa) were analyzed with the SIA system. The accuracy of the proposed SIA analyzer was evaluated by comparing results from the real samples of the SIA system with the values obtained with a standard procedure with an AutoAnalyser. The results shown in Table 13 revealed good correlation between the SIA system and the values obtained with the AutoAnalyser.

TABLE 13. Comparison of the results of a number of samples as determined with the proposed SIA system and an AutoAnalyser.

Sample	SIA ([] in mg.ℓ^{-1})	AutoAnalyser ([] in mg.ℓ^{-1})
S832804	45.5	47
S832841	32.8	33
S833330	27.8	26
S833468	25.3	24
S833481	4.89	4
S833584	35.9	32
S833493	10.7	12
S833444	16.2	14
S833559	19.4	18
S835313	35.9	37
S835910*	22.7	22
S835787	11.9	12
S835921	19.6	19
S836652	25.3	28

A method of standard addition was also used to determine the concentration in one of the samples (S835910). This was done to confirm the value obtained by the SIA procedure. A linear calibration curve (Fig. 7.13) was obtained (r = 0.9999) and the concentration of phosphate in the sample was calculated as 23.3 mg.ℓ^{-1} which compared well with both SIA and AutoAnalyser methods.

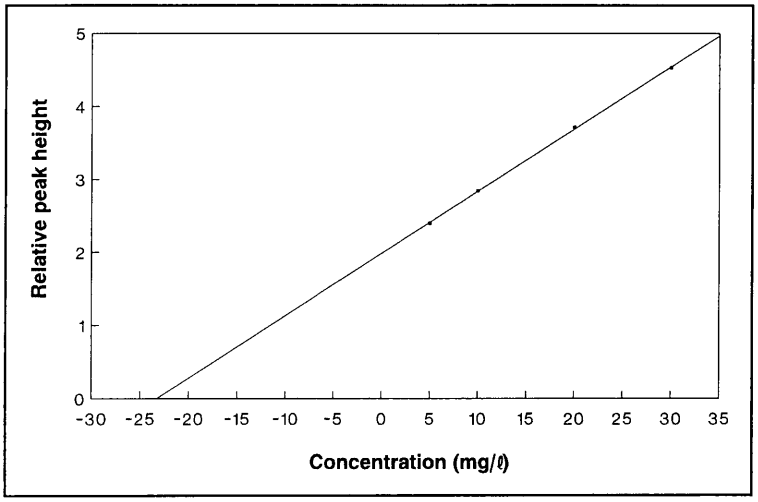

Fig. 7.13 Calibration curve obtained during standard addition. The concentration of the sample (S835910) was calculated as 23.3 mg.ℓ^{-1} phosphate.

7.4.3 Precision

The precision of the method was determined by 10 repetitions of standard solutions within the linear range of the specific method as well as 10 repetitions of samples within range. The results of the repetitions are listed in Table 14.

TABLE 14. Precision of the proposed SIA system

Standard/Sample ([] in mg.ℓ^{-1})	%RSD	Sample ([] in mg.ℓ^{-1})	%RSD
0	0.51	S832804	0.44
1	0.15	S832841	0.36
10	0.53	S833330	0.50
20	0.13	S833468	0.53
30	0.17	S833481	0.58
40	0.24	S833493	0.62
50	0.58	S833444	0.39
70	0.46	S833559	0.42
100	0.64	S835910	0.53
S835313	0.63	S835921	0.42
S835787	0.85	S833584	0.30

An excellent precision of less than 0.9% was obtained.

7.4.4 Detection limit

Detection limit is defined as the concentration of the analyte (phosphate) that will produce a signal two or three times the root mean square (rms) value of the baseline noise. In a sense, this is the lowest concentration that can be statistically differentiated from zero (the blank) [16]. The %RSD of the blank was calculated to be 0.51 (Table 14). Application of the above mentioned method (DL = 3σ; σ = 0.51) gave a value of 1.53 units. When this value is converted to absorbance units it correspond to a phosphate concentration of 7.1 mg.ℓ^{-1}. There is, however, reason to doubt this detection limit, because very well defined peaks were obtained with a 1 mg.ℓ^{-1} phosphate standard solution (relative peak height - 0.89, %RSD - 0.15).

The detection limit of the method was therefore calculated using the formula [17]

$$Detection\ limit = \frac{3 \times S_k}{100} \times K$$

where $S_k = 0.51$ is the relative standard deviation of the lowest concentration of the specific method and K = 1 mg.ℓ^{-1} is the lowest standard concentration for this method. A safety factor of 25% was built into the calculation. The detection limit was calculated to be 0.46 mg.ℓ^{-1}.

7.4.5 Sample interaction

The sample interaction, also referred to as the carry-over effect, was determined using the equation

$$Interaction = \frac{(A_3 - A_1)}{A_2} \times 100$$

where

A_1 = the true peak height of a sample with a low analyte concentration (10 mg.ℓ^{-1}),

A_2 = The true peak height of a sample containing ten times more analyte (100 mg.ℓ^{-1}) and

A_3 = The peak height for an interacted sample containing the same amount of analyte as A_1.

The relative peak heights of A_1, A_2 and A_3 were respectively 1.82, 8.98 and 1.86. The sample interaction between samples as calculated was 0.45% which is neglible.

7.4.6 Sample frequency

The sampling rate was calculated by dividing 3600 sec (1 h) through the time (in seconds) needed to complete one experiment. It took 205 sec to complete one sampling cycle which gave a sample frequency of about 18 samples per hour.

7.4.7 Interferences

There is little detailed information about the effects of interferences in the method. Generally, no interference problems are likely with unpolluted saline and fresh waters (e.g. there is no salt error). The possibility of interference should be considered, particularly with polluted samples and at phosphorus levels close to the limit of detection. A couple of the most important interferences will be described in the next paragraphs.

7.4.7.1 Arsenic

Arsenic present as arsenate is a potential source of serious error at high As : P ratios as it forms an analogous arsenomolybdenum blue complex [3]. Interferences from As(V) can be eliminated by reducing it to arsenite (As(III)) with an acidic mixture of bisulphite and thiosulphate [3]. To confirm the results that As(V) interfere in the determination of phosphate a 50 mg.ℓ^{-1} phosphate standard was spiked with ammonium arsenate. The following results

were obtained:

a) As : P in the ratio 1 : 1:- No interference of As(V) was experienced.

b) As : P in the ratio 1.5 : 1 :- An increase in relative peak height of 6.94% was experienced.

That As(V) interferes at levels higher than the 1 : 1 ratio of As : P was confirmed. The next question that arose was if As(III) interfere in the determination. A relative concentrated solution of As_2O_3 (solubility in water at 20 °C: 20 g.ℓ^{-1}) was prepared. Comparison between the relative peak heights of a 50 mg.ℓ^{-1} phosphate solution and a 50 mg.ℓ^{-1} phosphate solution spiked with the As_2O_3 solution confirmed that As(III) does not interfere in the determination of phosphate. It was, therefore, save to reduce the interfering As(V) to As(III) as suggested [3]. The reducing agent needed for the reduction was prepared as followed: 20 mℓ of 14% v/v sulphuric acid, 40 mℓ of 10% m/v sodium metabisulphite and 40 mℓ of 1% m/v sodium thiosulphate solutions were mixed together. This solution had to be prepared freshly as required [3].

The reducing agent had to be added to the sample, mixed and allow to stand for 15 minutes before final dilution to the required volume. In automated analytical systems, such as SIA, sample pretreatment has to be limited and kept to a minimum. To avoid this pretreatment of contaminated samples, attempts to combine the reducing agent with one of the reagents were made. Addition of the reducing agent to the molybdenum reagent was a total failure. As soon as HCl or H_2SO_4 was added to the reagent to adjust the pH, the mixture became yellow, then green and eventually turned dark blue. It is clear that the molybdenum in the reagent is

immediately reduced (in the absence of phosphate) by the reducing agent and that this mixture was unsuitable to use in the determination of phosphate.

Addition of the reducing agent to the ascorbic acid reagent resulted in a slightly yellow solution. This solution was, however, used to evaluate the influence of the reducing agent on the spiked phosphate standard. The relative peak height of the 50 mg.ℓ^{-1} phosphate standard was 4.03 units, while the relative peak height of the spiked solution (50 mg.ℓ^{-1} phosphate + 75 mg.ℓ^{-1} As) was 3.50 units. The result: an overall decrease in relative peak height of 13%. It is uncertain if this decrease in relative peak height was due to reduction of As(V) to As(III). The main reason for this dramatic decrease in relative peak height was that the viscosity of the ascorbic acid reagent was largely increased by the addition of the reducing agent, and this resulted in insufficient mixing of the ascorbic acid zone with the molybdenum and sample zones.

At this stage it was clear that the reducing agent could not be mixed with either of the reagents. To incorporate the reducing agent into the system via one of the ports of the valve did not seem to solve the problem. This would result in a stack of four zones that need to be mixed together (Fig. 7.14). Penetration of these four zones to form a well defined product zone seemed rather impossible, for it was found by Gübeli *et al* [14] that maximum three zones can be mixed together to ensure satisfactory zone overlap. The chances that the molybdenum reagent would be reduced by the reducing agent before it could react with the phosphate is highly possible and this would result in a peak profile due to the reduction of the molybdenum reagent and not due to the phosphate reaction. Another possibility was of course to redesign the complete SIA system and mixed the sample and reducing agent while

the molybdenum and ascorbic acid reagents were drawn up.

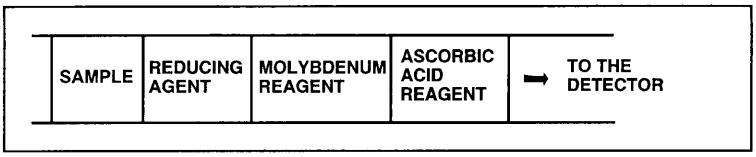

Fig. 7.14 Sequence of sample, reducing agent, molybdenum reagent, ascorbic acid reagent and detection.

Addition of the reducing agent to the sample prior to injection into the manifold, led to the following results:

TABLE 15. Influence of the reducing agent on the As(V) interference

Solution	Relative peak height	%RSD	Result
50 mg.ℓ^{-1} phosphate standard (a)	4.66	0.50	
50 mg.ℓ^{-1} phosphate standard + 75 mg.ℓ^{-1} As (b)	4.83	0.60	3.5% increase
50 mg.ℓ^{-1} phosphate standard + 75 mg.ℓ^{-1} As + 5 mℓ reducing agent	4.33	1.20	7.1% decrease from (a) 10.4% decrease from (b)

The relative peak height is recorded immediately after the addition of the reducing agent. A peak profile recorded 36 minutes after addition of the reducing agent showed a further decrease in relative peak height.

It seemed that the reducing agent reduced the As(V), but it also reduced the phosphate to phosphite and thereby lowered the relative peak height. A 50% v/v dilution of the reducing agent added to the spiked phosphate solution only reduced the As(V). The relative peak heights of the 50 mg.ℓ^{-1} phosphate standard and the spiked standard with diluted reducing

agent were 4.03 and 3.95 units respectively. This results were obtained immediately after the addition of the reducing agent to the spiked phosphate standard.

7.4.7.2 Silicate

Silica causes neglible interference in the determination of phosphate at room temperature as the formation of silicomolybdenum blue is inhibited by the high $[H^+]$:[Mo] ratio used [10]. Koroleff [18] has reported that 5 mg.ℓ^{-1} Si gives an absorbance of 0.003 at 880 nm in a 10 cm cuvette after 30 minutes. Interference from Si can be considerably reduced by carrying out the spectrophotometric measurements 6 - 10 minutes after addition of the mixed reagent as the kinetics of the formation of the molybdenum blue complex are relatively slow [3].

Despite the high $[H^+]$:[Mo] ratio (10.6 : 1) used and the rapid measurement of the formed product (measurements were carried out only two minutes after addition of the reagents), Si interfered tremendously in the determination of phosphate. The relative peak height of an 50 mg.ℓ^{-1} phosphate standard was 5.00 and the relative peak height of an 50 mg.ℓ^{-1} phosphate standard spiked with 10 mg.ℓ^{-1} Si was 8.37 units. This resulted in an increase in relative peak height of 67.2%!

Experiments with the ascorbic acid reagent, whereby the reducing agent was added (7.4.7.1 Arsenic), reduced the relative peak height of the spiked phosphate standard to 4.81 causing a nett increase of 12.2% in peak height, when compared to the 50 mg.ℓ^{-1} phosphate standard.

This decrease in sensitivity is not only due to insufficient mixing of the adjacent zones (because of the larger viscosity of the ascorbic acid reagent). When the reducing agent was added to the spiked sample prior to injection the relative peak height decreased to 5.85 from 8.37 units. The reducing agent is therefore responsible for the reduction of Si(V), causing a decrease in the interference.

Although addition of the reducing agent remove some of the interferent it is unable to suppress it. Si is thus a major interference in the determination of phosphate in water, because according to Pauer [6] the concentration of Si in surface water vary between 1 and 15 mg.ℓ^{-1}.

No interference from either arsenic or silicate was experienced in the analysis of the real water samples (Table 13) and the reducing agent was therefore not used as pretreatment of the samples.

7.4.7.3 Chromium

Cr(VI) is reported to interfere at 1 mg.ℓ^{-1} level [19]. Cr(VI) in the ratio 1 : 1 Cr : P showed however no interference in the determination.

7.4.7.4 Nitrite

A concentration of 1 mg.ℓ^{-1} N (as nitrite) may be tolerate in the presence of 0.1 mg.ℓ^{-1} phosphorus (as phosphate). The interference of nitrite is, however, both complex and variable

and appears to be related to exposure to air. A slight excess of sulphamic acid is effective in breaking down nitrite; 100 mg of the acid will deal with a nitrite concentration of 10 mg.ℓ^{-1} N in a 40 mℓ aliquot of test solution [3].

7.4.7.5 Nitrate

Interference from nitrate (NO_3^- : P, 2 : 1) caused an increase of 0.39% in relative peak height. This interference is neglible and confirms the result that nitrate may be tolerated up to 20 g.ℓ^{-1} (as N) provided that the absorbance is measured within 2 hours of colour development [3].

7.4.7.6 Sulphide

Interference of sulphide is complex, variable and dependent on conditions, reacting with both antimonate (catalyst) and molybdate to form thioacids. Complete removal by oxidation to sulphate or by aspiration with nitrogen is advocated [20].

7.4.7.7 Oxidizing agents

The action of oxidizing agents (oxalate and tartrate) in this method is complex. They may destroy the reducing agent, or subsequently reoxidize the phosphomolybdenum blue complex. The effect of oxidizing agents may be overcome by treatment with an excess of metabisulphite/thiosulphate in acid solution [21]. The presence of sulphur dioxide has no influence on the final production of molybdenum blue, but the treatment can only be applied

to determinations of inorganic phosphorus and total phosphorus, where hydrolysis is acceptable, as opposed to the determination of dissolved reactive phosphorus.

7.4.7.8 Mercury(II)chloride

The real samples obtained from the Institute for Water Quality Studies (Department of Water Affairs and Forestry, Pretoria) were preserved with 2 mg.ℓ^{-1} $HgCl_2$. It was found that $HgCl_2$ positively interfere at the ratio Hg(II) : P, 1 : 25. An increase in relative peak height of 2.9% was experienced. A concentration of 20 mg.ℓ^{-1} (Hg(II) : P) caused a 5% decrease in the relative peak height.

7.4.7.9 Barium, cesium and lead

The free molybdenum heteropoly acids and the salts of small cations are extremely soluble in water, but the salts of large cations such as Cs^+, Ba^{2+} and Pb^{2+} are usually insoluble [1]. From these three cations only Ba^{2+} was evaluated. A ratio Ba : P of 5 : 1 however showed no interference at all in the determination of phosphate. It can thus be concluded that the reaction between the molybdate and smaller P occurred much faster than the reaction between molybdate and barium.

7.4.7.10 Tellurium, iodine, cobalt and aluminium

Of these cations only Al^{3+} was tested as possible interference. All these cations form 1 : 6 octahedral complexes with molybdenum. This is however not the main reason why Al^{3+}

interfere in the determination of phosphate. Al^{3+}, like Ca^{2+}, forms insoluble salts with phosphates and lower thereby the free phosphate content of the samples. ($AlPO_4$:- K_{sp} = 3.7 x 10^{-41} and $Ca_3(PO_4)_2$:- K_{sp} = 1.2 x 10^{-29}) [22]. A ratio of 1 : 1 Al : P decreased the relative peak height with 8.6%.

7.4.7.11 Iron and copper

According to Pauer [6] Fe^{3+} and Cu^{2+} are present in limited quantities in surface and groundwater and it therefore do not interfere in the determination of phosphate. A ratio of 3 : 1 Cu : P cause a decrease in relative peak height of 3.7%. Fan and Fang [24] found that coexisting Fe^{3+} ions depress the signal obtained in the determination of phosphate. This interference would normally be overcome to some extent by masking in iron with tartrate.

The cations in 7.4.7.10 and 7.4.7.11 can easily be removed from the sample by using a cation exchange column in the uptake tube of the sample line.

7.4.7.12 Tin(II)chloride

Instead of ascorbic acid, tin(II)chloride can be used as reducing agent, therefore $SnCl_2$ can not really be seen as an interference, but the influence thereof in the presence of ascorbic acid was evaluated. Janse *et al* [23] mentioned that the reaction with ascorbic acid is too slow at low phosphate concentrations to produce sufficient sensitivity. The addition of 10 mg.ℓ^{-1} $SnCl_2$ improve the sensitivity and resulted in a 5% increase in relative peak height of

a 50 mg.ℓ^{-1} phosphate standard. $SnCl_2$ is however not used very frequently because it is easily oxidized by atmospheric oxygen and this led to unacceptable baseline drifts [6].

7.4.7.13 Antimony and vanadium

Antimony and vanadium are, like $SnCl_2$, not really interferences due to their use as catalysts in the reaction between molybdenum and phosphate. Addition of antimony as catalyst accelerate the reaction and improve the sensitivity [9]. Too high antimony concentrations resulted in turbid antimony solutions that complicated the automated SIA system tremendously [23].

7.4.7.14 Carbonate

However a neglible interference, it was found that the carbonate ion started to interfere at a ratio of 300 : 1 (CO_3^{2-} : PO_4^{3-}).

7.4.7.15 Phosphorous oxides

Both $P_2O_5^-$ and $P_2O_7^{2-}$ interfere positively to a great extent in the determination of phosphate. This interference is due to the rapid hydrolysis of the substances.

7.5 Conclusion

Proven feasible for automating the "Molybdenum Blue" method for phosphate monitoring, sequential injection analysis (SIA) presents some advantages in comparison to classical flow injection analysis (FIA) (such as simplicity of the manifold). A reduction in reagent and sample consumption is observed. The flow detector fouling with the product of the reaction between ascorbic acid and ammonium molybdate does not occur in SIA manifolds as the detector is in contact with water between analyses. In FIA manifolds, both reagents are mixed in the detector field causing fouling after a few hours of use [25]. As a consequence, very stable base lines are obtained by SIA and system cleaning during the operation time is unnecessary. The proposed system is fully computerised and is able to monitor phosphate in samples at a frequency of 18 samples per hour with a relative standard deviation of 0.9%. The calibration curve is linear between 0 and 70 mg.ℓ^{-1} phosphate. The detection limit is 0.46 mg.ℓ^{-1}. The major interferences were highlighted and attempts to remove them were offered. The proposed SIA method is accurate and reliable and will soon find numerous applications in the industries.

7.6 References

1. N. N. Greenwood and A. Earnshaw, **Chemistry of the Elements**, Chapter 12, pp. 546-637 and Chapter 23, pp 1167-1211, Pergamon, 1986.
2. J. Emsley, Phosphate Cycles, **Chem. Br.**, **13** (1977) 459.
3. **Phosphorus and Silicon in Waters, Effluents and Sludges.** Methods for the Examination of Waters and Associated Materials, HMSO, 1992.
4. D. F. Bolts, **Colorimetric Determination of Non-metals**, 2nd ed. Wiley-Interscience, New York, 1978.
5. M. K. Carroll and J. F. Tyson, **Applied Spectroscopy**, **48**(2) (1994) 276.
6. J. J. Pauer, **Die Vloei-inspuit Analise van Sekere Determinante in Oppervlak- en Grondwater**, MSc-Tesis, Universiteit van Pretoria, Maart 1989.
7. D. L. Kepert, **Isopolyanions and Heteropolyanions**, Chap 51 in Comprehensive Inorganic Chemistry, Vol 4, Pergamon press, Oxford, 1973, pp 607 - 672.
8. G. D. Marshall and J. F. van Staden, **Analytical Instrumentation**, **20** (1992) 79.
9. J. Murphy and J. P. Riley, **Anal. Chim. Acta.**, **27** (1962) 1431.
10. S. Pai, C. Yang and J. P. Riley, **Anal. Chim. Acta.**, **229** (1990) 115.
11. J. E. Going and S. J. Esenreich, **Anal. Chim. Acta.**, **70** (1974) 95.
12. H. K. Ludwak, **Analyst**, **78** (1953) 661.
13. G. D. Marshall, **Sequential-Injection Analysis**, PhD-Thesis, University of Pretoria, 1994.
14. T. Gübeli, G. D. Christian and J. Růžička, **Anal. Chem.**, **63** (1991) 2407.
15. J. Růžička and G. D. Marshall, **Anal. Chim. Acta.**, **237** (1990) 329.
16. G. D. Christian and J. E. O'Reilly, **Instrumental Analysis**, 2nd ed., Allyn and

Bacon, Inc., Boston, 1986.

17. J. F. van Staden and R. E. Taljaard, **Anal. Chim. Acta.**, In Press.

18. F. Koroleff in K. Grasshoff, M. Ehrhardt and K. Kremling (Eds), **Methods of Sea Water Analysis**, 2nd Ed., Verlag Chemie, Weinheim, (1983) 126-136.

19. F. J. Welcher (Ed), **Standard Methods of Chemical Analysis**, Vol 2 B, p 2467, 6th Ed., R. E. Kriegler, 1963.

20. V. N. de Jong and L. A. Villerius, **Marine Chemistry, 9** (1980) 191.

21. J. C. van Schouwenburg and I. Walinga, **Anal. Chim. Acta., 37** (1967) 271.

22. L. W. Potts, **Quantitative Analysis. Theory and Practice**, Harper and Row, New York, 1987, p 656.

23. T. A. H. M. Janse, P. F. A. van der Wiel and G. Kateman, **Anal. Chim. Acta., 155** (1983) 89.

24. S. Fan and Z. Fang, **Anal. Chim. Acta., 241** (1990) 15.

25. J. C. Masini, P. J. Baxter, K. R. Detwiler and G. D. Christian, **Analyst, 120** (1995) 1583.

26. J. F. van Staden, **Water SA, 13** (4) (1987) 107.

CHAPTER 8

Determination of Ammonia with the Indophenol Method using Sequential Injection Analysis

8.1 Introduction

Ammonia is a key parameter in many biological and industrial processes as well as an important indicator of the pollution of the environment [4]. The main nitrogen compounds in surface and groundwaters are nitrate (NO_3^-), nitrite (NO_2^-), ammonia (NH_4^+) and organic bounded nitrogen. Ammonia is the most reduced inorganic nitrogen form present in natural waters. Consequently, it is utilized in autotrophic processes in preference to nitrate and nitrite and is generated first from organic matter. Ammonia plays an important part in the nitrogen cycle of shallow and eutrophicated waters [14].

Most waters contain ammonium salts ("saline ammonia") and free ammonia in equilibrium with each other:

$$NH_4^+ + H_2O \rightleftharpoons NH_3 + H_3O^+$$

This equilibrium is extremely dependent on pH - with high pH favouring the free ammonia - and, to a lesser extent, on temperature, pressure and ionic concentration (or salinity) of the

water. The total concentration of the two species, more usually termed the "ammoniacal nitrogen" or "total ammonia" concentration, is generally understood to be the determinant in methods for the determination of ammonia in water [7]. Total nitrogen is defined as the value which is contributed by free ammonia, inorganic ammonium compounds and those types of organic nitrogen compounds that can be converted to ammonium sulphate by digestion with sulphuric acid [8].

Nitrogen plays an active part in the acidification of soils, where it is mainly present as organic nitrogen. The main organic forms are the ammonium and very mobile nitrate ions. Under aerobic conditions, ammonia is readily converted into nitrate owing to the activity of *Nitrosomonas* and *Nitrobacter* bacteria [26].

Ammonia plays a significant role in the atmosphere, because it is the only highly soluble common base present. It can neutralize different acids; the ammonium ion, NH_4^+, is a frequently found constituent of atmospheric aerosols and fogs. Ammonia is produced by biological processes from organic nitrogen compounds and hence exists in both clean and polluted atmospheres [26].

8.1.1 Properties of ammonia

NH_3 is a colourless, alkaline gas with an unique, penetrating odour that is first perceptible at concentrations of about 20 - 50 mg.ℓ^{-1}. Noticeable irritation to eyes and the nasal passages begins at about 100 - 200 mg.ℓ^{-1} and higher concentrations can be dangerous. Some physical and molecular properties of NH_3 are given in Table 1 [1].

TABLE 1. Physical and molecular properties of ammonia

Physical properties	Value	Molecular properties	Value
Melting point	195.42 K	Symmetry	C_{3v} (pyramidal)
Boiling point	239.74 K	Distance (N-H)	101.7 pm
Density (ℓ; 239 K)	0.6826 g.cm^{-1}	Angle (H-N-H)	107.8°
Density (g; rel. air = ℓ)	0.5963	Pyramid height	36.7 pm
η (239.5 K)	0.254 centipoise[(a)]	μ	1.46 Debye[(b)]
Dielectric constant ϵ (239 K)	22	Inversion barrier	24.7 kJ.mol^{-1}
K (234.3 K)	1.97 x 10^{-7} ohm^{-1}.cm^{-1}	Inversion frequency	23.79 GHz[(c)]
ΔH_f^0 (298 K)	-46.1 kJ.mol^{-1}	D (H-NH_2)	435 kJ.mol^{-1}
ΔG_f^0 (298 K)	-16.5 kJ.mol^{-1}	Ionization energy	979.7 kJ.mol^{-1}
S^0 (298 K)	192.3 J.K^{-1}.mol^{-1}	Proton affinity (gas)	841 kJ.mol^{-1}

[(a)] 1 centipoise = 10^{-3} kg.m^{-1}.s^{-1}
[(b)] 1 Debye = 10^{-18} esu = 3,335 64 x 10^{-30} cm
[(c)] GHz = 10^9 s^{-1}

8.1.2 Why is it necessary to determine ammonia?

The applications of ammonia are dominated (over 80%) by its use in various forms as a fertilizer. Of these, direct application is the most common (27.1%), followed by NH_4NO_3 (18.9%), urea (13.9%), ammonium phosphates (8.8%), N solutions and mixed fertilizers (8.2%) and $(NH_4)_2SO_4$ (3.5%) [1].

Particularly with regard to soil analysis agriculturalists are mainly interested in the nitrogen contents actually available to the growing plant. Because sewage sludge is applied to agricultural land as fertilizer there is a need to monitor application rates and to assess the

retention and/or availability of nitrogen by the analysis of soils and sediments; and to assess the uptake of nitrogen by plant material by the analysis of the plant material [8].

The agricultural value of the nitrogen present in sewage sludge depends on the form in which it is present together with the type of plant and time of year. "Free" ammonia is considered to be immediately available to pasture or plants although it may be rapidly lost by leaching, whilst organic nitrogen is released more slowly over longer periods [8].

During a fermentation process (yeast fermentation), it is desirable to know both the ammonium and ammonia concentrations. The ammonium-nitrogen indicates the level of nutrient, while significant amounts of ammonia indicate occurrence of undesirable metabolic pathways (anaerobic conditions) [4].

Industrial uses include (a) commercial explosives (5%) - such as NH_4NO_3, nitroglycerine, TNT and nitrocellulose, which are produced from NH_3 via HNO_3 - and (b) fibres/plastics (10%), e.g. in the manufacture of caprolactam for nylon-6, hexamethylenediamine for nylon-6,6, polyamides, rayon and polyurethanes. Other uses ($\sim$ 5%) include a wide variety of applications in refrigeration, wood pulping, detinning of scrap-metal and corrosion inhibition. It is also used as a rubber stabilizer, pH controller, in the manufacture of household detergents, in the food and beverage industry, pharmaceuticals, water purification and the manufacture of numerous organic and inorganic chemicals [1].

Ammonia is prepared industrially in larger amounts (number of moles) than any other single compound and the production of synthetic ammonia is of major importance in several

industries. Indeed, synthetic ammonia is the key to the industrial production of most inorganic nitrogen compounds, as indicated in Fig. 8.1 [1].

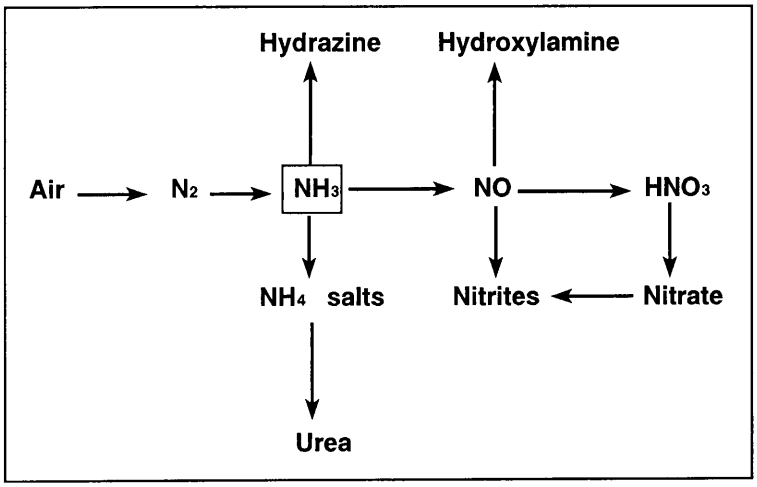

Fig. 8.1 Synthetic ammonia is the key to the industrial production of most inorganic nitrogen compounds.

Eutrophication and water pollution are nowadays a large problem. Estimation of ammonia, an important parameter to many ecosystems, is an important indicator of the pollution of the environment.

8.2 Sample collection and pretreatment

Samples can be collected in either glass or polyethylene containers. They should be analyzed as soon as possible after sampling, but if this should not be possible, storage at 4 °C is recommended in order to minimize ammonia concentration changes [7].

Samples that were taken at sites far from laboratories must be preserved and/or refrigerated as the absence of preservatatives and refrigeration results in an underestimation of NH_4^+ (especially when a considerably long lag-time exists between collection and analysis). Samples can be preserved with phenylmercuric acetate (0.1 mℓ/20 mℓ sample) [2].

Where delays in analysis is inevitable, and as a alternative to refrigeration, the sample may be brought to pH 2 with hydrochloric acid (d_{20} 1.18). The sample must be neutralized immediately prior to analysis with concentrated sodium hydroxide solution known to be free from ammonia. Differentiation between the forms of ammonia present in the preserved sample is not possible following such pretreatment [7].

Samples containing suspended matter should be allowed to settle prior to analysis, or preferably filtered through a glass fibre or membrane filter. Note, however, that ammonia can be absorbed during filtration. The filter medium must be first checked in this respect [7, 8].

Samples containing free chlorine should be dechlorinated at the time of sampling by the addition of a small crystal of sodium thiosulphate [7].

8.3 Choice of analytical method

There are several methods of determining ammonia and NH_4^+ in water. The manual spectrophotometric methods for ammonia are based on the following: Ammonia reacts with

hypochlorite ions, generated *in situ* by the alkaline hydrolysis of sodium dichloroisocyanurate, and with phenol at a pH of about 10.5, in the presence of potassium ferrocyanide, to form a coloured compound. The absorbance of the compound is measured spectrophotometrically [7]. The indophenol complex displays a broad absorption feature between 600 and 700 nm, with a maximum at 640 nm [26]. However, a method using sodium salicylate, instead of phenol, gave performance characteristics similar to those obtained with the former method. Because the high concentration of magnesium present in water, especially seawater, would be partially precipitated at the high pH value (required for stable colour formation) in the salicylate-based method, the phenol-based method (with a lower operating pH value) is preferred [7]. An advantage of the salicylate-based method is that it avoid the formation of the poisonous o-chlorophenol [14].

An alternative method of determining ammonia, oxidized nitrogen and most forms of organic nitrogen in raw and potable waters involves the oxidation of the sample with peroxodisulphate in alkaline conditions in an autoclave and subsequent determination of the formed nitrate [9]. Other methods include titrations [7], potentiometric determinations [7], ammonia selective electrodes [11] and determination of ammonia using carbon dioxide laser photocoustic spectroscopy [26].

The two most widely used colorimetric methods (adapted for flow injection systems) are the Nessler reaction [5] and the Berthelot reaction [6]. The Berthelot reaction is generally used because a number of organic substances in water interfere at the wavelength where ammonia is determined (when using the Nessler reaction). A reference channel is thus necessary. This complicates the methods tremendously [12]. The indophenol method is widely used for on-

site determination of ammonia [2] and evaluation of accuracy between various laboratories [2, 3]. Another method used in flow systems is to elevate the pH of the sample to at least pH 11 by addition of sodium hydroxide. The ammonia present in the sample is then released as gaseous ammonia which diffuses across a PTFE membrane into a buffered indicator (phenol red) stream. The change in absorption is measured spectrophotometrically at 592 nm [4, 10].

The indophenol method, as adapted for SIA by Lukkari *et al* [4], was chosen as analytical method for this study. This was done because the indophenol method is very suitable for direct routine analysis of ammonia in both fresh and seawater [14]. The method is also specific for ammonia, since organic nitrogen compounds, nitrate, nitrite and various electrolytes (in concentrations normally occurring in natural waters) do not interfere in the determination [12].

8.4 Principle of the reaction used for analysis

Ammonia in the sample reacts with hypochlorite ions to form monochloramine. This reacts with the phenolic compound in the presence of sodium tetraborate to form a blue indophenol-type compound which is measured spectrophotometrically at 640 nm. Fig. 8.2 shows the proposed reaction mechanism [12].

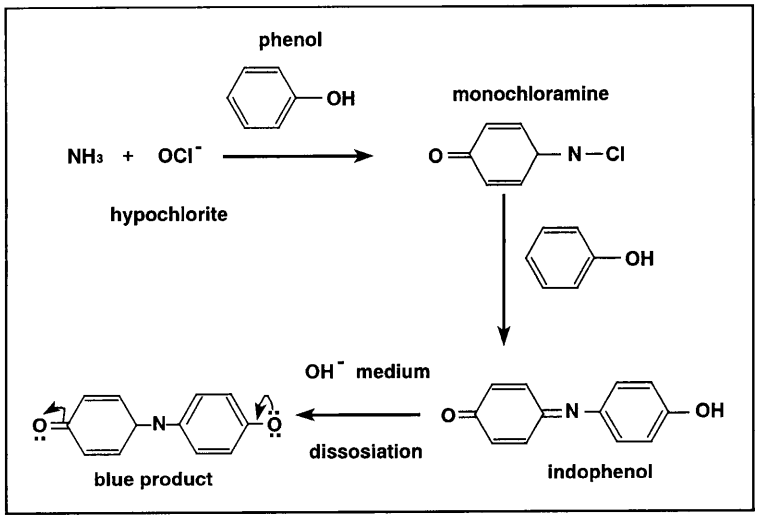

Fig. 8.2 Proposed reaction mechanism of the indophenol method.

8.5 Determination of ammonia with sequential injection analysis

8.5.1 Experimental

8.5.1.1 Reagents and solutions

All reagents were prepared from analytical-reagent grade unless specified otherwise. All aqueous solutions were prepared with doubly distilled deionised water. All solutions were degassed before measurements with a vacuum pump system.

Standard ammonium solutions: A stock solution containing 1 000 mg.ℓ^{-1} ammonium-N was prepared by dissolving 4.716 g $(NH_4)_2SO_4$ in distilled water and diluting it to 1 ℓ. Working solutions in the range 1 - 200 mg.ℓ^{-1} were prepared by suitable dilution of the stock solution.

Phenol reagent [4]: An alkaline phenol solution was prepared by dissolving 3.0 g pink phenol (Merck), 12.0 g of sodium hydroxide and 40 mℓ of ethanol in deionized water and diluting it to 100 mℓ.

Hypochlorite reagent [4]: An alkaline hypochlorite solution was prepared by dissolving 3 g of sodium hydroxide and 2 g of sodium tetraborate decahydrate in 60 mℓ of household bleach solution (containing 3.5% m/v sodium hydrochlorite) and diluting it to 100 mℓ.

Carrier: An alkaline carrier solution was prepared by dissolving 40 g sodium hydroxide in distilled water and diluting it to 1 ℓ.

Wash solution: A wash solution of 0.05 mol.ℓ^{-1} hydrochloric acid was used.

8.5.1.2 Apparatus

The sequential injection system were constructed from the following components: a Gilson minipuls peristaltic pump; a 10-port electrically actuated selection valve (Model ECSD10P; Valco Instruments, Houston, TX, USA); and a Unicam 8625 UV-visible spectrophotometer equipped with a 10-mm Hellma type flow-through cell (volume: 80 $\mu\ell$) for absorbance measurements. The formed indophenol product was monitored by measuring the absorbance at 640 nm. Data acquisition and device control were achieved using a PC30-B interface board (Eagle Electric, Cape Town, South Africa) and an assembled distribution board (MINTEK, Randburg, South Africa). The *FlowTEK* [13] software package (obtainable from MINTEK, Randburg, South Africa) for computer-aided flow-analysis was used throughout for device

control and data acquisition.

8.5.1.3 Manifold

The components of the SIA system were arranged as illustrated in Fig. 8.3. The holding coil was made of 2.0 m x 1.02 mm id coiled Tygon tubing, reaction coil 1 of 1.2 m x 1.02 mm id straight Tygon tubing and reaction coil 2 of 1.0 m x 0.76 mm id coiled Tygon tubing. The sampling, standard and reagent lines were made of 45 cm x 1.1 mm id Tygon tubing. The flow rate used, was 6.0 $m\ell.min^{-1}$.

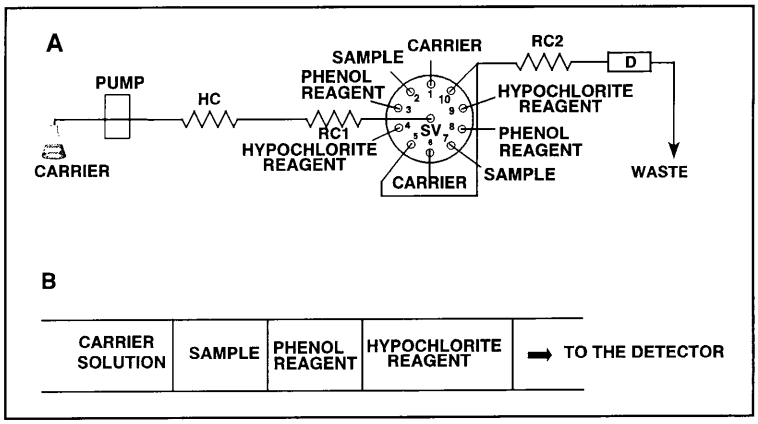

Fig. 8.3 Sequential injection system (A) used in the determination of ammonia. HC - holding coil, RC - reaction coil, SV - selection valve and D - detector. B: Sequence of zones.

8.5.1.4 Procedure

The device sequence for the determination of ammonia is outlined in Table 2. Two measurement cycles were used on one complete cycle of the 10-port selection valve. This

was done to utilise the full available capacity of the 10-port Valco valve. As seen from the sequential injection system depicted in Fig. 8.3 the first cycle (carrier, sample, phenol reagent, hypochlorite reagent and flushed to the detector) involved ports 1 to 5 of the selection valve. This was followed by an identical cycle involving ports 6 to 10.

TABLE 2. Device sequence for one cycle of the sequential injection system

Time (s)	Pump	Valve	Description
0	Off	Off	Pump and valve off
1		Carrier	Select carrier solution
5.5	Reverse		Draw up carrier solution
10.5	Off		Pump stop
11.5		Sample	Select sample solution
13	Reverse		Draw up sample solutions
18.5	Off		Pump stop
19.5		Phenol reagent	Select phenol reagent
20.5	Reverse		Draw up reagent
23	Off		Pump stop
24		Hypochlorite reagent	Select hypochlorite reagent
25	Reverse		Draw up reagent
33.5	Off		Pump stop
34.5		Detector	Select detector line
35.5	Forward		Pump stack of zones forward to penetrate each other
40.5	Off		Pump stop
50.5	Reverse		Pump stack of zones backwards to ensure mixing
60.5	Off		Pump stop
70.5	Forward		Pump stack of zones forward to ensure complete mixing
80.5	Off		Pump stop, stopped-flow period to allow reaction to develop
160.5	Forward		Pump formed product zone through detector
225	Off	Off	Return pump and valve to starting position

8.6 Optimization of the SIA system

8.6.1 Chemical parameters

As stated earlier most waters contain ammonium salts and free ammonia in equilibrium with each other:

$$NH_4^+ + H_2O \rightleftharpoons NH_3 + H_3O^+$$

This equilibrium is extremely dependent on pH - with high pH favouring the free ammonia - and, to a lesser extent, on temperature, pressure and ionic concentration of the water. The indophenol formation is a very slow process, but can be promoted by a catalyst. Sodium nitroprusside, found to be the most effective amongst the various catalysts [15], was unsuitable for use in sequential injection analysis due to the resulting high background values. It was therefore necessary to optimise the reagents to obtain an acceptable degree of sensitivity, reproducibility and sample frequency.

8.6.1.1 Phenol reagent

8.6.1.1.1 Concentration of the phenol reagent

It is clear from Fig. 8.4 that the relative peak height increases with increasing phenol concentration. Although it seemed that higher phenol concentrations would give rise to higher response values, a phenol concentration of 50 mg.ℓ^{-1} was used during the analysis. This was done, because the higher concentrations ($>$ 50 mg.ℓ^{-1}) become slightly yellow coloured and

this resulted in significant background values that is unacceptable in SIA.

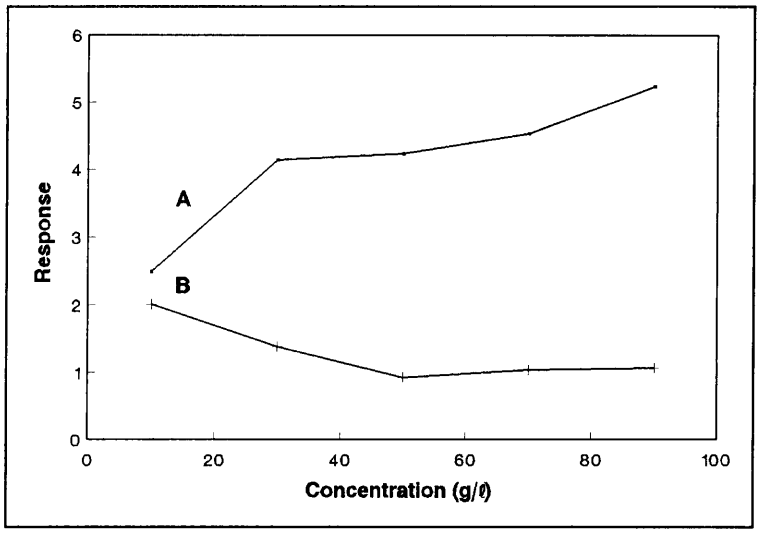

Fig. 8.4 Influence of phenol concentration on relative peak height (A) and precision (B - %RSD).

8.6.1.1.2 Concentration of NaOH in the phenol reagent

Because the determination of NH_3 is highly pH dependant and since high pH values favoured the formation of ammonia, it is necessary to perform the reaction in alkaline medium. Various NaOH concentrations were evaluated and the results are summarised in Table 3.

TABLE 3. Influence of the NaOH concentration on zone penetration and precision

Concentration ($g.\ell^{-1}$)	Relative peak height	%RSD
80	3.84	1.49
100	3.92	1.18
120	3.98	0.96
140	3.51	1.64
160	3.37	2.14

The 120 g.ℓ^{-1} NaOH solution was chosen as optimum, since it gave the best sensitivity and precision. The pH of the solution was approximately 10.8. The sudden decrease in response and reproducibility at concentrations higher than 120 g.ℓ^{-1} NaOH is due to the increase in viscosity of the solution. This resulted in smaller zone overlap due to insufficient mixing of the various zones.

8.6.1.1.3 Concentration of ethanol in the phenol reagent

Solórzano [17] dissolved the phenol in ethyl alcohol, since water solutions was found to be unstable. The use of ethyl alcohol as solvent is also recommended by Ivančič and Degobbis [14]. One of the advantages of this technique is that the phenol-alcohol reagent also serves as an efficient preservative for the samples [14]. Various water : ethanol ratios were evaluated. The results are summarised in Table 4.

TABLE 4. Influence of the water : ethanol ratio on sensitivity and precision

Water: ethanol ratio	Relative peak height	%RSD
1 : 0	1.70	2.55
7 : 3	3.78	1.42
6 : 4	5.04	1.09
1 : 1	5.53	2.50
4 : 6	6.50	2.80
0 : 1	7.12	3.05

The best precision was obtained with the 6 : 4 water : ethanol ratio. Better sensitivity was obtained with higher ethanol concentrations, but the reproducibility decreased tremendously.

This is probably due to the difference in viscosities between the adjacent zones.

8.6.1.2 Hypochlorite reagent

8.6.1.2.1 Source of hypochlorite

The most common source of hypochlorite ions is a dichloroisocyanurate solution [7 - 10]. The hypochlorite ions are generated *in situ* by the alkaline hydrolysis of the sodium dichloroisocyanurate. Another source of hypochlorite ions is common household bleach, like JIK (Reckitt & Colman, Elandsfontein, South Africa), which contain 3.5% m/v sodium hypochlorite. This sodium hypochlorite solution is considered less stable than dichloroisocyanurate solution [7].

8.6.1.2.2 Concentration of the hypochlorite

Fig. 8.5 shows the influence of the hypochlorite concentration on zone penetration and sensitivity. It is clear that the relative peak height increases with increasing hypochlorite concentration. The solution containing 60 mℓ of household bleach (as source of hypochlorite ions) was chosen as optimum due to the best reproducibility achieved. At higher hypochlorite concentrations ($>$ 60 mℓ per 100 mℓ solution) significant background values, probably due to differences in refraction index, were observed. The sensitivity of the method is found to be dependant on the freshness of the hypochlorite solution [24]. This reagent is stable for about a week and should be prepared weekly.

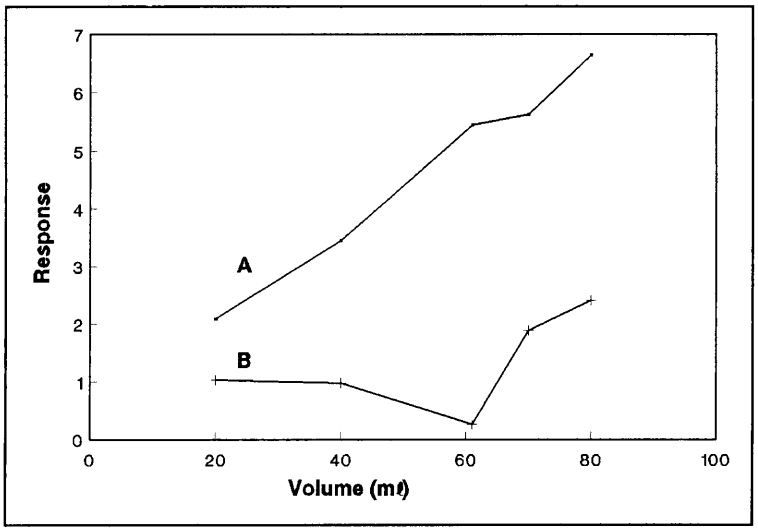

Fig. 8.5 Influence of hypochlorite concentration on relative peak height (A) and precision (B - %RSD).

8.6.1.2.3 Concentration of NaOH in the hypochlorite reagent

To ensure the high pH value needed for the reaction, NaOH was added to the hypochlorite reagent solution. Various concentrations of NaOH were evaluated. The results are given in Table 5.

TABLE 5. Influence of NaOH concentration in the hypochlorite solution on sensitivity and precision

Concentration ($g.\ell^{-1}$)	Relative peak height	%RSD
5	2.13	1.44
10	4.03	0.47
20	5.73	0.33
30	6.51	0.74
40	7.15	3.57

At NaOH concentrations below 10 $g.\ell^{-1}$ the pH of the reaction mixture is too low for the

reaction to develop at an acceptable rate. NaOH concentrations higher than 30 g.ℓ^{-1} resulted in more viscous solutions and therefore in insufficient mixing. The 30 g.ℓ^{-1} was therefore used in the analysis.

8.6.1.2.4 Concentration of sodium tetraborate decahydrate in the hypochlorite reagent

The added sodium tetraborate decahydrate had an effect on both the sensitivity and the reproducibility of the SIA method. The results of the various concentrations evaluated are summarised in Table 6.

TABLE 6. Influence of the concentration of $Na_2B_4O_7.10\ H_2O$ in the hypochlorite reagent on sensitivity and precision

Concentration (g.ℓ^{-1})	Relative peak height	%RSD
0	5.40	3.09
10	5.69	1.07
20	6.51	0.74
30	6.06	1.09
40	6.02	2.08

The response values increase with increasing concentration until a plateau is reached where an increase in concentration no longer results in an increase in relative peak height. The solution containing 20 g.ℓ^{-1} sodium tetraborate decahydrate was therefore chosen as optimum. This solution also gave the best reproducibility.

8.6.1.3 Catalyst

Acetone [23], Mn^{2+} [21], sodium nitroprusside [7 - 10, 12], sodium tetraborate decahydrate [4, 24] and ferrocyanide [22] are used as catalysts in the indophenol procedure. Mann [15] found that nitroprusside is a better catalyst than Mn^{2+} and Harwood and Huyser [23] showed that nitroprusside was a better catalyst than acetone. A drawback in the use of ferrocyanide is that it is necessary to irradiate the samples with fluorescent lamps in order to obtain the development of colour [26].

Addition of nitroprusside to the phenol reagent resulted in a reddish coloured solution which gave rise to large background values. It was further found that this solution was light sensitive. Attempts to protect the solution from light was not very successful. The reagent was stored in a dark bottle and the reagent line, holding coil and first reaction coil was covered with aluminium foil. After about 30 minutes the solution stabilized and a reproducible background value was obtained. This solution had to be prepared daily. It was clear that this solution was unsuitable for use in sequential injection analysis.

Addition of sodium tetraborate decahydrate to the hypochlorite solution gave a clear solution with no resulted background value. This solution is stable for up to a week and was used with great success in the proposed SIA system.

8.6.1.4 Sequences of sample and reagents

The order in which the different sequences of reagents and samples are drawn up depends

very much on the chemistry involved. Different possibilities were evaluated. The results are summarised in Table 7.

TABLE 7. Influence of order of reagents and sample on zone overlap and precision

Sequence	Relative peak height	%RSD
HPS*	5.48	0.61
PHS*	6.43	6.46
HSP*	8.29	5.10
PSH*	5.74	3.94
SPH*	5.57	0.78

* H - hypochlorite reagent
P - phenol reagent
S - sample

The sequences: PHS*, HSP* and PSH* resulted in high background values probably due to differences in the refraction indexes of the various zones. These sequences also gave rise to low precision. The sequence SPH* (sample, phenol reagent and then the hypochlorite reagent) was used. Contrary to the manual method (Fig.8.2), where the hypochlorite reagent is first added to the sample, the phenol reagent is first "added" to the sample in the SIA procedure.

8.6.1.5 Reaction time

The indophenol formation is a very slow process. After the reagents are added to the sample, in the manual determination, the mixture is allowed to react for 45 minutes [18]. A knowledge of the reaction rate is of particular value when adapting the process to sequential injection analysis, since the time spend in the manifold is too short for complete colour

development. As a stopped-flow period is easily incorporated into the SIA procedure, a waiting period of 80 seconds was used for the reaction to develop to an acceptable extent. The results of the various lengths of waiting periods are given in Table 8.

TABLE 8. Influence of the waiting period on sensitivity and precision

Waiting period (s)	Relative peak height	%RSD
0	2.82	1.20
10	2.99	2.99
20	3.24	1.50
30	3.71	1.72
50	4.27	1.32
70	4.59	0.95
80	5.11	0.84
90	5.06	1.03
110	4.12	2.13

A waiting period of 80 seconds seems to be long enough for the reaction to develop to a acceptable level. After 80 seconds dispersion of the formed product became dominant. This results in a decrease in relative peak height.

8.6.1.6 Flow reversals

It is the first flow reversal and its length which is the most effective in providing mutual zone penetration and since multiple flow reversals increase overall dispersion - and time to complete a measuring cycle - their use will remain restricted for difficult solution handling tasks, such as mixing zones of very different viscosities [25].

More than one flow reversal was needed in the determination of ammonia, due to insufficient mixing of the adjacent zones (because of their different viscosities). The stack of zones experienced three zone reversals before the formed product zone was eventually propelled to the detector. Note that waiting periods of 10 seconds each after the first two flow reversals and a waiting period of 80 seconds after the third flow reversal were incorporated into the SIA procedure (Table 2). It was found that this procedure gave better results (sensitivity and precision) than a procedure where the flow reversals followed each other without interruption. This surprising observation is probably due to the reaction kinetics of the formation of the indophenol product. Being a very slow process, longer reaction times is needed for complete colour development.

8.6.1.7 Temperature

In a modified, manual version of the indophenol method [19] it was shown that at temperatures of 20, 25, 37 and 75 °C, the sensitivity of the method was greatest at 75 °C, while time to reach maximum absorbance was greatest at 37 °C. Heating times were shown to be an important factor when reaction times and sensitivities were compared at 60 and 100 °C [20].

It was found by Stewart [18] that the rate of chromophore formation was generally enhanced by increasing the reaction temperature. However, as the temperature was raised, the final intensity of the blue chromophore decreased. The temperature had further no effect on the linearity of the calibration curve. It was, however, found by Pauer [12] that the most linear calibration curve is obtained at 42 °C (0 - 1.3 mg.ℓ^{-1} NH_4^+-N).

Stewart [18] also found that the final absorbance of the solution is fixed by the initial temperature of the reaction. From these studies it appears that a very fast initial reaction takes place. The amount of reactive intermediate produced by this initial reaction appears to decrease as the temperature is increased. It is this initial reaction which dictates the final absorbance of the solution. This is followed by the colour formation step, the rate of which can be increased by raising the temperature without affecting the final absorbance of the solution. Since the initial temperature of the mixture determines the sensitivity of the method all reagents, samples and standard solutions must be brought to the same temperature before mixing. This is particularly important where samples have been stored refrigerated prior to analysis.

8.6.1.8 Carrier

Initially distilled deionised water was used as carrier stream. This gave rise to large background values due to the large difference in viscosities of the reagent and sample zones with regard to the carrier stream. Multiple flow reversals reduced the background values but was unable to solve the problem. Changing the water carrier stream to a 1 mol.ℓ^{-1} NaOH solution reduced the background completely.

8.6.1.9 Wash solution

It is essential to rinse the complete system for at least one hour to remove all sodium hydroxide. Because of the high sodium hydroxide concentrations the selection valve and manifold become "sticky" and tend to become blocked. A 0.05 mol.ℓ^{-1} hydrochloric acid

solution was used as wash solution. The system was rinsed for about ten minutes with distilled deionised water after the acid treatment.

8.6.2 Physical parameters

Instead of using univariate optimization (Appendix B) as in the case of the chemical parameters, a method of alternating variable search (AVS) (Appendix C) was used to optimise the physical parameters.

The following parameters were optimized by the AVS method:

(i) Flow rate

(ii) Holding coil diameter

(iii) Reaction coil 1 diameter

(iv) Reaction coil 2 diameter

(v) Sample volume (V_S)

(vi) Phenol reagent volume (V_P)

(vii) Hypochlorite reagent volume (V_H)

As in the case of the simplex optimization (Chapter 7) the lengths of the holding coil and various reaction coils were not included into the AVS method. Because the geometries of the various coils do not have a significant influence on the sensitivity and precision of the proposed procedure, it is also excluded from the AVS method. The performance of the AVS method is shown in Table 9. The sample and reagent volumes are expressed as the time being drawn up.

TABLE 9. Progress of the AVS method for selected physical parameters

	Flow rate ($m\ell.min^{-1}$)	HC diameter (mm)	RC1 diameter (mm)	RC2 diameter (mm)	V_S (s)	V_P (s)	V_H (s)	Relative peak height	%RSD
Original conditions starting first cycle	5.9	1.02	1.02	0.76	5.5	2.5	7.5	5.16	0.21
	6.0							5.10	0.46
	6.1							5.24	2.60
	6.4							5.06	1.80
	5.8							4.76	2.99
	5.7							4.45	1.04
	6.1	1.02						5.01	1.40
		0.76						4.66	2.52
		0.51						4.02	0.97
		1.14						4.24	0.77
	6.1	1.02	1.02					4.48	1.36
			0.76					4.14	1.49
			0.51					3.49	2.37
			1.14					3.62	2.53
	6.1	1.02	1.02	0.76				4.11	0.63
				0.51				4.02	0.46
				0.46				3.98	1.04

TABLE 9. Continue

Flow rate ($m\ell.min^{-1}$)	HC diameter (mm)	RC1 diameter (mm)	RC2 diameter (mm)	V_S (s)	V_P (s)	V_H (s)	Relative peak height	%RSD
			1.02				3.51	1.85
			1.14				2.98	2.47
6.1	1.02	1.02	0.76	5.5			5.48	0.94
				4.5			4.67	0.77
				3.5			4.22	1.10
				6.5			4.80	1.36
				7.5			4.85	0.45
6.1	1.02	1.02	0.76	5.5	2.5		4.40	0.52
					3.5		4.30	2.51
					4.5		3.80	2.38
					1.5		3.17	1.12
					0.5		2.14	2.76
6.1	1.02	1.02	0.76	5.5	2.5	7.5	4.37	0.97
						6.5	4.30	0.74
						5.5	4.23	1.25
						8.5	4.44	0.65
						11.5	4.42	1.53

TABLE 9. Continue

	Flow rate ($m\ell.min^{-1}$)	HC diameter (mm)	RC1 diameter (mm)	RC2 diameter (mm)	V_S (s)	V_P (s)	V_H (s)	Relative peak height	%RSD
							10.5	4.38	1.02
End of first cycle	6.1	1.02	1.02	0.76	5.5	2.5	8.5	4.44	0.89
Starting second cycle	6.1							4.44	0.89
	6.2							4.35	1.04
	6.3							4.28	1.13
	6.0							4.56	0.97
	5.7							4.04	1.36
	5.8							4.24	1.28
	6.0	1.02						4.56	0.97
		0.76						4.31	1.32
		0.51						4.09	2.10
		1.14						4.46	0.99
	6.0	1.02	1.02					4.56	0.97
			0.76					4.14	1.23
			0.51					3.29	2.37
			1.14					4.30	1.06
	6.0	1.02	1.02	0.76				4.56	0.97

TABLE 9. Continue

	Flow rate ($m\ell.min^{-1}$)	HC diameter (mm)	RC1 diameter (mm)	RC2 diameter (mm)	V_S (s)	V_P (s)	V_H (s)	Relative peak height	%RSD
				0.51				4.48	1.11
				0.46				4.29	1.04
				1.02				3.51	1.85
				1.14				2.98	2.47
	6.0	1.02	1.02	0.76	5.5			4.56	0.97
					6.5			4.44	1.21
					7.5			4.41	1.18
					4.5			4.02	1.64
					3.5			3.89	2.13
	6.0	1.02	1.02	0.76	5.5	2.5		4.56	0.97
						3.5		4.18	1.64
						4.5		3.85	2.54
						1.5		4.48	1.01
						0.5		2.05	2.68
	6.0	1.02	1.02	0.76	5.5	2.5	8.5	4.56	0.97
							9.5	4.47	1.12
							10.5	4.36	1.75
							7.5	4.53	1.24
							6.5	4.40	1.50
End of second cycle	6.0	1.02	1.02	0.76	5.5	2.5	8.5	4.56	0.97

The AVS optimization was terminated after the second cycle, because no significant difference was obtained between the optimum values of the two cycles.

The optimum physical parameters were as followed:

(i) Flow rate: 6.0 $m\ell.min^{-1}$

(ii) Holding coil diameter: 1.02 mm

(iii) Reaction coil 1 diameter: 1.02 mm

(iv) Reaction coil 2 diameter: 0.76 mm

(v) Sample volume (V_S): 550 $\mu\ell$ (5.5 s)

(vi) Phenol reagent volume (V_P): 250 $\mu\ell$ (2.5 s)

(vii) Hypochlorite reagent volume (V_H): 850 $\mu\ell$ (8.5 s)

The configurations of the holding coil and reaction coils were determined by univariate optimization (Appendix B). In all cases the following geometries were evaluated: coiled, straight and knitted. The results are given in Table 10.

TABLE 10. Effect of the geometries of the holding and reaction coils on sensitivity and precision

	Configuration					
	Coiled		Straight		Knitted	
	RPH*	%RSD	RPH*	%RSD	RPH*	%RSD
Holding coil	5.11	0.84	4.86	0.63	4.77	1.65
Reaction coil 1	4.82	0.74	5.11	0.84	3.74	1.78
Reaction coil 2	5.14	0.78	4.96	1.75	4.97	1.33

* RPH = relative peak height

As seen from the results, the degree of zone penetration did not alter very much with the type of geometry used. The type of geometry did however effect the precision of the method. A coiled holding coil, straight first reaction coil and coiled second reaction coil were chosen for the proposed SIA system due to the best precision.

The holding coil length was determined as 2.0 m and the first reaction coil length as 1.2 m. The main function of the holding coil is to act as a reservoir to prevent the stack of zones of entering the pump conduit. Due to the coiled geometry of the second reaction coil a minimum length of 1.0 m was required. It is necessary to minimized the length of the second reaction coil in order to prevent dilution of the formed product zone.

8.7 Evaluation of the SIA method

The proposed sequential injection system was evaluated with regard to linearity, accuracy, precision, detection limit, sample interaction (carry-over), sample frequency and interferences.

8.7.1 Linearity

The response linearity of the proposed SIA system for the spectrophotometric determination of ammonia was calculated under the optimum conditions. The calibration curve is linear for ammonia concentrations between 0 and 50 mg.ℓ^{-1}. The relationship for relative peak height versus ammonia concentration was:

$$y = 0.044x + 2.035; r = 0.9994$$

where y = relative peak height and x = ammonia concentration. A representative run illustrating the actual peaks obtained for standards is given in Fig. 8.6.

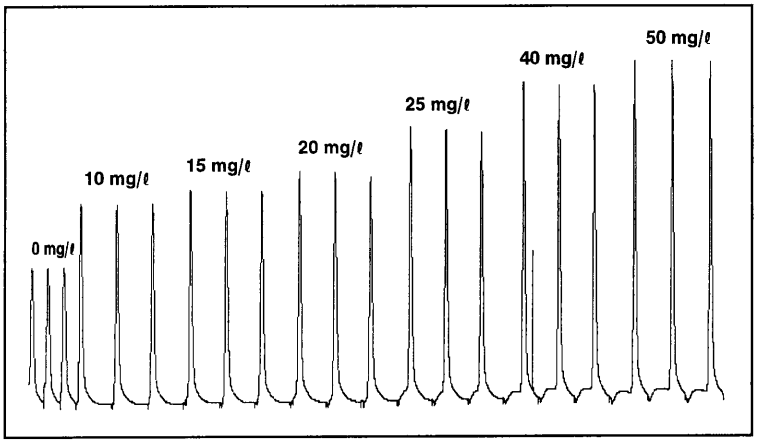

Fig. 8.6 A representative run of actual peaks obtained during calibration.

8.7.2 Accuracy

The accuracy of the proposed SIA analyzer was evaluated by comparing results from real samples obtained with the SIA system with results obtained with a standard procedure (AutoAnalyser). The results as shown in Table 11 revealed good agreement between the two methods.

TABLE 11. Comparison of the results of a number of samples as determined with the proposed SIA system and an AutoAnalyser

Sample	SIA ([ ] in mg.ℓ^{-1})	AutoAnalyser ([ ] in mg.ℓ^{-1})
S918401	40.3	41
S918188	4.9	5.0
S918498	28	25
S918425	32.8	36
S918413	15.6	15
S918504	0.2	0

Accuracy was also determined in terms of recovery using the samples in the presence of interfering ions normally found in real samples. The recovery was determined by analysing the samples (S918188 and S918504) to determine their analyte content, after which a known amount of analyte was added and the samples re-analyzed. Recovery was determined using the equation

$$Recovery\ (\%) = \frac{Determined\ ammonia}{Expected\ ammonia} \times 100$$

Table 12 gives the results obtained with the following samples: Sample A = S918188 + 20 mg.ℓ^{-1} NH_4^+-N, sample B = S918504 + 20 mg.ℓ^{-1} NH_4^+-N, sample C = S918188 + 40 mg.ℓ^{-1} NH_4^+-N, sample D = S918504 + 10 mg.ℓ^{-1} NH_4^+-N and sample E = S918504 + 5 mg.ℓ^{-1} NH_4^+-N.

TABLE 12. The % recovery of a number of ammonia samples

	Expected concentration ($mg.\ell^{-1}$)	Determined concentration ($mg.\ell^{-1}$)	% Recovery
Sample A	25	24.7	98.8
Sample B	20	20.6	103
Sample C	45	44.2	98.2
Sample D	10	9.8	98
Sample E	5	5.3	106

The percentage recovery of all samples was between 98 and 106%.

8.7.3 Precision

The reproducibility of the proposed method was tested on standard ammonia solutions and water samples (Table 13). The coefficient of variation for standard ammonia solutions and for water samples having different concentrations of ammonia, was less than 1.80 on 10 tests of each sample.

TABLE 13. Reproducibility test on a series of standard ammonia solutions as well as a series of water samples

Sample/Standard	Coefficient of variation (%)	Sample	Coefficient of variation (%)
0 mg.ℓ^{-1}	1.60	S918425	1.32
10 mg.ℓ^{-1}	1.20	S918413	1.65
20 mg.ℓ^{-1}	0.71	S918504	1.02
25 mg.ℓ^{-1}	1.15	Sample A	1.03
40 mg.ℓ^{-1}	0.95	Sample B	0.98
50 mg.ℓ^{-1}	1.32	Sample C	1.53
S918401	1.74	Sample D	1.78
S918188	1.80	Sample E	1.06
S918498	1.41		

8.7.4 Detection limit

The detection limit of the proposed SIA system was calculated using the formula

$$Detection\ limit = \frac{3 \times S_k}{100} \times K$$

where $S_k = 1.20$ is the relative standard deviation of the lowest concentration of the specific method and K = 10 mg.ℓ^{-1} is the lowest standard concentration for this method. A safety factor was built into the calculation. The detection limit was calculated to be 0.36 mg.ℓ^{-1}.

8.7.5 Sample interaction

The sample interaction (carry-over effect) between consecutive samples was determined by

analysing a sample with a low analyte concentration (10 mg.ℓ^{-1} ammonia) followed by one with a high analyte concentration (100 mg.ℓ^{-1} ammonia) which was again followed by a sample with a low analyte concentration (10 mg.ℓ^{-1} ammonia). The sample interaction between samples was then calculated using the following formula:

$$Sample\ interaction = \frac{(A_3 - A_1)}{A_2} \times 100$$

where A_1 = relative peak height of a sample containing 10 mg.ℓ^{-1} of ammonia followed by A_2 = relative peak height of a sample containing 100 mg.ℓ^{-1} of ammonia followed by A_3 = relative peak height of a sample containing the same amount of ammonia as A_1. The relative peak heights A_1, A_2 and A_3 were respectively 2.81, 4.57 and 2.84. The interaction between samples as calculated was 0.66%, which is negligible.

8.7.6 Sample frequency

It took 225 seconds to complete one analytical cycle. This gave a frequency of 16 samples per hour.

8.7.7 Interferences

The indophenol method is specific for ammonia species, since organic nitrogen compounds, nitrate, nitrite and various electrolytes (in concentrations normally occurring in natural waters) only slightly interfere [14]. The methyl and ethyl primary, secondary and tertiary

amines and volatile amines are known to interfere causing a reduction in response [7].

Urea and the common natural amino acids do not interfere if specified temperatures (± 30 °C) and pH values (± 10.5) are adhered to; at higher temperatures or pH values they are hydrolysed to ammonia and so included in the result [7].

The effect of certain combinations of other substances on the determination of ammonia is given in Table 14. More detailed information on the effects of individual interfering substances is lacking [7].

TABLE 14. Interference data in the determination of ammonia using the indophenol procedure

Other substances	Concentration of other substances ($mg.\ell^{-1}$)	Effect on a 1.0 $mg.\ell^{-1}$ ammonia standard (absorbance units)
Calcium	200	+ 0.100
Magnesium	150	
Calcium	200	+ 0.177
Magnesium	150	
Iron (III)	20	
Copper	1.5	
Nickel	1.0	
Cadmium	0.5	
Aluminium	1.0	
Lead	2.0	
Manganese	2.0	
Zinc	15	
Chloride	2 000	- 0.049
Nitrate (as N)	25	
Nitrite (as N)	10	
Sulphate	200	
Fluoride	10	
Anion detergent (as Manoxol OT)	10	- 0.101
Phenol	3	
Cyanide	0.1	
Thiocyanide	10	
Bicarbonate	800	

At pH values higher than 12 magnesium interfere by forming a precipitate of $Mg(OH)_2$. In order to avoid precipitation complexing agents are employed. Ca^{2+} and Mg^{2+} can be complexed by CDTA [16], EDTA or citrate [7]. None of the Group 1 elements tested (Na and K) interfere in the determination of ammonia. Ca^{2+} starts to interfere at a ratio of 3 : 1 Ca^{2+} : NH_4^+-N.

A dialyser unit is incorporated into the manifold for use in the analysis of samples, containing high levels of ammonia, which may be turbid. The dialyser unit is bypassed for the determination of low levels of ammonia.

8.8 Conclusions

A suitable SIA analyzer to determine ammonia in water is developed. This procedure is very suitable for direct routine analysis of ammonia in water. Because the method is specific for ammonia only a few components interfere in the determination. At the concentrations present in natural water these interferences are however insignificant. This method is fully computerised and is able to monitor ammonia in samples at a frequency of 16 samples per hour with a relative standard deviation better than 1.8%. The calibration curve is linear between 0 and 50 mg.ℓ^{-1}.

8.9 References

1. N. N. Greenwood and A. Earnshaw, **Chemistry of the Elements**, Pergamon Press, Oxford, 1984.
2. R. A. Rosemary and T. R. Seustedt, **Atmospheric Environment**, **24A** (12) (1990) 3093.
3. Analytical Quality Control (Harmonised Monitoring Committee), **Analyst**, **107** (1982) 680.
4. I. Lukkari, J. Růžička and G. D. Christian, **Fresenius J. Anal. Chem.**, **346** (1993) 813.
5. F. J. Krug, J. Růžička and E. H. Hansen, **Analyst**, **104** (1979) 47.
6. E. Strauss, J. P. Favier, D. D. Bicanic, K. van Asselt and M. Lubbers, **Analyst**, **116** (1991) 77.
7. **Ammonia in Waters.** Methods for the Examination of Waters and Associated Materials, HMSO, London, 1981.
8. **Total Nitrogen and Total Phosphorus in Sewage Sludge.** Methods for the Examination of Waters and Associated Materials, HMSO, London, 1985.
9. **Kjeldahl Nitrogen in Waters.** Methods for the Examination of Waters and Associated Materials, HMSO, London, 1987.
10. **Flow Injection Analysis. An Essay Review and Analytical Methods.** Methods for the Examination of Waters and Associated Materials, HMSO, London, 1990.
11. W. J. Schmidt, H-D. Meyer, K. Schügerl, W. Kuhlmann and K-H. Bellgardt, **Anal. Chim. Acta.**, **163** (1984) 101.
12. J. J. Pauer, **Die Vloei-Inspuitanalise van Sekere Determinante in Oppervlak- en**

Grondwater, M.Sc.-Tesis, Universiteit van Pretoria, 1989.

13. G. D. Marshall and J. F. van Staden, **Analytical Instrumentation**, **20** (1992) 79.

14. I. Ivančič and D. Degobbis, **Water Res.**, **18** (9) (1984) 1143.

15. L. T. Mann, **Anal. Chem.**, **35** (13) (1963) 2179.

16. R. T. Roskam and D. de Langen, **Anal. Chim. Acta.**, **30** (1964) 56.

17. L. Solórzano, **Limnol. Oceanogr.**, **14** (1969) 799.

18. B. M. Stewart, **Water Res.**, **19** (11) (1985) 1443.

19. M. W. Weatherburn, **Analyt. Chem.**, **39** (1967) 971.

20. P. J. Rommers and J. Visser, **Analyst**, **94** (1969) 653.

21. J. A. Russel, **J. Biol. Chem.**, **156** (1944) 457.

22. M. I. Liddicoat, S. Tibbitts and E. I. Butler, **Limnol. Oceanogr.**, **20** (1975) 131.

23. J. E. Harwood and D. J. Huyser, **Water Res.**, **4** (1970) 501.

24. L. C. Davis and G. A. Radke, **Anal. Biochem.**, **140** (1984) 434.

25. T. Gübeli, G. D. Christian and J. Růžička, **Anal. Chem.**, **63** (1991) 2407.

26. A. M. Sólyom, G. Z. Angeli, D. D. Bicanic and M. Lubbers, **Analyst**, **117** (1992) 379.

CHAPTER 9

Summary

The attributes of flow-injection analysis (FIA): speed, solution containment, capability of miniaturization, automated standardization, sample dilution, matrix removal, analyte preconcentration and the ability to control the time/concentration domain of any solution chemistry under investigation, are well recognized and exploited by the world wide community of flow injection enthusiasts.

Being able to use both selective and non-selective detector flow-injection systems, most likely in sequential injection configurations, will be recognized as universal inlets to both spectroscopic and electroanalytical instruments and will also, after suitable miniaturization, become integral parts of chemical sensors.

Sequential injection analysis (SIA) has been proposed to satisfy the demands for mechanical simplicity in FIA techniques. Minimizing the number of mechanical components to two (one pump and one valve) is beneficial for a process control environment as it increase the reliability of the apparatus. For laboratory applications, however, the drawbacks of the sequential injection (SI) system, with only one pump, need to be addressed. Therefore, one of the goals for future exploration is to design a flow scheme that combines the advantages of FIA and SIA and yet has none of their drawbacks.

Seen from a process analyst's viewpoint, the sequential injection analyzer is much less complicated than any present chemical analyzer, including traditional flow-injection schemes. The single liquid drive of the SIA system is likely to last many thousands of measurement cycles without need for servicing, thus providing the robustness for process analysis. The impulse-response mode of operation provides the possibility of recalibration and flushing of the detector cell, ensuring accuracy and precision. The multi-port selection valve replaces the check valves, normally needed in piston pumps, and serves as both an injector and selector. The volume of reagent consumption is minimal.

Possibly the greatest attribute of the system is that the same manifold configuration can accommodate a variety of chemistries, without the need of reconfiguration. In the conventional FIA system changing the sample volume requires reconfiguration of the sample loop and changes of the dispersion or reaction times require reconfiguration of the reactor coil. Additional reagents require additional flow lines with confluence points and extra pump channels. In the sequential injection system the same changes are obtained by reprogramming the pump speed and selector valve positions. These attributes, which are valuable for continuous monitoring and process control, will be rapidly exploited, provided that the complexibility of sequencing events during a measurement cycle can be overcome in a practical and readily accessible form. The adaption of chemistries to SIA is easy, as it can be based on the practice and theory of flow injection methodology, which provide guidelines for the design of sequential injection systems.

The inherent flexibility of SIA makes it an ideal tool for monitoring bioprocesses where sample matrix changes with time and different conditions of analysis may be required.

Another advantage of SIA is the possibility of clustering standards around the multiposition valve, so that the system might be automatically recalibrated as required. The detector is only exposed to the potentially harsh sample for a short time, the rest of the time, the detector is exposed to the wash solution. There is also the possibility of two assays being performed with an unique SIA system.

It is unlikely that SIA in its present form will replace FIA. Few sample manipulation techniques match FIA in flexibility. The only requirement for successful implementation in FIA is a repeatable flow pattern. In SIA careful planning and method design is required. Attention must be given to ensure that zones are contained within the reaction coil and that device events are carefully synchronized. This requires closer attention during the method development phase. Nevertheless, once a method has been developed, SIA tirelessly and slavishly repeats the device sequence which generates the desired analytical results.

Important guidelines were established to assist in the design of SIA manifolds. Of course, these guidelines must be interpreted in the light of the application at hand; it may not always be desirable to maximize sensitivity.

A wide range of successful applications of SIA were illustrated. The methodology developed during this study demonstrates the suitability of sequential injection analysis for the spectrophotometric determination of calcium in water, urine and pharmaceutical formulations. It was possible by using an optimized sequence of sample and reagents to eliminate any background originating from coloured free indicator species.

A sequential injection analyzer was developed to monitor the sulphate concentration in the effluents of chemical process industries as well as natural waters downstream. Incorporation of an alkaline buffer-EDTA solution in the correct sequence of the system redissolved accumulated barium sulphate precipitate to give a high degree of sensitivity, accuracy and precision.

On-line dilution with sequential injection analysis had been evaluated for sulphate monitoring in industrial effluents using a dilution coil in the conduits of the manifold system and a dilution step as part of the timing sequence. The manifold of the SIA system with the dilution coil is more complex than the system including the dilution step. The former method needs more complicated programming as well. Shorter analysis time favoured the dilution with the dilution step, but the limited linear range is a large drawback of the method. The large linear range of the SIA system with the dilution coil makes it very suitable to be used as a process analyzer.

Proven feasible for automating the 'Molybdenum Blue' method for phosphate monitoring, SIA presents some advantages in comparison to classical FIA (such as simplicity of the manifold). The flow detector fouling with the product of the reaction between ascorbic acid and ammonium molybdate does not occur in the sequential injection manifold as the detector is in contact with water between analyses. In flow-injection manifolds, both reagents are mixed in the detector field causing fouling after a few hours of use. As a consequence, very stable baselines are obtained by sequential injection analysis and system cleaning during the operation time is unnecessary.

A suitable sequential injection analyzer for the direct spectrophotometric determination of ammonia in water is developed. SIA makes determinations based on slower reactions feasible, because, unlike FIA, the flow can be halted for a fixed time to allow the reaction to develop. Reaction between reagents with very different viscosities is also feasible in SIA due to sufficient mixing by multiple flow reversals.

Successful applications of SIA in a number of different applications are developed and for the foreseeable future, it can be expected that sequential injection process analyzers will be proliferated in modern chemical, biochemical, metallurgical and environmental applications.

APPENDIX A

APPENDIX A

Simplex Optimization

1 Introduction

The response surface of an analytical system can be represented with isoresponse contours. The position of these contours is unknown to the researcher. The process of finding a minimum or maximum in this response surface is called optimization. Simplex optimization is based on a set of rules using a geometrical figure, called a simplex. A simplex is defined by a number of vertices that is one more than the number of factors (dimensions) that have to be optimized. A simplex in two dimensions is thus a triangle and a simplex in three dimensions a tetraheder.

Fig. A1 represent a two-dimensional simplex superimposed on a contourdiagram of isoresponse lines of a function with two variables (factors). A, B and C is response values that were determined at the corresponding co-ordinates of factor 1 and factor 2.

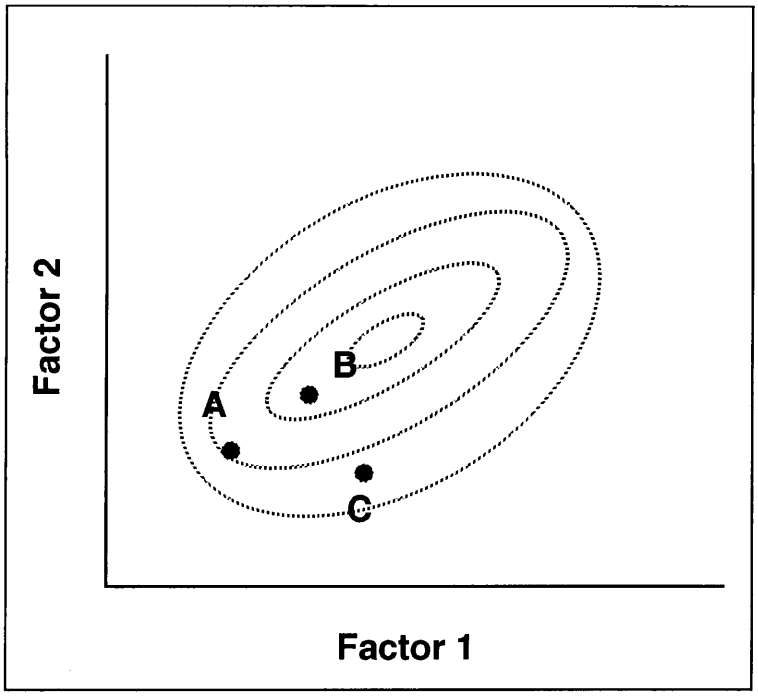

Fig. A1 Two dimensional simplex superimposed on a contour diagram of isoresponse lines.

2 Experimental

The optimization must move the simplex in the direction of the maximum response. To achieve this a number of rules must be obeyed.

(1) A response is measured after every move.

(2) A move is made in the direction of the adjacent simplex by rejecting the least desirable response of the original simplex and replacing it with the mirrorimage of the rejected vertex. In Fig. A2 three moves from ABC to DEF is shown. In the original simplex A had the lowest response and was rejected. Reflection of A creates D and a new simplex BCD. A response is measured at D. C, now the least desirable

response, was rejected leading to simplex BDE, with E the reflection of C. Experimental results shown that B was to reject next leading to the fourth simplex, EDF.

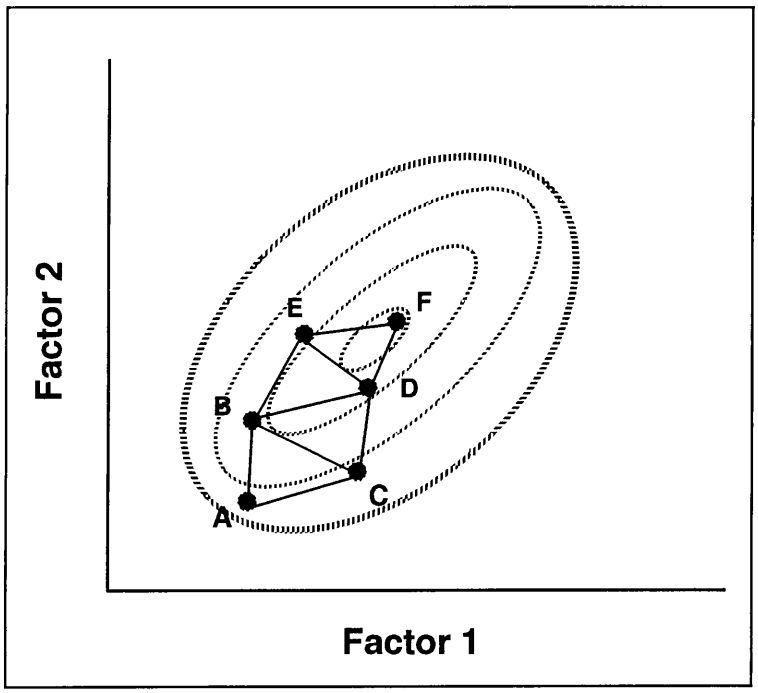

Fig. A2 Progress of simplex optimization.

For a k-dimensional simplex with co-ordinate vectors

$$P_1, P_2, \ldots, P_j, \ldots, P_k, P_{k+1}$$

elimination of the least wanted response P_j gives the symmetry axis

$$P_1, P_2, \ldots, P_{j-1}, P_{j+1}, \ldots, P_k, P_{k+1}$$

with centroid

$$\bar{P} = 1/k(P_1 + P_2 + ... + P_{j-1} + P_{j+1} + ... + P_k + P_{k+1}).$$

The new simplex is defined as the symmetry axis together with a new vertex P_j^* which is the reflection of the rejected vertex P_j over the centroid P,

$$P_j^* = \bar{P} + (\bar{P} - P_j)$$

(3) If the reflected point gives the lowest response in the new simplex, the second lowest response in the new simplex is rejected.

(4) If a vertex has remained unrejected for k+1 simplexes, the response corresponding to that co-ordinates is repeated. If the high response was due to an error, a re-evaluation of the response at that vertex corrects the mistake and eventually eliminates the vertex.

(5) If a reflected vertex falls outside the boundaries of the factors a highly undesirable response is assigned to it. Rules 2 and 3 bring the simplex back within the boundaries.

When a optimum is reached, the rules force the simplex to move in a circle as shown in Fig. A3. The movement of the triangles makes it obvious when an optimum is reached in the case of two factors, but with tetrahedra and polyhedra of higher dimensions it is not always obvious when an optimum is reached.

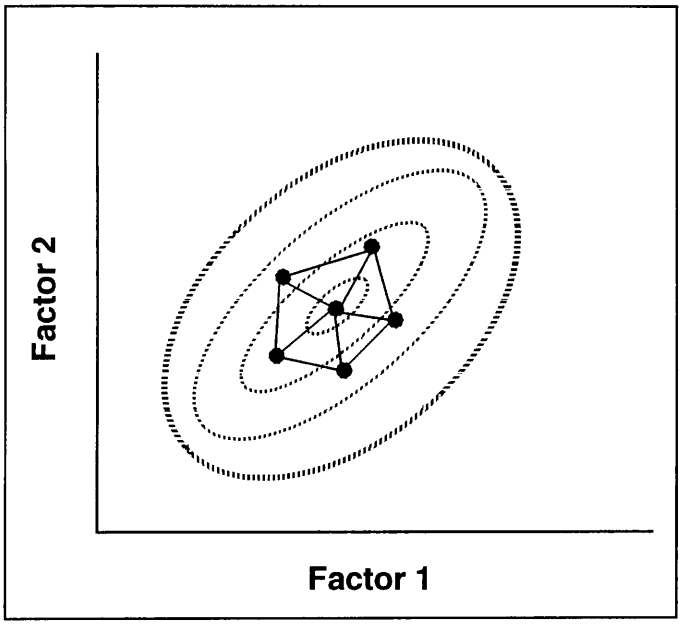

Fig. A3 Representation of the optimum reached with simplex optimization.

3 Modified simplex optimization

Advance towards the optimum can be accelerated by a simplex which can vary in size. The choice of the initial simplex is also not critical as it can be expanded or contracted as the method proceeds. A modification of the simplex method by Nelder and Mead involves the operations of expansion and contraction.

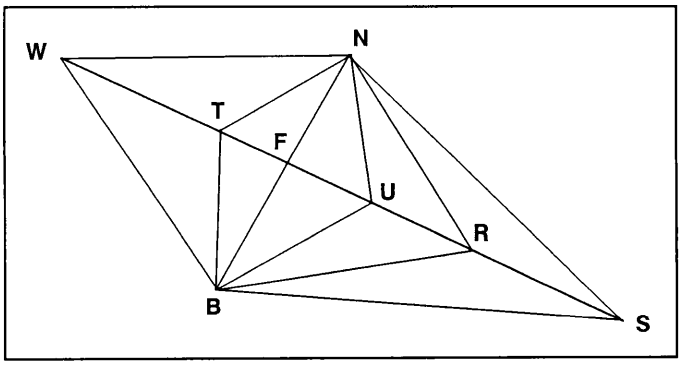

Fig. A4 Representation of the modified simplex optimization.

Fig. A4 shows the starting simplex BNW. B is the best response, W the worst response and N the second best response. $\bar{P}$ is the centroid of the symmetry axis BN. Reflection of W across BN give vertex R.

$$P_r = \bar{P} + (\bar{P} + P_w)$$

There is three possibilities available depending on the response of vertex R. The possibilities are:

1) The response at R is better than the response at B. This means movement is in the right direction and favour further investigation. Thus the segment WR is expanded:

$$P_S = \bar{P} + \epsilon(\bar{P} - P_W)$$

where ϵ is the expansion coefficient ($\epsilon > 1$). The response is evaluated at vertex S.

If S is better than B, the new simplex is BNS. If S is worse than B, the new simplex is BNR.

2) The response at R is not better or worse than B. There is no need for expansion or contraction and the new simplex is BNR.

3) The response is less desirable than the response at N. Movement is in the wrong direction and contraction in this direction is desirable. If the response at R is less desirable than the worst previous vertex (W) then the new contracted simplex should be at T which is closer to W than to R.

$$P_T = \bar{P} + ß(\bar{P} - P_W)$$

where ß is the contraction coefficient and $0 < ß < 1$. If the response at R is not less desirable than the lowest previous vertex (W), then the new contracted simplex is at U which is closer to R than to W.

$$P_U = \bar{P} + ß(\bar{P} - P_W)$$

The simplex is terminated when the size of the steps become smaller than a previously determined size, e.g. when the response differences become close to the value of the indeterminate error.

In contrast to factorial design (Appendix B), the number of experiments required in the

simplex method do not increase rapidly with the number of factors. Therefore all factors thought to have a bearing on the result should be included in the optimization.

4 References

1. C. Rozynki, **Chem. Anal.**, (Warsaw), **38** (6) (1993) 681.

APPENDIX B

APPENDIX B

Univariate Optimization

1 Introduction

Univariate optimization is probably the most frequently used technique in optimisation of an analytical procedure. This technique must not be confused with factor analysis which is based on linear algebra. With factor analysis one is trying to express a given set of data in terms of a linear model. Using univariate optimization, the researcher makes some experimental measurements and then plots two-dimentional graphs, trying to relate the change in response to the change in function of the independent variable.

2 Experimental

Univariate optimization is done by varying one factor and keeping n - 1 factors constant until the optimum of the factor is reached. That factor should be set at the optimum value, a second factor should be varied, while the n - 2 factors are kept constant, until the optimum of the second factor is achieved. This process continues until all n factors are optimized.

In using univariate optimization, the investigators make one of two major assumptions:

(i) the response is a function of only one variable or

(ii) if the data are multi-dimensional; that the response responds to the dominant or controlling variable in the model.

3 Reference

1. P. H. Weiner, **Chemtech**, (1977) 321.

APPENDIX C

APPENDIX C

Alternating Variable Search (AVS) Method

1 Introduction

Optimization may be considered as the process by which a maximum (or minimum) in a factor space is located. What is required is an efficient strategy for locating the maximum value on an n + 1 dimensional response surface, where n is the number of factors contributing to the response. The efficiency of optimization is quantified in terms of the time taken to locate the maximum. This has an effect on the mechanism of the search strategy in terms of selection of (a) the size step and (b) the criterion for stopping.

2 Experimental

Several variations of the AVS method can be used, all of which involved initial decisions concerning the boundaries or limits of the factor space and of the initial step size for each factor. Step sizes are chosen to be between 0.1 and 0.05 of the appropriate factor space. As a rough guide for the choice of step size, the criterion that two steps from the starting position should cause a significant difference in the response value is used. For all methods the standard deviation of the response is estimated after the first successful cycle by replicate measurement. The search is terminated when the responses obtained at the end of two

successive cycles were within 10% of each other.

(a) Fixed step size method

Two methods are used which differed only in the rule for changing direction. In the first (fixed AVS-1) the search changes direction after one step in a bad direction (i.e. a decrease in response) whereas in the second (fixed AVS-2) a change in direction was made after two successive bad steps had been taken.

(b) Rosenbrock's method

This is a variable step size method in which the step is increased by a factor of three if the search is proceeding in a good direction. If the search direction is bad, a contracted step of half the previous step size is taken and then the search direction is changed.

(c) Hybrid method

In this method the first cycle of the factors (i.e. all factors taken in turn) proceed with a fixed step size. For subsequent cycles the initial step is increased by a factor of three if the search is proceeding in a good direction. As long as the response increase, the initial step size is repeated following by a "triple jump". If the factor of the three expansions gives a bad response, a step (of initial size) is taken in the reverse direction (equivalent to a replacement step of factor two expansion). The direction is then changed. When a bad response is obtained for the initial step size, following a triple jump, a further unit step is taken. If two

successive bad steps have been taken, the search direction is changed, otherwise a triple jump is taken. The flow diagram of this hybrid method is shown in Fig. C1.

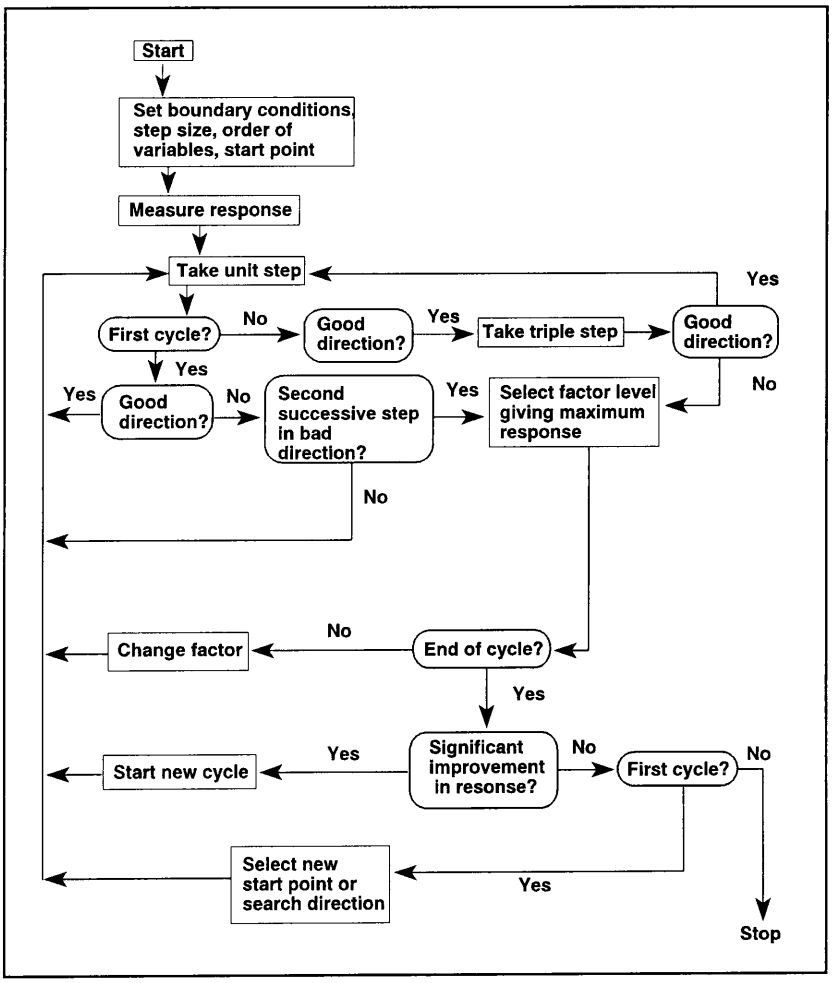

Fig. C1 Flow diagram for the hybrid AVS method.

The AVS methods are critised on the basis that the optimum found depends on the starting position for the search, and the order in which the factors are taken. The number of steps necessary to find the optimum is also given as a drawback of the AVS methods.

3 References

1. S. J. Chalk and J. F. Tyson, **Anal. Chem.**, **66** (1994) 660.

2. S. Greenfield, M. S. Salman, M. Thomsen and J. F. Tyson, **Journal of Analytical Atomic Spectroscopy**, **4** (1989) 55.

APPENDIX D

APPENDIX D

Publications and Presentations

1. J. F. van Staden and R. E. Taljaard, *Determination of Calcium in Water, Urine and Pharmaceutical Samples by Sequential injection Analysis*, **Anal. Chim. Acta.**, In Press, (1996).
2. J. F. van Staden and R. E. Taljaard, *Determination of Sulphate in Natural Waters and Industrial Effluents by Sequential Injection Analysis*, **Anal. Chim. Acta.**, In Press, (1996).
3. J. F. van Staden and R. E. Taljaard, *On-line Dilution with Sequential Injection Analysis. A System for Monitoring Sulphate in Industrial Effluents*, Submitted to **Fresenius J. Anal. Chem.**, (1996).
4. R. E Taljaard and J. F. van Staden, *Determination of Phosphate in Natural Waters by Sequential Injection Analysis*, In Preparation, (1996).
5. J. F. van Staden and R. E. Taljaard, *Determination of Ammonia in Water and Industrial Effluent Streams with the Indophenol Method using Sequential Injection Analysis*, Submitted to **Anal. Chim. Acta.**, (1996).

R. E. Taljaard, Student Symposium: Akademie vir Wetenskap en Kuns, Pretoria, November 1995.

R. E. Taljaard and J. F. van Staden, Poster, 33rd SACI Convention, Cape Town, January 1996.